UNIVERSITY OF GLASGOW

CHEMISTRY DEPARTMENT

ELECTRON PARAMAGNETIC RESONANCE STUDIES OF SOME SYSTEMS OF CHEMICAL INTEREST

being

A thesis submitted in part fulfilment

of the requirement for the

DEGREE OF DOCTOR OF PHILOSOPHY

by

ARCHIBALD A. McCONNELL

October 1970

ProQuest LLC.
789 East Eisenhower Parkway
P.O. Box 1346
Ann Arbor, MI 48106 – 1346

Ph.D. Thesis October 1970 Archibald A. McConnell

ELECTRON PARAMAGNETIC RESONANCE STUDIES OF SOME SYSTEMS OF CHEMICAL INTEREST

Summary

This thesis is subdivided into four parts, which are summarised separately below.

Part I

An elementary account of the principles of electron paramagnetic resonance spectroscopy and a brief description of the spectrometer system are contained in this, the introductory section, of this thesis.

Part II

This section describes a study of nitroxide radicals obtained from caryophyllene nitrosite.

Eight different nitroxide radicals have been derived from caryophyllene nitrosite. Two are obtained by allowing caryophyllene nitrosite in chloroform solution to react with iodine or with bromine; two by irradiating solid caryophyllene nitrosite with red light, or by irradiating solutions of caryophyllene nitrosite in toluene or in benzene with red light; two are obtained by irradiating solutions of caryophyllene nitrosite in ethanol with red light; one by irradiating solid caryophyllene nitrosite with ultraviolet radiation, and one by dissolving

the last radical in chloroform. Three of these radicals have been isolated as pure, stable solids. Electron paramagnetic resonance spectra of the eight radicals are described and spin Hamiltonian parameters, extracted from spectra of "glasses" formed at 77°K by dispersing them in chloroform:toluene (3:2) solution or from room-temperature spectra, are given. Structures for the nitroxide radicals, and some information about the mechanisms of the red and ultraviolet photolyses reactions, are deduced from the electron paramagnetic resonance data.

Part III

This section deals with a study of the small free radical, di-tertiary-butylnitroxide, within the cavities of Dianin's compound.

Polycrystalline and single crystal electron paramagnetic resonance spectra of di-tertiary-butylnitroxide in Dianin's compound have been examined over the temperature range $77°K \lesssim T \lesssim 430°K$. The orientations of the radicals in the crystal have been determined, and the motions of the radicals and the magnitudes of the energy barriers hindering these motions in the clathrate, have been characterised. Changes in van der Waals interactions as the temperature changes appear to affect hyperfine tensor components, but it has not been possible to obtain quantitative information about changes in the electron

distribution responsible for these effects. Other radicals do not appear to be formed as the temperature is raised. At higher temperatures the lattice sublimes.

Part IV

In this section the effects of axial interactions on electron paramagnetic resonance spectra of copper(II) chelates are described.

X-band e.p.r. spectra in chloroform:toluene (60:40) glasses at 77°K show that chloroform forms weak complexes with some planar compounds of copper(II). Spin Hamiltonian parameters for some "isolated" cupric chelates and for some corresponding chloroform-chelate complexes are reported, and these parameters are equated to the atomic orbital coefficients in some of the molecular orbitals involved in bonding in both types of compound. The relative ordering of the energies of the B_{2g} and A_{1g} levels in planar copper(II) compounds may change if the ligand is changed. Effects of axial perturbations which arise from two axial dipoles acting on planar cupric complexes are considered, and first-order perturbation theory is used to obtain relationships which connect the spin Hamiltonian parameters for the "isolated" complexes with those for the perturbed complexes: experimental observations are in accord with the theoretical treatment. Relaxation arising from rotation about the long

axis of these cupric complexes controls the line widths in their e.p.r. spectra recorded at 295°K: the effect of chloroform complexing on paramagnetic relaxation phenomena in these complexes is noted. E.p.r. methods may be used to discriminate between different isomers of polyketone complexes of copper(II).

Acknowledgements

The author wishes to express his appreciation of the assistance and encouragement given by Dr. A. L. Porte throughout this work. He thanks also Professor J. M. Robertson in whose laboratories this work was carried out.

Helpful discussions with staff and research students of the Chemistry Department of the University of Glasgow, in particular with former colleagues, Drs. J. M. Barbour, N. M. D. Brown, and D. A. Tong, are acknowledged.

The author thanks Dr. J. S. Roberts for advice on the subject of nitroxide radicals obtained from caryophyllene nitrosite, and Dr. D. D. MacNicol for supplying the compounds studied in Part III of this thesis and for advice thereon.

Thanks are also due to Mrs. K. Love and to Mr. F. B. Wilson for providing photographic prints; and especially to Miss Janette Pollock for performing the unenviable task of typing the manuscript of this thesis.

Finally he acknowledges with gratitude the award of a Carnegie Research Scholarship during the tenure of which this work was carried out.

Preface

This thesis deals with the application of electron paramagnetic resonance spectroscopy to three distinct chemical problems. The thesis has been subdivided into four parts, the first of which consists of a general introduction to electron paramagnetic resonance spectroscopy. Part II describes a study of a number of nitroxide free radicals obtained from caryophyllene nitrosite by photochemical and by other means. Part III is concerned with the study of the behaviour of the nitroxide radical, di-tertiary-butylnitroxide within the cavities of Dianin's compound over the temperature range $77°K < T < 430°K$. Part IV describes the effect of axial perturbation by molecules of chloroform (solvent) on planar complexes of copper(II) and discusses the relaxation of these copper(II) complexes in solution.

Summaries of Parts II, III, and IV are given at the end of each part.

The work described in this thesis is original, and was carried out in partial fulfilment of the requirements for the degree of Ph.D. in the University of Glasgow.

October, 1970 A. A. McConnell.

TABLE OF CONTENTS

PART I

AN INTRODUCTION TO ELECTRON PARAMAGNETIC RESONANCE SPECTROSCOPY

PART II

ELECTRON PARAMAGNETIC RESONANCE STUDIES OF NITROXIDE RADICALS OBTAINED FROM CARYOPHYLLENE NITROSITE

PART III

AN ELECTRON PARAMAGNETIC RESONANCE STUDY OF DI-TERTIARY -BUTYLNITROXIDE IN DIANIN'S COMPOUND

PART IV

THE EFFECTS OF AXIAL INTERACTIONS ON ELECTRON PARAMAGNETIC RESONANCE SPECTRA OF COPPER(II) CHELATES: WEAK COMPLEXES OF COPPER(II) AND CHLOROFORM

PART I

AN INTRODUCTION TO ELECTRON PARAMAGNETIC RESONANCE SPECTROSCOPY

1. Magnetic moments of electrons and nuclei

Electrons, protons and neutrons undergo various kinds of closed-loop like motion. An angular momentum, G, generated in this way may be decomposed into its components along three mutually perpendicular directions x, y and z.

$$G^2 = G_x G_x + G_y G_y + G_z G_z \qquad 1.1$$

and the quantum mechanical properties of angular momentum operators show that:

(a) the eigenvalues of G^2 may be written in the form $n(n+1)\hbar^2$ where $\hbar = 6{\cdot}6256 \times (2\pi)^{-1} \times 10^{-27}$ erg. sec. and 2n is an integer

(b) the eigenvalues of G_z are $m\hbar$ where m can have any of the (2n + 1) values n, (n - 1), ···, -n.

In general both spin and orbital motions contribute to the observed angular momentum.

The spin quantum numbers of the electron, proton and neutron all have values of one half. The total angular momentum of a nucleus is made up of contributions from individual nucleons, the actual value of I, the spin

quantum number of the nucleus as a whole depending on the way in which the spin and orbital angular momenta of the nucleons involved are coupled together. I can have values of 0, or $\frac{1}{2}$, or 1, or 3/2, ···. The total angular momentum of an electron is the resultant of a spin and an orbital contribution, the spin contribution being defined by the qunatum numbers S and m_S (or S_z) and the orbital contribution being defined by the quantum numbers ℓ and m_ℓ.

Any charged particle which has an angular momentum must also possess a magnetic dipole moment. For an electron, in general, both the orbital and spin angular momentum contribute to the magnetic moment, $\underline{\mu}$, which is given by

$$\underline{\mu} = \gamma \underline{G} \qquad 1.2$$

where γ, the magnetogyric ratio is defined by

$$\gamma = - \frac{g_e e}{2mc} \qquad 1.3$$

where e and m are respectively the charge and the mass of the electron, c is the velocity of light, and g_e is the electronic g factor. For a single electron with the spin and orbital angular momenta coupled together, the total angular momentum is:

$$\underline{G} = \sqrt{\underline{j}(\underline{j}+1)}\ \hbar \qquad 1.4$$

where $\underline{j} = \underline{l} + \underline{s}$, and the g factor is

$$g_j = 1 + \frac{j(j+1) + s(s+1) - l(l+1)}{2j(j+1)} \qquad 1.5$$

An unpaired electron situated in the valence shell of an atom or molecule in a solid or in a liquid, i.e. one which is in a chemically interesting situation, experiences strong electrostatic fields due to the presence of neighbouring atoms. Such fields uncouple the spin and orbital angular momenta, with the result that, so far as the spin is concerned, the orbital angular momentum is effectively zero. When the orbital angular momentum is "quenched" in this way, the g factor has the spin-only value of 2·00232; the slight difference from exactly two is a consequence of relativistic effects. That the g factors of single unpaired electrons in free radicals and transition metal ions deviate significantly from this spin-only value, is due to the reintroduction of some spin-orbit coupling, often because of the presence of low-lying excited states. In cases where the ground state spin eigenfunction has only a second order contribution from orbital paramagnetism, the electronic magnetic moment may be written as

$$\mu = - g_{eff}\sqrt{s(s+1)}\ e\hbar(2mc)^{-1} \qquad 1.6$$

where the orbital contribution is taken into the effective g factor and the magnetic moment is considered to arise from the spin alone. g_{eff} is a tensor quantity.

The magnetic moment of the nucleus may be written

$$\underline{\mu}_N = \gamma_N \underline{G}_N \qquad 1.7$$

where the nuclear magnetogyric ratio, γ_N, is defined by

$$\gamma = \frac{g_N e}{2Mc} \qquad 1.8$$

where e and M are respectively the charge and mass of the proton, c is the velocity of light, and g_N is the nuclear g factor, a constant characteristic of the nucleus in question. In magnetic resonance studies the orbital and spin angular momenta of the nucleus are not considered separately and their resultant is described by the particular value of g_N for the nucleus in question. It is conventional to describe the nuclear angular momentum by a nuclear spin quantum number I, so that

$$\underline{\mu}_N = \frac{g_N e}{2Mc} \hbar \underline{I} \qquad 1.9$$

$$\text{where } \underline{I}^2 = I(I+1)$$

2. Zeeman interaction

When a magnetic dipole interacts with an applied magnetic field, H, the magnetic contribution to the Hamiltoniam for the system may be written in the form

$$\mathcal{H} = - \underline{\mu}.\underline{H} \qquad 1.10$$

In the case of interaction between an unpaired electron and a steady magnetic field applied in the z-axis direction of a Cartesian frame of reference, this becomes

$$\begin{aligned} \mathcal{H} &= - (\mu_e)_z H \\ &= + (g_e)_z \beta_e H S_z \end{aligned} \qquad 1.11$$

where β_e, the electronic Bohr magneton, is a constant equal to $e\hbar(2mc)^{-1} = 0{\cdot}92732 \times 10^{-20}$ erg/gauss, and S_z is the spin operator defining the z-axis component of the electron's angular momentum. In what follows, whenever the g factor is unsubscripted, the implication is that it is that component of the g tensor along the direction defined by an applied steady magnetic field. Since $S = \frac{1}{2}$ for the electron, the value of S_z can be either $+\frac{1}{2}$ or $-\frac{1}{2}$, which correspond to alignment of the electronic magnetic moment roughly parallel and anti-parallel respectively, to the applied magnetic field. The eigenvalues of the Hamiltonian 1.11 are

$$E = g_e \beta_e H m_S$$

$$= \pm \tfrac{1}{2} g_e \beta_e H \qquad 1.12$$

with the lower state corresponding to the $m_S = -\frac{1}{2}$ eigenvalue of S_z.

Similarly, for a nuleus possessing a magnetic dipole moment, interaction with a steady magnetic field applied in the z-axis direction may be described by the Hamiltonian

$$\mathcal{H} = - \gamma_N \hbar \underline{H} . \underline{I}$$

$$= - \gamma_N \hbar H I_z \qquad 1.13$$

where I_z is the nuclear spin operator along the z-axis direction. The eigenvalues of this Hamiltonian are

$$E = - \gamma \hbar H m$$

where $m = I, I - 1, \cdots, - I$.

3. Hyperfine coupling

If an unpaired electron is surrounded by magnetic nuclei, as is often the case in chemically interesting systems, the magnetic dipoles of the electron and the nuclei may couple together. If such hyperfine coupling is present in a system of one unpaired electron and one magnetic nucleus in a steady magnetic field, the perturbation of the electronic Zeeman energy levels may be thought of as arising from the presence of an extra

magnetic field, whose magnitude and direction depends on the magnetic energy of the nucleus. When the applied magnetic field lies along the z-axis direction, the extra magnetic field due to the nucleus is considered to result approximately from the z-component of the nuclear magnetic moment reinforcing or diminishing the applied field according to the particular eigenvalue of I_z which describes the nuclear Zeeman level. The net result is to split the electronic Zeeman energy level into (2I + 1) equally spaced sublevels. At room temperature, the differences in population between these various sublevels are negligibly small.

In general, the Hamiltonian representing such an interaction between an unpaired electron and a magnetic nucleus may be written in the form

$$\mathcal{H}_{IS} = \sum_{\substack{\alpha,\alpha' \\ = x,y,z}} T_{\alpha\alpha'} S_{\alpha} I_{\alpha'} \qquad 1.14$$

The hyperfine coupling tensor T is always Hermitian. It is always possible to find a principal axis system such that this tensor is diagonal, and the hyperfine coupling is then written

$$\mathcal{H}_{IS} = T_{xx}S_xI_x + T_{yy}S_yI_y + T_{zz}S_zI_z \qquad 1.15$$

Very often the principal axis system of this hyperfine

tensor coincides with that of the g tensor, and consequently the analysis is considerably simplified. This coincidence is assumed in the present treatment.

It is convenient at this point to discuss the mechanism of hyperfine coupling between the unpaired electron and the magnetic nucleus. In general, there are two contributions to be considered: dipolar and contact coupling. The first of these is basically the classical interaction of two magnetic dipoles $\underline{\mu}_e$ and $\underline{\mu}_N$, separated by a distance $\underline{r}$, which may be represented by the Hamiltonian

$$\mathcal{H}_{dipolar} = \frac{g_e\beta_e g_N\beta_N}{\underline{r}^3}\left[\underline{I}.\underline{S} - \frac{3(\underline{I}.\underline{r})(\underline{S}.\underline{r})}{\underline{r}^2}\right] \quad 1.16$$

where $\underline{I}$ is the nuclear spin and $\underline{S}$ the electron spin. The anisotropy of this interaction is a consequence of the orientation dependence of the vector $\underline{r}$, and it may be shown that

$$\mathcal{H}_{dipolar} = g_e\beta_e g_N\beta_N \left\langle \frac{1 - 3\cos^2\varphi}{r^3} \right\rangle_{AV} \underline{I}.\underline{S} \quad 1.17$$

where φ is the angle between the axis of the dipoles and the line joining them. The orientation dependent term has been replaced by its spacial average over the whole orbital occupied by the unpaired electron. When the unpaired electron distribution is spherically symmetric

or when the orientation-dependent term has a spherically symmetric time-average, as is the case for example in solution due to the Brownian motion, then the dipolar contribution to the hyperfine coupling is zero. The dipolar contribution may thus be represented by a tensor of zero trace:

$$T_{dipolar} = \begin{vmatrix} t^{D}_{xx} & 0 & 0 \\ 0 & t^{D}_{yy} & 0 \\ 0 & 0 & t^{D}_{zz} \end{vmatrix}$$

in a principal axis system.

The second mechanism of hyperfine coupling is non-classical and it requires the presence at the magnetic nucleus of a finite unpaired electron spin density. This interaction is isotropic and it may be represented by the Hamiltonian

$$\mathcal{H}_{contact} = a h \underline{I}.\underline{S} \qquad 1.18$$

where $$a = -\frac{8\pi}{3} g_e \beta_e g_N \beta_N (2S)^{-1} |\psi(o)|^2$$

where $\psi(o)$ is the wavefunction of the unpaired electron evaluated at the position of the nucleus. In the cases discussed in this work, $S = \frac{1}{2}$, and so the Hamiltonian for the contact interaction involving several nuclei is written in these cases as

$$\mathcal{H}_{contact} = -\frac{8\pi}{3} g_e \beta_e g_N \beta_N \sum_i \delta(\underline{r}_i - \underline{r}) \underline{I}_i . \underline{S} \qquad 1.19$$

where $\underline{r}_i$ and $\underline{r}$ are the radius vectors of the i^{th} nucleus and of the unpaired electron respectively, and $\underline{I}_i$ is the nuclear spin operator for the i^{th} nucleus and $\delta(\underline{r}_i - \underline{r})$ is the Dirac delta function. The contact interaction is dependent on the amount of s-character of the orbital in an atom, or the σ- character of an orbital in a molecule, occupied by the unpaired electron. The sign of 'a', the isotropic hyperfine coupling constant, is dependent on the sign of g_N and also on the sign of the electronic spin density, $|\psi(o)|^2$. An unpaired electron in an orbital which has no s-character whatsoever, may give rise to a contact interaction by polarisation of electrons in inner orbitals.

4. The spin Hamiltonian

The spin Hamiltonian for an unpaired electron interacting with a system of magnetic nuclei in an applied magnetic field $\underline{H}$ lying along the z-axis direction, is thus

$$\mathcal{H} = \beta_e \underline{H} . \underline{g} . \underline{S} + \sum_i \underline{S}_i . \underline{T}_i . \underline{I}_i \qquad 1.20$$

where the label i refers to the i^{th} magnetic nucleus. The Zeeman interaction between the magnetic nuclei and the applied magnetic field is one or two orders of

magnitude less than the interaction between the electronic and nuclear spins, and it is ignored in this first-order treatment. The effect of nuclear quadrupolar interactions is also neglected at this stage. If the system being considered consists of a paramagnetic species with $S = \frac{1}{2}$ in solution, the Hamiltonian is

$$\mathcal{H} = g\beta_e \underline{S}.\underline{H} + \sum_i a_i \underline{S}.\underline{I}_i \qquad 1.21$$

and for high values of the magnetic field, of the magnitude normally used in electron paramagnetic resonance spectroscopy, the eigenvalues of this Hamiltonian are

$$E_{m_S,\, m_I} = g\beta_e m_S H + a m_I m_S \qquad 1.22$$

5. Electron paramagnetic resonance conditions

In a study of the transitions between a set of electronic Zeeman energy levels normally an alternating magnetic field is applied at right angles to the static field. The Hamiltonian for such a magnetic field may be written

$$\mathcal{H}'(t) = g_e\beta_e[H_x(t)S_x + H_y(t)S_y] \qquad 1.23$$

where $H_x(t)$ and $H_y(t)$ are the x and y components of the alternating field, $2H_1 \cos\omega t$ where ω is the angular frequency of this field. S_z can connect only those states with $\Delta m_S = 0$ whereas S_x and S_y can connect only those states with $\Delta m_S = \pm 1$. It is for this reason that the

alternating field is applied in the xy plane. Such a field can then induce transitions between adjacent energy levels, provided that the energy of this alternating field is equal to the energy separation between adjacent levels, i.e. provided

$$\Delta E = \hbar\omega = h\nu \qquad 1.24$$

If the system consists of one unpaired electron, then the electronic Zeeman energy level scheme is as shown below:

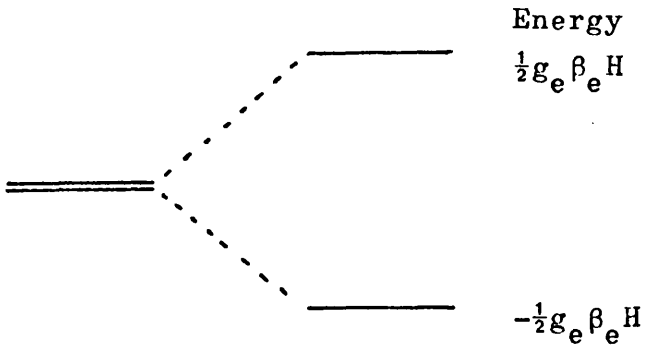

In this case $\Delta E = g_e\beta_e H$, and so

$$\omega = g_e\beta_e H(\hbar)^{-1} \qquad 1.25$$

An applied field of 3×10^3 gauss gives an electron paramagnetic resonance at frequencies about 9000 MHz., corresponding to a wavelength of about 3 cm.

6. Electron paramagnetic resonance in bulk matter

The application of electron paramagnetic resonance

spectroscopy to systems of chemical interest usually involves studies of bulk matter i.e. liquids and solids. An example of such a more realistic system, viz. an assembly of identical paramagnetic molecules of electron spin $S = \frac{1}{2}$ located in the solid or liquid state, will now be discussed. The material containing the unpaired electrons is called the "lattice", even when it is a liquid.

When this assembly of unpaired electrons is subjected to a steady magnetic field $\underline{H}$, applied along the z-axis direction, each unpaired electron has two possible energy levels, separated in energy by $g_e \beta_e H$. Hyperfine interactions are neglected in order to simplify the analysis. If this system is perturbed by applying radiation of the correct frequency, polarised to lie in a direction perpendicular to $\underline{H}$, then transitions between the two energy levels occur. The probability of a transition from the lower $| - \frac{1}{2} >$ level to the upper $| + \frac{1}{2} >$ level which results in absorption of radiant energy is equal to the probability of transition downwards by stimulated emission. Thus, only if the lower state is more densely populated than the upper one will a net absorption of energy from the perturbing field occur. At the microwave frequencies

employed in electron paramagnetic resonance spectroscopy, spontaneous emission of radiation may be neglected.

At thermal equilibrium, the populations of the two levels are related by the Boltzmann expression,

$$\frac{N_{-\frac{1}{2}}}{N_{+\frac{1}{2}}} = e^{\Delta E/kT} = e^{g_e\beta_e H/kT} \qquad 1.26$$

where $N_{-\frac{1}{2}}$ is the population of the $|-\frac{1}{2}>$ level, and $N_{+\frac{1}{2}}$ is the population of the $|+\frac{1}{2}>$ level. If Δn is the population difference between the lower and upper states, and if the total number of unpaired electrons is N, then it is easily shown that

$$\Delta n = \tfrac{1}{2}N\left[\exp\left(\frac{g_e\beta_e H}{kT}\right) - 1\right]$$

$$\text{so that} \quad \Delta n = Ng_e\beta_e H/2kT \qquad 1.27$$

provided $g_e\beta_e H(kT)^{-1}$ is small, i.e. provided $\Delta n/N$ is small. It is this quantity Δn which results in the absorption of microwave energy in electron paramagnetic resonance spectroscopy. From the discussion so far, it would appear that when the resonance condition is fulfilled, eventually Δn would fall to zero, and that when this occurred the absorption of microwave energy would cease. The fact that most electron paramagnetic resonance signals do not fade in intensity with time, means that there must be a mechanism, or mechanisms, whereby the unpaired electrons in the upper state are able

to get rid of their excess energy by processes which do not involve the emission of microwave radiation. That such processes do exist is implicit in the assumption that the populations of the two magnetic energy levels may be described by the Boltzmann distribution, since before the steady magnetic field was applied the number of electrons in the spin state $| + \frac{1}{2} >$ must have been equal to the number in the spin state $| - \frac{1}{2} >$, neglecting the effect of the earth's magnetic field.

Processes which bring about dissipation of energy are called relaxation processes. Before the discussion of relaxation processes, a second way of describing this phenomenon is discussed. The decrease in the value of Δn with absorption of microwave energy, may be described by saying that the spin temperature, T_S, rises as microwave energy is absorbed, while the temperature of the lattice remains unaltered. Interaction between the spin system and the lattice will provide a means of bringing the two systems into thermal equilibrium. Since the thermal capacity of the lattice is very much greater than that of the spin system, the equilibrium temperature is very close to the original lattice temperature. In the absence of spin-lattice interactions the spin temperature will continue to rise

until it reaches the value $T_S = \infty$ when the populations of the two states are equal.

A general relaxation process will now be discussed. The lattice is at thermal equilibrium, and the probabilities of spontaneous spin transitions up and down are different. Let the upward relaxation probability be W_{-+} and let the downward one be W_{+-}, with $W_{-+} \neq W_{+-}$. The rate of change of $N_{-\frac{1}{2}}$ is given by

$$\frac{dN_{-\frac{1}{2}}}{dt} = N_{+\frac{1}{2}} W_{+-} - N_{-\frac{1}{2}} W_{-+} \qquad 1.28$$

When thermal equilibrium has been established,

$$\frac{dN_{-\frac{1}{2}}}{dt} = 0$$

and if the equilibrium populations are $N^o_{-\frac{1}{2}}$ and $N^o_{+\frac{1}{2}}$, then

$$\frac{N^o_{+\frac{1}{2}}}{N^o_{-\frac{1}{2}}} = \frac{W_{-+}}{W_{+-}} \qquad 1.29$$

By the use of the Boltzmann expression, it may be shown that

$$\frac{W_{-+}}{W_{+-}} = \exp(-\Delta E/kT) \qquad 1.30$$

If $N_{+\frac{1}{2}}$ and $N_{-\frac{1}{2}}$ are expressed in terms of Δn and N, then

$$\frac{d\Delta n}{dt} = -\Delta n(W_{+-} + W_{-+}) + N(W_{+-} - W_{-+}) \qquad 1.31$$

Rearrangment yields

$$\frac{d\Delta n}{dt} = -\frac{(\Delta n - \Delta n_o)}{T_1} \qquad 1.32$$

where Δn_o is the population difference at thermal equilibrium and is equal to

$N(W_{+-} - W_{-+}) / (W_{+-} + W_{-+})$ and T_1 is equal to $(W_{+-} + W_{-+})^{-1}$. T_1 is called the spin-lattice relaxation time, and it has the dimensions of time. A large value of T_1 indicates slow relaxation, i.e. the system requires a long time to reach thermal equilibrium.

For a complete description of this system it is necessary to include the effects of induced transitions which arise in the presence of the microwave field. Quantum mechanics shows that the probabilities of upward and downward stimulated transitions are equal; let this probability be P. Then it is easily shown that

$$\frac{d\Delta n}{dt} = -2P\Delta n \qquad 1.33$$

for the induced transitions, and the rate of absorption of energy from the microwave field is

$$\frac{dE}{dt} = nP\Delta E \qquad 1.34$$

Combining the effects of the microwave field and the relaxation process, yields

$$\frac{d\Delta n}{dt} = -2P\Delta n - (\Delta n - \Delta n_o)T_1^{-1} \qquad 1.35$$

and at thermal equilibrium

$$\Delta n = \frac{\Delta n_o}{(1 + 2PT_1)} \qquad 1.36$$

so that the equilibrium rate of absorption of microwave energy is

$$\frac{dE}{dt} = nP\Delta E$$
$$= \Delta n_o \Delta E P (1 + 2PT_1)^{-1} \qquad 1.37$$

So long as $2PT_1 \ll 1$, the electron paramagnetic resonance absorption signal is not liable to fade to zero, or to use the spectroscopist's phrase, the signal is not liable to become saturated.

T_1 is also known as the longitudinal relaxation time.

As a result of relaxation the spin states have a finite lifetime, and consequently the resonance absorption line cannot be represented by a delta function. The line width due to spin-lattice relaxation is of the order of T_1^{-1}.

One of the conclusions which may be drawn from the preceeding discussion is that although spin-lattice relaxation decreases the lifetime of the spin states, it does not affect their relative energies. There are, however, other relaxation processes which vary the relative energies of the spin levels without affecting the lifetime of the spin states. The relaxation time for this process, T_2', is called the spin-spin relaxation time, or the transverse relaxation time. Spin-spin relaxation and spin-lattice relaxation are closely

related since any interaction which can decrease the lifetime of a spin state may also be capable of modulating the energy levels involved. It may be shown that the total line width T_2^{-1} consists of two parts; the first arises from spin-lattice relaxation and equals $(2T_1)^{-1}$, and the second results from spin-spin relaxation and is equal to $(T_2')^{-1}$.

In the case of spin-lattice relaxation, energy is transferred between different spin states i.e. states of different S_z value, whereas in spin-spin relaxation it is the S_x and S_y components of spin which are involved.

7. The Bloch equations and lineshapes

In order to discuss the line shapes of electron paramagnetic resonances in quantitative terms, it is convenient to employ the classical approach of Bloch. Consider the bulk magnetic moment $\underline{M}$ of a sample of electron spins at one particular temperature, and let there be $N_{-\frac{1}{2}}$ electrons in the state $| -\frac{1}{2} >$ and $N_{+\frac{1}{2}}$ in the state $| +\frac{1}{2} >$. If the z-component of the bulk magnetic moment is M_z, then

$$M_z = -g_e\beta_e(N_{-\frac{1}{2}} - N_{+\frac{1}{2}}) = -g_e\beta_e\Delta n \qquad 1.38$$

and spin-lattice relaxation effects bring about an exporential decay to equilibrium

$$\frac{d\Delta n}{dt} = -\frac{\Delta n}{T_1} \qquad 1\cdot39$$

i.e. since M_z is directly proportional to Δn

$$\frac{dM_z}{dt} = -\frac{M_z}{T_1} \qquad 1.40$$

In the absence of an applied magnetic field there is no distinction between the x, y and z axis directions so that M_x and M_y, the x and y components of magnetisation, obey the same decay equation as M_z.

If a steady magnetic field is now applied along the z-axis, M_z will decay not to zero, as before, but to a steady value M_o which is given by

$$M_o = -g_e\beta_e\Delta n_o = \chi_o H_o \qquad 1.41$$

where $\chi_o = N(g_e\beta_e)^2 S(S+1)(3kT)^{-1}$

χ_o is the static magnetic susceptibility of the total number of spins, and Δn_o is the equilibrium value of the population difference between the two spin levels.
The decay equation for M_z is now

$$\frac{dM_z}{dt} = -\frac{M_z - M_o}{T_1} \qquad 1.42$$

where M_o is the equilibrium value of M_z, while those for M_x and M_y are

$$\frac{dM_x}{dt} = -\frac{M_x}{T_2'}$$

and

$$\frac{dM_y}{dt} = -\frac{M_y}{T_2'} \qquad 1.43$$

where T_2' is the transverse relaxation time for these two components of the magnetic moment $\underline{M}$. Now it is found that the motion of the bulk magnetisation in an applied magnetic field follows that laws of classical mechanics

i.e. $$\frac{d\underline{M}}{dt} = -g_e\beta_e(\hbar)^{-1}(\underline{M} \times \underline{H}) \qquad 1.44$$

If relaxation is ignored, then the rates of change of the components of $\underline{M}$ are given by

$$\begin{aligned} \frac{dM_x}{dt} &= \omega_o M_y \\ \frac{dM_y}{dt} &= -\omega_o M_x \qquad 1.45 \\ \frac{dM_z}{dt} &= 0 \end{aligned}$$

ω_o is the electronic resonance frequency

$$\omega_o = -g_e\beta_e H(\hbar)^{-1}$$

One solution of these equations is

$$\underline{M} \equiv (M_x, M_y, M_z) = (M_{\underline{1}}\cos\omega_o t, -M_{\underline{1}}\sin\omega_o t, M_{11}) \qquad 1.46$$

This represents a vector moving in an anticlockwise direction around the surface of a cone with uniform angular velocity ω_o. The magnitude of the component of $\underline{M}$ parallel

to the field direction is M_{11} (the longitudinal component), and that perpendicular to this direction is $M_{\underline{1}}$ (the transverse component). In the case of no relaxation these remain constant, i.e. if relaxation is neglected, $\underline{M}$ precesses about $\underline{H}$ with an angular frequency of ω_o. This angular frequency, ω_o, is called the Larmor frequency, and the precessional motion is known as the Larmor precession.

It is the sign of the magnetogyric ratio which determines the direction of precession; for electrons

$$\gamma = - \frac{g_e \beta_e}{\hbar} \qquad 1.47$$

i.e. γ is negative, and the electronic spins precess anticlockwise about the magnetic field direction.

It is now necessary to include the effects of relaxation at this point. From equations 1.42, 1.43 and 1.44, we arrive at the well-known Bloch equations

$$\begin{aligned} \frac{dM_x}{dt} &= \omega_o M_y - \frac{M_x}{T_2'} \\ \frac{dM_y}{dt} &= - \omega_o M_x - \frac{M_y}{T_2'} \\ \frac{dM_z}{dt} &= - \frac{M_z - M_o}{T_1} \end{aligned} \qquad 1.48$$

These equations describe a damped precession of the spins,

with the rotating transverse components of $\underline{M}$ decaying to zero with characteristic time T_2', and the longitudinal component M_z decaying towards its equilibrium value M_o with a decay time T_1.

From this macroscopic description of the resonance phenomenon in bulk matter, it is possible to go further and predict a definite line shape for the resonance.

Consider an assembly of electron spins in a steady magnetic field $\underline{H}$; a circularly polarised microwave field $\underline{H}_1$ is then applied in the xy plane rotating anticlockwise, in the same sense as the precession of the spins, with a uniform angular velocity ω which need not be equal to the resonance frequency ω_o. The Bloch equations give

$$\frac{d\underline{M}}{dt} = \gamma_e(\underline{M} \times \underline{H}) + \gamma_e(\underline{M} \times \underline{H}_1) - \frac{(\underline{i}M_x + \underline{j}M_y)}{T_2'} - \frac{\underline{k}(M_z - M_o)}{T_1} \qquad 1.49$$

where γ_e is the magnetogyric ratio of the electron, and $\underline{i}$, $\underline{j}$, $\underline{k}$ are unit vectors along the x, y and z axes, and

$$\underline{H}_1 = H_1(\underline{i}\cos\omega t - \underline{j}\sin\omega t) \qquad 1.50$$

A transformation to a new coordinate system which rotates with $\underline{H}_1$, at an angular velocity ω about the z axis, is now carried out. In this new coordinate system the axes

are x', y', z', and the z'-axis is parallel to the steady field $\underline{H}$, while the x'-axis lies in the direction of $\underline{H}_1$.

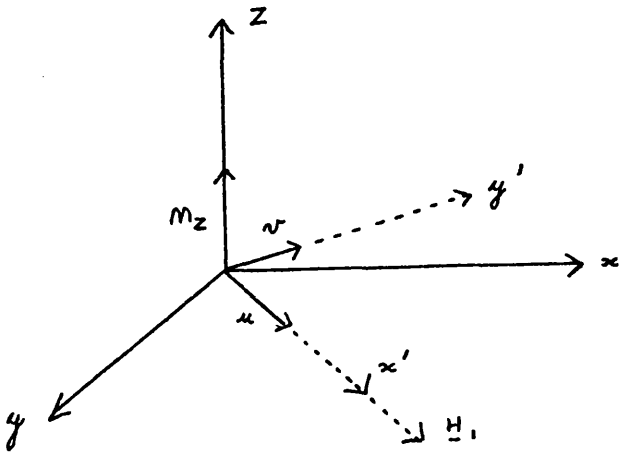

Figure 1

The coordinate system.

The transverse components of the magnetic moment along the x' and y' directions are denoted by u and v. In the new system of axes, the vectors $\underline{M}$, $\underline{H}_1$ and $\underline{\omega}$ become

$$\begin{aligned} \underline{M}' &= \underline{i}'u + \underline{j}'v + \underline{k}'M_z \\ \underline{H}_1' &= \underline{i}'H_1 \\ \underline{\omega}' &= 0 \end{aligned} \qquad 1.51$$

An observer in the rotating coordinate system would see the unit vectors $\underline{i}'$, $\underline{j}'$ and $\underline{k}'$ as fixed and the rate of change of $\underline{M}'$ would appear to be

$$\frac{\delta \underline{M}'}{\delta t} = \underline{i}' \frac{du}{dt} + \underline{j}' \frac{dv}{dt} + \underline{k}' \frac{dM_z}{dt} \qquad 1.52$$

On the other hand, an observer in the fixed frame of reference would see a set of unit vectors rotating with angular velocity $\underline{\omega}$. The rate of change of $\underline{i}'$ would be

$$\frac{d\underline{i}'}{dt} = \underline{\omega} \times \underline{i}' \qquad 1.53$$

and the rate of change of $\underline{M}'$ would be

$$\frac{d\underline{M}}{dt} = \underline{i}' \frac{du}{dt} + \underline{j}' \frac{dv}{dt} + \underline{k}' \frac{dM_z}{dt}$$

$$+ u \frac{d\underline{i}'}{dt} + v \frac{d\underline{j}'}{dt} + M_z \frac{d\underline{k}'}{dt}$$

$$= \frac{\delta \underline{M}'}{\delta t} + \underline{\omega} \times \underline{M}' \qquad 1.54$$

If, at time $t = 0$, the axes xyz and $x'y'z'$ coincide, then by substituting the last equation into equation 1.49, the Bloch equations in the rotating frame are obtained

$$\frac{\delta \underline{M}'}{\delta t} = \gamma_e \underline{M}' \times \left(\underline{H}' + \frac{\underline{\omega}}{\gamma_e}\right) + \gamma_e (\underline{M}' \times \underline{H}_1')$$

$$- \frac{(\underline{i}'u + \underline{j}'v)}{T_2'} - \frac{\underline{k}'(M_z - M_o)}{T_1} \qquad 1.55$$

Separation into components along x', y' and z' gives

$$\frac{du}{dt} = (\omega_o - \omega)v - \frac{u}{T_2'}$$

$$\frac{dv}{dt} = -(\omega_o - \omega)u + \gamma_e H_1 M_z - \frac{v}{T_2'}$$

$$\frac{dM_z}{dt} = -\gamma_e H_1 v - \frac{(M_z - M_o)}{T_1} \qquad 1.56$$

If the microwave field has been applied for a sufficiently long time, then a steady state is reached and the stationary solution for the Bloch equations just given is

$$u = M_o \frac{\gamma_e H_1 (T_2')^2 (\omega_o - \omega)}{1 + (T_2')^2(\omega_o - \omega)^2 + \gamma_e{}^2 H_1{}^2 T_1 T_2'}$$

$$v = M_o \frac{\gamma_e H_1 T_2'}{1 + (T_2')^2(\omega_o - \omega)^2 + \gamma_e{}^2 H_1{}^2 T_1 T_2'}$$

$$M_z = M_o \frac{1 + (T_2')^2(\omega_o - \omega)^2}{1 + (T_2')^2(\omega_o - \omega)^2 + \gamma_e{}^2 H_1{}^2 T_1 T_2'}, \qquad 1.57$$

Although the above discussion has involved a perturbing field $\underline{H}_1$ which is a rotating field, in experimental electron paramagnetic resonance spectroscopy the perturbing field is an oscillating linearly polarised field. A linearly polarised field of strength $2H_1 \cos\omega t$ in the x-direction can, however, be treated as the sum of two counter-rotating fields of magnitude H_1 with Cartesian components $(H_1 \cos\omega t, -H_1 \sin\omega t, 0)$ and $(H_1 \cos\omega t, H_1 \sin\omega t, 0)$. Only the field which rotates in

an anticlockwise sense can be in resonance with the electron spins, the other rotating field having very little effect. It is a very good approximation to regard the single field rotating in an anticlockwise sense as equivalent to an oscillating field of maximum amplitude $2H_1$.

The transverse component of $\underline{M}$ along the x-axis, u, oscillates in phase with H_1, and v is 90° out of phase. In the fixed system of axes

$$H_{1x} = 2H_1 \cos\omega t$$

$$M_x = u\cos\omega t + v\sin\omega t \qquad 1.58$$

The rotating xy components of the oscillating field, $\underline{H}_1$, and of the magnetic moment, $\underline{M}$, may be written as complex numbers

$$H_1 = 2H_1 \exp(-i\omega t)$$

$$M_{xy} = 2H_1\chi(\omega) \exp(-i\omega t) \qquad 1.59$$

where $\chi(\omega)$, the complex magnetic susceptibility, is

$$\chi(\omega) = \chi'(\omega) + i\chi''(\omega) \qquad 1.60$$

Thus,

$$M_x = H_1[\chi(\omega)e^{-i\omega t} + \chi^*(\omega)e^{i\omega t}]$$

$$= 2H_1\chi'(\omega)\cos\omega t + 2H_1\chi''(\omega)\sin\omega t \qquad 1.61$$

It is obvious that u and v are proportional to $\chi'(\omega)$ and

$\chi''(\omega)$ respectively. From equations 1.57, 1.58 and 1.59

$$\chi'(\omega) = \tfrac{1}{2}\chi_o\omega_o \frac{T_2'^2(\omega_o - \omega)}{1 + T_2'^2(\omega_o - \omega)^2 + \gamma_e^2 H_1^2 T_1 T_2'} \qquad 1.62$$

$$\chi''(\omega) = \tfrac{1}{2}\chi_o\omega_o \frac{T_2'}{1 + T_2'^2(\omega_o - \omega)^2 + \gamma_e^2 H_1^2 T_1 T_2'}$$

Note that $\chi_o H_o = M_o$.

If now the frequency of $\underline{H}_1$ is gradually changed, so that the resonance condition is passed through, then $\chi'(\omega)$ changes sign with the result that $\underline{M}$ is 180° out of phase with the microwave field at the high frequencies. $\chi''(\omega)$ shows a very large increase near resonance, and since the spin system absorbs energy from the rotating field at a rate

$$\frac{dE}{dt} = 2\omega\chi'' H_1^2 \qquad 1.63$$

it is this power absorption which is used to follow the resonance. The result of the rotating field $\underline{H}_1$ acting on the magnetic moments of the spins is to produce a torque with a component, vH_1 in magnitude, about the z-axis. This component does work on the precessing spins, and the rate of work is $\omega v H_1$. The average power absorption is

$$\frac{dE}{dt} = 2\omega H_1^2 \chi''(\omega)$$

$$= H_1^2 \chi_o \omega \omega_o \frac{T_2'}{1 + (T_2')^2(\omega_o - \omega)^2 + \gamma_e^2 H_1^2 T_1 T_2'} \qquad 1.64$$

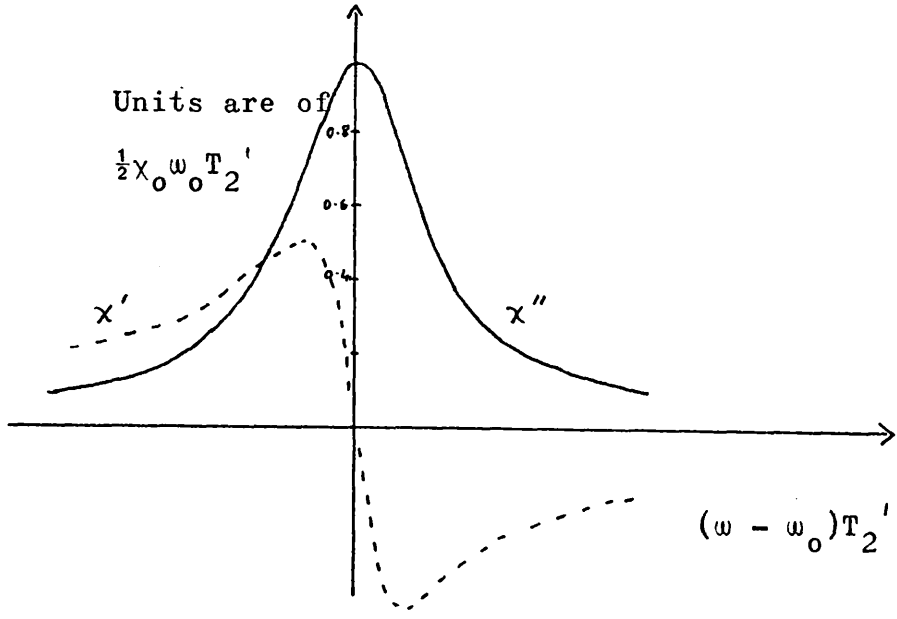

Figure 2

Absorption and dispersion line shapes derived from the Bloch equations.

Provided the microwave power is not great enough to cause saturation, i.e. provided that $\gamma_e^2 H_1^2 T_1 T_2'$ is small, the absorption line is Lorentzian in shape, i.e. of the form

$$g(\omega) = \frac{T_2'}{\pi} \frac{1}{1 + (T_2')^2(\omega - \omega_o)^2} \qquad 1.65$$

If the microwave field is strong, however, the equation describing energy absorption becomes

$$\frac{dE}{dt} = n_o \Delta E \frac{P(\omega)}{1 + 2P(\omega)T_1} \qquad 1.66$$

where $P(\omega) = (\frac{1}{2})\pi\gamma_e{}^2 H_1{}^2 g(\omega)$. This expression gives the transition probability. The effect of saturation is to reduce the intensity of the central part of the resonance line relative to the wings, thereby producing apparent broadening of the spectrum, which may be so strong as to reduce the signal intensity to zero in extreme cases.

The precession of the spins in phase is weakly damped in many systems, and for some time after the field H_1 is removed its effects may still be observed. The coherence of phase of the individual electronic magnetic moments soon disappears and the phases become randomly distributed. The oscillations of $\underline{M}$ die away. This residual effect forms the basis of a number of methods of measuring relaxation times.

To return to the description of the resonance line-shape, the maximum of the Lorentzian function 1.65 occurs at $\omega = \omega_o$ and the width of the absorption line between points where its height is half the maximum is $2(T_2')^{-1}$. It is, however, only in situations where electron spin

exchange interactions are important that the Lorentzian function may be used to describe the resonance lineshape of paramagnetic molecules in bulk matter. Usually it is magnetic dipolar interactions which define the broadening of the resonance lineshape, and if the distribution of magnetic dipoles is random with respect to the electron undergoing resonance, then the resultant lineshape is Gaussian, i.e. of the form

$$g(\omega) = \frac{T_2'}{\sqrt{2\pi}} \exp[-\tfrac{1}{2}(T_2')^2(\omega - \omega_o)^2] \qquad 1.67$$

Because of computational difficulties in dealing with the shape of a line broadened by magnetic dipolar interactions, the resonant lineshape is often assumed to be Gaussian. In electron paramagnetic resonance spectroscopy it is usually the first derivative of the absorption lineshape which is recorded. The distance from the maximum to the minimum value of the derivative curve is $2(T_2')^{-1}$ for a Gaussian curve and $2[T_2'\sqrt{3}]^{-1}$ for a Lorentzian one.

The lineshape functions just discussed apply only to the unsaturated line; if the microwave field is strong enough to cause saturation of the resonance line, saturation broadening effects become important and equation 1.66 must be used to describe the lineshape.

8. Effects of motions on electron paramagnetic resonance spectra

If the molecules of the paramagnetic species being studied undergo motion, then some of the properties of the spin Hamiltonian may be modified.

Consider the symmetric tensor T which is referred to axes x, y, z in space. Let this tensor describe a suitable property of the molecule, so that its components are constant in an axis system α, β, γ attached to the molecule as it rotates rapidly in solution. While the components $T_{\alpha\alpha}$, $T_{\alpha\beta}$, etc., in the molecular axis are constant, the values of the components referred to the space-fixed axes, T_{xx}, T_{xy}, etc., fluctuate randomly. If T is the hyperfine coupling tensor, then it may be shown that the effect of rapid random motions in solution, is to average out the dipolar contribution while leaving the Fermi contact contribution unchanged.

The dipole-dipole interaction between two magnetic moments $\underline{\mu}_1$ and $\underline{\mu}_2$ which are connected in space by the vector distance $\underline{r}$, may be written

$$V = \frac{\underline{\mu}_1 \cdot \underline{\mu}_2}{r^3} - \frac{3(\underline{\mu}_1 \cdot \underline{r})(\underline{\mu}_2 \cdot \underline{r})}{r^5} \qquad 1.68$$

Now, using a spherical polar coordinate system,

$$V = \frac{\underline{\mu}_1 \cdot \underline{\mu}_2}{r^3} - \frac{3}{r^5}[\mu_{1z} r\cos\theta + r\sin\theta(\mu_{1x}\cos\varphi + \mu_{1y}\sin\varphi)]$$
$$[\mu_{2z} r\cos\theta + r\sin\theta(\mu_{2x}\cos\varphi + \mu_{2y}\sin\varphi)] \qquad 1.69$$

The normal transformation between Cartesian and polar coordinate systems has been used, viz.,

$$x = r\sin\theta\cos\varphi, \qquad y = r\sin\theta\sin\varphi$$
$$z = r\cos\theta$$

If rotation of the molecule in solution is random, the direction of $\underline{r}$ varies randomly, so that the average over many rotations involves all solid angles, $d\Omega$, with equal probability:

$$d\Omega = \sin\theta d\theta d\varphi$$

Now,

$$\langle \cos\theta\sin\theta\cos\varphi \rangle = \frac{1}{4\pi} \int_0^{2\pi} \cos\varphi d\varphi \int_0^{\pi} \cos\theta\sin^2\theta d\theta$$
$$= 0$$

and

$$\langle \cos\theta\sin\theta\sin\varphi \rangle = \langle \sin^2\theta\cos\varphi\sin\varphi \rangle$$
$$= 0$$

but

$$\langle \sin^2\theta\cos^2\varphi \rangle = \langle \sin^2\theta\sin^2\varphi \rangle$$
$$= \langle \cos^2\theta \rangle$$
$$= \tfrac{1}{3}$$

Thus

$$\langle V \rangle = \frac{1}{r^3}[\underline{\mu}_1 \cdot \underline{\mu}_2 - 3(\tfrac{1}{3}\mu_{1z}\mu_{2z} + \tfrac{1}{3}\mu_{1x}\mu_{2x} + \tfrac{1}{3}\mu_{1y}\mu_{2y})]$$
$$= 0 \qquad 1.70$$

The effect of motion on a free radical in solution is to remove the dipolar contribution to the hyperfine coupling tensor.

The second important effect of motion on electron paramagnetic resonance spectra concerns relaxation processes. Since both longitudinal and transverse relaxation processes involve the effects of time-dependent magnetic and/or electric fields on the unpaired electron, any motion which gives rise to such fields may be capable of effecting relaxation of the spin system. Two conditions must be fulfilled for relaxation to occur:

i. there must be present an interaction which couples with the spin system,

ii. this interaction must have a time-dependent Fourier component at the resonance frequency or at twice this frequency.

In solids an important source of relaxation is the vibrational motions of the lattice. In liquids the main relaxation mechanisms involve rotational and diffusional motions. Intramolecular motions

and chemical exchange may also be important in some cases. As the main area of interest in relaxation in this thesis is concerned with the liquid state, a more detailed consideration of relaxation in solution is now given.

For a radical or ion with electron spin quantum number $S = \frac{1}{2}$ in solution, two intramolecular sources of relaxation are important. As the paramagnetic species tumbles about in solution, time-dependent interactions arise from anisotropy in the g tensor and from anisotropy in the dipolar hyperfine coupling to magnetic nuclei. Neither of these interactions is strong and the spectral lines are usually sharp. A further source of relaxation in solution, lies in the possibility that the rotational motion of the paramagnetic molecule may generate a time-dependent magnetic dipole moment. If the solutions being studied are sufficiently dilute, the interactions between unpaired electrons may be neglected. It is normal to remove electron-electron interactions by diluting the solution to be studied until there is no further decrease in spectral line width.

A more quantitative description of some aspects of solution relaxation will now be presented.

9 Correlation

Consider a force f(t) which varies randomly with time

about a mean value of zero. Its strength may be measured through the mean square average $\overline{f^*(t)f(t)}$. If a sample of this force is considered in a time interval from $-T$ to $+T$, its Fourier transform is

$$f_T(\omega) = \int_{-T}^{T} f(t)e^{i\omega t}\, dt \qquad 1.71$$

Now $f_T(\omega)$ is also a random function with average value zero, but its modulus squared $| f_T(\omega) |^2$ has a non-zero average value. A function $J(\omega)$ may be defined in such a way as to represent the power or "spectral density" at angular frequency ω

$$J(\omega) = \lim_{T \to \infty} \frac{1}{2T} \overline{f_T^*(\omega)f_T(\omega)} \qquad 1.72$$

and this function tends to a definite limit.

It may be shown, by making use of the Wiener-Khintchin theorem, that the power spectrum is related to the autocorrelation function of $f(t)$, which is defined by

$$G(\tau) = \overline{f^*(t + \tau)f(t)} \qquad 1.73$$

and which is a measure of the persistence of the fluctuations. If, for example, $f(t)$ is some quantity arising from the Brownian motion of molecules in a liquid, then for short times $G(\tau)$ is large; and as τ increases, $G(\tau)$ falls to zero. The autocorrelation

function often has the form

$$G(\tau) = \overline{f^*(t)f(t)} \exp(-|\tau|/\tau_c) \qquad 1.74$$

which represents a quantity decreasing exponentially with a decay time τ_c, the correlation time, which represents the time for a normal fluctuation to decrease to zero. It may be shown that

$$J(\omega) = \int_{-\infty}^{\infty} G(\tau) \exp(i\omega\tau)\, d\tau \qquad 1.75$$

i.e. the power spectrum of f(t) is the Fourier transform of the autocorrelation function.[1]

The interaction between two magnetic dipoles in solution varies with time, and if this interaction is considered in two parts, one time-independent, the other time-dependent, then this latter part amounts to a random perturbation arising from local fields which may, in the case of systems where the spin quantum number is $\frac{1}{2}$, be represented by the 2 x 2 matrix,

$$V(t) = \begin{vmatrix} v_{\alpha\alpha}(t) & v_{\alpha\beta}(t) \\ v_{\beta\alpha}(t) & v_{\beta\beta}(t) \end{vmatrix} \qquad 1.76$$

where α and β refer to the spin states $|+\frac{1}{2}>$ and $|-\frac{1}{2}>$ respectively. T_1 and T_2' may be expressed in terms of the autocorrelation functions of the matrix

elements of the perturbation $\bar{V}(t)$. It may be shown that T_1 depends on the power spectrum of $v_{\alpha\beta}(t)$ at the resonance frequency ω_o, or at twice this frequency, whereas T_2' is also dependent on fluctuations in the relative energies of the spin states which occur with frequencies close to zero.[2]

If the fluctuations causing relaxation are the local magnetic fields $\underline{H}(t)$ generated by the random motions of the molecules in solution, and if the auto-correlation function for this motion is given by

$$G(\tau) = \overline{f^*(t)f(t)} \exp(-|\tau|/\tau_c) \qquad 1.77$$

then

$$(T_1)^{-1} = 2\hbar^{-2}\,\overline{|v_{\alpha\beta}|^2} \cdot 2\tau_c (1 + \omega_o^2\tau_c^2)^{-1} \qquad 1.78$$

and

$$(T_2')^{-1} = \tfrac{1}{2}\hbar^{-2}\,\overline{|v_{\alpha\alpha} - v_{\beta\beta}|^2} \cdot 2\tau_c + (2T_1)^{-1} \qquad 1.79$$

Now the matrix elements of V in the field $\underline{H}$ are

$$v_{\alpha\beta} = \pm \tfrac{1}{2} g_j \beta_j (H_x - iH_y) \qquad 1.80$$

$$v_{\alpha\alpha} - v_{\beta\beta} = \pm g_j \beta_j H_z \qquad 1.81$$

where H_x, H_y and H_z are respectively the x, y and z components of the magnetic field $\underline{H}$, and g_j and β_j are respectively the g factor and the value of the magneton (electronic or nuclear) of the magnetic species giving rise to the fluctuating field. The relaxation times

may thus be shown to be

$$(T_1)^{-1} = \tfrac{1}{2}(g_j\beta_j)^2\hbar^{-2}\overline{(H_x^2 + H_y^2)}2\tau_c(1 + \omega_o^2\tau_c^2)^{-1} \qquad 1.82$$

and

$$(T_2')^{-1} = \tfrac{1}{2}(g_j\beta_j)^2\hbar^{-2}\{2\tau_c\overline{H_z^2} + \tfrac{1}{2}\overline{(H_x^2 + H_y^2)}2\tau_c(1 + \omega_o^2\tau_c^2)^{-1}\} \qquad 1.83$$

If the Brownian motion is isotropic, then the mean square averages of H_x, H_y and H_z are equal and the ratio of T_1 to T_2' is determined by the relative strengths of the fluctuations at angular frequencies $\omega = \omega_o$ and $\omega = 0$. For long correlation times, $(1 + \omega_o^2\tau_c^2)$ is large and $T_1 < T_2'$, but for very rapid Brownian motion, $\omega_o\tau_c$ is small and T_1 and T_2' are almost equal.

10. Brownian motion

Debye[3] developed a theory of random tumbling in solution and this will be sketched roughly to define the main points. The unpaired electron is assumed to be fixed at the centre of a sphere, of radius r, while a magnetic species, for example, a magnetic nucleus or an unpaired electron tumbles randomly around the surface of this sphere. Let this moving species begin at point A, and arrive some time later at point B with polar coordinates (θ, φ). The quantity of interest is

the probability, $p(\theta, \varphi; t)$, that a molecule reaches the point B at a time t after beginning from point A at time $t = 0$. Ω is assumed to be the mean angular velocity of rotation, and α, assumed small, is the "mean free path" i.e. the mean angle through which the molecule turns between collisions. Thus $\Omega t\alpha^{-1}$ collisions occur in time t and the mean square angle turned through between collisions is $2\alpha^2$. It can be shown that the mean square displacement is

$$\overline{\theta^2} = 2\alpha\Omega t = 4D't \qquad 1.84$$

where D' is the spherical diffusion coefficient. Debye showed that the probability $p(\theta, \varphi; t)$ is described by the differential equation for diffusion on the surface of a sphere

$$\frac{1}{D'}\frac{\partial p}{\partial t} = \nabla^2 p = \frac{1}{\sin\theta}\frac{\partial}{\partial\theta}\left(\sin\theta\frac{\partial p}{\partial\theta}\right) + \frac{1}{\sin^2\theta}\frac{\partial^2 p}{\partial\varphi^2} \qquad 1.85$$

The general solution of this equation may be shown to be an expansion in a series of normalised spherical harmonies $Y_{\ell m}(\theta, \varphi)$

$$p = \sum_{\ell,m} C_{\ell m} Y_{\ell m}(\theta, \varphi) \exp\left(-D'\ell(\ell+1)t\right) \qquad 1.86$$

The coefficients C_{lm} may be obtained for any set of initial conditions through the use of the expansion theorem for spherical harmonics. It may be shown that for random Brownian motions, the average value of any angular function $F(\theta, \varphi)$ which may be expressed as a spherical harmonic of order l, will decay exponentially to zero.[4]

If

$$\overline{F(t)} = \int_0^{\pi} \int_0^{2\pi} F(\theta, \varphi) p(\theta, \varphi; t) \sin\theta d\theta d\varphi$$

then

$$\overline{F(t)} = \overline{F(0)} \exp(-D' l(l+1)t) \qquad 1.87$$

In the magnetic resonance experiment, the spherical harmonics are of the second order i.e. $l = 2$, since we are dealing with tensors, and relaxation involves a characteristic rotational correlation time, τ_c. For a local perturbing field from a bar magnet of moment $g\beta I$, quantised in a steady field H_o, the local field has a component

$$H_z = \pm g\beta r^{-3}[\tfrac{1}{2}(3\cos^2\theta - 1)] \qquad 1.88$$

parallel to H_o and a component

$$H_{\perp} = g\beta r^{-3}[(3/2)\sin\theta\cos\theta] \qquad 1.89$$

perpendicular to H_o, where θ is the angle between the electron - bar magnet vector and the applied field direction. It is then easily shown that

$$\overline{\tfrac{1}{2}[3\cos^2\theta(t) - 1]} = \exp(-6D't) = \exp(-t/\tau_c) \qquad 1.90$$

An approximate value of τ_c may be obtained by considering the molecule containing the unpaired electron as a sphere of radius a in a fluid of viscosity η. The torque exerted by the viscosity on the rotating sphere is given by $8\pi\eta a^3 \left(\frac{d\theta}{dt}\right)$ and the following relation has been deduced

$$D' = kT(8\pi\eta a^3)^{-1}$$

or

$$\tau_c = 4\pi\eta a^3(3kT)^{-1} \qquad 1.91$$

This theoretical approach to motion in solution is obviously an oversimplification and it must not be relied on to produce quantitatively reliable results under all circumstances.

It has been found that equation 1.91 is approximately valid when the polar solute molecule is at least three times as large as the surrounding non-polar solvent molecules.[5-7]

11. The Decca X3 electron paramagnetic resonance spectrometer

All of the electron paramagnetic resonance spectra discussed in this study were recorded on a Decca X3

spectrometer, operating in the X-band region at a frequency of 9270 MHz., and using a standard H_{102} cavity. The magnet used was a Newport Instruments 11" electromagnet, and the magnetic field was calibrated by standard proton magnetic resonance techniques. A block diagram of the spectrometer is given in Figure 3.

The magnetic field calibration system was checked with a reference g-marker which consisted of a finely powdered sample of diphenylpicrylhydrazyl whose g-factor is known accurately.

Spectra of single crystals were obtained with the crystal mounted on the end of a spectrosil rod by means of "Araldite" cement. The crystal was oriented optically, observations being carried out with a travelling microscope. A marker on the top of the spectrosil rod was used in conjunction with a circular scale marked in degrees at the top of the cavity to measure the orientation about the axis of mounting.

The measurement of electron paramagnetic resonance spectra over a range of temperature was carried out by means of a flow system. For cooling, a stream of gaseous nitrogen was passed through a coil immersed in a Dewar of liquid nitrogen and then passed over the sample; for

heating, the gaseous nitrogen was passed over an electrically heated coil before reaching the sample. Temperature was measured with a copper-constantan thermocouple.

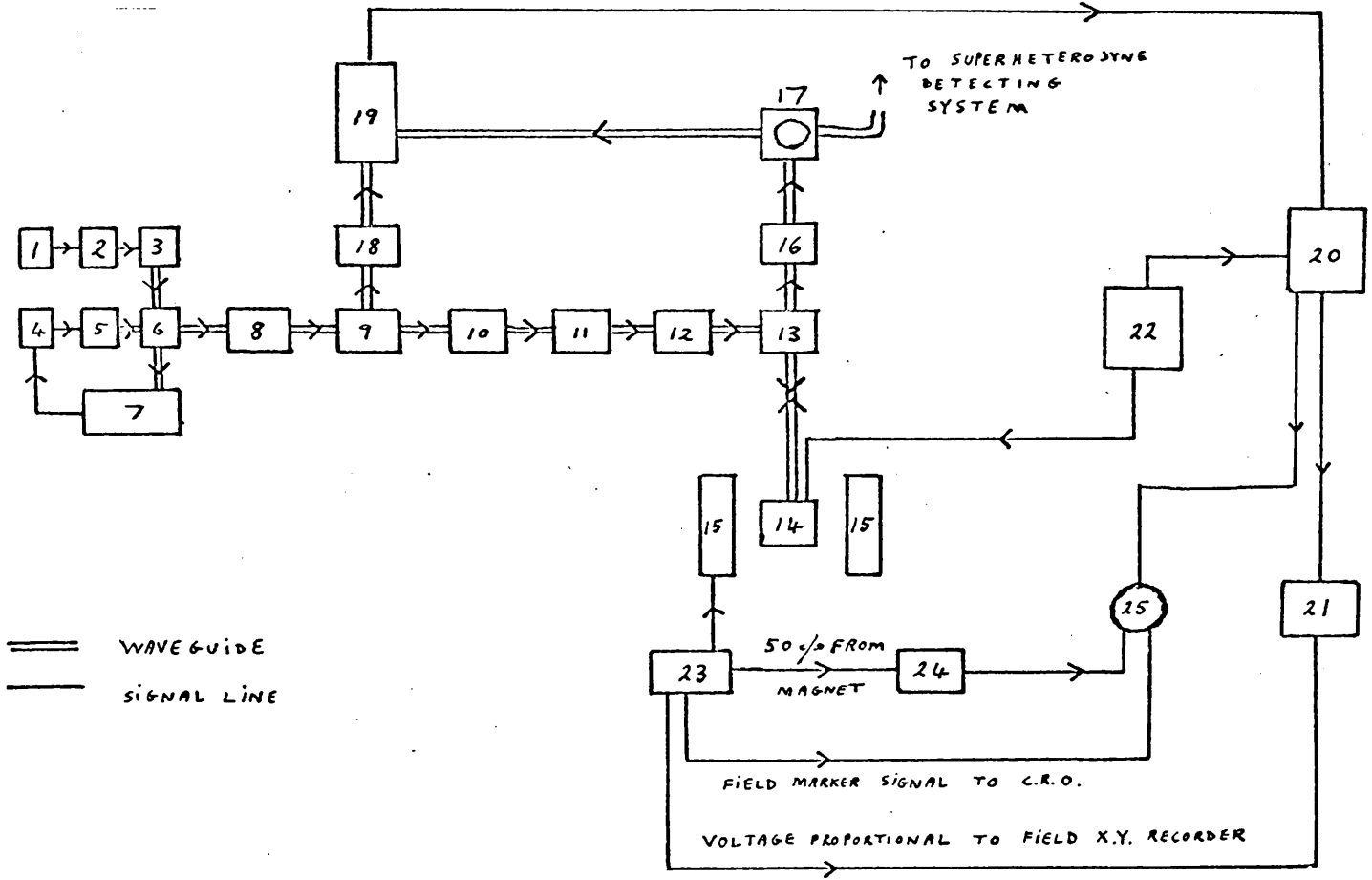

FIG 3 BLOCK DIAGRAM DECCA - NEWPORT E. P. R. SPECTROMETER

The Decca X3 Spectrometer System.

Key to Diagram.

1. 30 Mc/s Crystal controlled Oscillator
2. 30-300 Mc/s Multiplier
3. Harmonic Generator (9300 Mc/s)
4. Phase sensitive Detector
5. Signal Klystron
6. Crossguide Coupler
7. 30 Mc/s Phase Lock amplifier, and mixer.
8. Isolator
9. Coupler
10. Phase Shifter
11. Switched Attenuator
12. Variable Attenuator
13. 6dB. coupler (high directivity)
14. Sample cavity
15. Poles of electromagnet
16. Isolator
17. Waveguide switch
18. Shutter Switch
19. 100 Kc/s Pre-amplifier, and balanced mixer
20. 100 Kc/s Amplifier, and Phase sensitive Detector
21. Recorder X.Y.

22. 100 Kc/s Oscillator, and Phase Shifter

23. Magnet control and Power supply

24. Phase shifter

25. C. R. Oscilloscope

References to Part I

The treatment of the theory of electron paramagnetic resonance spectroscopy given to Part I of this thesis has been based on the following sources:

A C.P. Slichter, "Principles of Magnetic Resonance," Harper and Row, New York, 1963.

B A. Carrington, A.D. McLachlan, "Introduction to Magnetic Resonance," Harper and Row, New York, 1967.

C P.B. Ayscough, "Electron Spin Resonance in Chemistry," Methuen, London, 1967.

D J.D. Memory, "Quantum Theory of Magnetic Resonance Parameters," McGraw-Hill, New York, 1968.

1 Source B, page 257.

2 Source B, page 252.

3 P. Debye, "Polar Molecules," Dover, New York, 1945, Chapter 5.

4. Source B, page 259.

5. R.J. Meakins, Trans. Farad. Soc., 1958, 54, 1160.

6. D.A. Pitt, C.P. Smyth, J. Phys. Chem., 1959, 63, 582.

6. R.D. Nelson, C.P. Smyth, J. Phys. Chem., 1964, 68, 2704.

PART II

ELECTRON PARAMAGNETIC RESONANCE STUDIES OF NITROXIDE RADICALS OBTAINED FROM CARYOPHYLLENE NITROSITE

1. Introduction

The first nitroxide compound to be made was Fremy's salt (A), an inorganic radical[1]; the first organic nitroxide to be prepared was porphyrexide (B), a heterocyclic free radical[2]:

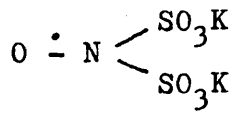

A

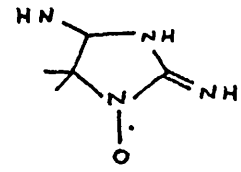

B

It is only in recent years, especially as a result of the development of e.p.r. spectroscopy, that this class of compound has been extensively studied, and used in the study of physico-chemical and biological problems. The recent book by Forrester, Hay and Thomson[3] gives an excellent review of nitroxide free radicals.

Methods of formation of nitroxide radicals which are relevant to the work discussed in this thesis are now briefly outlined.

Hoffmann[4] has formed stable dialkylnitroxides by addition of tertiary alkyl radicals to tertiary-nitroso-alkanes:

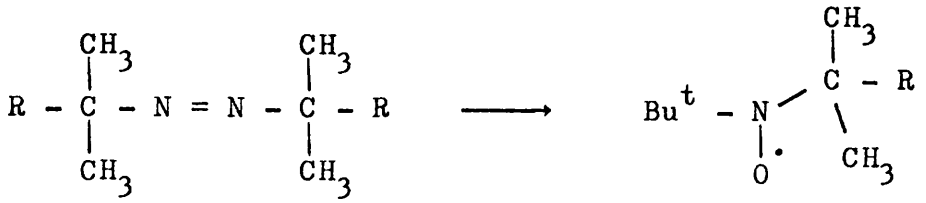

80°C for 6 hrs. in

presence of t-nitrosobutane.

R = CN and COOMe

Ultraviolet irradiation of solutions of aromatic nitroso compounds in methanol or in tetrahydrofuran produces diarylnitroxides.[5,6]

Nitroxides may be formed by irradiating tertiary-aliphatic nitroso compounds with red visible light at room temperature, or by similarly treating primary and secondary nitroso compounds at higher temperatures.[7,8] The higher temperature is necessary in the latter cases in order to shift the monomer-dimer equilibrium in favour of the monomer; for the tertiary compound steric effects favour the monomer and heating is unnecessary. There are two possible mechanisms for this reaction: in the first of these mechanisms, alkyl or aryl radicals produced in the photodissociation of the nitroso compound, attack a second molecule of the latter; in the second case, a photochemically excited molecule of nitroso compound reacts with a second, unexcited, molecule of nitroso compound. The second mechanism

may be written

$$RNO \xrightarrow{h\nu} RNO^{*}$$

$$RNO^{*} + RNO \rightarrow R_2NO + NO$$

Di-tertiary-alkylnitroxides have been detected in systems containing methylmethacrylate and nitrogen dioxide or nitric oxide.[9-11]

2. Caryophyllene nitrosite

The recent renewal of interest in the photochemistry of caryophyllene and its derivatives,[12-14] together with the extensive compilation of magnetic characteristics of nitroxide radicals[7,8,15-33] has suggested the use of electron paramagnetic resonance spectroscopy to re-examine the properties of caryophyllene nitrosite (I).[34,35]

This compound is a brilliant blue solid and it was used in early work on the Cotton effect[36] and on studies of asymmetric photochemical decompositions.[37] It is well-known as a derivative for the characterisation of caryophyllene.[38] Some previous studies of the effect of light on caryophyllene nitrosite were carried out as far back as 1892, but many of the results are inconclusive.[37,39-42] Although nitrogen and some nitrogen oxides have been identified, the major photolysis products do not appear to have been characterised.

Preliminary observations from studies being carried out on the photochemical properties of caryophyllene nitrosite are now given.

3. Radicals obtained when caryophyllene nitrosite reacts with bromine or with iodine

If caryophyllene nitrosite (I) is treated with bromine in chloroform solution at room temperature, a stable crystalline "bromo-nitrosite" can be isolated. A 10^{-3} M. solution of this compound in a 3:2 chloroform: toluene mixture at room temperature (295°K) gives an intense electron paramagnetic resonance spectrum consisting of a 1:1:1 triplet. The isotropic g value of the radical responsible for this spectrum is $2{\cdot}0057 \pm 0{\cdot}0002$, and the isotropic coupling constant a $(^{14}N) = 43{\cdot}2 \pm 0{\cdot}3$ MHz. $(15{\cdot}4 \pm 0{\cdot}1$ gauss). No further resolution of hyperfine splitting can be effected even though the solution is diluted and thoroughly degassed.

The first derivative of the e.p.r. spectrum of this solution at 77°K is shown in the upper half of Figure 1. If the spin Hamiltonian for the nitroxide radical is written in the form

$$\mathcal{H} = \beta_e \underline{H}.\underline{g}.\underline{S} + \underline{S}.\underline{T}.\underline{I}$$

then Figure 1 can be analysed in terms of a superposition of three curves of the type described by Kneubühl[43] (see appendix A), and the principal components of the g tensor and the hyperfine tensor T, along with the line-broadening parameter, β, can be obtained from it. These parameters are listed in the following table. One of the assumptions made by Kneubühl in this method of analysis is that the paramagnetic molecules are oriented completely randomly throughout the glass. It has been found in this study that glasses of all of the compounds described in this section show a definite orienting effect such that the nitroxide radicals have a greater probability of being in an orientation with the sigma framework of their nitroxide groups perpendicular to the applied magnetic field. These solutions at 77°K. are not therefore pure glasses; there is some tendency towards crystallisation inside the specimen tubes used in recording the spectra. This crystallising effect results in the wings of the spectrum gaining intensity at the expenses of the centre of the spectrum. In the case under discussion, the "bromonitrosite", it appears that twice as many radicals have their (RR')N-O sigma electronic framework perpendicular to the applied field as there would have been for a completely random distribution. The first derivative

of the absorption spectrum expected from a polycrystalline sample of nitroxide radicals with the parameters of radical IIb in Table 1 and with the intensity weighted to give such a spacial distribution is shown in the bottom half of Figure 1.

This work was carried out before the publication by Leigh[44] of an account of the effects of dipolar interactions in glassy or polycrystalline spectra whereby the intensity of the central region of the spectrum is reduced in intensity in comparison with the "wings" of the spectrum. It is, however, thought that in the cases described in this section, the glasses are sufficiently dilute to preclude any significant contribution from this effect.

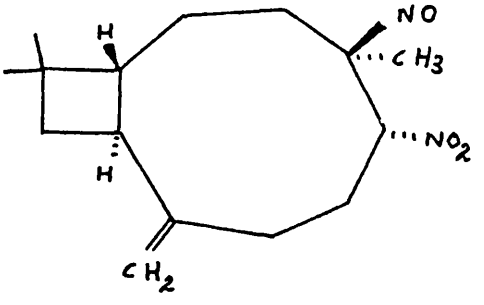

I

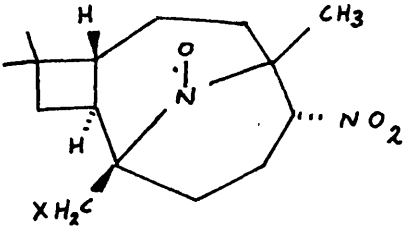

IIa ; X = I

IIb ; X = Br

By comparing the intensity of the e.p.r. spectrum

obtained from a solution containing a known weight of the "bromo-nitrosite" with that of the spectrum from a solution containing a known number of electron spins, in a similar environment and at a similar concentration, the molecular weight of the "bromo-nitrosite" was found to be 375 $\pm$ 25. By analogy with the product (IIa) obtained[34,35] from the corresponding reaction involving iodine and caryophyllene nitrosite, the structure IIb is therefore assigned to the "bromo-nitrosite".

The magnetic tensor components extracted from the e.p.r. spectra of dilute solutions of radical IIa in chloroform:toluene (3:2) glass, at 77°K, are included in Table 1. To obtain a theoretical spectrum with the correct intensity distribution, it is necessary to have a distribution of radicals such that three times as many of them have their sigma electronic framework perpendicular to the applied magnetic field as would be expected from a completely random distribution. The experimental and simulated first derivative spectra for a glassy sample of IIa, weighted according to this scheme, are shown in Figure 1.

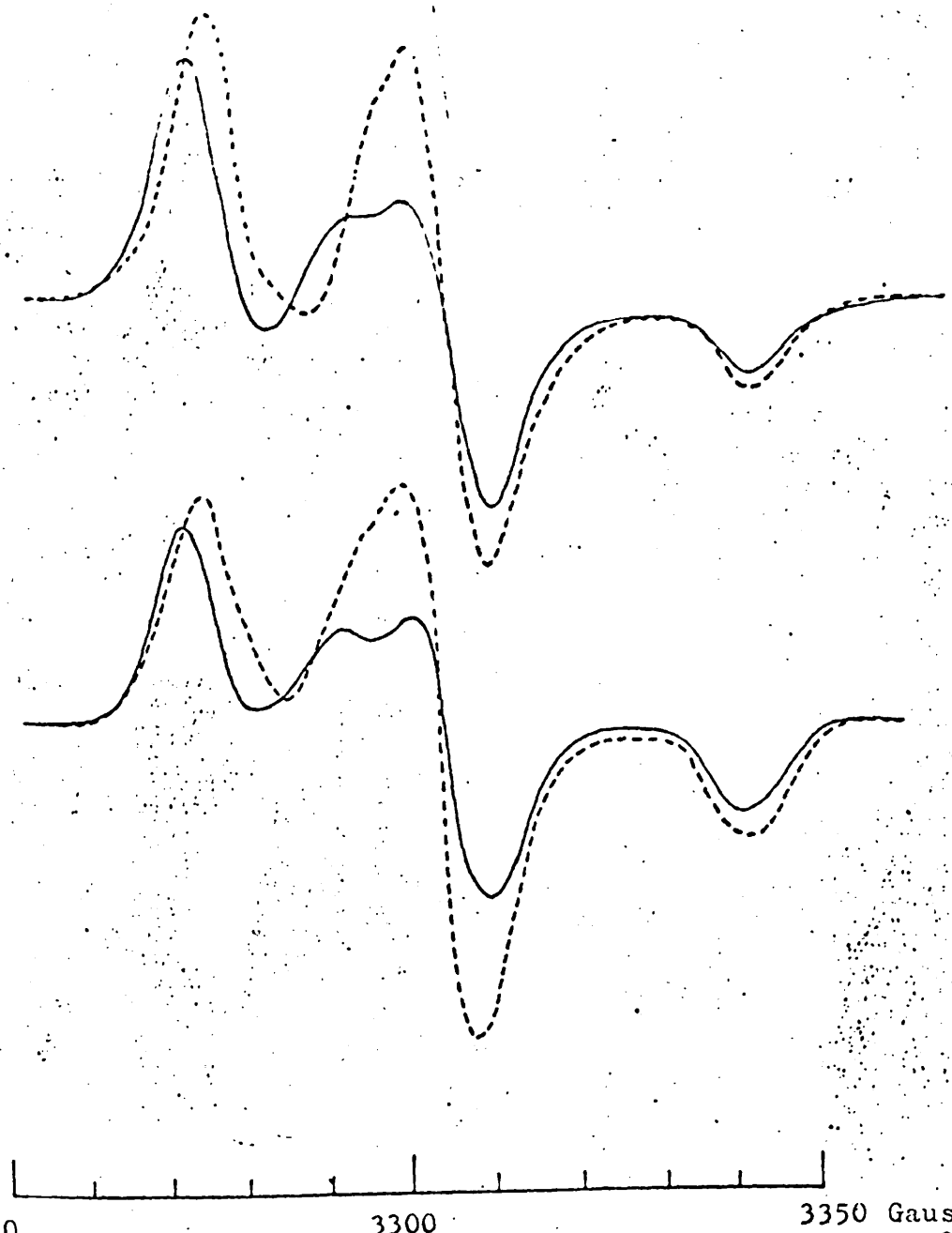

Figure 1 Observed and calculated e.p.r. spectra for 10^{-3} M solutions of radicals IIa(——) and IIb(----) dispersed in chloroform: toluene (3:2) glass at 77°K. The parameters used in calculating these spectra are listed in Table 1. The upper curves are the observed spectra. The lower curves are the calculated spectra.

Table 1

Principal g-tensor components, hyperfine tensor components and line broadening parameters for caryophyllene bromo-nitrosite and for caryophyllene iodo-nitrosite. The broadening functions are assumed to have the Gaussian form $(2\pi)^{-\frac{1}{2}}\beta^{-1}\exp[-(h'-h)^2(2\beta^2)^{-1}]$. Hyperfine tensor components are in M.Hz. units. Limits of error for g and T components are ± 0·0006 and ± 2 M.Hz. respectively.

Radical	g_{11}	g_{22}	g_{33}	$\langle g \rangle$
IIa	2·0083	2·0052	2·0034	2·0056
IIb	2·0071	2·0068	2·0028	2·0056

Radical	$T_{11}(^{14}N)$	$T_{22}(^{14}N)$	$T_{33}(^{14}N)$	$a(^{14}N)$	β
IIa	11	14	95	40(=14·2 gauss)	3·5
IIb	11	11	102	41(=14·6 gauss)	4·0

4. Radicals obtained when

(i) caryophyllene nitrosite and

(ii) solutions of caryophyllene nitrosite,

are irradiated with red light

Caryophyllene nitrosite shows two regions of absorption in the ultraviolet - visible range of the electromagnetic spectrum. There is absorption of ultraviolet at 2700 Å, and there is absorption of red visible light at 6700 Å. This latter transition, the $\pi^* \leftarrow n$ transition of the nitroso group, is responsible for the blue colour of solid caryophyllene nitrosite. Irradiation of this solid, in the absence of air, with red light from a filtered tungsten lamp, results in decomposition to a yellow viscous liquid and nitrogen, nitrous oxide, and nitric oxide are evolved.[42] The presence of at least four major constituents has been demonstrated by thin layer chromatography. The e.p.r. spectrum of this viscous liquid was recorded at 290°K., and is shown in Figure 2. The magnetic parameters obtained from this spectrum are given

$g_{11} = 2{\cdot}0061 \pm 0{\cdot}0006$; $g_{22} = 2{\cdot}0061 \pm 0{\cdot}0006$;

$g_{33} = 2{\cdot}0029 \pm 0{\cdot}0006$; $\langle g \rangle = 2{\cdot}0050 \pm 0{\cdot}0006$;

$T_{11}(^{14}N) = 12{\cdot}4 \pm 2$ MHz.; $T_{22}(^{14}N) = 12{\cdot}4 \pm 2$ MHz.;

$T_{33}(^{14}N) = 95{\cdot}6 \pm 2$ MHz.; $a(^{14}N) = 40{\cdot}1 \pm 2$ MHz.

$= 14{\cdot}3 \pm 0{\cdot}7$ gauss

The e.p.r. spectrum of a dilute solution of this yellow substance dissolved in chloroform is shown in Figure 3. This solution spectrum shows that there are two nitroxide radicals present, their isotropic g factors, $\langle g \rangle$, being identical ($2{\cdot}0055 \pm 0{\cdot}0001$) and their isotropic hyperfine coupling constants, $a(^{14}N)$, being $42{\cdot}4 \pm 0{\cdot}3$ MHz. ($15{\cdot}1 \pm 0{\cdot}1$ gauss) and $35{\cdot}4 \pm 0{\cdot}3$ MHz. ($12{\cdot}6 \pm 0{\cdot}1$ gauss) respectively. No further splitting of the spectrum was observed. The low value of the second of these two $a(^{14}N)$ parameters suggests that a significant amount of delocalisation of the unpaired electron away from its π^* orbital on the nitrogen atom has occurred.

The spectrum of the viscous yellow liquid itself (Figure 2) indicates that any tumbling motion of the radicals must be of such a low frequency that it does not average out the magnetic anisotropies in the g and hyperfine coupling tensors. This suggests that the nitroxide radicals concerned are of fairly high molecular weight.

All of the above observations are in accord with the photolysis scheme A in which an unpaired electron in the sigma framework in a red-excited nitroso-group attacks

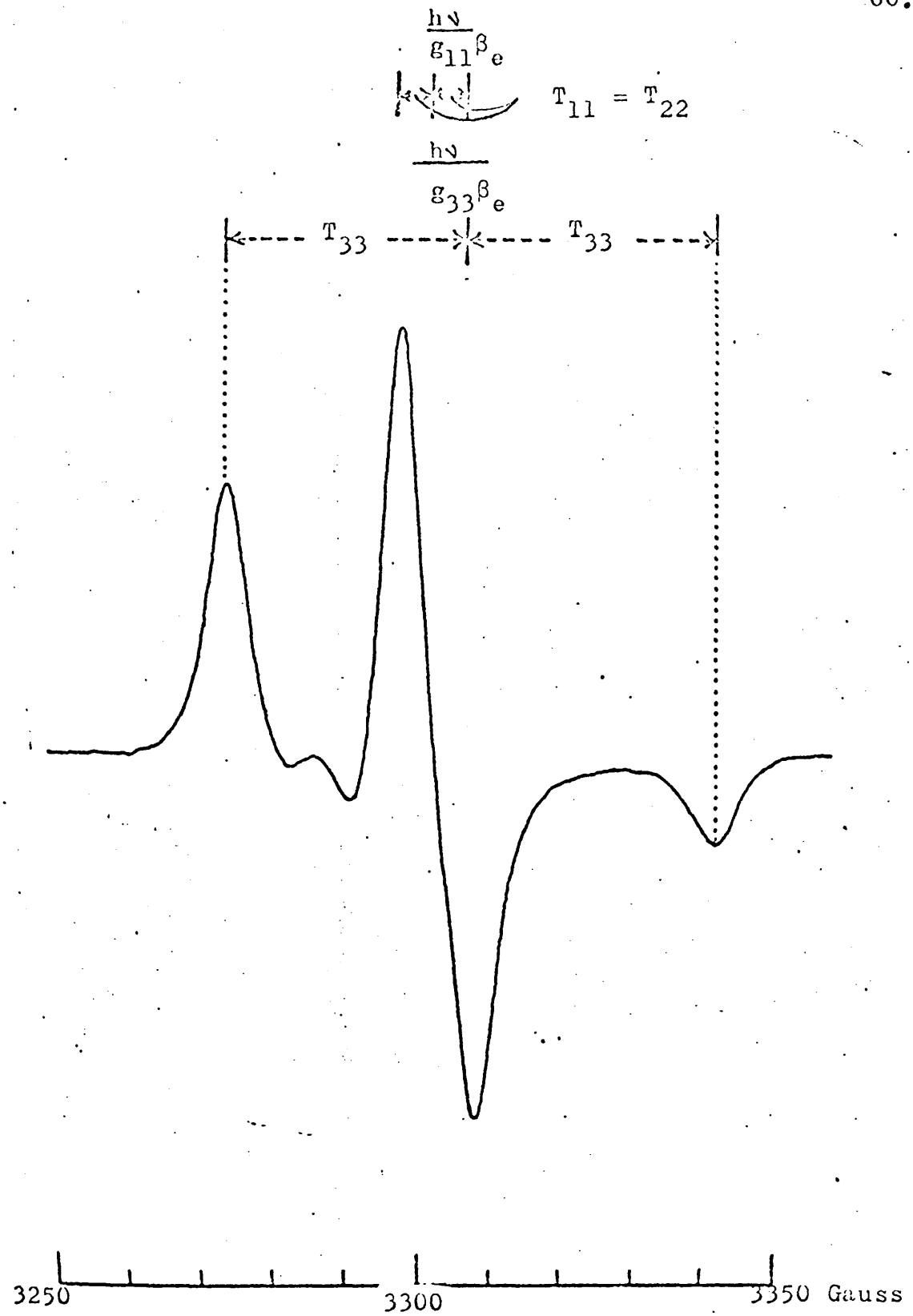

Figure 2. The e.p.r. spectrum of the viscous yellow liquid obtained, at 290°K., by irradiating caryophyllene nitrosite with red light.

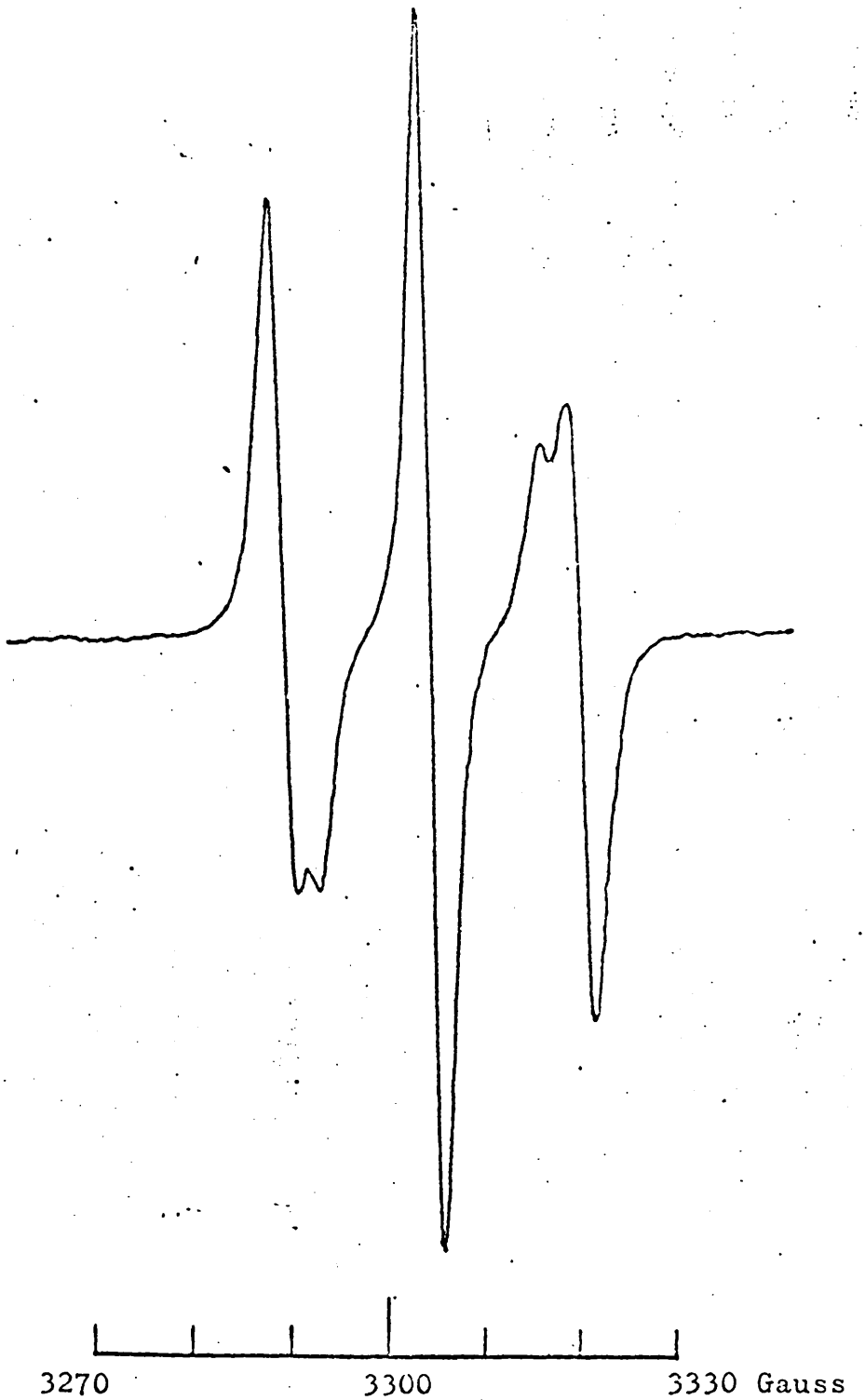

Figure 3 The e.p.r. spectrum of a dilute solution in chloroform of the viscous yellow liquid obtained by irradiating caryophyllene nitrosite with red light. The spectrum was recorded at 290°K.

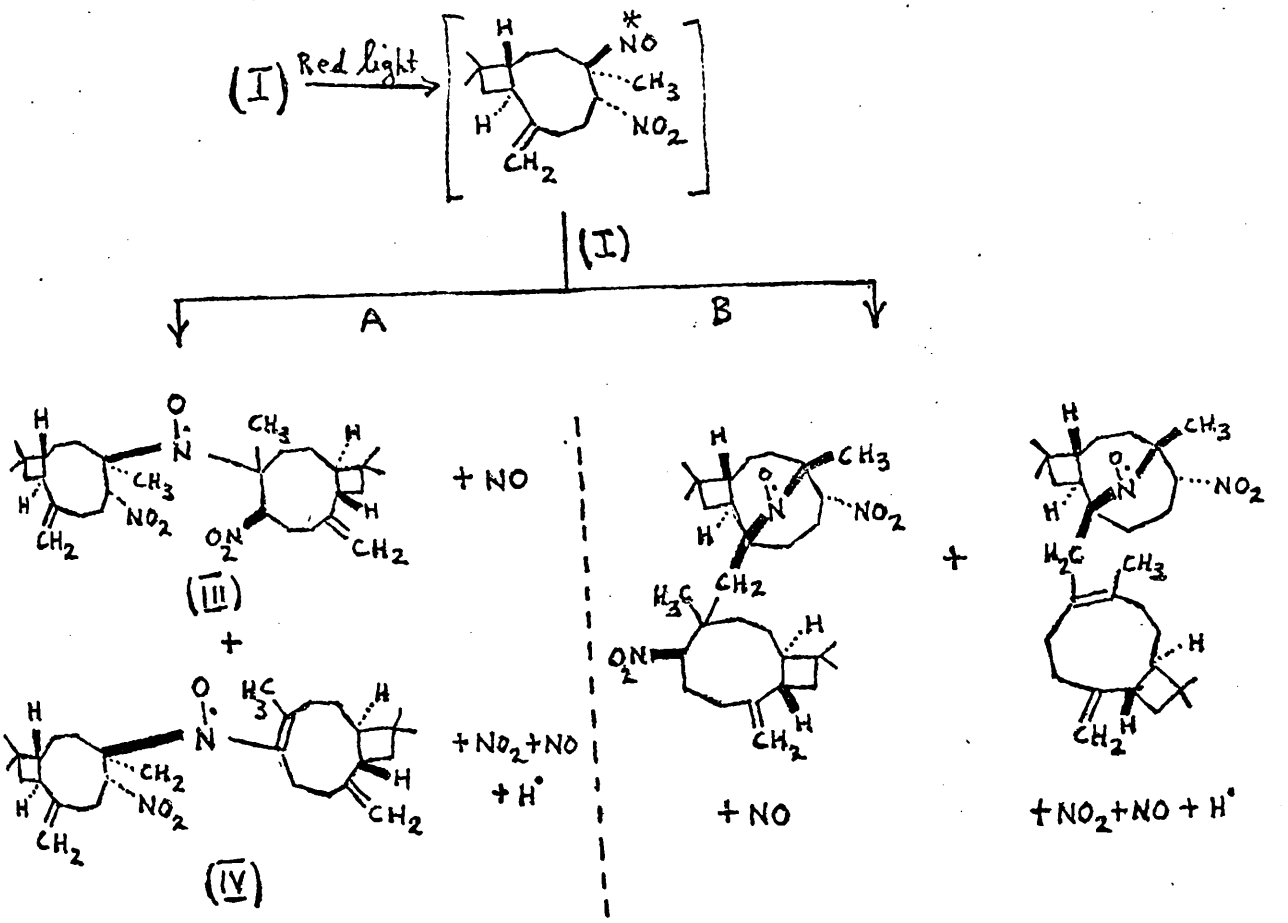
(I) Red light
(I)
A
B
+ NO
(III)
+
(IV)
+ NO2 + NO
+ H°
+ NO
+
+ NO2 + NO + H°

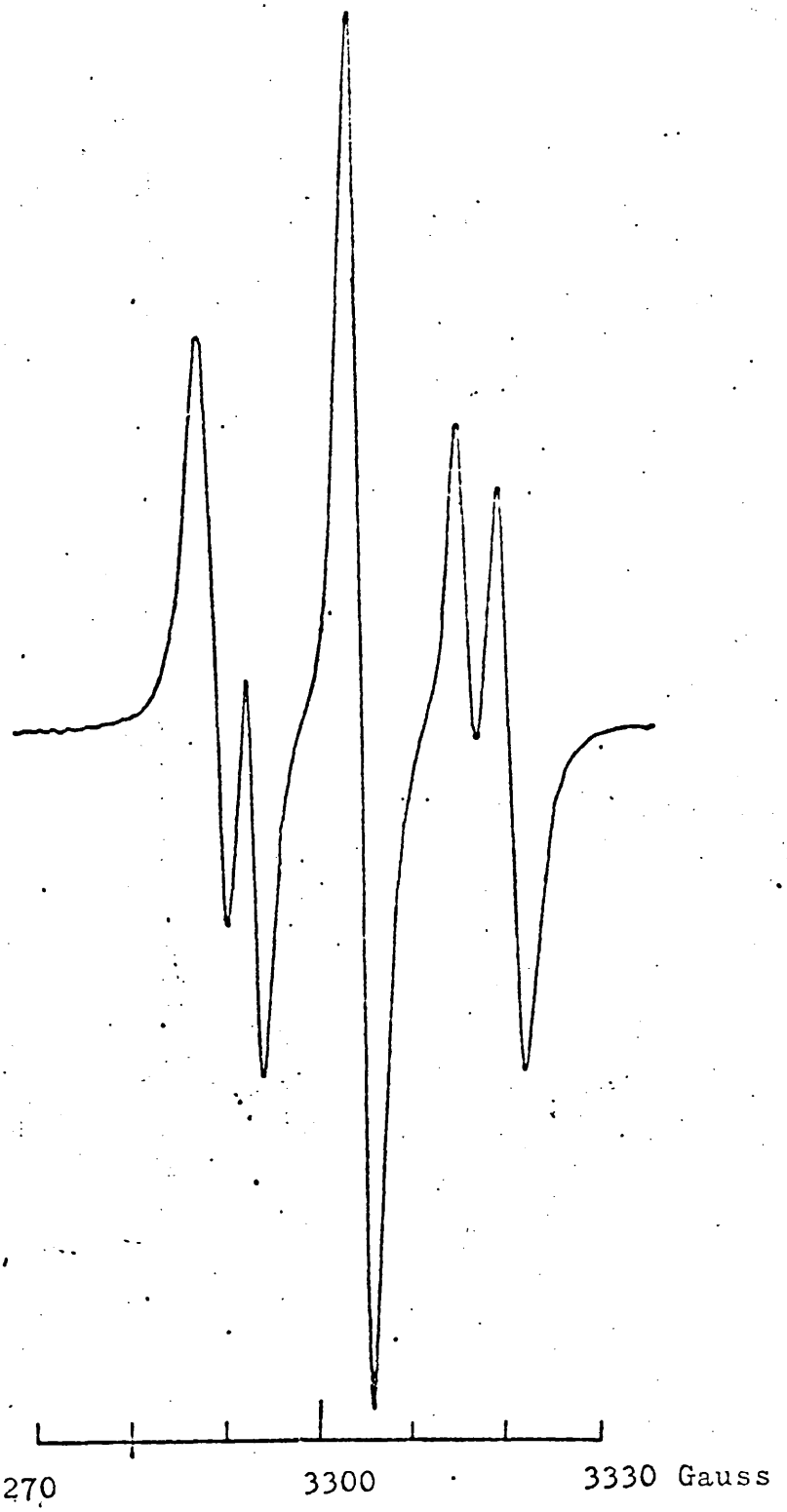

Figure 4 The e.p.r. spectrum of the radicals obtained by irradiating a dilute solution of caryophyllene nitrosite in toluene with red light. The spectrum was recorded at 290°K.

a neighbouring caryophyllene nitrosite molecule in the crystal. Although the reaction scheme A must be regarded as a suggestion consistent with a limited amount of experimental data, the alternative photolysis scheme B can be firmly rejected since it would not result in the formation of a nitroxide radical in which the $a(^{14}N)$ hyperfine coupling constant is 12·6 gauss.

When a 10^{-2} M solution of caryophyllene nitrosite in toluene is irradiated with red light, then the e.p.r. spectrum obtained is consistent with the formation of compounds III and IV. This spectrum, which is shown in Figure 4, arises from two nitroxide radicals with identical isotropic g factors, $\langle g \rangle = 2{\cdot}0053 \pm 0{\cdot}0002$ and with isotropic hyperfine coupling constants $a(^{14}N)$ of $43{\cdot}5 \pm 0{\cdot}6$ MHz. ($15{\cdot}5 \pm 0{\cdot}2$ gauss) and $34{\cdot}5 \pm 0{\cdot}6$ MHz. ($12{\cdot}3 \pm 0{\cdot}2$ gauss) respectively. If the irradiated solution is left standing for some time, radical IV decomposes and eventually the spectrum of radical III alone is observed. Similar results are obtained if benzene, rather than toluene, is used as solvent in this experiment. The photo-excited caryophyllene nitrosite molecule does not appear to react with toluene or with benzene.

When chloroform or ethanol are used as solvents in

this photolysis with red light, the photo-excited caryophyllene nitrosite molecule does react with the solvent, and the primary products do not give an e.p.r. spectrum. If a solution of caryophyllene nitrosite in ethanol is irradiated with red light for about two hours and then the ethanol is allowed to evaporate off and the solid products dissolved in toluene, then at least four products are obtained. Two of these are nitroxide radicals. The first radical [$< g >$ = 2·0063 ± 0·0001; $a(^{14}N)$ = 21·9 ± 0·3 MHz. (7·8 ± 0·1 gauss)] is an unstable compound which it was not possible to isolate. The second is a yellow crystalline solid whose molecular weight lies between 560 and 600 (e.p.r. and osmometry). In chloroform-toluene (3:2) solution it gives rise to the e.p.r. spectrum shown in Figure 5: this compound therefore contains the molecular fragment $(R^1R^2R^3)CN\dot{O}CH(R^4R^5)$. Its isotropic spin Hamiltonian parameters are $< g >$ = 2·0061 ± 0·0002; $a(^{14}N)$ = 39·9 ± 0·3 MHz. (14·2 ± 0·1 gauss); $a(^{1}H)$ = 6·5 ± 0·3 MHz. (2·3 ± 0·1 gauss) which are consistent with structure V for the yellow compound, provided the neighbouring C-H bond lies nearly in the sigma framework of the NO group.[32] The unusual stability of structure V is ascribed to spacial congestion in the neighbourhood

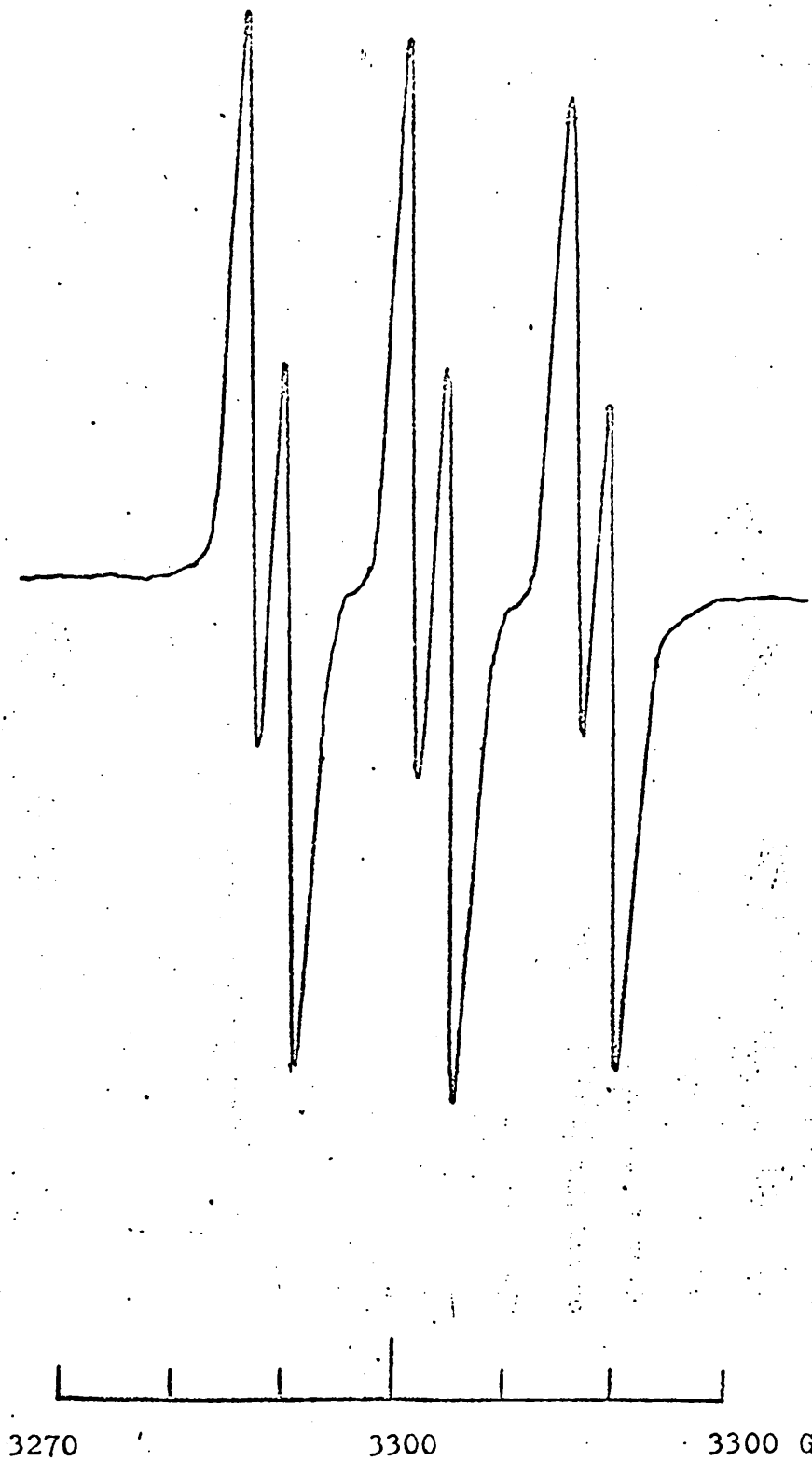

Figure 5 The e.p.r. spectrum of a 10^{-2}M solution, in chloroform: toluene (3:2) at 290°K, of the yellow solid isolated after irradiating caryophyllene nitrosite in ethanol with red light.

of the α-hydrogen atom: nitroxide radicals containing the structural unit $(R^1R^2R^3)CN^{\bullet}OCH(R^4R^5)$ are known to disproportionate readily unless steric overcrowding protects this position in the molecule.[45]

The nature of the unstable nitroxide radical obtained from ethanolic solution is not understood. The low value of its hyperfine coupling constant, $a(^{14}N)$ = 21·9 $\pm$ 0·3 MHz., means that the unpaired electron spin density at the nitrogen nucleus is considerably less than in the case of a normal di-tertiary-alkylnitroxide. Its spin Hamiltonian parameters are consistent with the presence of a carbonyl group α to the NO residue;[31] this compound may be VI.

Since the red-irradiated solution of caryophyllene nitrosite in ethanol is diamagnetic, the radicals V and VI cannot themselves be primary photolysis products but may be derived by oxidation of the corresponding hydroxylamines.

Another radical, claimed to have the structure Vb, has recently been isolated from the products obtained when caryophyllene nitrosite in ethanol, is irradiated with red light.[46]

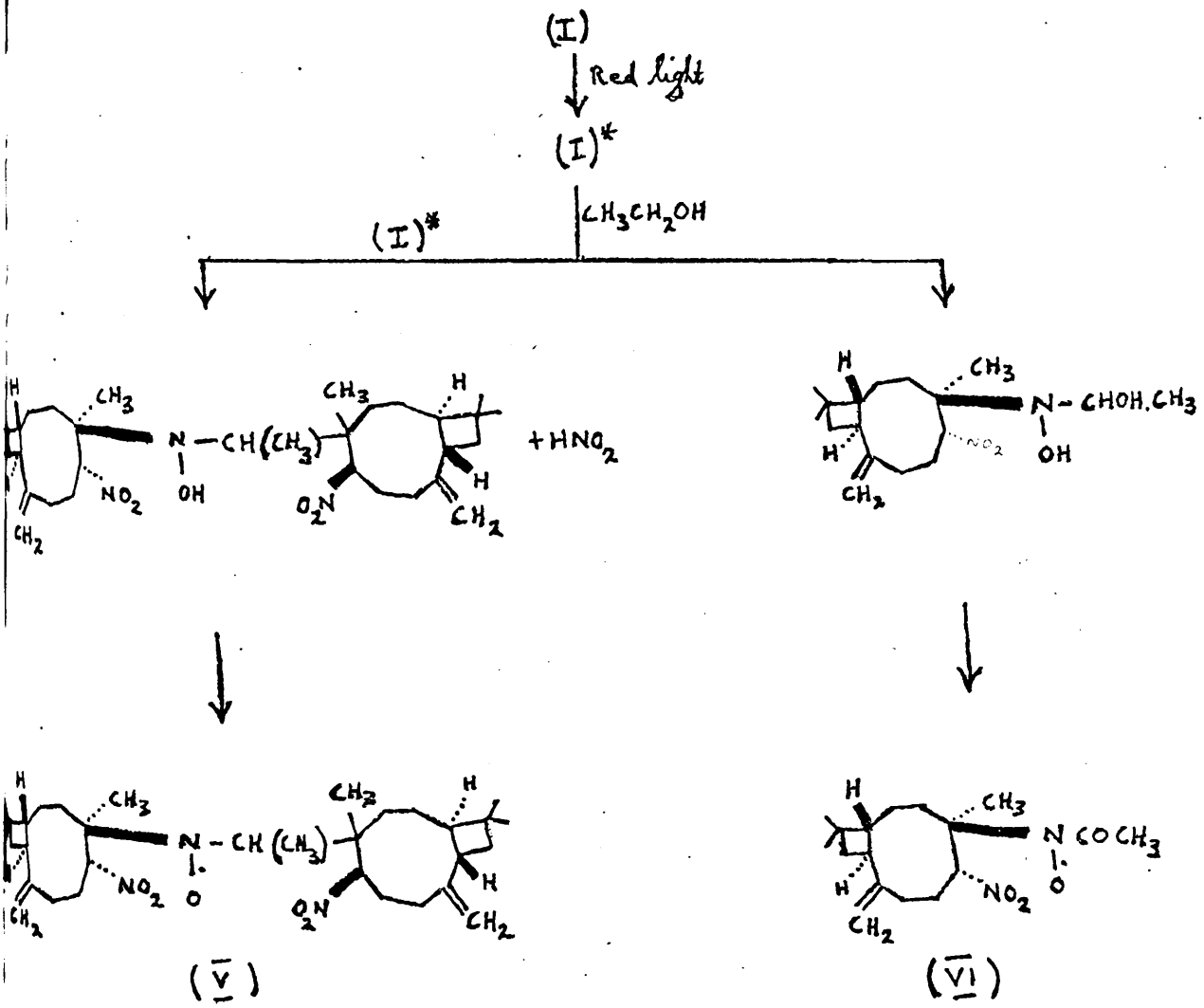
(I)
Red light
(I)*
(I)*
CH3CH2OH
+HNO2
(V)
(VI)

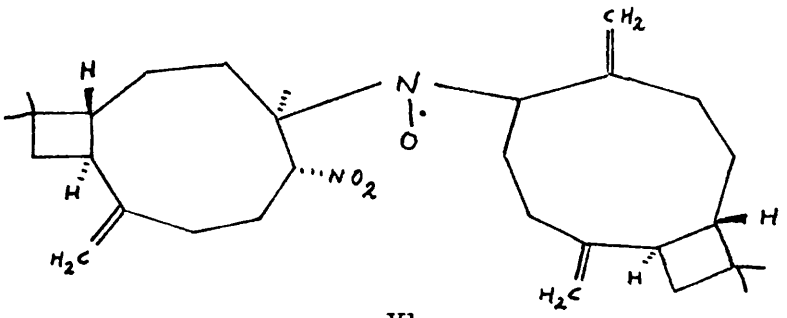

Vb

5. Radicals obtained when caryophyllene nitrosite is irradiated with ultraviolet light

Irradiation of a polycrystalline sample of caryophyllene nitrosite with ultraviolet radiation from a medium pressure mercury arc causes the blue colour to take on a greenish hue. This irradiated solid is paramagnetic and its e.p.r. spectrum, recorded at 290°K., is shown in Figure 6. As long as this irradiated solid is not exposed to light, the radical which gives the e.p.r. signal shown may be seen for a number of months. If this solid is taken into solution, however, the radical quickly disappears. The spectrum of a freshly prepared solution of this irradiated solid in chloroform is shown in Figure 7; the isotropic g factor is $\langle g \rangle = 2{\cdot}0054 \pm 0{\cdot}0002$, and the isotropic hyperfine coupling constant is $a(^{14}N) = 40{\cdot}4 \pm 0{\cdot}6$ MHz. ($14{\cdot}4 \pm 0{\cdot}2$ gauss). No proton hyperfine coupling is

observed, and the spectrum gradually disappears on allowing the solution to stand.

The spectrum shown in Figure 6 arises from an unpaired electron interacting with one ^{14}N nucleus and with one proton. The spin Hamiltonian parameters are given below

$g_{11} = 2{\cdot}0063 \pm 0{\cdot}0006$; $g_{22} = 2{\cdot}0062 \pm 0{\cdot}0006$;
$g_{33} = 2{\cdot}0032 \pm 0{\cdot}0006$; $\langle g \rangle = 2{\cdot}0052 \pm 0{\cdot}0003$
$T_{11}(^{14}N) = 12 \pm 3$ MHz.; $T_{22}(^{14}N) = 12 \pm 3$ MHz.;
$T_{33}(^{14}N) = 78 \pm 3$ MHz.; $a(^{14}N) = 34 \pm 5$ MHz. (12 ± 2 gauss)
$T_{11}(^{1}H) = 23 \pm 3$ MHz.; $T_{22}(^{1}H) = 23 \pm 3$ MHz.;
$T_{33}(^{1}H) = 35 \pm 3$ MHz.; $a(^{1}H) = 27 \pm 5$ MHz. (10 ± 2 gauss).

The ultraviolet radiation is absorbed by the $-NO_2$ group of the nitrosite, but the spin Hamiltonian parameters are not in accord with radicals of the type $R\dot{C}HNO_2$ or $R\text{-}\dot{N}\overset{O}{\underset{OH}{\nearrow}}$, which have been observed in the γ-irradiation of nitroalkanes.[47] Iminoxy radicals, $RCH = \dot{N}O$, are also inconsistent with this set of magnetic parameters.[48-50] A nitroxide radical of type $(R_1R_2R_3)C\dot{N}OCH(R_4R_5)$ would fit this data;[51] and furthermore, the $a(^{14}N)$ value of 12 gauss extracted from Figure 6, and the green colour developed on ultraviolet irradiation,[31,33] suggest that a five-membered nitroxide ring which contains

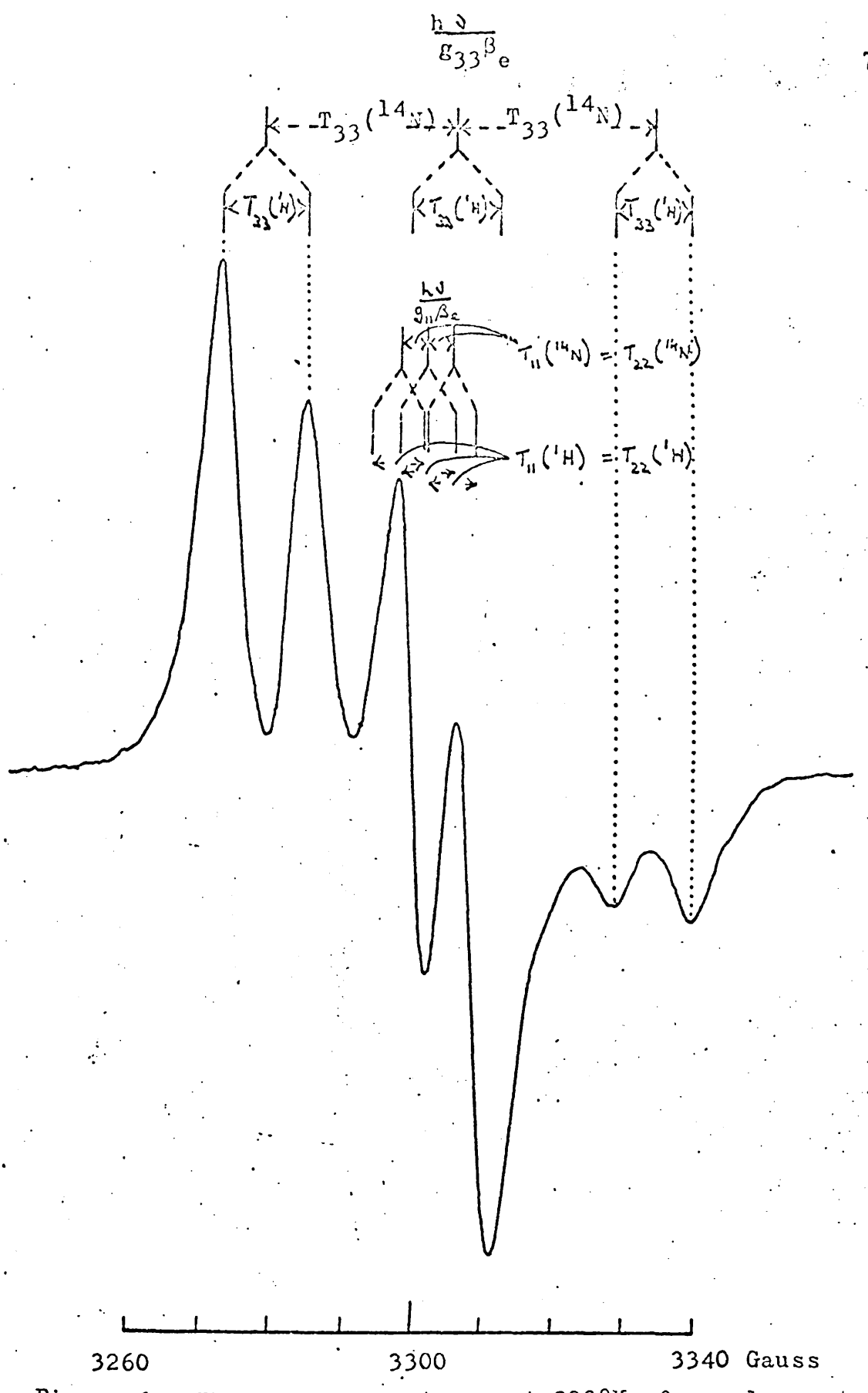

Figure 6 The e.p.r. spectrum, at 290°K, of a polycrystalline sample of caryophyllene nitrosite after irradiation with U.V. ligh

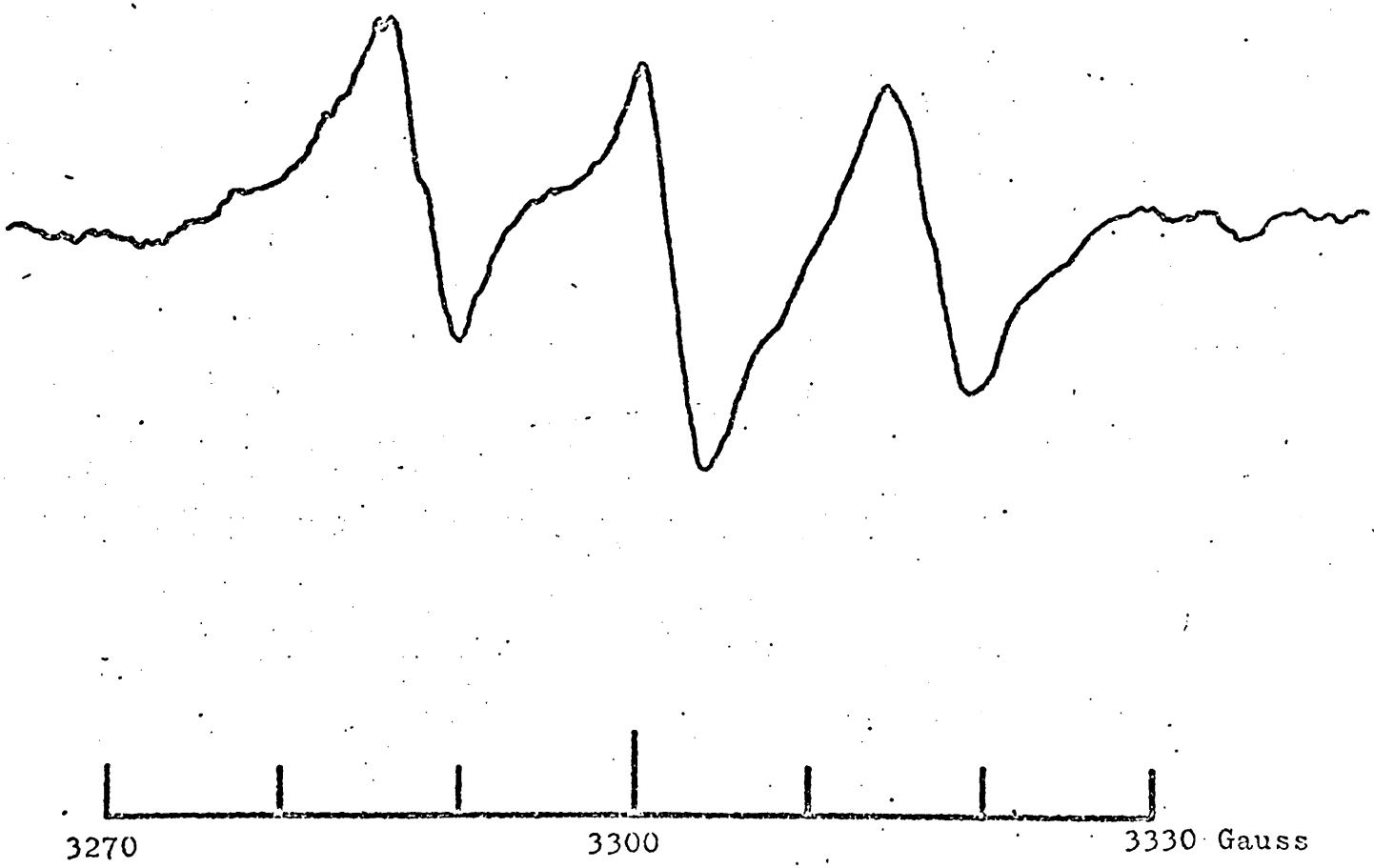

Figure 7 The e.p.r. spectrum of a dilute solution, in chloroform at 290°K., of U.V. irradiated (solid) caryophyllene nitrosite

a β-carbonyl residue, has been formed during the photolysis. Structure VII is therefore assigned to this radical formed in the solid. Formation of VII implies that the conformation of caryophyllene nitrosite in the blue solid is VIII and that is is converted into VII by the reaction sequence shown

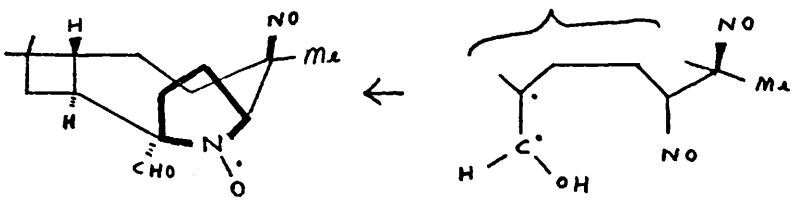

VII

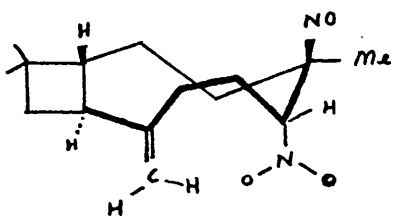

VIII

When this radical is dissolved in chloroform, the β-proton hyperfine coupling observed in the solid (Figure 6) is no longer visible, i.e. some further rearrangement occurs on dissolution in chloroform. The a(^{14}N) value in Figure 7, of 14·4 gauss, however, shows that, in at least the early stages of this additional reaction, the five-membered nitroxide ring is still present.

6. Summary of Part II

Eight different nitroxide radicals have been derived from caryophyllene nitrosite. Two are obtained by allowing caryophyllene nitrosite in chloroform solution to react with iodine or with bromine; two by irradiating solid caryophyllene nitrosite with red light, or by irradiating solutions of caryophyllene nitrosite in toluene or in benzene with red light; two are obtained by irradiating solutions of caryophyllene nitrosite in ethanol with red light; one by irradiating solid caryophyllene nitrosite with ultraviolet radiation, and one by dissolving the last radical in chloroform. Three of these radicals have been isolated as pure, stable solids. Electron paramagnetic resonance spectra of the eight radicals are described and spin Hamiltonian parameters, extracted from spectra of "glasses" formed at 77°K by dispersing them in chloroform:toluene (3:2) solution, or from room-temperature spectra, are given. Structures for the nitroxide radicals, and some information about the mechanisms of the red and ultraviolet photolyses reactions, are deduced from the electron paramagnetic resonance data.

References to Part II

1. E. Fremy, Ann. Chim. Phys., 1845, 15, 459.
2. O. Piloty, B. Graf Schwerin, Ber., 1901, 34, 1870.
3. A.R. Forrester, J.M. Hay, R.H. Thomson, "Organic Chemistry of Stable Free Radicals," Academic Press, London, 1968.
4. A.K. Hoffmann, U.S. Patent 1966, 3,253, 015; Chem. Abs., 1966, 65, 15225.
5. K. Maruyama, R. Tanikaga, R. Goto, Bull. Chem. Soc., Japan, 1964, 37, 1893.
6. H. Mauser, H. Heitzer, Z. Naturforsch., 1965, 20b 200.
7. A. Mackor, Th.A.J.W. Wajer, Th.J. De Boer, J.D.W. van Voorst, Tet. Letters, 1966, 19, 2115.
8. E.T. Strom, A.L. Bluhm, Chem. Commun., 1966, 115.
9. M. Elbert, J. Law, Nature, 1965, 205, 1193.
10. J.A. McRae, M.C.R. Symons, Nature, 1966, 210, 1259.
11. W.M. Fox, J.A. McRae, M.C.R. Symons, J. Chem. Soc. A, 1967, 1773.
12. K.H. Schulte-Elte, G. Ohloff, Helv. Chim. Acta, 1968, 51, 494.
13. K.H. Schulte-Elte, G. Ohloff, Helv. Chim. Acta, 1968, 51, 548.
14. G. Gollnick, G. Schade, Tet. Letters, 1968, 6, 689.

15. R.H. Hoskins, J. Chem. Phys., 1956, 25, 788.

16. J.R. Thomas, J. Amer. Chem. Soc., 1960, 82, 5955.

17. A.K. Hoffmann, A.T. Henderson, J. Amer. Chem. Soc., 1961, 83, 4675.

18. J.C. Baird, J.R. Thomas, J. Chem. Phys., 1961, 35, 1507.

19. G.M. Coppinger, J.D. Swalen, J. Amer. Chem. Soc., 1961, 83, 4900.

20. J.C. Baird, J. Chem. Phys., 1962, 37, 1879.

21. R. Brière, H. Lemaire, A. Rassat, Bull. Soc. chim. France, 1965, 3273.

22. G. Chapelet-Letourneaux, H. Lemaire, A. Rassat, Bull. Soc. Chim. France, 1965, 3283.

23. R. Brière, R. Dupeyre, H. Lemaire, C. Morat, A. Rassat, P. Rey, Bull. Soc. chim. France, 1965, 3290.

24. H. Lemaire, Bull. Soc. chim. France, 1966, 559.

25. A.M. Vasserman, A.L. Buchachenko, Zhur. Strukt. Khim., 1966, 7, 673.

26. J.Q. Adams, S.W. Nicksic, J.R. Thomas, J. Chem. Phys., 166, 45, 654.

27. E.G. Rozantsev, Russ. Chem. Rev., 1966, 35, 658, and references therein.

28. Th.A.J.W. Wajer, A. Mackor, Th.J. de Boer, J.D.W. van Voorst, Tetrahedron, 1967, 23, 4021.

29. R. Brière, H. Lemaire, A. Rassat, P. Rey, A. Rousseau, Bull. Soc. chim. France, 1967, 4479.

30. A. Calder, A.R. Forrester, Chem. Commun., 1967, 682.

31. A. Rassat, "Molecular Spectroscopy," The Institute of Petroleum, London, 1968, p. 145, and references therein.

32. G. Chapelet-Letourneaux, H. Lemaire, R. Lenk, M.-A. Marechal, A. Rassat, Bull. Soc. chim. France, 1968, 3963.

33. R.M. Dupeyre, H. Lemaire, A. Rassat, Tet. Letters, 1964, 1781.

34. D.M. Hawley, J.S. Roberts, G. Ferguson, A.L. Porte, Chem. Commun., 1967, 942.

35. D.M. Hawley, G. Ferguson, J.M. Robertson, J. Chem. Soc. B, 1968, 1255.

36. S. Mitchell, J. Chem. Soc., 1928, 3258.

37. S. Mitchell. J. Chem. Soc., 1930, 1829.

38. E. Deussen, J. prakt. Chem., 1926, 114, 63, and references therein.

39. E. Kremers, O. Schreiner, Pharm. Arch., 1892, 2, 287.

40. J. Simonsen, "The Terpenes," Cambridge University Press, 1932, vol. 2, p. 515.

41. E. Deussen, Annalen, 1909, 369, 44.

42. R.M. Hoffman, J. Amer. Chem. Soc., 1934, 56, 1894.

43. F.K. Kneubühl, J. Chem. Phys., 1960, 33, 1074.

44. J.S. Leigh, J. Chem. Phys., 1970, 52, 2608.

45. M. Iwamura, N. Inamoto, Bull. Chem. Soc. Japan, 1967, 40, 703.

46. J.S. Roberts, W. Motherwell, personal communication.

47. C. Chachaty, C. Rosilio, J. Chim. phys., 1967, 64, 777.

48. A.K. Hoffman, W.G. Hodgson, W.H. Jura, J. Amer. Chem. Soc., 1961, 83, 4675.

49. J.R. Thomas, J. Amer. Chem. Soc., 1964, 86, 1446.

50. P.W. Atkins, M.C.R. Symons, "The Structure of Inorganic Radicals," Elsevier, London, 1967, pp. 140 - 142.

51. P.B. Ayscough, "Electron Spin Resonance in Chemistry," Methuen, London, 1967, pp. 282 - 286, and references therein.

PART III

AN ELECTRON PARAMAGNETIC RESONANCE STUDY OF DI-TERTIARY-BUTYLNITROXIDE IN DIANIN'S COMPOUND

1. Introduction

There has been a renewal on interest in clathrate compounds in recent years and a number of reviews on this subject have appeared.[1-18] Molecules of "guest", G, are trapped within cavities which exist in the lattice of the "host", H, and the clathrate of composition G.nH can be stable over a wide range of values of n. Maximum and minimum values of n are determined largely by geometrical considerations.

Clathrates are of interest to physical chemists for a number of reasons, amongst which may be included the following

(1) They may be used to separate two very similar compounds if one is able to fit inside the clathrate cavity and the other is too large to do so. This technique is used both in research and on the industrial scale.[19]

(2) Theoretical studies of van der Waals interactions may be tested on clathrates since the environment of the "guest" molecule is then well-defined. Cell-models which are used in theories of liquids and of solid solutions, in particular, may be tested on clathrates.

A "guest" molecule in a clathrate may be regarded as an example of a simple "particle-in-a-box".[20-22]

(3) Reactive species and transient intermediates in chemical reactions may often be prevented from diffusing and hence may be stabilised, if they are produced within, or are introduced into, the cavities in a clathrate.[23,24]

(4) Spectroscopic studies of "guest" molecules in clathrates are often particularly informative, since the environment of the species being examined is well-defined and the complexities which arise from the fluctuating solvation effects found in solutions are not present. Infra-red,[25-30] dielectric,[30-35] magnetic susceptibility,[36-39] nuclear magnetic resonance[40-53] and electron paramagnetic resonance methods[24,54-59] have all been used to study clathrates. Nuclear magnetic resonance and electron paramagnetic resonance spectra are particularly sensitive to motional and to environmental changes and so the magnetic resonance methods are especially suited to investigating "guest" species.

Dianin's compound, 4-p-hydroxyphenyl-2,2,4-trimethylchroman, I, has been known for a considerable time,[60,61] but it was not until 1955 that Baker and McOmie deduced,[62]

from chemical evidence, the formula I, and showed that Dianin's compound forms crystalline inclusion compounds with a great variety of substances.

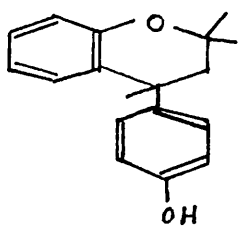

I

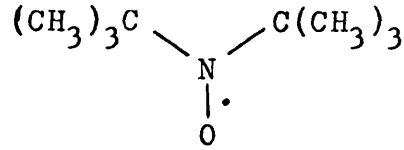

II

At the same time Powell and Wetters[63] published a preliminary communication on a postulated structure of the argon clathrate, $Ar.6C_{18}H_{20}O_2$, but full details of the crystal structure of the compound were not given. Hoffman, Breeden and Liggett[64] have reported that carbohydrates can be included in the cavities of Dianin's compound. Davies and Williams[33] have studied dielectric relaxation of several "guest" molecules in Dianin's compound. Bhatnagar[65] has written a general review of clathrates formed from Dianin's compound.

The structure of Dianin's compound was unknown when the work described in this thesis was started, but recently a report of this structure has been given,[66] and a preliminary communication on the isomorphorus clathrate "host", 4-p-hydroxyphenyl-2,2,4-trimethylthia-

chroman, has also been published.[67] Both of these substances crystallise in the trigonal system in which a hexagonal unit cell containing eighteen molecules of the "host" may be defined. The space group is $R\bar{3}$, and in the structure six molecules of Dianin's compound are linked by hydrogen-bonding through their OH group to form a complex which then links up with similar complexes to form cages in which "guest" molecules of suitable size may be trapped. Figure 1 shows a projection of the structure along the a axis of the hexagonal unit cell defined in reference 67. In this 2/3 of the contents of a unit cell are shown (two of the six molecules in each complex of the cage are represented by their oxygen atoms alone so that the cavity may be seen more clearly). The complete structure consists of columns of molecules similar to the one illustrated, packed along the c axis and forming cages around the points (0, 0, $\frac{1}{2}$), (1/3, 2/3, 1/6) and (2/3, 1/3, 5/6).

Di-tertiary-butylnitroxide (DTBN), II, is a stable free radical whose structure has been examined by electron diffraction methods,[68] and its spin Hamiltonian parameters have been extensively studied.[69] It forms a clathrate with Dianin's compound and since it is a relatively large

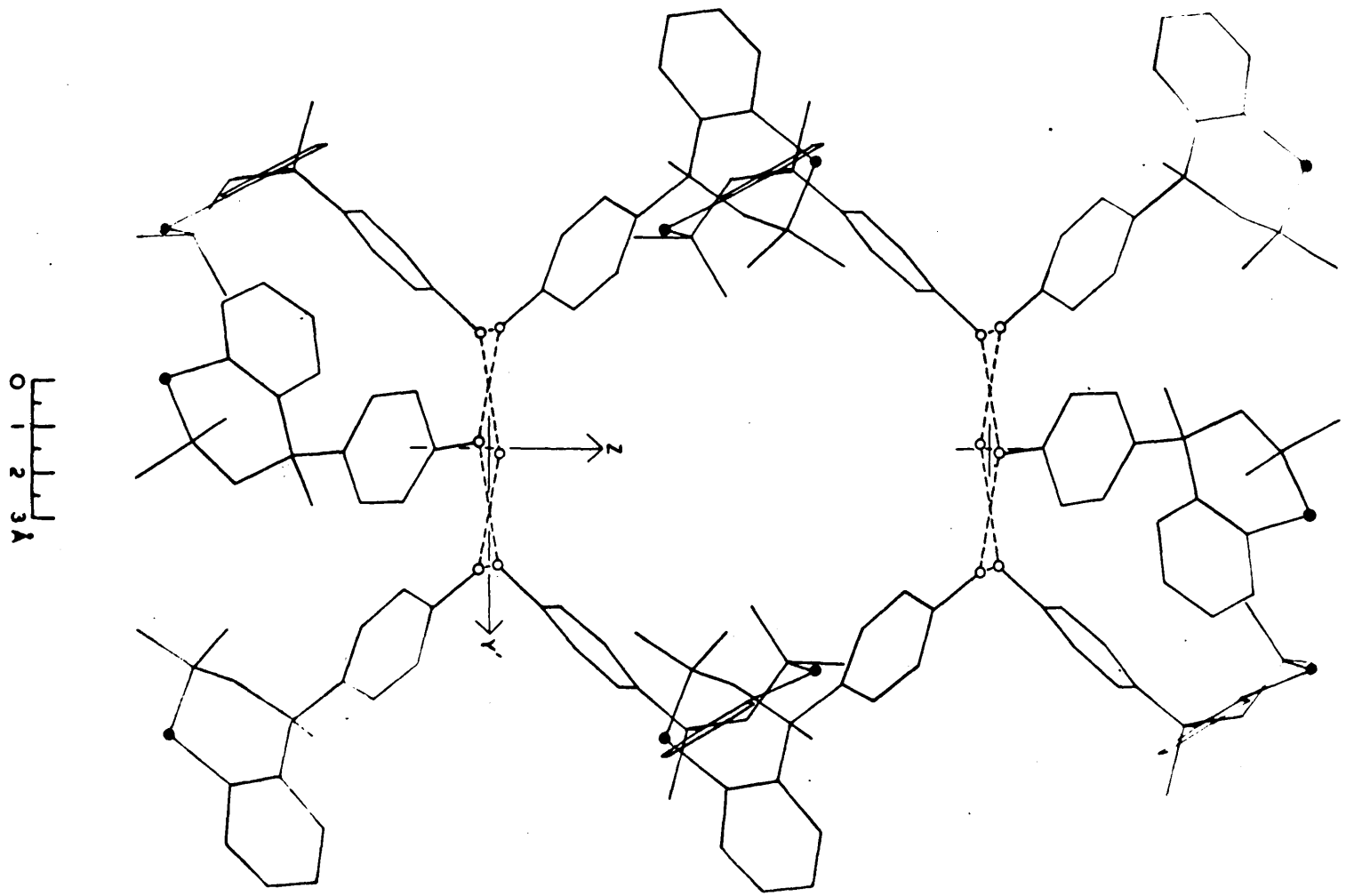

Figure 1. The structure of Dianin's compound projected along the a-axis. Two molecules of (I), which lie directly above and below the cavity as viewed in this direction, have been excluded apart from their hydroxyl oxygen atoms. Y' is perpendicular to the a- and c-axes.

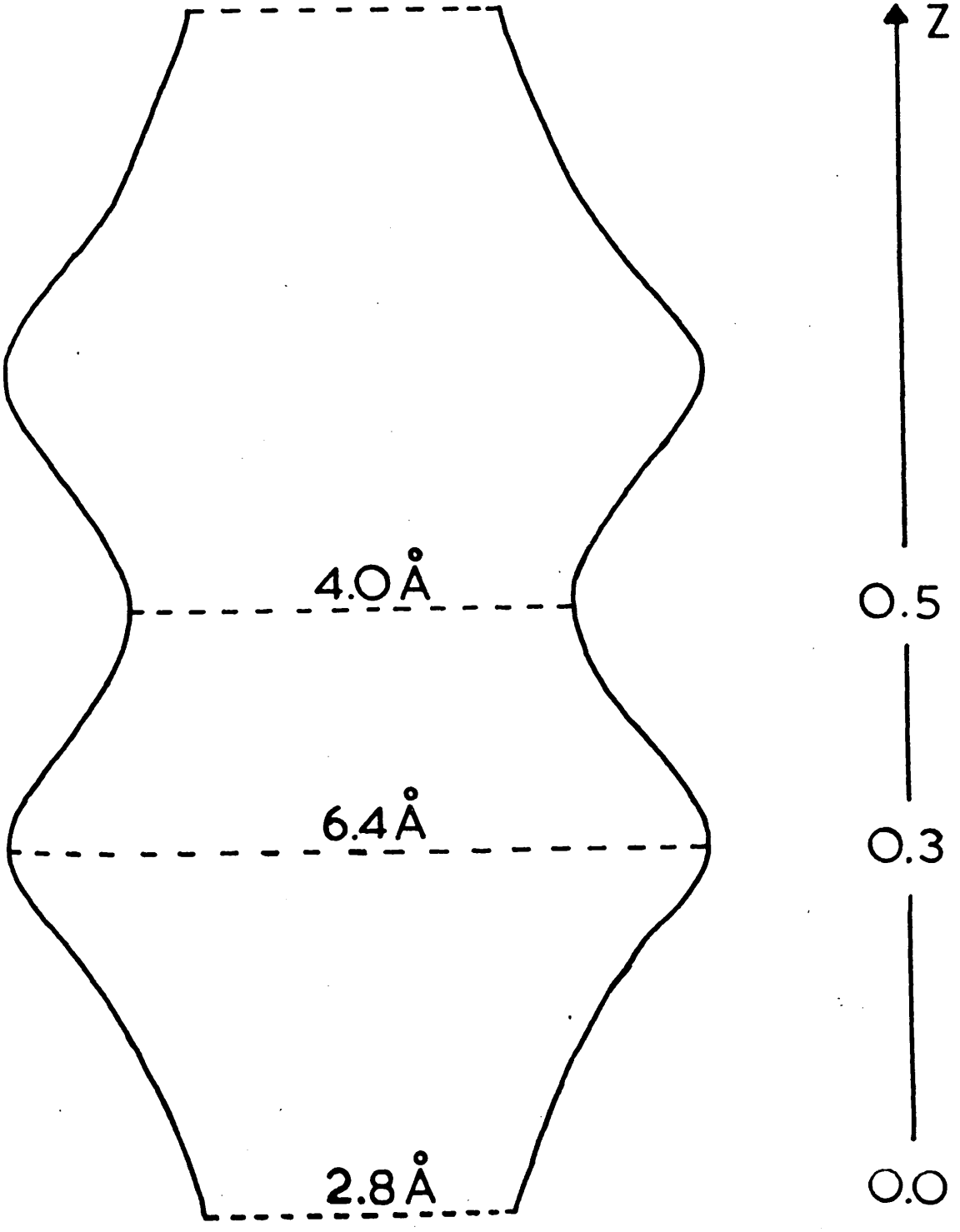

Figure 2. The structure of Dianin's compound projected along the a-axis, in terms of van der Waals radii.

molecule it should interact appreciably with the "host" compound. It was therefore decided to prepare single crystals of this clathrate and to study their electron paramagnetic resonance properties over a wide range of temperature, and so try to obtain information about

(a) the orientation(s) of the radical(s) in the crystal,

(b) the motions of the radicals and the magnitudes of the energy barriers hindering these motions in the clathrate,

(c) the effects of van der Waals interactions on the unpaired electron distribution within the radical, and

(d) the possible formation of compounds when the radicals acquire enough energy to attack the cavity walls formed by the "host" molecules.

2. Experimental procedure and results

Dianin's clathrate containing di-tertiary-butyl-nitroxide was prepared in the following manner. 0·14 g. of di-tertiary-butylnitroxide was added to a solution of 600 mg. of Dianin's compound in 10 ml. of n-decanol, and the solution was left to crystallise slowly for three months. This resulted in the formation of well-formed hexagonal single crystals about 2 mm. along the hexagonal axis and about 0·5 mm. x 0·5 mm. in cross-section, as shown in the accompanying diagrams. In analysing electron

paramagnetic resonance spectra it is convenient to work in terms of a right-handed rectangular coordinate system (see Figure 3). The framework chosen for this purpose was that defined by the vectors $\underline{p}$, $\underline{q}$ and $\underline{r}$ in this figure. These are related to the crystallographic hexagonal unit cell as shown. The angles, θ, are defined later.

Electron paramagnetic resonance derivative spectra were recorded on a Decca-Newport spectrometer system operating at a frequency of 9270 MHz. Standard techniques using 100 KHz. audiomodulation followed by phase-sensitive detection, calibration using proton resonance methods, and temperature variation using a flow system employing gaseous nitrogen as the fluid, were used.

The second moments of the electron paramagnetic resonance absorption spectra of a polycrystalline sample of the clathrate were examined over the temperature range $77^{\circ}K \lesssim T \lesssim 430^{\circ}K$. The experimental second moments obtained are plotted as a function of temperature in Figure 4. Table 1 of Appendix B lists the actual second moment values. In Figure 4 the points marked ▾ were obtained as the sample temperature was reduced;

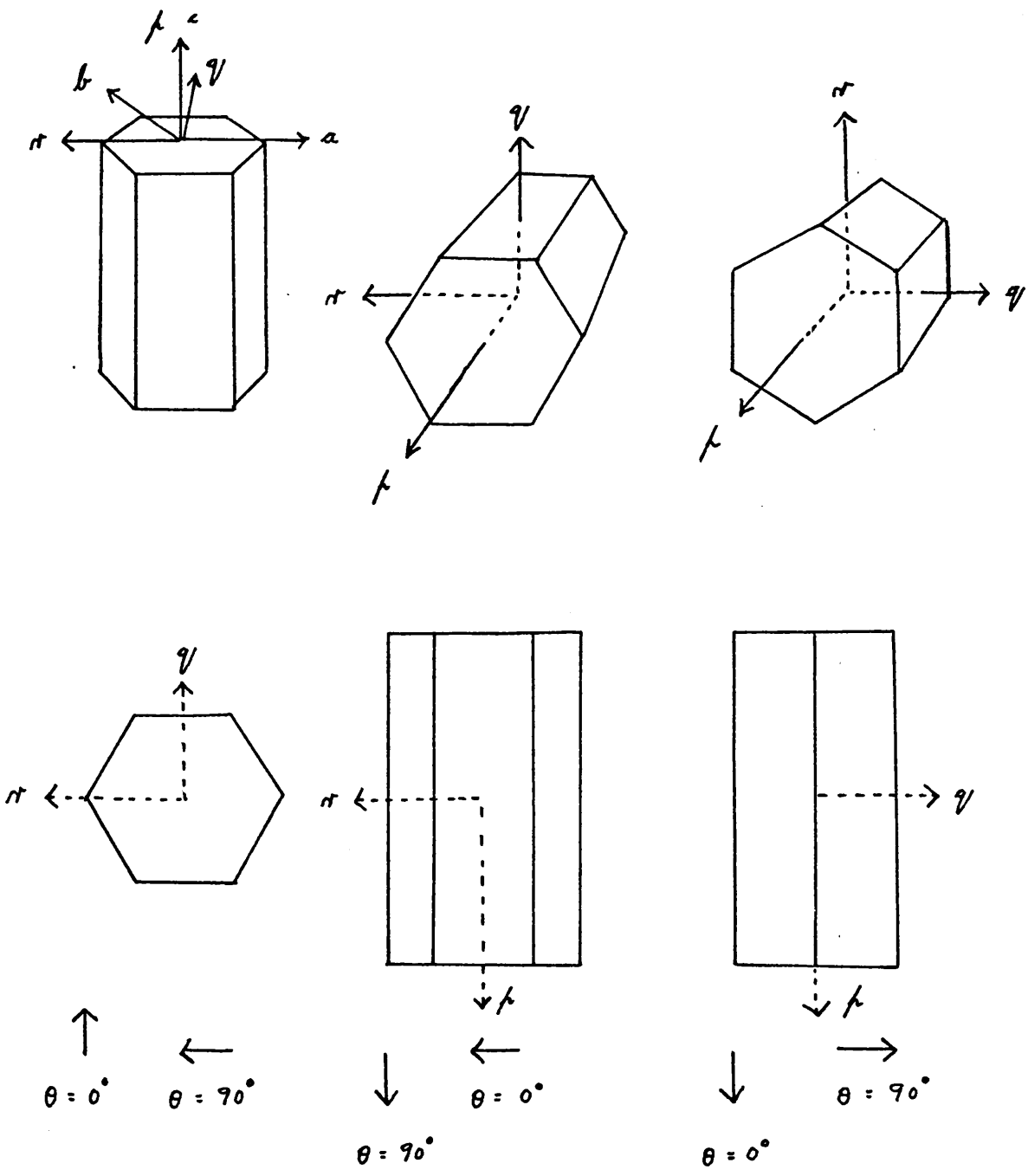

Figure 3

Relationship between the crystallographic axes, a, b, c and the orthogonal axes p, q, r used in this study.

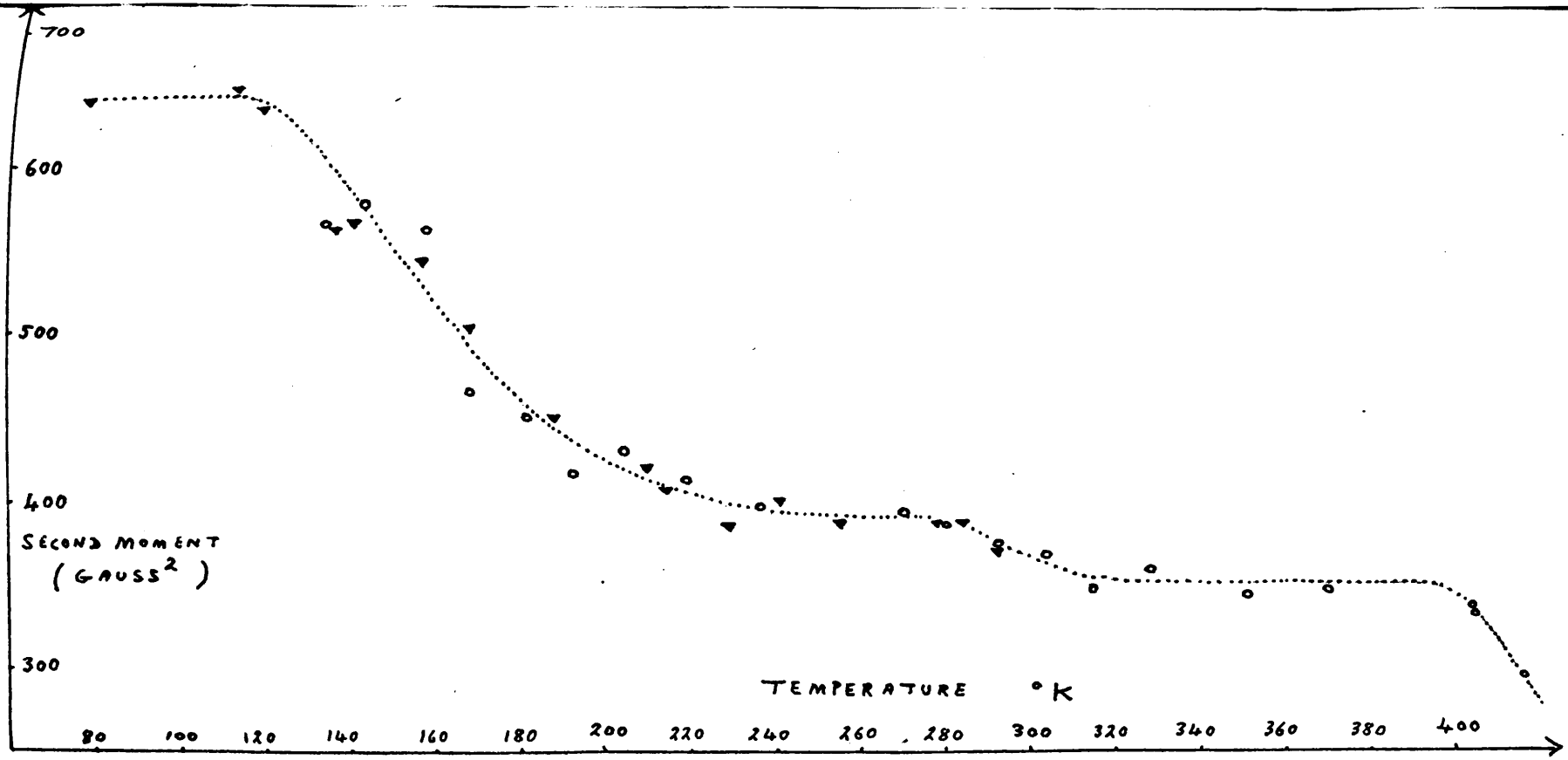

Figure 4

Polycrystalline sample of Dianin's compound containing di-tertiary-butyl-nitroxide: second moment of electron paramagnetic resonance absorption spectrum versus temperature.

the points marked o were obtained as the sample temperature was increased. No hysteresis effects were observed, i.e. this curve implies that no phase changes occur between 77°K and the temperature of sublimation.

First derivative electron paramagnetic resonance line shapes of polycrystalline samples recorded at 77°K, at 260°K, and at 293°K were analysed in detail using Kneubühl's method.[70] Figures 5, 6 and 7 contain experimental derivative curves observed at these temperatures.

Detailed analyses of electron paramagnetic resonance spectra of single crystals were carried out at 93°K, 260°K and 293°K, and at 353°K. Typical single crystal spectra at these temperatures are shown in Figures 8, 9, 10 and 11. Hyperfine coupling and g tensor components were extracted from spectra obtained at 260°K, 293°K, and at 353°K, and in each of these cases the changes in these tensor components were followed as the orientation of the single crystal in the magnetic field was changed. Plots of these tensor components obtained with the crystal mounted about axes p, q and r respectively are shown in the Figures 1 to 24 in Appendix B.

Because of the overlap from several resonances it was not possible to analyse quantitatively spectra recorded at

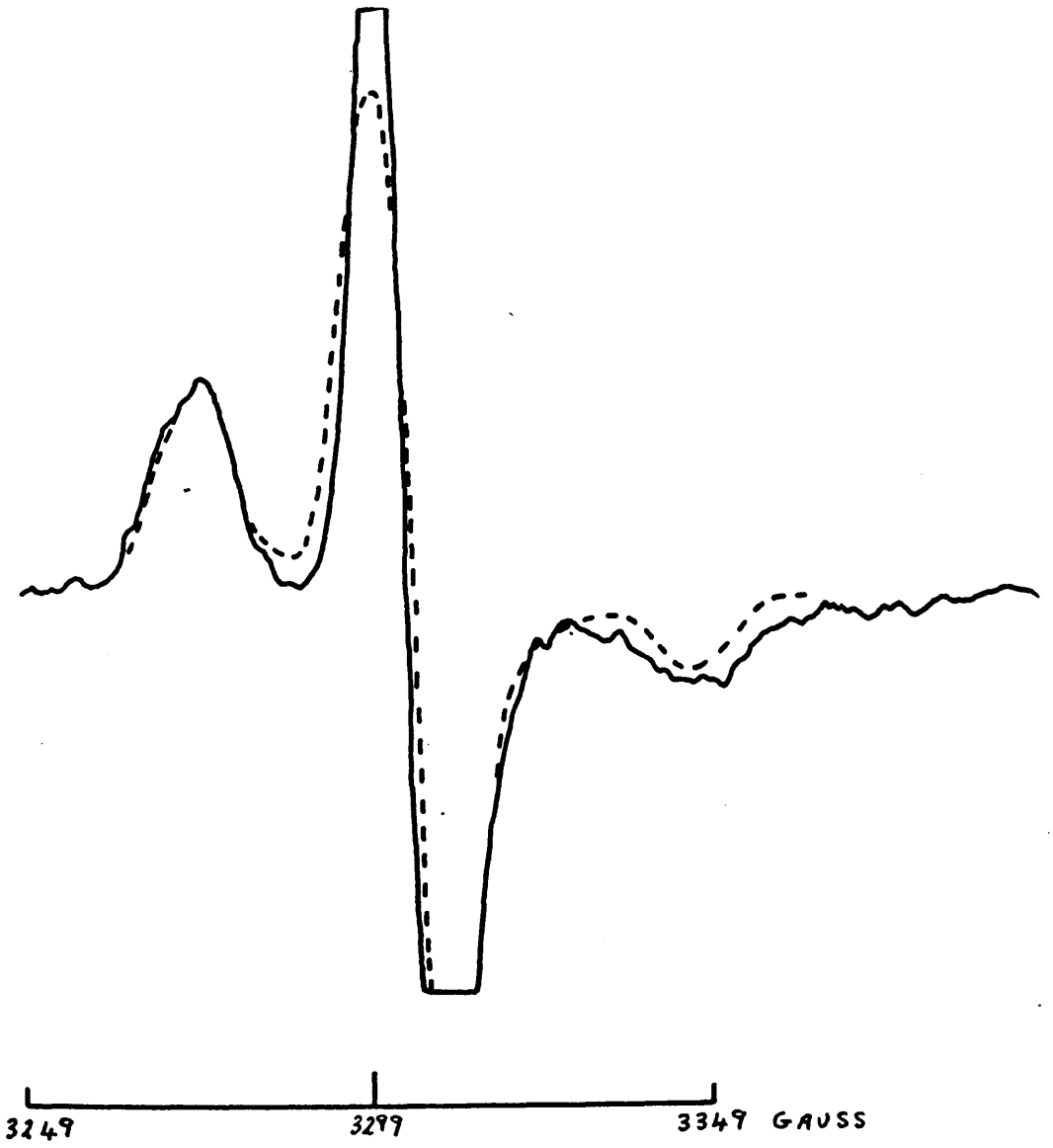

Figure 5

Electron paramagnetic resonance derivative spectrum of a powdered sample of di-tertiary-butylnitroxide in Dianin's compound, recorded at 77°K. The dotted line represents the simulated spectrum due to a polycrystalline magnetically dilute sample of the two nitroxide radicals (in equal concentration) with the magnetic parameters listed in Table I.

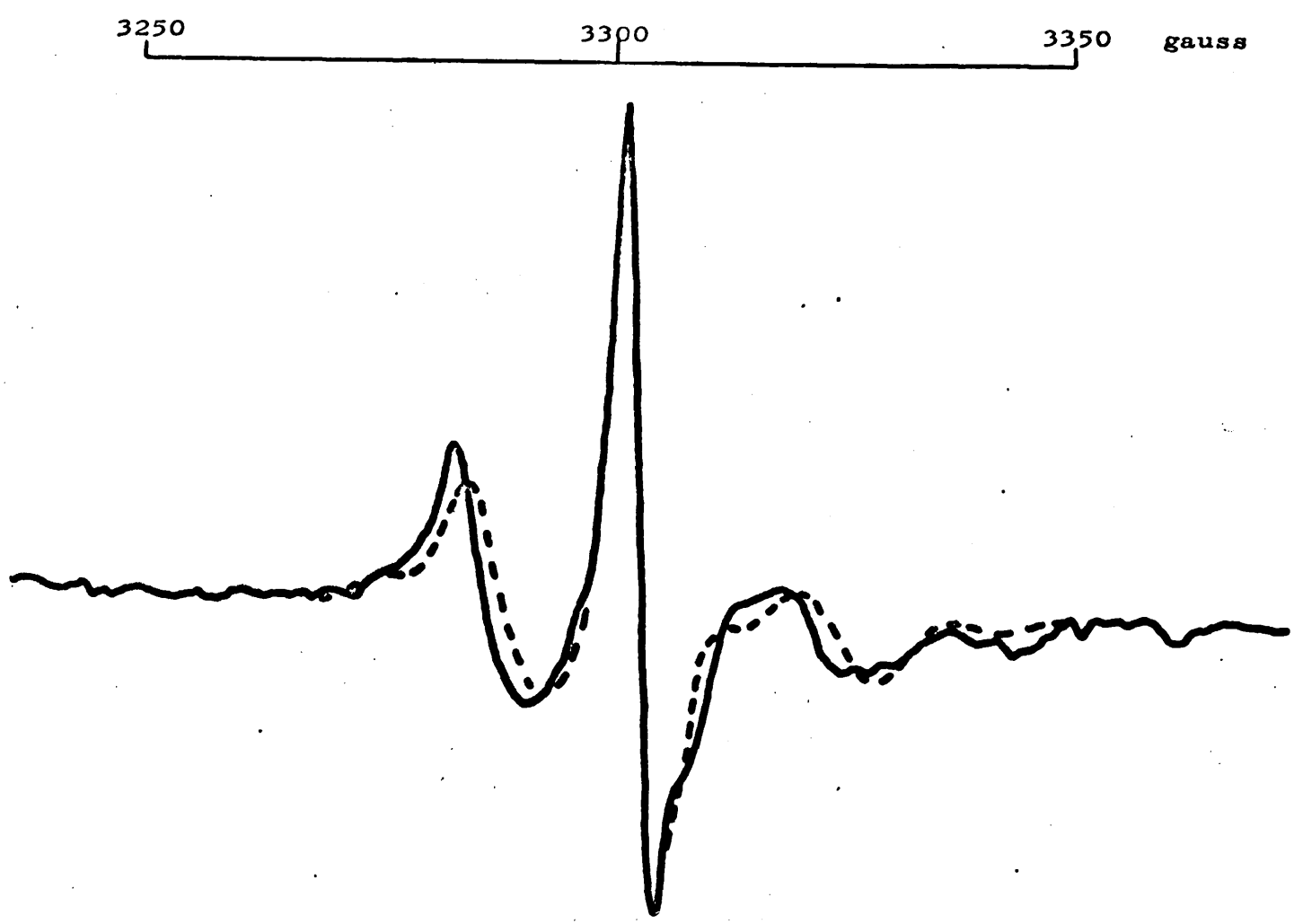

Figure 6

Electron paramagnetic resonance derivative spectrum of a powdered sample of di-tertiary-butylnitroxide in Dianin's compound, recorded at 260°K. The dotted line represents the simulated spectrum due to a polycrystalline magnetically dilute sample of the two nitroxide radicals (in equal concentration) with the magnetic parameters listed in Table II.

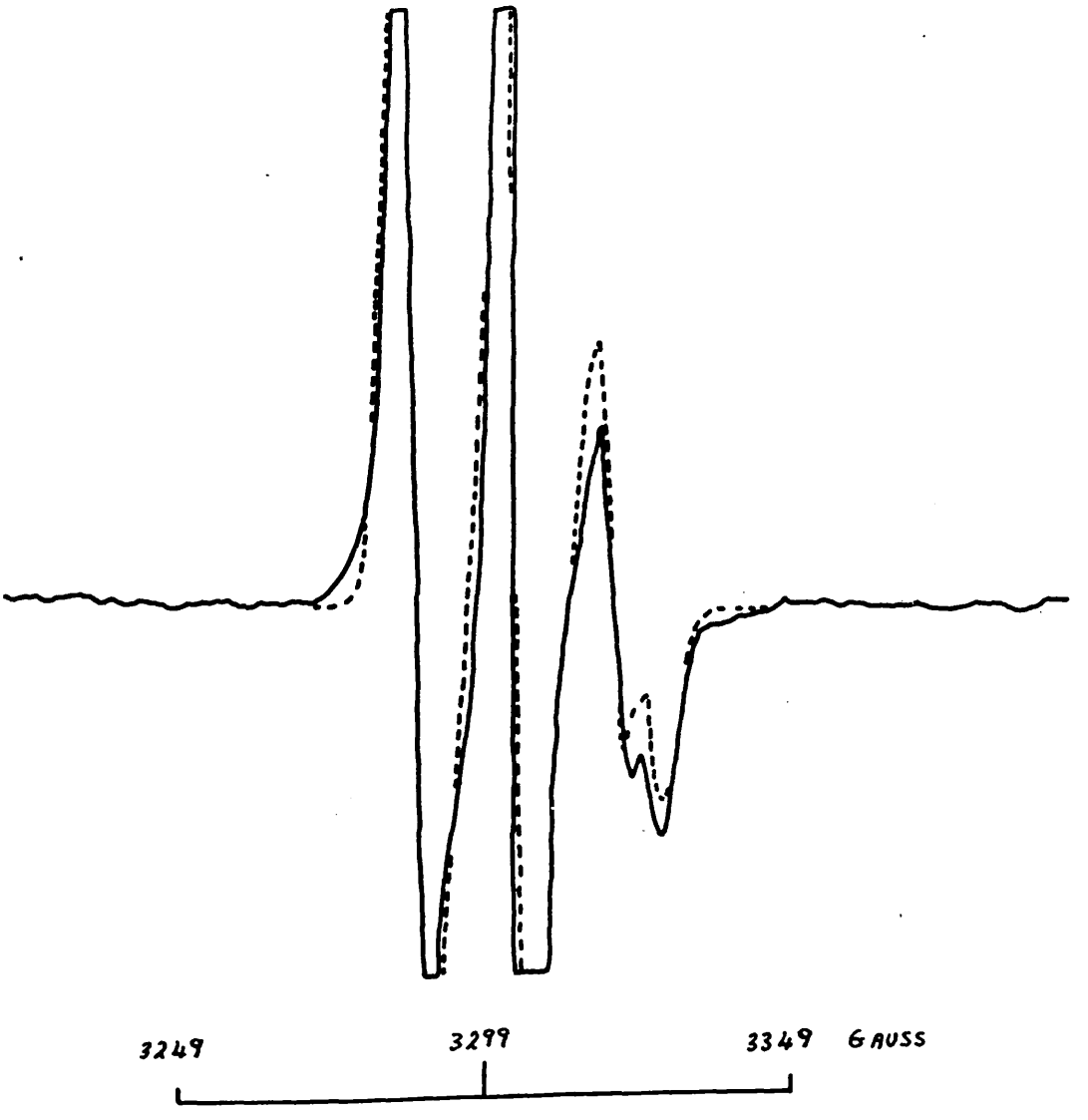

Figure 7

Electron paramagnetic resonance derivative spectrum of a powdered sample of di-tertiary-butylnitroxide in Dianin's compound, recorded at 293°K. The dotted line represents the simulated spectrum due to a polycrystalline magnetically dilute sample of the two nitroxide radicals (in equal concentration) with the magnetic parameters listed in Table III.

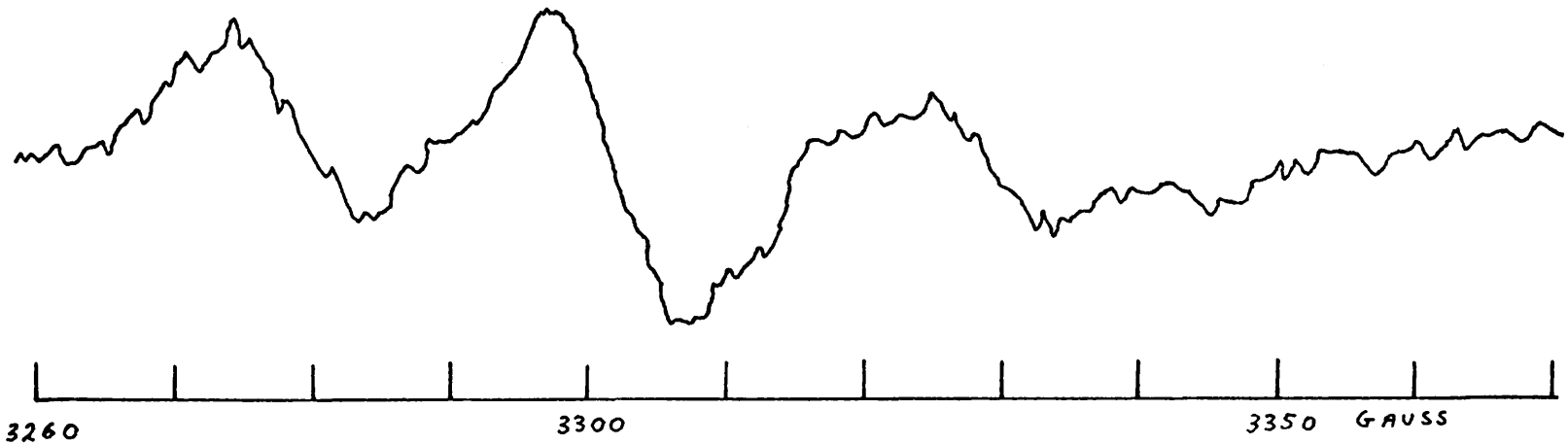

Figure 8

Electron paramagnetic resonance derivative spectrum, recorded at 93°K. of a single crystal of Dianin's compound containing di-tertiary-butylnitroxide, mounted on axis r, at an orientation with $\theta = 90°$.

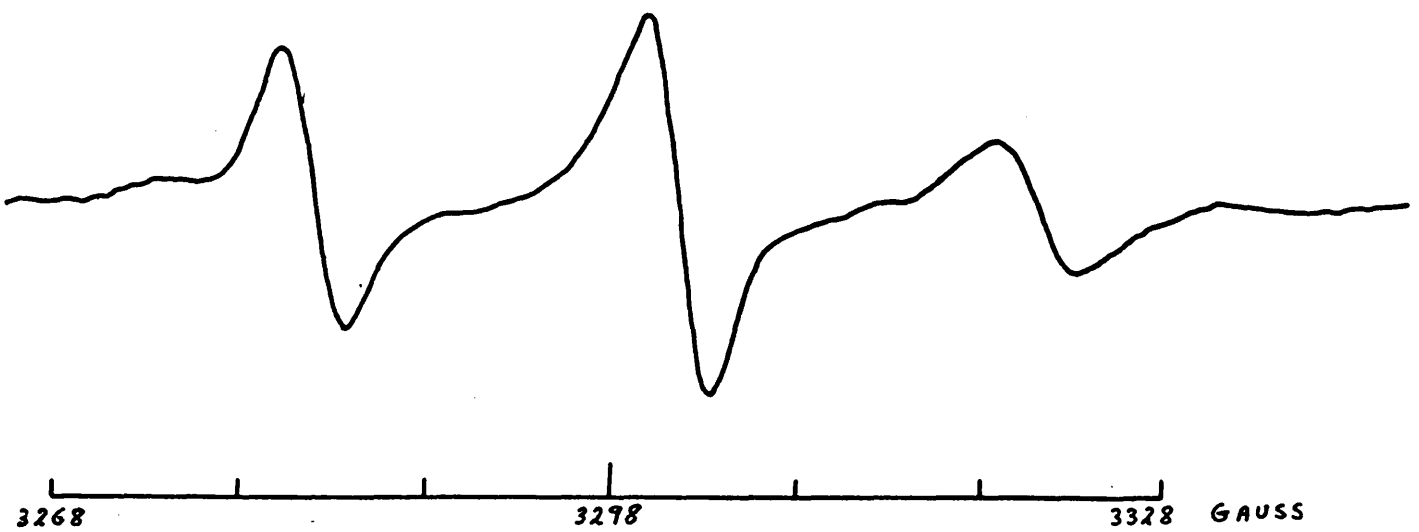

Figure 9

Electron paramagnetic resonance derivative spectrum, recorded at 260°K. of a single crystal of Dianin's compound containing di-tertiary-butylnitroxide, mounted on axis r, at an orientation with $\theta = 90°$.

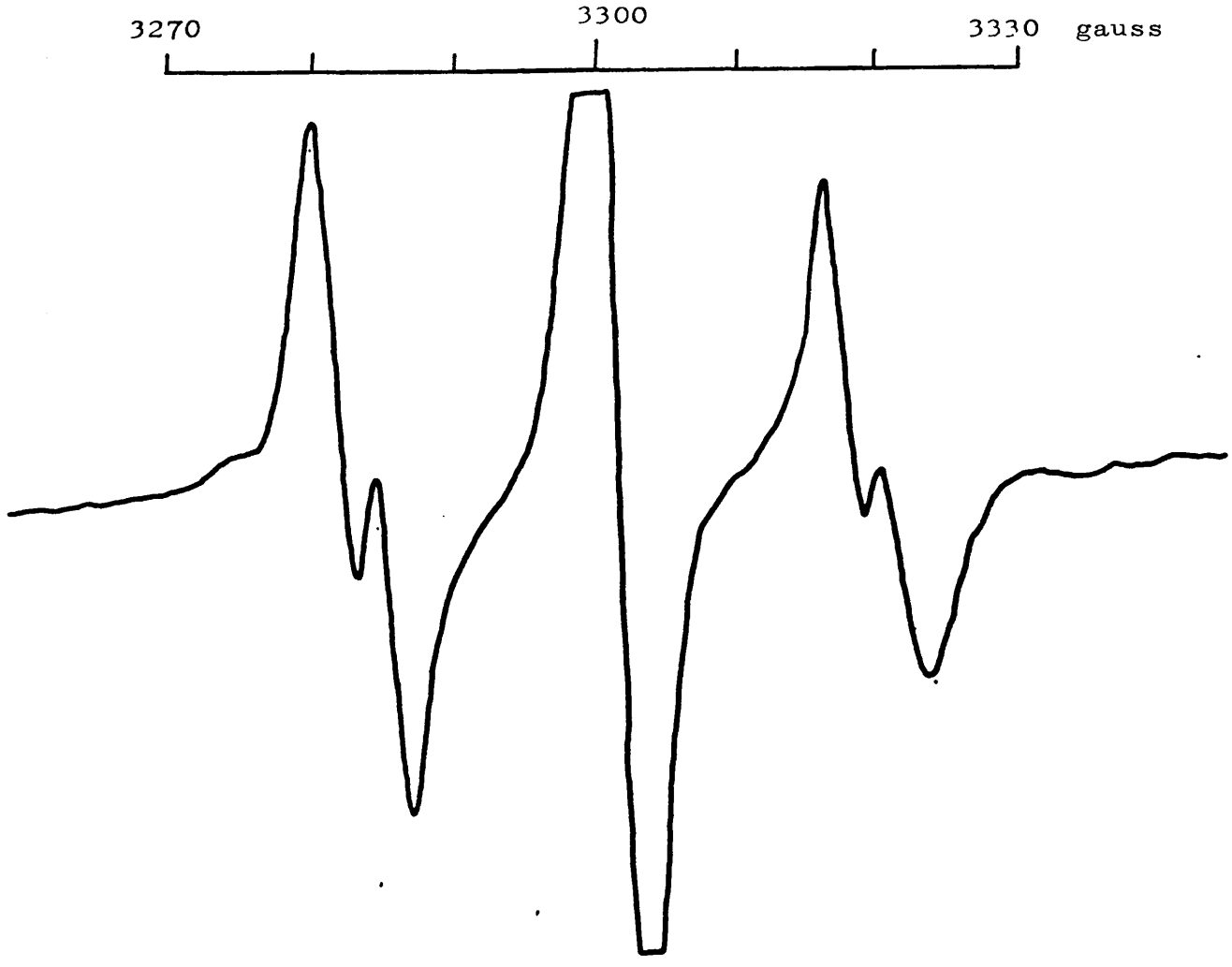

Figure 10

Electron paramagnetic resonance derivative spectrum, recorded at 293°K. of a single crystal of Dianin's compound containing di-tertiary-butylnitroxide, mounted on axis r, at an orientation with $\theta = 90°$.

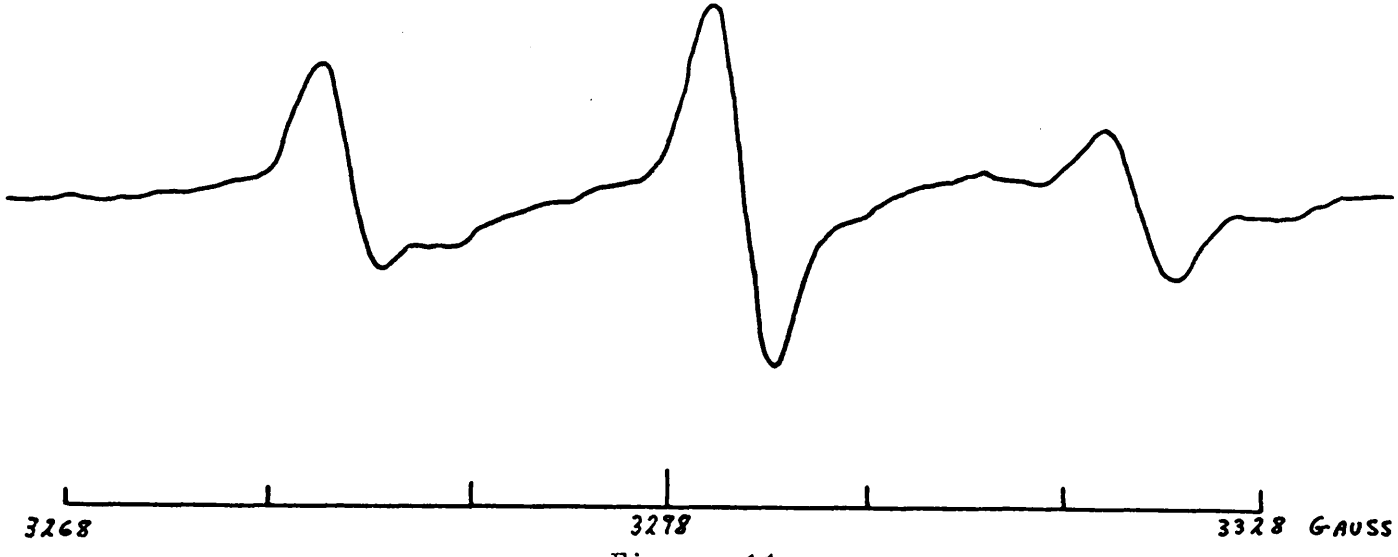

Figure 11

Electron paramagnetic resonance derivative spectrum, recorded at 353°K, of a single crystal of Dianin's compound containing di-tertiary-butylnitroxide, mounted on axis r, at an orientation with $\theta = 90°$.

93°K, though it was obvious that at this temperature spectra were reproduced at 60° intervals when the crystal was mounted along the p axis direction.

3. Interpretation and discussion of results

A. The polycrystalline spectra

The curve of second moment versus temperature shows that there is unlikely to be any motion which could affect the absorption spectrum below about 120°K. Consequently the derivative of the absorption curve at 77°K represents the electron paramagnetic resonance absorption spectrum of the rigid lattice. By making use of van Vleck's expression[71] it may be shown that the second moment of the electron paramagnetic resonance absorption spectrum for a polycrystalline sample of magnetically dilute, rigid nitroxide free radical is given by

$$\langle \Delta H^2 \rangle = \frac{4}{15}\gamma_N^2 h^2 I_N(I_N + 1) \langle r^{-6} \rangle + \frac{2}{3} a^2$$

where a is the ^{14}N isotropic hyperfine coupling constant, $I_N = 1$, and $\gamma_N = 1{\cdot}9335 \times 10^3$ gauss^{-1}sec^{-1}. $\underline{r}$ is the vector joining the unpaired electron to the ^{14}N nucleus. In this expression it is assumed that only intramolecular effects are important contributors to the second moment and that intermolecular interactions may be ignored. Since $\langle \Delta H^2 \rangle$ is a function of $\langle r^{-6} \rangle$ this is a good approximation. 'a' (see later) is 14 ± 1 gauss.

$< \Delta H^2 >$ at 77°K. is 640 ± 10 gauss^2, therefore,

$$640 = 2{\cdot}2171 \times 10^{-48} < r^{-6} > + \frac{2}{3}(14)^2$$

giving

$$\left(\frac{1}{< r^{-6} >}\right)^{\frac{1}{6}} = 0{\cdot}41 \pm 0{\cdot}01 \text{ Å}$$

This may be taken as a measure of r, the average distance of the unpaired electron from the nitrogen nucleus in di-tertiary-butylnitroxide inside the clathrate at 77°K.

If the spin Hamiltonian for the radical is written in the form 3.1

$$\mathcal{H} = \beta_e \underline{H}.\underline{g}.\underline{S} + \underline{S}.\underline{T}.\underline{I} \qquad 3.1$$

then the first derivative of the electron paramagnetic resonance absorption spectrum of the polycrystalline sample at 77°K (Figure 5) can be analysed in terms of superpositions of curves of the kind described by Kneubühl[70] (see Appendix A) and the principal components of the g tensor and of the hyperfine tensor, $\underline{T}$, and the line broadening function β [$\beta = f(m_I)$] can be obtained from it. Broadening functions are assumed to have the Gaussian form, $(2\pi)^{-\frac{1}{2}}\beta^{-1} \exp[-(h' - h)^2 (2\beta^2)^{-1}]$. In order to account for the shoulders on the extremities of Figure 5 it is necessary to assume that two nitroxide radicals with slightly different spin Hamiltonian parameters contribute to the spectrum. The spin Hamiltonian

parameters for these two radicals are given in the following table. The polycrystalline line shape function calculated from them is shown superposed in Figure 5.

Table I

Radical	g_{11}	g_{22}	g_{33}	$< g >$	$T_{11}(^{14}N)$	$T_{22}(^{14}N)$
A	2·01072	2·00585	2·00076	2·00578	15·00	2·00
B	2·00950	2·00463	2·00136	2·00516	5·00	4·00

Radical	$T_{33}(^{14}N)$	$a(^{14}N)$	$\beta(m_I = 1)$	$\beta(m_I = 0)$	$\beta(m_I = -1)$
A	34·00	17·00	5·0	2·5	3·0
B	40·40	16·47	4·0	2·5	3·0

T values are given in gauss.

Limits of error for g_{11}, g_{22}, g_{33}, T_{11}, T_{22}, T_{33}, and for β are 0·001, 0·001, 0·001, 0·3 gauss, 0·3 gauss, 0·3 gauss and 0·4 respectively. The anisotropic contributions $A^D_{11}(^{14}N)$, $A^D_{22}(^{14}N)$ and $A^D_{33}(^{14}N)$ for these radicals are (in gauss)

Radical	$A^D_{11}(^{14}N)$	$A^D_{22}(^{14}N)$	$A^D_{33}(^{14}N)$
A	-2·00	-15·00	17·00
B	-11·47	-12·47	23·93

At 115°K the nitroxide radicals undergo some kind of reorientational motion within the cavities of the clathrate and the second moment gradually falls. It is not until a temperature of 260°K is attained that this motion is fully established, at which temperature the second moment becomes 390 ± 10 gauss.[2] Further information can be obtained about the nature of this motion from a quantitative study of the first derivative of the electron paramagnetic resonance absorption line shape at 260°K (Figure 6). This figure shows that there are two kinds of nitroxide radical present in the polycrystalline sample; each of these contributes its own Kneubühl spectrum to the observed absorption. The normalised absorption line shape function for a polycrystalline sample at 260°K can therefore be written as

$$F(h') = \omega_1 f_1(h') + (1 - \omega_1) f_2(h')$$

where ω_1 is the fraction of radicals of kind 1. $f_1(h')$ is the normalised line shape function for these radicals and $f_2(h')$ is the normalised line shape function for radicals of kind 2. $f_1(h')$ and $f_2(h')$ are the Kneubühl curves appropriate to radicals 1 and 2, respectively. Analysis of Figure 6 shows that $\omega_1 = 0{\cdot}5$ and gives the following spin Hamiltonian parameters

Table II

Radical	g_{11}	g_{22}	g_{33}	$< g >$	$T_{11}(^{14}N)$	$T_{22}(^{14}N)$	$T_{33}(^{14}N)$
1	2·00767	2·00603	2·00233	2·00534	11·00	4·70	33·25
2	2·00585	2·00463	2·00439	2·00496	5·20	20·60	20·60

Radical	$a(^{14}N)$	$\beta(m_I = 1)$	$\beta(m_I = 0)$	$\beta(m_I = -1)$
1	16·32	2·70	1·60	2·70
2	15·47	2·50	1·70	3·60

T values are given in gauss.

Limits of error are the same as in Table I.

Half of the radicals are still rigidly held within the clathrate and the others, radical 2, undergo rapid reorientational motion about an axis fixed in the molecular framework of the radical. Under these conditions it can be shown that the van Vleck expression is modified to[72]

$$< \Delta H^2 > = \omega_1 [\tfrac{4}{15}\gamma_N^2 \hbar^2 I_N(I_N + 1) < r^{-6} > + \tfrac{2}{3} a^2]$$

$$+ (1 - \omega_1)\{[\tfrac{4}{15}\gamma_N^2 \hbar^2 I_N(I_N + 1) < r^{-6} >][\tfrac{1}{4}(3\cos^2\gamma - 1)^2] + \tfrac{2}{3} a^2\}$$

i.e. $390 = 0{\cdot}5\ [640] + 0{\cdot}5\{[509][\tfrac{1}{4}(3\cos^2\gamma - 1)^2 + 131]\}$

i.e. $\gamma = 49°29' \pm 6°$ or $60°21' \pm 7°$

i.e. the angle formed by the axis of reorientation and the mean electron-nuclear vector is $49° \pm 6°$, or $60° \pm 7°$.

At 275°K. the second moment of the polycrystalline absorption curve falls again until the temperature reaches 325°K, at which temperature it has a value of 350 ± 10 gauss^2. The additional motion responsible for this change in the second moment and the spin Hamiltonian parameters at 293°K and at 353°K will be considered in greater detail when the spectra obtained from single crystals are discussed. At 395°K the second moment again falls drastically as a result of sublimation and consequent breakdown of the clathrate structure.

The first derivative of the absorption spectrum of the polycrystalline sample at 293°K is shown in Figure 7, together with the theoretical first derivative spectrum arising from two distinct kinds of nitroxide radical calculated by Kneubühl's method. The spin Hamiltonian parameters of these radicals are given below.

Table III

Radical	g_{11}	g_{22}	g_{33}	$\langle g \rangle$	$T_{11}(^{14}N)$	$T_{22}(^{14}N)$	$T_{33}(^{14}N)$
aniso- tropic species	2·00555	2·00391	2·00379	2·00442	5·50	20·70	20·60
iso- tropic species	2·00536	2·00515	2·00500	2·00517	16·20	16·35	16·40

Radical	$a(^{14}N)$	$\beta(m_I = 1)$	$\beta(m_I = 0)$	$\beta(m_I = -1)$
	15·60	2·60	2·60	2·60
	16·32	2·60	2·60	2·60

T values are given in gauss.

Limits of error are the same as in Table I.

If a simple Boltzmann expression is used to calculate the energy of activation for these two motions described above, then that which commences at 115°K is found to have an activation energy of 0·21 ± 0·05 Kcal/mole, while that which is manifested in the neighbourhood of room temperature has an activation energy of 0·41 ± 0·05 Kcal/mole. These low values imply that only van der Waals forces have to be overcome for motion to begin.[2,33,73]

B. Spectra obtained from single crystals

The experimental data given in Figures 1 to 24 in Appendix B were fitted by means of least squares analysis to curves of the type

$$g^2 = g_{pp}^2\cos^2\theta + g_{qq}^2\sin^2\theta + 2g_{pq}^2\cos\theta\sin\theta$$

and

$$T^2 = T_{pp}^2\cos^2\theta + T_{qq}^2\sin^2\theta + 2T_{pq}^2\cos\theta\sin\theta$$

and thereby the elements of the g^2 tensor and of the T^2

tensor referred to the rectangular frame pqr were determined.[74] These tensors at temperatures of 260°K, 293°K and 353°K are given below and calculated g^2 and T^2 values using this data are plotted in the appropriate figures in Appendix B.

g^2 and T^2 tensors at 260°K

$$g^2 = \begin{vmatrix} 4{\cdot}02528 \pm 0{\cdot}00020 & 0{\cdot}00 \pm 0{\cdot}01 & 0{\cdot}00 \pm 0{\cdot}01 \\ 0{\cdot}00 \pm 0{\cdot}01 & 4{\cdot}02372 \pm 0{\cdot}00020 & 0{\cdot}00 \pm 0{\cdot}01 \\ 0{\cdot}00 \pm 0{\cdot}01 & 0{\cdot}00 \pm 0{\cdot}01 & 4{\cdot}02372 \pm 0{\cdot}00020 \end{vmatrix}$$

$$T^2 = \begin{vmatrix} 236 \pm 5 & 0 \pm 10 & 0 \pm 10 \\ 0 \pm 10 & 2942 \pm 5 & 0 \pm 10 \\ 0 \pm 10 & 0 \pm 10 & 2945 \pm 5 \end{vmatrix}$$

The spectra of the stationary species noted in the polycrystalline spectrum were too weak to be observed in the single crystal spectra at 260°K.

g^2 and T^2 tensors at 293°K

anisotropic species

$$g^2 = \begin{vmatrix} 4{\cdot}02528 \pm 0{\cdot}00020 & 0{\cdot}00 \pm 0{\cdot}01 & 0{\cdot}00 \pm 0{\cdot}01 \\ 0{\cdot}00 \pm 0{\cdot}01 & 4{\cdot}02408 \pm 0{\cdot}00020 & 0{\cdot}00 \pm 0{\cdot}01 \\ 0{\cdot}00 \pm 0{\cdot}01 & 0{\cdot}00 \pm 0{\cdot}01 & 4{\cdot}02384 \pm 0{\cdot}00020 \end{vmatrix}$$

$$T^2 = \begin{matrix} 289 \pm 17 & 0 \pm 10 & 0 \pm 10 \\ 0 \pm 10 & 2872 \pm 17 & 0 \pm 10 \\ 0 \pm 10 & 0 \pm 10 & 2887 \pm 17 \end{matrix}$$

isotropic species

$$g^2 = \begin{vmatrix} 4{\cdot}02412 \pm 0{\cdot}00020 & 0{\cdot}00 \pm 0{\cdot}01 & 0{\cdot}00 \pm 0{\cdot}01 \\ 0{\cdot}00 \pm 0{\cdot}01 & 4{\cdot}02396 \pm 0{\cdot}00020 & 0{\cdot}00 \pm 0{\cdot}01 \\ 0{\cdot}00 \pm 0{\cdot}01 & 0{\cdot}00 \pm 0{\cdot}01 & 4{\cdot}02388 \pm 0{\cdot}00020 \end{vmatrix}$$

$$T^2 = \begin{vmatrix} 1985 \pm 25 & 0 \pm 10 & 0 \pm 10 \\ 0 \pm 10 & 2058 \pm 25 & 0 \pm 10 \\ 0 \pm 10 & 0 \pm 10 & 2045 \pm 25 \end{vmatrix}$$

g^2 and T^2 tensors at 353°K

$$g^2 = \begin{vmatrix} 4{\cdot}02524 \pm 0{\cdot}00020 & 0{\cdot}00 \pm 0{\cdot}01 & 0{\cdot}00 \pm 0{\cdot}01 \\ 0{\cdot}00 \pm 0{\cdot}01 & 4{\cdot}02355 \pm 0{\cdot}00020 & 0{\cdot}00 \pm 0{\cdot}01 \\ 0{\cdot}00 \pm 0{\cdot}01 & 0{\cdot}00 \pm 0{\cdot}01 & 4{\cdot}02359 \pm 0{\cdot}00020 \end{vmatrix}$$

$$T^2 = \begin{vmatrix} 294 \pm 17 & 0 \pm 10 & 0 \pm 10 \\ 0 \pm 10 & 2981 \pm 17 & 0 \pm 10 \\ 0 \pm 10 & 0 \pm 10 & 2954 \pm 17 \end{vmatrix}$$

The components of the T^2 tensor are given in MHz^2.

Table IV

The principal components of the g tensor of di-tertiary-butylnitroxide within Dianin's compound.

Radical	Temp.	g_{pp}	g_{qq}	g_{rr}	$< g >$
anisotropic species	260°K	2·00631	2·00592	2·00592	2·00605
anisotropic species	293°K	2·00631	2·00601	2·00595	2·00609
isotropic species	293°K	2·00602	2·00598	2·00596	2·00599
anisotropic species	353°K	2·00630	2·00588	2·00589	2·00602

The mean error on the g values is 0·00005.

Table V

The principal components of the T tensor of di-tertiary-butylnitroxide within Dianin's compound.

Radical	Temp.	$T_{pp}(^{14}N)$	$T_{qq}(^{14}N)$	$T_{rr}(^{14}N)$	$a(^{14}N)$
anisotropic species	260°K	15·4±0·2 (5·5±0·1)	54·2±0·1 (19·4±0·03)	54·3±0·1 (19·4±0·03)	41·3±0·1 (14·8±0·05)
anisotropic species	293°K	17·0±0·5 (6·1±0·2)	53·6±0·2 (19·1±0·1)	53·7±0·2 (19·2±0·1)	41·4±0·3 (14·8±0·1)
isotropic species	293°K	44·5±0·3 (15·9±0·1)	45·4±0·3 (16·2±0·1)	45·2±0·3 (16·2±0·1)	45·0±0·3 (16·1±0·1)
anisotropic species	353°K	17·1±0·5 (6·1±0·2)	54·6±0·2 (19·5±0·1)	54·3±0·2 (19·4±0·1)	42·0±0·3 (15·0±0·1)

The T tensor components are given in MHz. and the corresponding value in gauss is given in brackets.

Several interesting conclusions can immediately be drawn from these results.

(1) The axes p, q and r are principal axes at 260°K, at 293°K and at 353°K. In the cases where $g^2_{qq} = g^2_{rr}$ and

$T^2_{qq} = T^2_{rr}$, the radicals described by these tensors are rotating about the $\bar{3}$ axis of the crystal, i.e. axis p.

(2) At 260°K and at 353°K only one kind of rotating species is present and these species seem to be magnetically identical within the limits of accuracy of the experimental data. At 293°K, on the other hand, there are two magnetically different radicals present. The first of these is identical, again within the limits of accuracy of the experimental data, with the species at 260°k and 353°K, described in (1) on previous page. The second species, present in equal concentration, is rotating rapidly and randomly within cavities in the clathrate. There is not enough room within the cages described earlier in this thesis for di-tertiary-butyl-nitroxide to undergo random rotation, hence at least half of the nitroxide radicals trapped within the clathrate must be held between the columns of molecules of the kind shown in Figure 1, or in grossly malformed cages.

(3) The isotropically rotating species disappears between 293°K and 353°K and reappears reversibly when the temperature is again lowered to 293°K. This implies that the unpaired electron of this kind of nitroxide radical is being exchanged reversibly with the lattice,

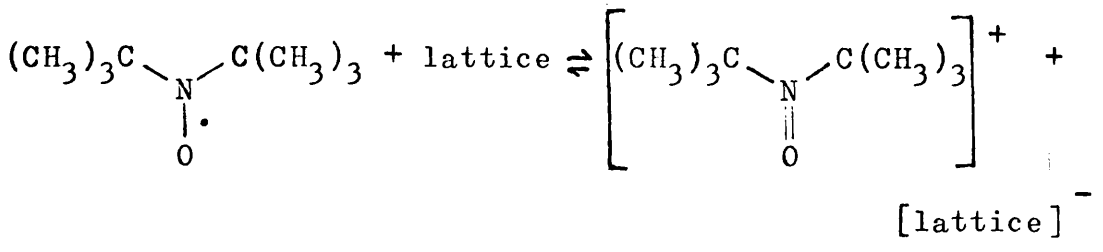

and that the hyperfine interactions resulting from this exchange are broadening the spectrum to such an extent that the electron paramagnetic resonance spectrum of the radical species participating in this equilibrium is too broad to be observed. It is possible that this exchange is the first step in the breakdown of the crystal structure at higher temperatures.

(4) As already explained, because of overlapping of spectra, it was not possible to carry out detailed single crystal analyses at 93°K, i.e. it was not possible to obtain direct estimates of the principal components of the g and hyperfine tensors for rigidly held di-tertiary-butylnitroxide molecules in the clathrate. Values of these g and T components with respect to the molecular framework x, y and z shown in Figure 12, have already been given by McConnell.[69] These values are:

g_{xx} = 2·0089 ± 0·0003; g_{yy} = 2·0061 ± 0·0003; g_{zz} = 2·0027 ± 0·0003; T_{xx} = 19·9 ± 1·5 MHz (7·1 ± 0·5 gauss); T_{yy} = 15·7 ± 1·5 MHz. (5·6 ± 0·5 gauss);

T_{zz} = 89·6 ± 4·2 MHz. (32 ± 1·5 gauss).

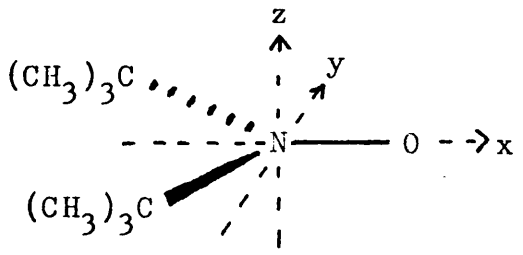

Figure 12

The x-axis lies along the N - O bond, the z-axis along the π-orbital of nitrogen, and the y-axis in a direction perpendicular to the x- and z-axes.

If the axis about which rapid rotation takes place makes angles of $\cos^{-1}\alpha$, $\cos^{-1}\beta$ and $\cos^{-1}\gamma$ with the principal axes x,y and z respectively, then the principal hyperfine interactions parallel and perpendicular to the rotation axis are[75]

$$T_{11\ell} = \alpha^2 T_{xx} + \beta^2 T_{yy} + \gamma^2 T_{zz}$$

$$T_{1r} = \tfrac{1}{2}[(1 - \alpha^2)T_{xx} + (1 - \beta^2)T_{yy} + (1 - \gamma^2)T_{zz}]$$

Analogous equations may be written for the relationship between the observed g tensor components and those given by McConnell for the static system. By using the values obtained at 293°K for the g and hyperfine components of the anisotropically rotating species together with McConnell's

values for the corresponding components of the static system, it is easily shown that

$$\cos^{-1}\alpha = 86°59'$$
$$\cos^{-1}\beta = 9°43'$$
$$\cos^{-1}\gamma = 80°45'$$

Since the axis of rotation coincides with the $\bar{3}$ axis in the crystal, these direction cosines immediately define the orientation of the rotating molecule in the crystal. However, because of computational effects in evaluating α, β and γ and because of the rather large limits of error in the values quoted by Griffith, Cornell and McConnell[69] for their hyperfine tensor components, these angles may be as much as 10° in error.

4. Summary of Part III

Polycrystalline and single crystal electron paramagnetic resonance spectra of di-tertiary-butylnitroxide in Dianin's compound have been examined over the temperature range $77^{\circ}K \lesssim T \lesssim 430^{\circ}K$. The orientations of the radicals in the crystal have been determined, and the motions of the radicals and the magnitudes of the energy barriers hindering these motions in the clathrate, have been characterised. Changes in van der Waals interactions as the temperature changes appear to affect hyperfine tensor components, but it has not been possible to obtain quantitative information about changes in the electron distribution responsible for these effects. Other radicals do not appear to be formed as the temperature is raised. At higher temperatures the lattice sublimes.

References to Part III

1. K.A. Kobe, W.G. Domask, Petroleum Refiner, 1952, 31, 106.
2. D.F. Evans, R.E. Richards, Proc. Roy. Soc. (London), 1954, A, 223, 238.
3. F.D. Cramer, Rev. Pure Appl. Chem., 1955, 5, 143.
4. G. Montel, Bull. Soc. chim. France, 1955, 1013.
5. W. Schlenk, Svensk Kem. Tidskr., 1955, 67, 435.
6. L. Mandelcorn, Chem. Rev., 1959, 59, 827.
7. J.H. van der Waals, J.C. Platteeuw, Adv. Chem. Phys., 1959, 2, 1.
8. J.R. Meakins, Progr. Dielectrics, 1961, 3, 191 - 192.
9. M.M. Hagan, J. Chem. Educ., 1963, 40, 643.
10. V.M. Bhatnagar, Def. Sci. J. (N. Dehli), 1963, Suppl. 13, 57.
11. C. Asselineau, J. Asselineau, Ann. Chim. (Paris), 1964, 9, 461.
12. W.C. Child, Q. Rev., 1964, 18, 321.
13. G.A. Jeffrey, R.K. McMullan, Progr. Inorg. Chem., 1967, 8, 43.
14. V.M. Bhatnagar, J. Struct. Chem., 1967, 8, 513.
15. V.M. Bhatnagar, "Clathrate Compounds" Chand, New Dehli, 1968.
16. T. Iwamoto, Bussei, 1969, 10, 304.

17. A. Sopkova, J. Jaluvka, Chem. Listy, 1969, 63, 273.

18. W. Schlenk, Chem. Unserer Zeit, 1969, 3, 120.

19. G. Gawalek, "Physicochemical Separating and Measuring Methods," Deut. Verlag Wissenschaft, Berlin, 1969, Vol. 15.

20. J.H. van der Waals, Trans. Faraday Soc., 1956, 52, 184.

21. R.K. Gosavi, C.N.R. Rao, Indian J. Chem., 1967, 5, 162.

22. Y. Hazony, S.L. Ruby, J. Chem. Phys., 1968, 49, 1478.

23. P. Goldberg, J. Chem. Phys., 1964, 40, 427.

24. D.E. Wood, T.M. Pietrzak, J. Chem. Phys., 1967, 46 2973.

25. V.M. Bhatnagar, Z. Anorg. Allg. Chem., 1968, 363, 318.

26. V.M. Bhatnagar, Enperientia, 1968, 24, 319.

27. V.M. Bhatnagar, J. Prakt. Chem., 1969, 311, 302.

28. V.M. Bhatnagar, Z. Anorg. Allg. Chem., 1969, 370, 110.

29. F. Casellato, B. Casu, Spectrochim. Acta, Part A, 1969, 25, 1407.

30. M. Jaffrain, J.-L. Siemons, A. Libreton, C.R. Acad. Sci. (Paris), Ser. C, 1969, 268, 2240.

31. J.S. Dryden, J.R. Meakins, Nature, 1952, 169, 324.

32. M. Davies, J. Chim. phys., 1966, 63, 67.

33. M. Davies, K. Williams, Trans. Faraday Soc., 1968, 64, 529.

34. W.S. Brey, H.P. Williams, J. Phys. Chem., 1968, 72, 49.

35. M. Jaffrain, J.L. Siemons, C.R. Acad. Sci. (Paris), Ser. C, 1968, 266, 1323.

36. D.E. Evans, R.E. Richards, J. Chem. Soc., 1952, 3295.

37. A.H. Cooke, H. Meyer, W.P. Wolf, D.F. Evans, R.E. Richards, Proc. Roy. Soc. (London), 1954, A, 225, 112.

38. A.H. Cooke, H.J. Duffus, Proc. Phys. Soc., 1954, 67A, 525.

39. H. Meyer, M.C.M. O'Brien, J.H. van Vleck, Proc. Roy. Soc. (London), 1958, A, 243, 414.

40. D.F.R. Gilson, C.A. McDowell, Nature, 1959, 183, 1183.

41. V.M. Bhatnagar, H. Nakajima, Chim. Anal. (Paris), 1967, 49, 206.

42. C.A. McDowell, P. Raghunathan, Mol. Phys., 1967, 13, 331.

43. C.A. McDowell, P. Raghunathan, Proc. Int. Conf. Spectrosc., 1st, Bombay, 1967, 2, 462.

44. S. Brownstein, D.W. Davidson, D. Fiat, J. Chem. Phys., 1967, 46, 1454.

45. B.L. Afanas'ev, V.I. Kvlividze, G.G. Malenkov, Dokl. Akad. Nauk SSSR, 1968, 183, 360.

46. D.D. Eley, M.J. Hay, K.F. Chew, W. Derbyshire, Chem. Commun., 1968, 1474.

47. V.M. Bhatnagar, Chim. Anal. (Paris), 1968, 50, 81.

48. C.A. McDowell, P. Raghunathan, Mol. Phys., 1968, 15, 259.

49. C.A. McDowell, P. Raghunathan, J. Mol. Struct., 1968, 2, 359.

50. J.P. McTague, J. Chem. Phys., 1969, 50, 47.

51. Y.A. Majid, S.K. Garg, D.W. Davidson, Can. J. Chem., 1969, 47, 4697.

52. J.D. Bell, R.E. Richards, Trans. Faraday Soc., 1969, 65, 2529.

53. P.V. Demarco, A.L. Thakkar, J. Chem. Soc. (D), 1970, 2.

54. O.H. Griffith, J. Chem. Phys., 1964, 41, 1093.

55. O.H. Griffith, J. Chem. Phys., 1965, 42, 2644.

56. O.H. Griffith, J. Chem. Phys., 1965, 42, 2651.

57. T. Miyoshi, T. Iwamoto, Y. Sasaki, Inorg. Chim. Acta, 1968, 2, 329.

58. K. Reiss, H. Shields, J. Chem. Phys., 1969, 50, 4368.

59. H. Ohigashi, Y. Kurita, J. Magn. Resonance, 1969, 1, 464.

60. A.P. Dianin, J. Russ. Phys. Chem. Soc., 1914, 46, 1310.

61. A.P. Dianin, Chem. Zentr., 1915, 1, 1063.

62. W. Baker, J.F.W. McOmie, Chem. and Ind., 1955, 256.

63. H.M. Powell, B.D.P. Wetters, Chem. and Ind., 1955, 256.

64. H.L. Hoffman, G.R. Breedon, R.W. Liggett, J. Org. Chem., 1964, 29, 3440.

65. V.M. Bhatnagar, Chem. Age India, 1963, 14, 688.

66. J.L. Flippen, J. Karle, I.L. Karle, J. Amer. Chem. Soc., 1970, 92, 3749.

67. D.D. MacNicol, H.H. Mills, F.B. Wilson, Chem. Commun., 1969, 1332.

68. B. Andersen, P. Andersen, Acta Chem. Scand., 1966, 20, 2728.

69 O.H. Griffith, D.W. Cornell, H.M. McConnell, J. Chem. Phys., 1965, 43, 2909.

70. F.K. Kneubühl, J. Chem. Phys., 1960, 33, 1074.

71. J.H. van Vleck, Phys. Rev., 1948, 74, 1168.

72. H.S. Gutowsky, G.E. Pake, J. Chem. Phys., 1950, 18, 162.

73. R.K. Gosavi, C.N.R. Rao, Indian J. Chem., 1967, 5 162.

74. P.B. Ayscough, "Electron Spin Resonance in Chemistry," Methuen, London, 1967, p. 157 onwards.

75. W.L. Hubbell, H.M. McConnell, Proc. Natl. Acad. Sci. U.S.A., 1969, 64, 20.

PART IV

THE EFFECTS OF AXIAL INTERACTIONS ON ELECTRON PARAMAGNETIC RESONANCE SPECTRA OF COPPER(II) CHELATES : WEAK COMPLEXES OF COPPER(II) AND CHLOROFORM

1. Transition-metal ion complexes

In the compounds of the transition elements and rare-earths, unpaired d- or f-electrons may give rise to electron paramagnetic resonance spectra. A brief introductory survey of the magnetic properties of these elements will now be presented.

Provided the temperature is not too low and provided certain conditions are fulfilled, measurement of the static magnetic susceptibility, χ_o, of compounds of the rare-earth series, yields via the relationship

$$\chi_o = N\mu^2\beta_e^2(3kT)^{-1} = CT^{-1} \qquad 4.1$$

a value for the magnetic moment, μ, of the paramagnetic species; C, the Curie constant, is characteristic of the substance concerned. For rare-earth compounds, with only a few exceptions, the values of μ so obtained agree reasonably well with the values calculated from the equation

$$\mu = - g_J \beta_e \sqrt{J(J + 1)} \qquad 4.2$$

where J is the total electronic angular momentum quantum number for the ion.

In the first transition series, susceptibility measurements give μ values which are in approximate agreement with the spin-only relationship

$$\mu = - g_e \beta_e \sqrt{S(S + 1)} \qquad 4.3$$

where S is the quantum number which defines the total spin angular momentum for the ion. Similarly, in the case of the second and third transition series, compounds have g values near to those expected for the spin-only case.

Thus, spin-orbit coupling is strong in the case of the compounds of the rare-earth elements, while for those elements with partially filled d-orbitals, the spin-orbit coupling is almost completely quenched; this is exactly what is expected from theoretical considerations.

To return to the study of magnetic susceptibility, it is known that many substances obey a modified Curie relationship, viz.,

$$\chi_o = \frac{C}{T - W} \qquad 4.4$$

where W is the Weiss constant. Other forms of para-

magnetism are known, with somewhat less simple relationships between χ_o and temperature and between χ_o and magnetic field. The two most important cases are ferromagnetism and antiferromagnetism.

When considering the energy level scheme of transition metal ions in a steady magnetic field, it is simplest to make use of the perturbation approach. The most important term in the Hamiltonian is considered first, and the next most important term is treated as a perturbation on the first. This procedure is then repeated until all the terms in the Hamiltonian have been considered. It is difficult in general to arrange the various terms in the Hamiltonian in decreasing order of importance, since this order varies from one group of compounds to another; for example, the spin-orbit interaction is more important than most crystal field effects in rare-earth complexes, whereas in complexes of the d-transition elements this order is usually reversed.

Having very briefly considered the magnetic properties of transition metal compounds, it is proposed now to consider specifically the $3d^n$ transition metal ions. In this case, the Hamiltonian may be written,

$$\mathcal{H} = V_F + V_{XL} + V_{LS} + V_{SS} + V_H + V_N + V_h + V_Q \qquad 4.5$$

where V_F = the free ion energy $\sim 10^5$ cm^{-1}

V_{XL} = the crystal field energy $\sim 10^4$ cm^{-1}

V_{LS} = the spin-orbit coupling energy $\sim 10^2$ cm^{-1}

V_{SS} = the electron spin-spin interaction ~ 1 cm^{-1}

V_H = the electronic Zeeman interaction ~ 1 cm^{-1}

V_N = the electron-nuclear interaction $\sim 10^{-1}$ - 10^{-3} cm^{-1}

V_h = the nuclear Zeeman interaction $\sim 10^{-3}$ cm^{-1}

V_Q = the nuclear quadrupole-electric field interaction $\sim 10^{-3}$ cm^{-1}

The first term is

$$\mathcal{H}_F = \sum_k \frac{p^2_k}{2m} - \frac{Ze^2}{r_k} + \sum_{j<k} \frac{e^2}{r_{jk}} \qquad 4.6$$

where p_k is the momentum of the k^{th} electron, and e and m are the electronic charge and mass respectively, Ze is the nuclear charge and r_k is the distance from the k^{th} electron to the nucleus while r_{jk} is the distance between the j^{th} and k^{th} electrons. The free ion has, in general, spin and orbital energy degeneracy, and it is characterised by a group of (2L + 1) (2S + 1) - fold degenerate levels, where the L values are determined by Hund's rule of maximum multiplicity. The appropriate values of n and of the quantum numbers L and S for the ground states

of the ions of the $3d^n$ series are given

n	0	1	2	3	4	5	6	7	8	9	10
L	0	2	3	3	2	0	2	3	3	2	0
S	0	$\frac{1}{2}$	1	3/2	2	5/2	2	3/2	1	$\frac{1}{2}$	0

In the case of Cu^{2+} the configuration of the ion is $3d^9$ which can be regarded as a positive hole in the completed $3d^{10}$ shell. The eigenvalues of V_F for the Cu^{2+} ion are the d_{+2}, d_{+1}, d_o, d_{-1}, d_{-2} solutions of the Schrödinger equation; these levels are five-fold degenerate.

The ground state of Cu^{2+} is ^2D; in the free ion this level is split into two sublevels, with $J = 5/2$ and $J = 3/2$, where the $J = 5/2$ level is the lower, by the spin-orbit interaction. This spin-orbit coupling, however, is broken down in the crystalline complex by the strong effect of V_{XL} which is considered next.

If the ion is now placed in an octahedral crystal field, then the Hamiltonian becomes

$$\mathcal{H} = V_F + V_{XL}$$

which has eigenfunctions

$$d_{x^2 - y^2} = \frac{1}{\sqrt{2}} \left\{ d_{+2} + d_{-2} \right\}$$

$$d_{xy} = \frac{1}{i\sqrt{2}} \{d_{+2} - d_{-2}\}$$

$$d_{z^2} = d_o \qquad 4.7$$

$$d_{xz} = -\frac{1}{\sqrt{2}} \{d_{+1} - d_{-1}\}$$

$$d_{yz} = -\frac{1}{i\sqrt{2}} \{d_{+1} + d_{-1}\}$$

It is usual for chemical purposes to make use of the real funstions d_{xz} and d_{yz}, although d_{+1} and d_{-1} could be used instead. The boundary surfaces of these orbitals are illustrated below:

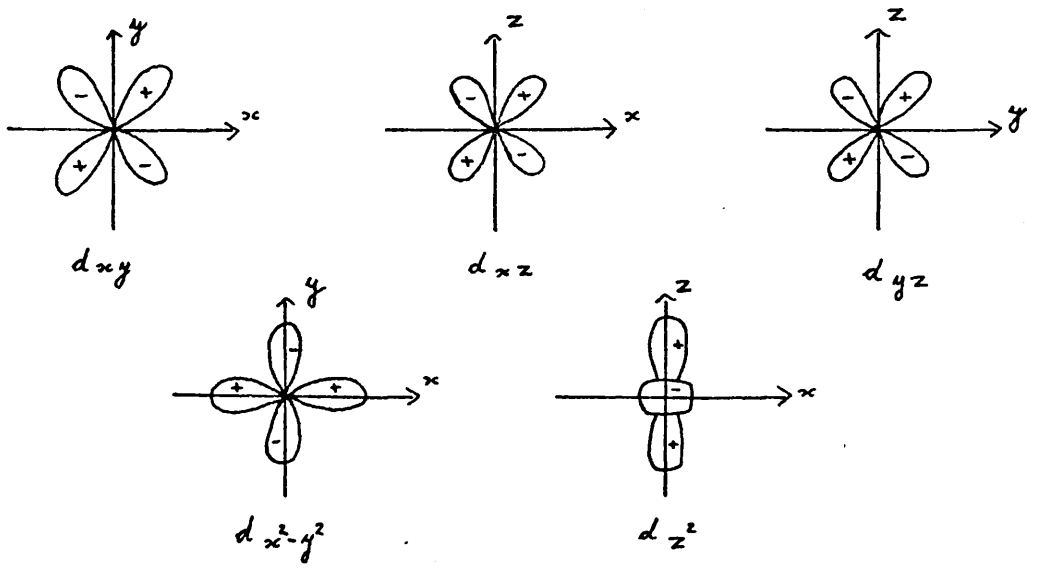

Figure 1.

Boundary surfaces of e_g and t_{2g} electronic densities.

Bethe[1] has shown that the effect of V_{XL}, if it has

octahedral symmetry, is to split the five-fold degeneracy of the D-state into a triplet composed of the d_{xz}, d_{yz} and d_{xy} orbitals (called t_{2g}) and a doublet made up of the other two d orbitals (e_g).

For Cu^{2+} the energy level scheme for various environments is given below with the e_g orbitals being lower in energy than the triplet t_{2g} orbitals. For many copper(II) complexes the octahedron is distorted by the ligands lying along the z-axis moving further away from, and those along the x and y axes coming closer to the central metal ion. This lowers the energy of the $d_{x^2 - y^2}$ and d_{xy} orbitals while raising that of the d_{z^2}, d_{xz} and d_{yz} orbitals.

Sometimes it is possible for the tetragonal distortion to become strong enough to raise the energy level of the d_{z^2} orbital above that of the d_{xy} orbital; whether or not this actually happens in any particular case, even in the limit of a square planar complex, depends on the metal ion and ligands concerned. Theoretical considerations indicate that for Cu(II) square planar complexes the energy level scheme, for the positive hole, is as given overleaf

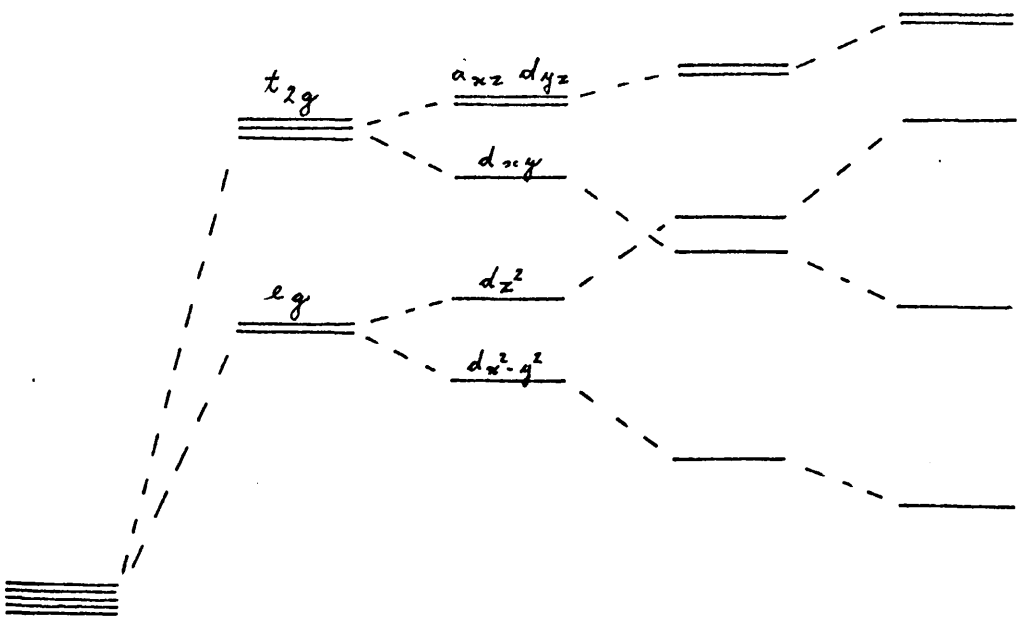

Figure 2

Energy level scheme for the Cu(II) ion in various environments, using the standard positive hole formalism. This diagram is not drawn to scale.

Each of these levels is still two-fold degenerate, as predicted by Kramer's theorem which states that a

purely electrostatic field acting on a system with an odd number of electrons, can never reduce the degeneracy below two. A magnetic field is required to remove this Kramer's degeneracy.

For tetragonal copper(II) complexes the positive hole occupies the lowest level E_o, which is doubly degenerate. The ground state wave functions involved are $\psi_o\alpha$ and $\psi_o\beta$ where α and β are the spin functions with $S_z = +\frac{1}{2}$ and $S_z = -\frac{1}{2}$ respectively. For tetragonal complexes, the positive hole occupies the $d_{x^2-y^2}$ or d_{z^2} orbital, depending on the type of tetragonal distortion involved, and in the case of square planar complexes, the positive hole is in the $d_{x^2-y^2}$ orbital.

The effect of spin-orbit coupling will now be discussed

$$V_{LS} = \lambda \underline{L}.S = \lambda[L_zS_z + \tfrac{1}{2}(L_+S_- + L_-S_+)] \qquad 4.8$$

where the λ is positive when the 3d shell is less than half-filled and negative when more than half-filled; thus for Cu^{2+} λ is negative. One of the main effects of V_{LS} is to mix other states, ψ_n, with the ground state ψ_o. The new ground states may be determined by first-order perturbation theory,

$$(\psi_o\alpha)' = \psi_o\alpha - \sum_n \psi_n \frac{\langle n \mid \lambda \underline{L}.\underline{S} \mid o, \tfrac{1}{2}\rangle}{E_n - E_o}$$

$$(\psi_o\beta)' = \psi_o\beta - \sum_n \psi_n \frac{\langle n \mid \lambda \underline{L}.\underline{S} \mid o, -\tfrac{1}{2}\rangle}{E_n - E_o} \qquad 4.9$$

$\psi_n\alpha$ may be mixed with $\psi_o\alpha$, and $\psi_n\beta$ with $\psi_o\beta$ by the L_zS_z part of $\underline{L}.\underline{S}$, i.e. the operator L_zS_z does not change the electron spin. Mixing of the α and β ground states with the β and α excited states, respectively, is brought about by the L_+S_- and L_-S_+ terms. Thus, the eigenfunctions of

$$\mathcal{H} = V_F + V_{XL} + V_{LS}$$

are

$$\Psi = (\psi_o\alpha)' = \psi_o\alpha - \tfrac{1}{2}\lambda \sum_n \frac{\langle \psi_n \mid L_z \mid \psi_o\rangle}{E_n - E_o} \psi_n\alpha$$

$$- \tfrac{1}{2}\lambda \sum_n \frac{\langle \psi_n \mid L_+ \mid \psi_o\rangle}{E_n - E_o} \psi_n\beta \qquad \text{and}$$

$$\Psi = (\psi_o\beta)' = \psi_o\beta + \tfrac{1}{2}\lambda \sum_n \frac{\langle \psi_n \mid L_z \mid \psi_o\rangle}{E_n - E_o} \psi_n\beta$$

$$- \tfrac{1}{2}\lambda \sum_n \frac{\langle \psi_n \mid L_- \mid \psi_o\rangle}{E_n - E_o} \psi_n\alpha \qquad 4.10$$

It is this mixing of excited states with the ground state which determines the extent to which the orbital angular momentum is "unquenched". To first-order this spin-orbit coupling has no effect on the energies of the levels,

except for cases of orbitally degenerate levels.

Omitting electron-electron spin-spin interactions, an approximation valid for d^9 ions if the paramagnetic species is sufficiently diluted by a diamagnetic host lattice or by a solvent, the interaction of the unpaired electron with a magnetic field will now be considered. Now,

$$V_H = \beta_e \underline{H}.\ (\underline{L} + g_e \underline{S}) \qquad 4.11$$

First-order perturbation theory yields,

$$< \Psi_o \mid \mathcal{H}_H \mid \Psi_o > = \beta_e < \Psi_o \mid \underline{H}.\ (\underline{L} + g_e \underline{S}) \mid \Psi_o > \qquad 4.12$$

Second-order perturbation theory yields a second term

$$\sum_{n \neq o} \frac{< \Psi_o \mid \mathcal{H}_H \mid \Psi_n > < \Psi_n \mid \mathcal{H}_H \mid \Psi_o >}{E_n - E_o}$$

$$= - g_e \beta_e \lambda S_i H_j \sum_{n \neq o} \frac{< \Psi_o \mid L_i \mid \Psi_n > < \Psi_n \mid L_j \mid \Psi_o >}{E_n - E_o}$$

$$= - g_e \beta_e \lambda \Lambda_{ij} S_i H_j \qquad 4.13$$

where Ψ_o and Ψ_n are the ground and excited state wavefunctions before the application of the Zeeman perturbation. Addition of equations 4.12 and 4.13 therefore gives, for the complete Zeeman interaction,

$$V_H = g_e\beta_e(\delta_{ij} - \lambda\Lambda_{ij})\, S_i H_j$$

$$= \beta_e S_i g_{ij} H_j \qquad 4.14$$

where g is now an anisotropic tensor;

$$g_{ij} = g_e(\delta_{ij} - \lambda\Lambda_{ij}) \qquad 4.15$$

i.e. g_{ij} is a symmetric tensor of second rank, with principal values g_{xx}, g_{yy} and g_{zz}.

For the case of axial symmetry, $g_{xx} = g_{yy} = g_{\perp}$ and $g_{zz} = g_{11}$, and for the case of cubic symmetry $g_{11} = g_{\perp}$. Λ_{ij} is a real symmetric tensor which measures the amount of mixing of higher states with the ground state by spin-orbit coupling and by interaction with the applied field.

With Cu^{2+} in a tetragonal field, $\Lambda_{xx} = \Lambda_{yy} = \Lambda_{\perp}$

$$= [E_{(d_{xz})} - E_{(d_{x^2-y^2})}]^{-1}$$

and

$$\Lambda_{zz} = \Lambda_{11} = 4[E_{(d_{xy})} - E_{(d_{x^2-y^2})}]^{-1} \qquad 4.16$$

if the positive hole occupies the $d_{x^2-y^2}$ orbital, and

$$\Lambda_{xx} = \Lambda_{yy} = \Lambda_{\perp} = 3[E_{(d_{xz})} - E_{(d_{z^2})}]^{-1}$$

and $\Lambda_{zz} = \Lambda_{11} = 0$ $\qquad 4.17$

if the positive hole occupies the d_{z^2} orbital. It is

because of the negative value of λ for Cu^{2+} that g values greater than the spin-only value of 2·0023 are found.

Measurement of the g value will obviously provide information about the type of orbital occupied by the positive hole. Experimentally it has been found that the postive hole usually occupies a perturbed $d_{x^2 - y^2}$ orbital i.e. the distortion from octahedral symmetry is brought about by lengthening of the ligand-to-copper distances along the z axis. An exception to this rule is the case of complex fluorides with Cu(II) and alkali metals, M_2CuF_4 and $MCuF_3$, in which the distortion consists of a compression along the z axis with the result that the positive hole is in the perturbed d_{z^2} orbital.[2]

2. The molecular orbital approach

Up till this point the possibility of covalent bonding between the central metal ion and its ligands has not been considered. A crystal field description has been used and for most complexes this is not a completely valid description. An alternative approach, molecular orbital theory, employing the usual symmetry and energy criteria of bonding, takes the possibility of overlap between the ligand system of orbitals and the central metal ion's

orbitals into account.[3]

For first row transition metals, the orbitals 3d, 4s, 4p have comparable energies, and so these are all available for bonding with the ligand system. When symmetry requirements are met, and orbitals combine to give new molecular orbitals, the number of new orbitals formed is equal to the number of combining orbitals, and one of the new orbitals is less, and one of them is more stable than any of the original orbitals.

The d_{z2}, d_{x2-y2}, s, p_x, p_y, and p_z metal orbitals point along the metal-ligand bond directions and so are available for σ-bonding. The three p-orbitals and the d_{xy}, d_{xz} and d_{yz} orbitals are of the correct symmetry for π-bonding to suitable ligand orbitals. It is best to consider the ligand orbital system as a whole, and the six σ-orbitals (one from each ligand) are combined to give six "symmetry" orbitals, each of these new orbitals being constructed in such a way as to overlap with a particular one of the six metal ion orbitals available for σ-bonding. These two sets of orbitals are then combined in matching pairs, to form a bonding and an anti-bonding molecular orbital for each pair of combining orbitals.

Some, but not all, ligands also have π-orbitals

available for bonding with the central metal ion, and again these may be combined to give "symmetry" orbitals which can then be overlapped with the metal ion's π-orbitals to give a system of bonding and anti-bonding π-orbitals.

This process is illustrated diagramatically for σ-bonding alone in Figures 3 and 4, the first indicating the initial and final orbital energy levels, and the second showing the metal orbitals and their matching ligand group orbitals.

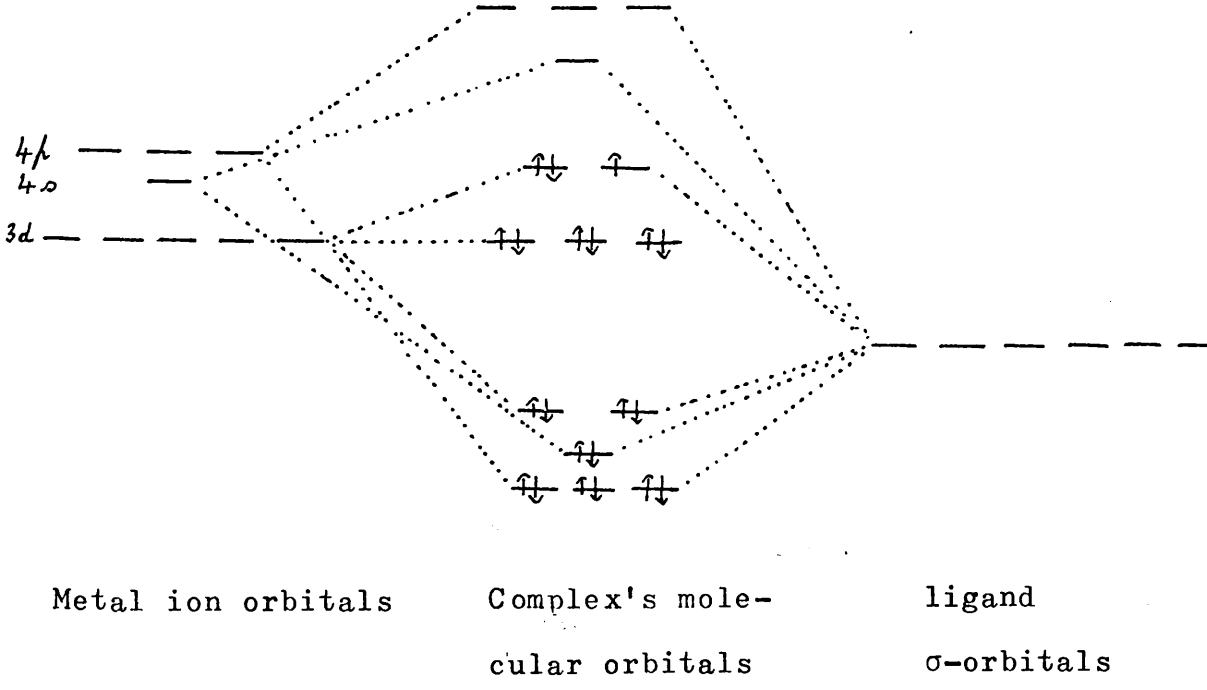

Figure 3

Initial and final orbital energy levels for octahedral transition metal ion complex.

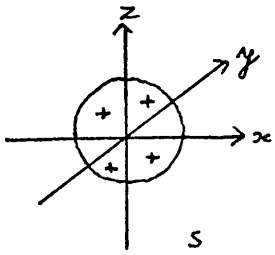

s

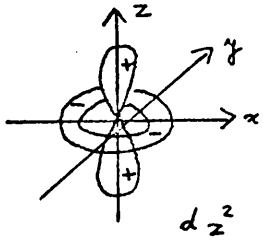

d_{z^2}

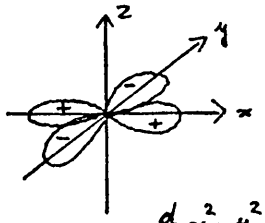

$d_{x^2-y^2}$

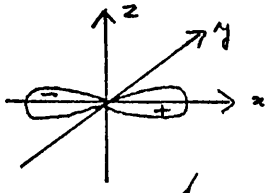

p_x

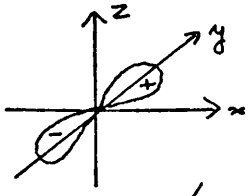

p_y

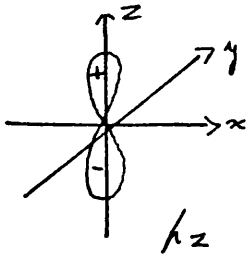

p_z

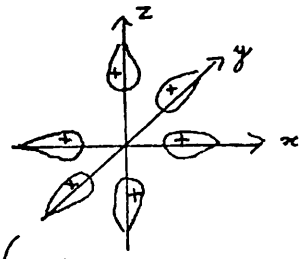

$\frac{1}{\sqrt{6}}(\sigma_x + \sigma_{-x} + \sigma_y + \sigma_{-y} + \sigma_z + \sigma_{-z})$

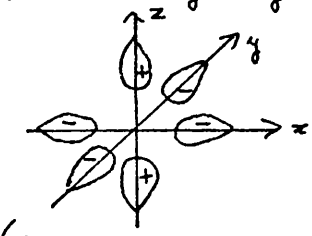

$\frac{1}{2\sqrt{3}}(2\sigma_z + 2\sigma_{-z} - \sigma_x - \sigma_{-x} - \sigma_y - \sigma_{-y})$

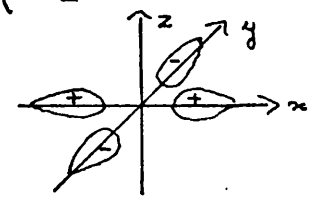

$\frac{1}{2}(\sigma_x + \sigma_{-x} - \sigma_y - \sigma_{-y})$

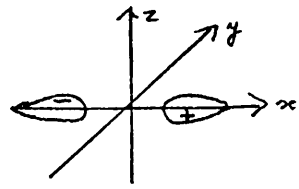

$\frac{1}{\sqrt{2}}(\sigma_x - \sigma_{-x})$

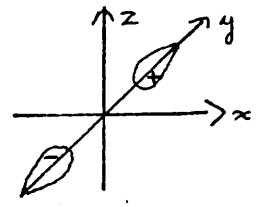

$\frac{1}{\sqrt{2}}(\sigma_y - \sigma_{-y})$

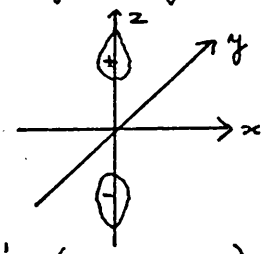

$\frac{1}{\sqrt{2}}(\sigma_z - \sigma_{-z})$

Figure 4

Metal and ligand group orbitals involved in σ-bonding.

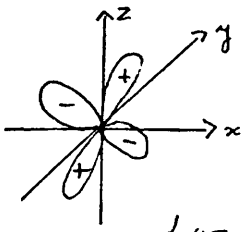

d_{yz}

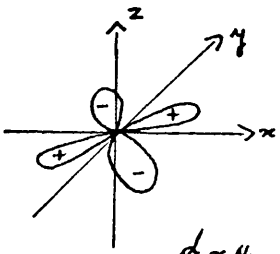

d_{xy}

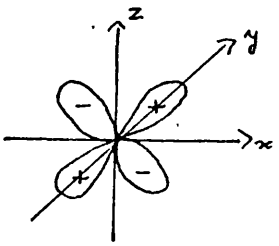

d_{xz}

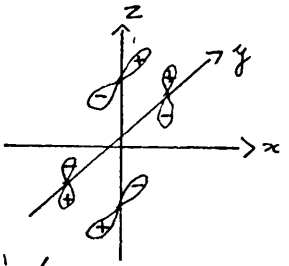

$\frac{1}{2}\left(f_z(y) - f_z(-y) + f_y(z) - f_y(-z)\right)$

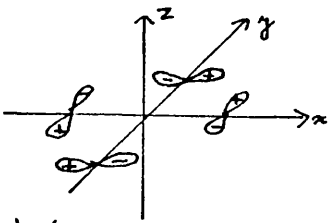

$\frac{1}{2}\left(f_x(y) - f_x(-y) + f_y(x) - f_y(-x)\right)$

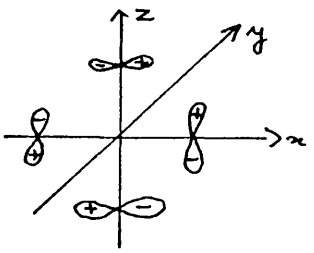

$\frac{1}{2}\left(f_x(z) - f_x(-z) + f_z(x) - f_z(-x)\right)$

Figure 5

Metal d-orbitals and ligand group orbitals suitable for π-bonding.

If the system of molecular orbitals shown in Figure 3 is subjected to a tetragonal distortion due to lengthening of the metal-ligand bonds along the z-axis of the complex, then some of the degeneracy is removed and in Cu(II) complexes the positive hole will occupy the

anti-bonding molecular orbital constructed from the $d_{x^2 - y^2}$ orbital and the appropriate ligand group-orbital.

The spin-orbit coupling interaction $\lambda \underline{L}.\underline{S}$ now perturbs these molecular orbitals, mixing them to some extent, changing their energies in the manner described earlier, and unquenching some orbital paramagnetism.

As before when a magnetic field is applied, the energy of these levels changes by an amount

$$V_H = \beta_e S_i g_{ij} H_j$$

where $$g_{ij} = g_e(\delta_{ij} - \lambda \Lambda_{ij})$$

and this time λ, defined by equation 4.13 is a function of matrix elements of a molecular orbital.

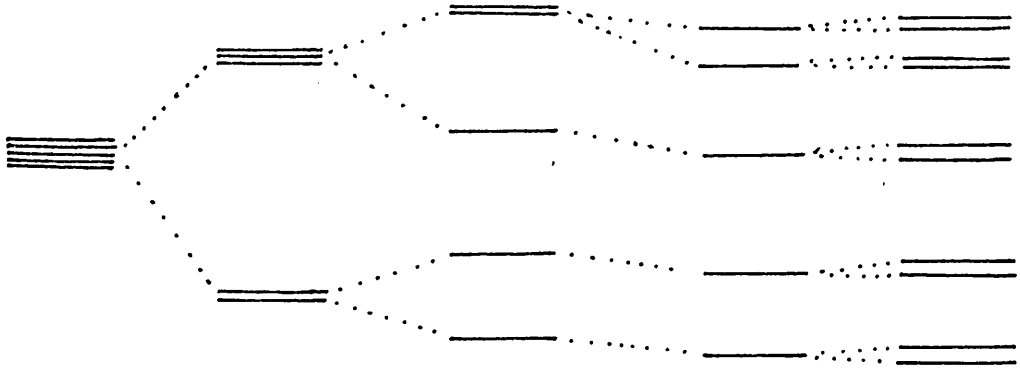

Figure 6

Energy level scheme for Cu(II) ion in various environments.

If the magnetic field is applied parallel to the z-axis of the tetragonal copper complex, then the energy of separation between the two Zeeman levels of the molecular orbital occupied by the positive hole is

$$E = g_{11}\beta_e H$$

Likewise when H is applied perpendicular to the z-axis of the complex, the energy difference between the levels is

$$E = g_{\perp}\beta_e H$$

In general, for a single crystal of Cu^{2+} in a tetragonal environment, electron paramagnetic resonance may occur when the value of the magnetic field strength is

$$H = h\nu/g_e\beta_e \qquad 4.18$$

where $$g_e^2 = g_{11}^2\cos^2\theta + g_{\perp}^2\sin^2\theta$$

and θ is the angle between the z-axis of the complex, i.e. the symmetry axis, and the magnetic field vector $\underline{H}$. The intensity of the resonance absorption, as well as its position, is orientation-dependent; the transition probability, P is proportional to $(g_x\beta_e S_x H_1)^2$, where H_1 is the amplitude of the microwave field applied in the x-axis direction, so that the variation in intensity of absorption with orientation of the complex in the magnetic

field may be written

$$I(\theta)\alpha \quad g_{\underline{1}}^{\,2} + g_{11}^{\,2} - g_{\theta}^{\,2} \qquad 4.19$$

3. Effects of hyperfine interactions on copper(II) electron paramagnetic resonance

Up to this point nuclear interactions have been ignored and the spin Hamiltonian for a copper complex of tetragonal symmetry in a steady magnetic field has been taken as

$$\mathcal{H}_s = g_{11}\beta_e H_z S_z + g_{\underline{1}}\beta_e (H_x S_x + H_y S_y) \qquad 4.20$$

i.e. only perturbations arising from V_{XL}, V_{LS} and V_H have been considered. The effect of magnetic copper nuclei will now be introduced in two parts; V_N the magnetic interaction between the positive hole and the nucleus through their magnetic moments, and V_Q the electrostatic interaction between the positive charge and the electric quadrupole moment of the nucleus. The former interaction is linear in I, the nuclear spin, the latter is quadratic in I. Higher magnetic and electric multipoles are not normally considered as the magnitude of their interaction is extremely small. It may be shown that[4,5] these interactions are given by

$$V_N + V_Q = 2\gamma_N\beta_e\beta_N \left\{\frac{(\underline{l} - \underline{s}).\underline{I}}{r^3} + \frac{3(\underline{r}.\underline{s})(\underline{r}.\underline{I})}{r^5} + \frac{8\pi}{3}\delta(\underline{r})(\underline{s}.\underline{I})\right\}$$

$$+ \frac{eQ}{2I(2I-1)}\left\{\frac{I(I+1)}{r^3} - \frac{3(\underline{r}.\underline{I})^2}{r^5}\right\} \qquad 4.21$$

where $\underline{l}$ and $\underline{s}$ are the orbital and spin angular momenta of the positive hole, β_e is the electronic Bohr magneton, β_N is the nuclear magneton, γ_N is the nuclear magnetogyric ratio in units of $e/2Mc$, Q is the quadrupole moment of the nucleus, and $\underline{r}$ is the distance of the positive hole from the nucleus. The Fermi contact term is represented by the delta function. V_N and V_Q are usually written in tensor form, $S_iA_{ij}I_j$ and $I_iQ_{ij}I_j$ respectively, where A_{ij} is the hyperfine coupling tensor and Q_{ij} is the quadrupole moment tensor. In cases of tetragonal symmetry, taking the z axis of the complex to be this symmetry axis, there are two principal values, parallel and perpendicular to this axis, for these tensor components. It is then usual to write

$$V_N + V_Q = AS_zI_z + B(S_xI_x + S_yI_y) + Q'[I_z^2 - \tfrac{1}{3}I(I+1)] \qquad 4.22$$

Now, in the crystal field description of a Cu(II) ion

in a tetragonal field, it has been shown that the following relationships are approximately true:[5]

$$A = P[-4/7 - K_o + g_{11} - 2 + \tfrac{3}{7}(g_{\perp} - 2)]$$

$$B = P[2/7 - K_o + g_{\perp} - 2 - \tfrac{3}{14}(g_{\perp} - 2)]$$

$$Q' = 3eQq[4I(2I - 1)]^{-1} \qquad 4.23$$

with $P = 2\gamma_N\beta_e\beta_N \langle r^{-3} \rangle$ where $\langle r \rangle$ is the effective radius of the $d_{x^2 - y^2}$ orbital. K_o is a constant representing the admixture of configurations with unpaired s-electrons. In the case of Cu(II), the configurations $3s3d^{10}$ and $3d^84s$ are admixed with the ground state and the value of K_o is 3/7.[6] eQq is the quadruple coupling constant of the transition metal nucleus in the complex: for ^{65}Cu and ^{63}Cu the value of I is 3/2, and since their magnetic moments are nearly equal, they give rise to almost identical hyperfine structures, which can be separated experimentally only under favourable conditions. The hyperfine structure due to the terms A and B by themselves would consist of (2I + 1) equally spaced lines in strong magnetic fields, but the quadrupolar term makes the hyperfine structure more complex when the external field is at an angle to the symmetry axis.

Equations 4.23 are not appropriate when a molecular orbital description is used: the modifications required in that case are considered later.

The last term to be considered is the nuclear Zeeman term, which shifts the energy levels of the system by a small amount

$$V_h = \gamma_N \beta_N \underline{H}.\underline{I} \qquad 4.24$$

The complete spin Hamiltonian for a Cu(II) complex with tetragonal symmetry in a steady magnetic field is thus,

$$\mathcal{H} = g_{11}\beta_e H_z S_z + g_{\perp}\beta_e (H_x S_x + H_y S_y) + A S_z I_z + B(S_x I_x + S_y I_y) + Q'[I_z^2 - \tfrac{1}{3} I(I+1)] - \gamma_N \beta_N \underline{H}.\underline{I} \qquad 4.25$$

which gives rise to the energy level scheme below:

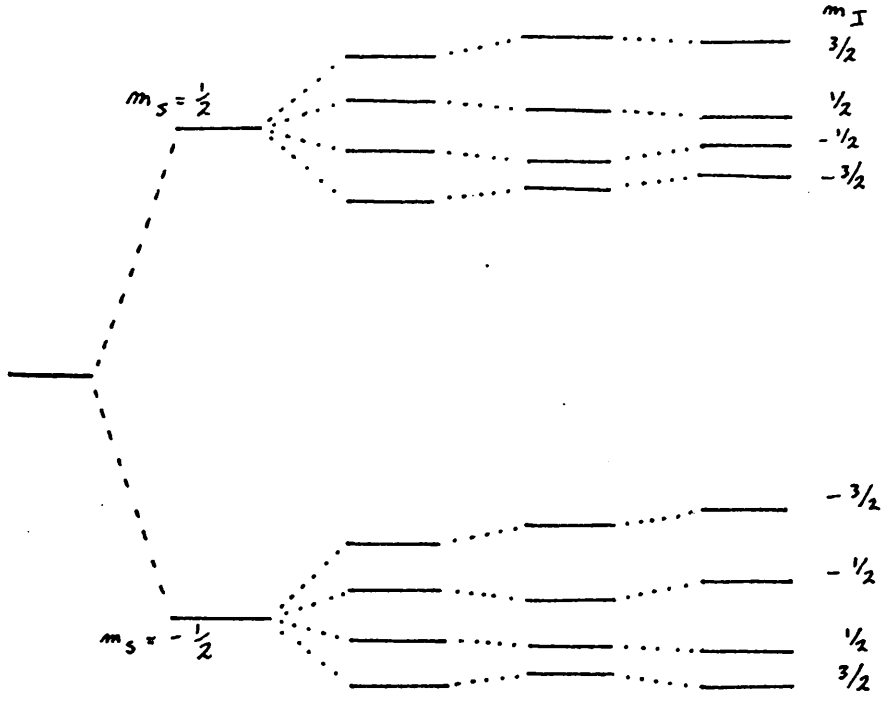

Figure 7

Energy level scheme derived from the Hamiltonian 4·25, for a Cu(II) complex with tetragonal symmetry.

4. Selection rules

Having considered the energy levels, it is now necessary to see which transitions are allowed by the selection rules. The standard selection rule for the system being considered is $\Delta m_S = \pm 1$, and $\Delta m_I = 0$, and because of the change in order of the $(2I + 1)$ levels on going from the $m_S = +\frac{1}{2}$ to the $m_S = -\frac{1}{2}$ electronic levels, four hyperfine transitions of this kind are allowed for each copper isotope. Weaker transitions are often observed corresponding to the selection rules $\Delta m_S = \pm 1$, $\Delta m_I = \pm 1$ and $\Delta m_S = \pm 1$, $\Delta m_I = \pm 2$. These transitions which are normally forbidden in e.p.r. spectroscopy, become "allowed" because of the presence of the x and y components of the magnetic hyperfine contribution and because of the quadrupolar interaction. Those mix together nuclear spin states so that m_I is no longer a good quantum number, and this causes the normal selection rules to be not so rigorously applicable.

Thus, in the e.p.r. spectra of copper(II) complexes three groups of transitions are expected for each structurally different type of cupric species. Each group will consist of four transitions for each copper isotope, ^{63}Cu, and ^{65}Cu. In the first group, the nuclear spin quantum number , m_I, does not change, the selection rules

being $\Delta m_S = \pm 1$ and $\Delta m_I = 0$. In the second and third groups of transitions, the nuclear spin quantum number does change, but it has been shown that[7,8] the intensities of these transitions are significant only when θ lies in the range $60^\circ \lesssim \theta \lesssim 90^\circ$. θ is defined for a single crystal as the angle between the applied field and the "tetragonal" axis of the complex.

5. Electron paramagnetic resonance spectra of some copper(II) β-ketoenolates in magnetically dilute glasses

It is not always possible to grow magnetically dilute, doped, single crystals of transition metal ion complexes, and so magnetically dilute polycrystalline samples are often used instead. In such samples, each of the randomly oriented crystallites contributes separately to the observed e.p.r. spectrum. Such a spectrum thus consists of a superposition of the spectra from crystallites with all possible values of θ, weighted in proportion to the probability of finding the complex at that particular angle. Often it is not possible even to obtain polycrystalline samples, and instead glasses are used. The e.p.r. spectra of magnetically dilute samples of cupric complexes homogenously dispersed in glasses may

be treated as very finely powdered polycrystalline samples. The two cases give identical spectra if the degree of powdering is fine enough.

E.p.r. spectra from such samples have been discussed by a number of authors,[9-11] and it has been shown that the derivative spectra of cupric chelates in glasses are of the form exhibited by, for example, compound IX in a glass of chloroform and toluene (60:40) at 77°K. This spectrum is shown in Figure 8.

In the case of planar complexes of copper(II), the difference between g_{11} and $g_{\perp}$ is sufficiently large to enable the peaks a, b, c, d and e in Figure 8, which are due to contributions from complexes in which H is roughly parallel to the "tetragonal" axis, to be separated from that part of the spectrum which comes from those crystallites in which H lies roughly in the plane perpendicular to the "tetragonal" axis. In Figure 8, the peaks a and b are due to the two isotopic species ^{65}Cu and ^{63}Cu respectively: the peaks to the high-field side of e arise from complexes which are oriented with H roughly in the plane perpendicular to the "tetragonal" axis of the complex. In this region occur transitions $\Delta m_S = \pm 1$, $\Delta m_I = 0$, and also transitions which obey the selection rules $\Delta m_S = \pm 1$, $\Delta m_I = \pm 1$, and $\Delta m_S = \pm 1$, $\Delta m_I = \pm 2$.

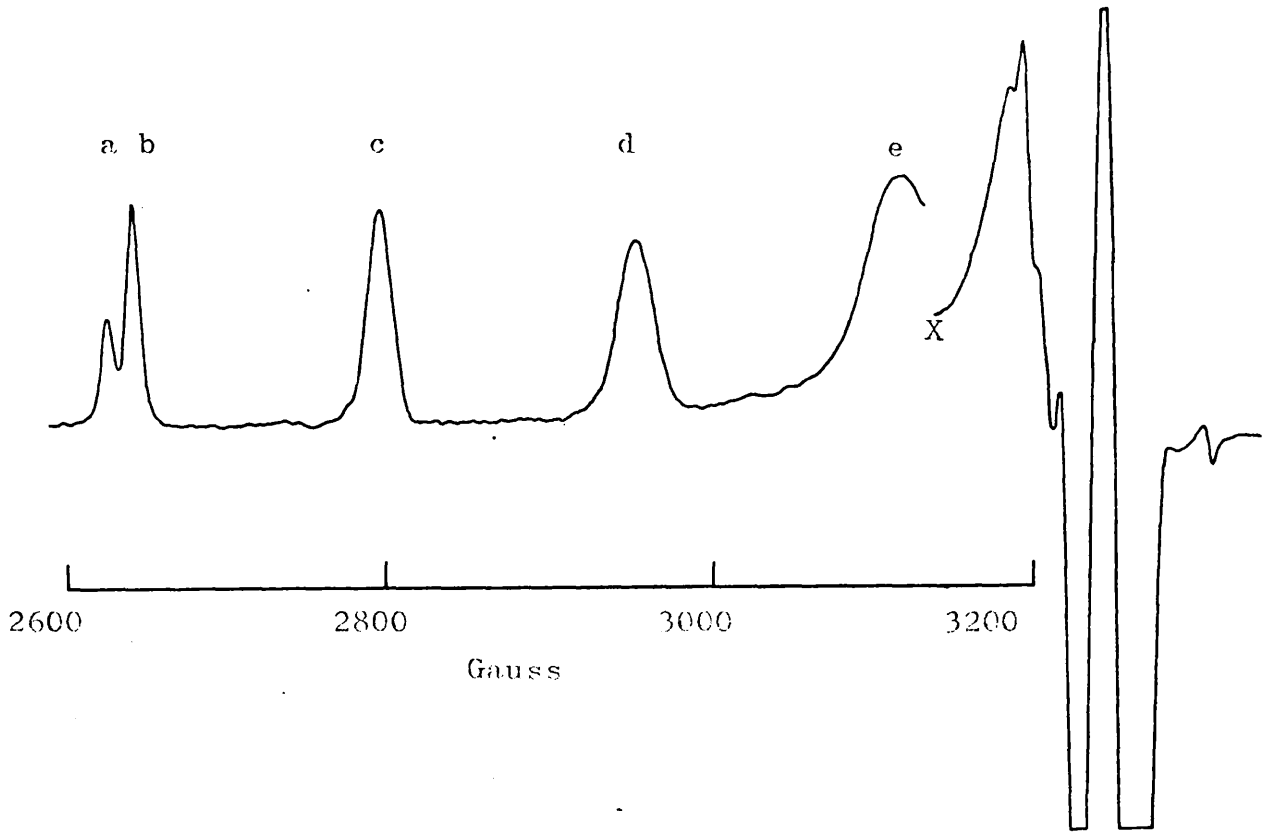

Figure 8 E.P.R. spectrum of a 10^{-3}M solution of IX dispersed in chloroform:toluene glass (60:40) at 77°K. At fields higher than that marked X the spectrometer gain is reduced by a factor of 5.0.

Many of the theoretical treatments[9-11] ignore such contributions from these combination transitions to this region of the spectrum, but they are not negligible, and ought to be taken into account. The extreme high field region of the spectrum contains an additional peak which arises from a singularity in the function which describes the intensity of the glassy spectrum.

Occasionally, additional unexpected peaks have been observed in e.p.r. spectra of β-ketoenolates of copper(II); see, for example, Figure 9. This section of the thesis is concerned with studies of such spectra carried out in order to account for the origin of these additional extra resonances and to examine any chemical significance which they might have.

6. Experimental procedure and results

10^{-3} M. solutions of the copper(II) complexes, (I) - (X), in chloroform:toluene glasses (chloroform:toluene ratio is 60:40) were studied at 77°K in a Decca X3 spectrometer in combination with a Newport Instruments 11-inch magnet system. Calibration of the resonant fields was effected by the use of standard proton magnetic resonance techniques. The magnetic parameters g_{11}, $A(^{63}Cu)$, and

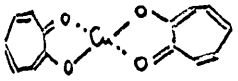

I

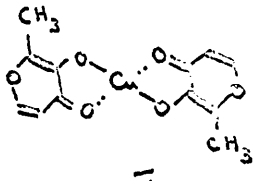

II

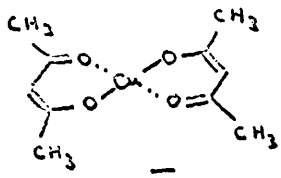

III

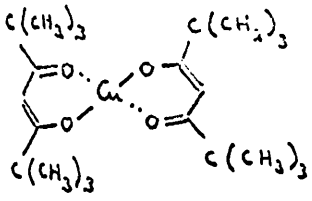

IV

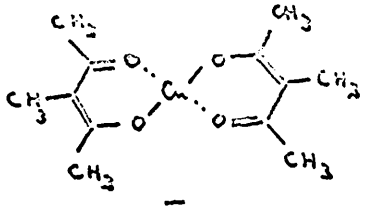

V

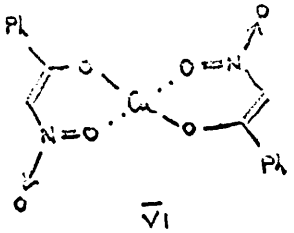

VI

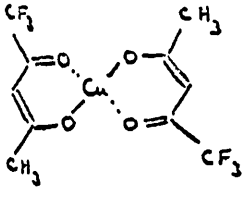

VII

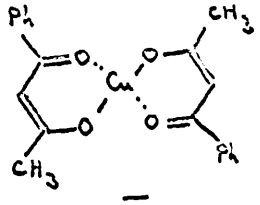

VIII

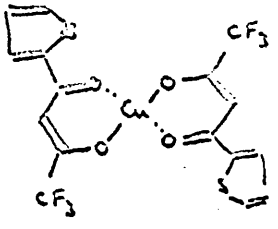

IX

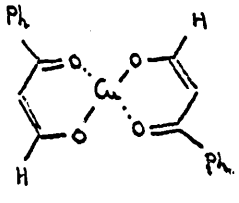

X

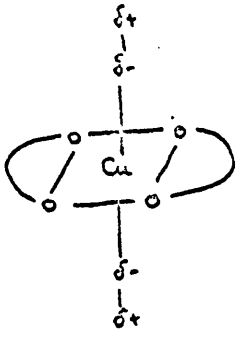

XI

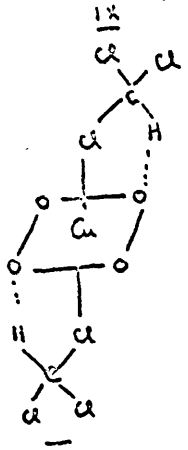

XII

$A(^{65}Cu)$ were obtained from the spectra of glasses at 77°K, while the parameters $< g >$, the isotropic g-value, and $< A >$, the isotropic hyperfine coupling constant, were obtained from solution spectra at 300°K. The limits of error on these parameters obtained experimentally were as follows:

$g_{11} \pm 0{\cdot}0005$, $A(^{63}Cu)$ and $A(^{65}Cu) \pm 0{\cdot}5 \times 10^{-4}$ cm^{-1},

$< g > \pm 0{\cdot}0005$, $< A > \pm 0{\cdot}5 \times 10^{-4}$ cm^{-1}.

The parameters $g_{\perp}$, $B(^{63}Cu)$ and $B(^{65}Cu)$ were evaluated from the approximate relationships

$$< g > = \frac{1}{3}(g_{11} + 2g_{\perp})$$

$$< A > = \frac{1}{3}(A + 2B)$$

Owing to the fact that the g and hyperfine tensor components are temperature dependent,[12] the limits of error in the values calculated for $g_{\perp}$ and B at 77°K, by means of this procedure, may be as large as $\pm 0{\cdot}005$ and $\pm 4 \times 10^{-4}$ cm^{-1}, respectively.

Table 1 contains the magnetic parameters obtained from the e.p.r. spectra, recorded at 77°K, from cupric tropolonate in chloroform:toluene (60:40) and in bromoform:toluene (60:40) glasses, and also from the unstable glass which may be made by suddenly quenching a solution

Table 1

E.P.R. spectral parameters of 10^{-3} M solutions of cupric tropolonate homogeneously dispersed in glasses. Hyperfine tensor components are in units of 10^{-4} cm^{-1}. The parameters marked * could not be obtained from the spectra because the features on which they depend were not resolved.

Glass	⟨g⟩	⟨A⟩	$g_{\parallel}$	$g_{\perp}$	$A(^{63}Cu)$	$B(^{63}Cu)$	$A(^{65}Cu)$	$B(^{65}Cu)$
chloroform: toluene(60:40)	2·123	77·6	2·284	2·043	178·1	27·3	187·3	22·7
			2·257	2·056	196·3	18·2	*	*
bromoform: toluene(60:40)	2·123	78·9	2·253	2·058	194·9	21·0	205·2	15·8
chloroform	2·122	78·8	2·284	2·041	177·4	29·5	186·7	24·8

of cupric tropolonate in chloroform to 77°K. Typical spectra thus obtained are shown in Figure 9.

Bromoform-toluene glasses and chloroform glasses give rise to normal spectra. The spectrum obtained from the chloroform glass is identical with that obtained from the paramagnetic species which gives rise to the peaks, a, b, c, d, and e in the chloroform:toluene glass spectrum: the spectrum obtained from the bromoform:toluene glass is virtually identical with that obtained from the species which gives rise to the peaks, a', b', c', d', and e' in the chloroform-toluene glass spectrum. On increasing the concentration of cupric tropolonate in chloroform: toluene to 10^{-2}M, no significant changes were observed in the relative intensities of the groups of peaks aa', bb', ••• ee'. On the other hand, if the ratio of chloroform to toluene is increased, then the intensity ratios a:a', b:b' •••, e:e' increase.

On examining the e.p.r. spectra obtained from glasses of compounds (II) through (X) in chloroform:toluene at 77°K it was found that compounds (II) through (VI) gave rise to doubled spectra, while compounds (VII) through (X) gave normal spectra in these glasses. Each of the compounds (I) through (VI) give rise to two species in chloroform:toluene glasses. One of these species consists of the chelate surrounded by toluene molecules and it gives the peaks a', b', •••, e'.

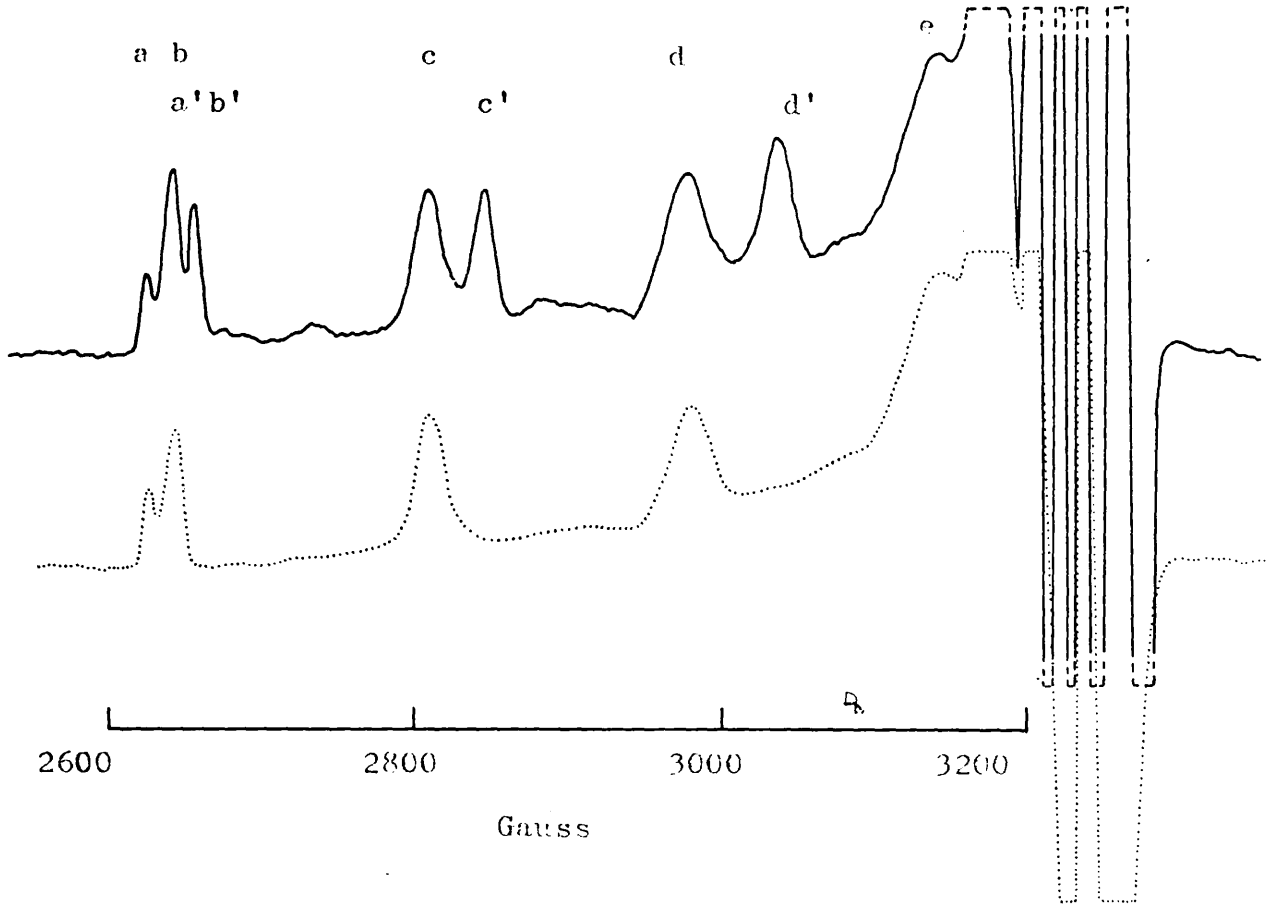

Figure 9. E.P.R. spectra of 10^{-3} M solutions of cupric tropolonate (I) dispersed in chloroform: toluene glass (60:40) (—) and in chloroform glass (...) at 77°K.

The second species gives the peaks a, b, c, ···, e; and it appears that the electron distribution in the transition metal ion complex is noticeably perturbed by interaction with contiguous chloroform molecules in this case. As expected the ratio of intensities a:a', b:b', ···, e:e' in the spectra given by compounds (II) through (VI) increase when the ratio of chloroform to toluene is increased. The magnetic parameters evaluated from e.p.r. spectra of compounds (II) through (X) in chloroform-toluene glasses at 77°K, are given in Table 2.

These results suggest that in chloroform-containing glasses of compounds (I) through (VI) there is formed a weak complex (XI), in which the negative ends of the electric dipoles of two chloroform molecules interact with and perturb the d_{z^2} orbital of the cupric chelate. The absence of such a weak complex in the case of compounds (VII) through (X) may be explained by the presence in them of bulky, or negatively charged, side groups. Cis-trans isomerism cannot explain this doubling of the spectra in compounds (I) through (VI).

7. Equation of the spin Hamiltonian parameters to molecular orbital coefficients in copper(II) complexes

If spin-orbit coupling, Zeeman interactions, and hyperfine interactions are all neglected, then, as

Table 2

E.P.R. spectral parameters of 10^{-3} M solutions of copper(II) complexes homogeneously dispersed in chloroform-toluene glasses (chloroform: toluene = 60:40) at 77°K. Hyperfine tensor components are in units of 10^{-4} cm^{-1}. Parameters marked * could not be determined because the spectral features on which they depend were not resolved.

Compound	$\langle g \rangle$	$\langle A \rangle$	$g_{\parallel}$	$g_{\perp}$	$A(^{63}Cu)$	$B(^{63}Cu)$	$A(^{65}Cu)$	$B(^{65}Cu)$
II	2·130	71·1	2·296	2·047	168·8	22·3	178·9	17·2
			2·254	2·068	192·3	10·5	*	*
III	2·123	75·7	2·273	2·043	181·8	22·7	191·7	17·8
			2·246	2·062	196·6	15·3	*	*
IV	2·121	77·6	2·303	2·030	165·8	33·4	174·7	29·0
			2·238	2·062	193·9	19·4	204·2	14·2
V	2·119	78·2	2·277	2·041	182·6	26·0	191·2	21·7
			2·241	2·108	197·4	18·5	*	*
VI	2·131	66·4	2·342	2·026	145·9	26·8	*	*
			2·309	2·043	157·7	20·7	*	*
VII	2·128	69·9	2·300	2·042	168.2	20·8	178·2	15·8
VIII	2·130	77·1	2·274	2·042	180·4	25·4	190·1	20·5
IX	2·132	70·8	2·299	2·049	169·2	21·6	*	*
X	2·123	76·2	2·286	2·042	173·4	27·5	182·6	23·0

already explained, it may be shown that the positive hole is in an antibonding orbital $\psi(B_{1g})$, built from the cupric ion $d_{x^2-y^2}$ orbital and the appropriate ligand σ orbitals. In the case of diketonates, the σ orbitals employed are considered to be made up from the "lone pair" sp^2 hybridised σ orbitals of the oxygen atoms in the chelating ligands. The $\psi(B_{1g})$ antibonding orbital and the higher antibonding orbitals are given in order of increasing energy, in the standard hole formalism, by

$$\psi(B_{1g}) = \alpha d_{x^2-y^2} - \left(\frac{\alpha'}{2}\right)\left(-\sigma_x^{(1)} + \sigma_y^{(2)} + \sigma_x^{(3)} - \sigma_y^{(4)}\right)$$

$$\psi(B_{2g}) = \beta_1 d_{xy} - \left(\frac{\beta_1'}{2}\right)\left(p_y^{(1)} + p_x^{(2)} - p_y^{(3)} - p_x^{(4)}\right)$$

$$\psi(A_{1g}) = \alpha_1 d_{z^2} - [\alpha_1'/2(1 + 2c_1^2)^{\frac{1}{2}}]\,[\sigma_x^{(1)} + \sigma_y^{(2)} - \sigma_x^{(3)} - \sigma_y^{(4)} - 2c_1(\sigma_z^{(5)} - \sigma_z^{(6)})]$$

$$\psi(E_g') = \beta d_{xz} - [\beta'/2(2 + 8c_2^2)^{\frac{1}{2}}]\,[p_z^{(1)} - p_z^{(3)} + 2c_2(p_x^{(5)} - p_x^{(6)})]$$

$$\psi(E_g^2) = \beta d_{xz} - [\beta'/(2 + 8c_2^2)^{\frac{1}{2}}]\,[p_z^{(2)} - p_z^{(4)} + 2c_2(p_y^{(5)} - p_y^{(6)})] \qquad 4.26$$

Tetragonal distortion in the z-axis direction has been taken into account by including the parameters c_1 and c_2. For a complex with octahedral symmetry, c_1 and c_2 would both equal unity; for a square coplanar complex

with no tetragonal distortion, c_1 and c_2 would both be zero. The coordinate system used in defining these orbitals is a right-handed Cartesian system, and ligands 1, 2 and 5 are placed on the positive x, y and z axes, and ligands 3, 4 and 6 on the negative x, y and z axes respectively. Following standard procedure, spin-orbit coupling, nuclear magnetic interactions, and nuclear quadrupolar interactions are then considered as perturbations affecting the basis functions. The contribution to the Hamiltonian due to these interactions is

$$\begin{aligned}\mathcal{H}' &= \lambda(r)\underline{L}.\underline{S} + \beta_e\underline{H}.(\underline{L} + 2{\cdot}0023\underline{S}) \\ &+ 2\gamma_N\beta_e\beta_N\left\{[(\underline{L} - \underline{S}).\underline{I}/r^3] + 3(\underline{r}.\underline{S})(\underline{r}.\underline{I})/r^5] \right. \\ &+ \left.\frac{8\pi}{3}\delta(r)\underline{S}.\underline{I}\right\} + \left[\frac{eQ}{2I(2I-1)}\right]\left\{[I(I+1)/r^3]\right. \\ &- \left. 3(\underline{r}.\underline{I})^2/r^5\right\} - \gamma_N\beta_N\underline{H}.\underline{I} \qquad 4.27\end{aligned}$$

and the matrix elements of these perturbation interactions are then equated with the corresponding matrix elements of the spin Hamiltonian 4.25, and from the resulting equations the spin Hamiltonian parameters may be expressed as functions of the coefficients of the anti-bonding orbitals given above.[5,13,14] This procedure results in the following relationships,

$$g_{11} = 2{\cdot}0023 - 8(\lambda_o/\Delta E_{xy})[\alpha^2\beta_1^2 - f(\beta_1)] \qquad 4.28$$

$$g_{\underline{1}} = 2{\cdot}0023 - 2(\lambda_o/\Delta E_{xz})[\alpha^2\beta^2 - g(\beta)] \qquad 4.29$$

$$A = P\{-\alpha^2(\tfrac{4}{7} + K_o) - 2\lambda_o\alpha^2[(4\beta_1{}^2/\Delta E_{xy}) + (3\beta^2/7\Delta E_{xz})]\} \qquad 4.30$$

$$B = P\{\alpha^2(\tfrac{2}{7} - K_o) - (22\lambda_o\alpha^2\beta^2)/(14\Delta E_{xz})\} \qquad 4.31$$

In these equations λ_o is the spin-orbit coupling constant for the free copper ion[15] and

$$P = 2\gamma_N\beta_e\beta_N < d_{x2-y2}|r^{-3}|d_{x2-y2} >, \qquad 4.32$$

and may be estimated theoretically through calculations involving Hartree wave functions; alternatively P may be obtained experimentally from the optical hyperfine structure intervals of copper; Abragam and Pryce give a value of P equal to 0·036 cm^{-1} for cupric complexes.[16] K_o is a correction term to allow for the presence of Fermi contact contributions from excited-state configurations, mainly the $3s3d^{10}$ and the $3d^84s$ configurations, of copper(II); the value of K_o has been shown to be 3/7.[6]

The functions $f(\beta_1)$ and $g(\beta)$ are defined by

$$f(\beta_1) = \alpha\alpha'\beta_1{}^2 s + \alpha\alpha'\beta_1(1 - \beta_1{}^2)^{\frac{1}{2}}T(n)/2 \qquad 4.33$$

$$g(\beta) = \alpha\alpha'\beta^2 s + \alpha\alpha'\beta(1 - \beta^2)^{\frac{1}{2}}T(n)/\sqrt{2} \qquad 4.34$$

where s is the overlap integral

$$s = \tfrac{1}{2} \langle d_{x^2-y^2} | - \sigma_x^{(1)} + \sigma_y^{(2)} + \sigma_x^{(3)} - \sigma_y^{(4)} \rangle$$

$$= 2 \langle d_{x^2-y^2} | - \sigma_x^{(1)} \rangle \qquad 4.35$$

and it has been shown[14] that the value of s is 0·076. The constant T(n) is an integral over ligand functions and it arises in the calculation of the matrix elements of the Hamiltonian with the wave functions; it has been shown[13] to have the value 0·22.

Equation 4.30 may be written[14]

$$\alpha^2 = (-\tfrac{A}{P}) + (g_{11} - 2) + \tfrac{3}{7}(g_{\perp} - 2) + 0{\cdot}04 \qquad 4.36$$

The term 0·04 is an approximate average value for the several integrals in equations 4.28 and 4.29. α may thus be obtained from equation 4.36, and α' may be calculated from the normalising condition,

$$\alpha^2 + (\alpha')^2 - 4\alpha\alpha' \langle d_{x^2-y^2} | - \sigma_x^{(1)} \rangle = 1 \qquad 4.37$$

Equations 4.28 and 4.29 may be used to evaluate β_1 and β, if the d-d transition energies are known.

8. d-d transition energies and α-values in cupric chelates I - X

The visible-ultraviolet spectrum of cupric tropolonate consists of a weak absorption at 14, 700 cm^{-1}

($\epsilon \sim 100$) and a very intense charge-transfer band at 26,000 cm^{-1}. The maltol complex(II) exhibits a weak absorption at 14,600 cm^{-1}, a very weak inflexion at 17,500 cm^{-1} and an intense charge-transfer band at 26,000 cm^{-1}, tailing to 19,000 cm^{-1} in toluene solution. Taking ΔE_{xy} to be 14,700 cm^{-1} and using this value in equation 4.28 results in unreasonable values for the degree of in-plane π-bonding. It is therefore assumed that 14,700 cm^{-1} is the energy of the transition $\psi(A_{1g}) \leftarrow \psi(B_{1g})$; this assignment is supported by the fact that changes in the solvent give rise to changes in the absorption frequency. The other d-d transitions are masked by charge-transfer bands, but lower limits of 20,000 and 22,000 cm^{-1} can be assigned to ΔE_{xy} and ΔE_{xz} respectively. The use of the latter transition energies in equation 4.28, however, results in unreasonably large estimates of the degree of π-bonding in the six-membered ring chelates, whereas with the assignment of a value of 14,700 cm^{-1} to ΔE_{xy} reasonable descriptions are obtained in these cases. It is thought that the relative order of the energies of the B_{2g} and the A_{1g} levels inverts on going from a six-membered to a five-membered chelate ring; the B_{2g} level is lower in the six-membered ring systems, while the A_{1g} level is lower in the five-membered ring chelates.

Values of α^2 are listed in Table 3.

Table 3

B_{1g} molecular orbital coefficients, α^2, for compounds I - VI, and for their chloroform complexes.

Compound	I	II	III	IV	V	VI
uncomplexed species	0·866	0·858	0·854	0·843	0·876	0·806
complexed species	0·836	0·825	0·841	0·816	0·841	0·799

9. Bonding in complexes of copper(II) chelates and chloroform

The spin Hamiltonian parameters for the chloroform complexes may be treated in the same way, and the α^2 values are also listed in Table 3. It can be seen that complexing with chloroform results in a small increase in the electron delocalisation in the σ-framework of these compounds.

10. Axial perturbation in cupric chelates

Consider two electric dipoles, each of moment μ, centred at the points (o, o, a) and (o, o, - a) respectively, as shown in Figure 10. The effect of these dipoles is to alter the energy of a positive charge at the point

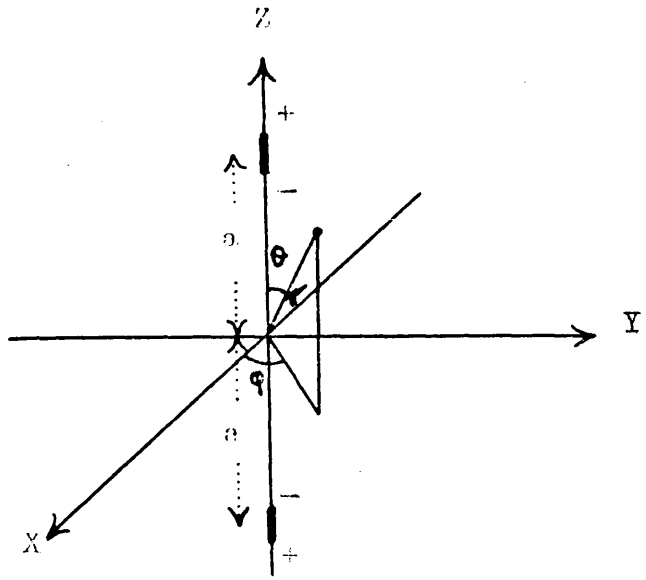

Figure 10.

Axial perturbation of planar complexes by electric dipoles situated on the z axis at points (o, o, a) and (o, o, -a).

(r, θ, φ) by an amount

$$\mathcal{H}' = e\mu a^{-2}\left\{2 + 3r^2a^{-2}(3\cos^2\theta - 1)\right\} \qquad (r < a)$$

The molecular orbitals in the chloroform complexes may be described in terms of the orbitals of the isolated cupric chelates perturbed by the axial interaction $\mathcal{H}'$. The molecular orbitals described in equation 4.26 have no off-diagonal matrix elements of $\mathcal{H}'$ and so they are not mixed by this axial perturbation. Their energies, however, are altered by amounts given, to first order, by the appropriate diagonal elements of $\mathcal{H}'$. Using simple Slater functions for the d-contributions to the orbitals 4.26, these diagonal elements can be shown to be

$$\begin{aligned}
\langle \psi(B_{1g})|\mathcal{H}'|\psi(B_{1g})\rangle &= \alpha^2(2e\mu a^{-2} - 216e\mu a^{-4}a_o{}^2Z_{eff}^{-2}) \\
\langle \psi(B_{2g})|\mathcal{H}'|\psi(B_{2g})\rangle &= \beta_1{}^2(2e\mu a^{-2} - 216e\mu a^{-4}a_o{}^2Z_{eff}^{-2}) \\
\langle \psi(A_{1g})|\mathcal{H}'|\psi(A_{1g})\rangle &= \alpha_1{}^2(2e\mu a^{-2} + 216e\mu a^{-4}a_o{}^2Z_{eff}^{-2}) \\
\langle \psi(E_g{}^1)|\mathcal{H}'|\psi(E_g{}^1)\rangle &= \langle \psi(E_g{}^2)|\mathcal{H}'|\psi(E_g{}^2)\rangle \\
&= \beta^2(2e\mu a^{-2} + 108e\mu a^{-4}a_o{}^2Z_{eff}^{-2})
\end{aligned} \qquad 4.38$$

where $a_o = h^2(4\pi^2\mu e^2)^{-1}$

and $Z_{eff}e$ is the effective core potential experienced by the positive hole.

The effect of these axial interactions is therefore to decrease the separations ΔE_{xy} and ΔE_{xz} by amounts given by:

$$\Delta' E_{xy} = -(hc)^{-1}(\beta_1^2 - \alpha^2)(2e\mu a^{-2} - 216e\mu a^{-4} a_o^2 Z_{eff}^{-2}) \text{ cm}^{-1} \quad 4.39$$

$$\Delta E_{xz} = -(hc)^{-1}\{(\beta^2 - \alpha^2)(2e\mu a^{-2}) + (\beta^2 + 2\alpha^2)(108e\mu a^{-4} a_o^2 Z_{eff}^{-2})\} \text{ cm}^{-1} \quad 4.40$$

The differences in the parallel components of the g and hyperfine tensors of the isolated complexes and the perturbed complexes, Δg_{11} and ΔA, may be expressed, through substituting equation 4.39 into equations 4.28 and 4.30, as follows:

$$\Delta g_{11} = g_{11}(\text{perturbed}) - g_{11}$$

$$= [(g_{11} - 2{\cdot}0023)/\Delta E_{xy}][(hc)^{-1}(\beta_1^2 - \alpha^2)(2e\mu a^{-2} - 216e\mu a^{-4} a_o^2 Z_{eff}^{-2})] \quad 4.41$$

$$\Delta A = A(\text{perturbed}) - A$$

$$= -1{\cdot}86P\lambda_o a^2 (hc)^{-1}\{[4\beta_1^2/(\Delta E_{xy})^2](\beta_1^2 - \alpha^2)(2e\mu a^{-2} - 216e\mu a^{-4} a_o^2 Z_{eff}^{-2}) + (\tfrac{3}{7})[\beta^2/(\Delta E_{xz})^2][(\beta^2 - \alpha^2)2e\mu a^{-2} + (\beta^2 + 2\alpha^2)108e\mu a^{-4} a_o^2 Z_{eff}^{-2}]\} \quad 4.42$$

where g_{11} and A refer to the isolated cupric chelates, and g_{11} (perturbed) and A (perturbed) refer to the chloroform complexes. These equations 4.41 and 4.42, along with 4.39 and 4.40 predict the following changes.

(1) The parallel components of the g tensor for the chloroform complexes should be greater than the corresponding components in the isolated cupric chelates, provided that the perturbing dipoles are oriented in the manner shown in Figure 10. This prediction is borne out by the experimental observations.

(2) Since A and λ_o for copper(II) are both negative, then the hyperfine tensor components, A, for the chloroform complexes should be numerically smaller than those for the isolated cupric chelates, provided the perturbing dipoles are oriented in the manner shown in Figure 10. Again, this prediction is verified by the experimental observations.

The experimental A and g values, together with those calculated from equations 4.41 and 4.42, are listed in Table 4. For the calculated entries, the following values of the parameters in these equations are assumed:

$$\beta_1^2 = \beta^2 = 0{\cdot}95$$

$$\mu = 4{\cdot}8 \times 10^{-18} \text{ e.s.u.}$$

$$a = 2{\cdot}8 \times 10^{-8} \text{ cm}$$

$$Z_{eff} = 11{\cdot}86$$

Within the limits of the approximations used, the observed and predicted changes in the spin Hamiltonian parameters agree, except in the case of compound(VI) in which the predicted changes are higher than those observed. It is thought that, in this case, the perturbing dipoles are unable to approach the cupric ion as closely as in the case of compounds(I) through (V).

From a consideration of these results it appears that the chlorine atoms in the chloroform molecule act as ligands in these complexes. If the interaction between the complex and the chloroform were to occur by hydrogen bonding of chloroform molecules to the A_{1g} orbitals of the isolated complex, the changes in g_{11} and in A would have been in senses opposite to those which have been observed. Infra-red studies have indicated[17] that weak hydrogen bonds are formed between chloroform and planar metal β-ketoenolates. The paramagnetic resonance evidence presented here, together with this infra-red evidence, suggests that at 77°K the structures of these complexes are as shown in (XII). The magnetic

Table 4

Calculated and observed changes in g_{11} and in $A(^{63}Cu)$ when copper(II) chelates complex with chloroform

	I	II	III	IV	V	VI
Δg_{11} (calculated)	0·030	0·034	0·045	0·050	0·036	0·087
Δg_{11} (observed)	0·027	0·042	0·027	0·065	0·036	0·033
ΔA (calculated) (cm^{-1})	11×10^{-4}	14×10^{-4}	26×10^{-4}	28×10^{-4}	20×10^{-4}	36×10^{-4}
ΔA (observed) (cm^{-1})	18×10^{-4}	23×10^{-4}	15×10^{-4}	28×10^{-4}	15×10^{-4}	12×10^{-4}

resonance evidence does not permit a distinction between cupric chelate: $2(CHCl_3)$ and cupric chelate: $CHCl_3$.

11. Paramagnetic relaxation in solutions of β-ketoenolates of copper(II)

The electron paramagnetic resonance spectrum, recorded at room temperature, of a 0·001 M. solution of cupric tropolonate dissolved in chloroform, is shown in Figure 11.

If the orbital contribution to the paramagnetic moment of the complex had been completely quenched by the ligand field, then the magnetic moment would have been due entirely to spin, and the g factor would have been 2·00232, and the magnetic properties would have been independent of the orientation of the complex relative to the magnetic field, i.e. the magnetic properties would have been isotropic. Under such conditions, one should expect a quartet consisting of four equally intense peaks separated by the same amount due to the isotropic interaction of the electron with the ^{63}Cu and ^{65}Cu nuclei. The magnetogyric ratios of these two nuclei are very similar to each other, and one would expect to see the spectra form the two isotopic species to be superimposed, thereby giving rise to the four equally intense peaks mentioned.

In fact, a spectrum of this sort is not observed. Four peaks are obtained but they appear to differ in intensity, and they are not equally speced. The peaks to the low field side of the spectrum appear to be less intense and are broader than those on the high field side of the spectrum. See Figure 11. To understand this phenomenon, it is necessary to consider the Hamiltonian for the problem. The magnetic terms in the Hamiltonian for the unpaired electron in a tetragonal[18,19] cupric complex can be written in the form,

$$\mathcal{H} = g_r\beta_e H_r S_r + g_p\beta_e H_p S_p + g_q\beta_e H_q S_q + A_r S_r I_r + A_p S_p I_p + A_q S_q I_q \qquad 4.43$$

where the r axis is the symmetry axis, in a right-handed axis system. In a tetragonal complex,

$$g_r = g_{11} \neq g_p = g_q = g_{\perp}$$

and $A_r = A \neq A_p = A_q = B$

Now, in solution the complex undergoes rotational motions and the Brownian motions tend to average out the anisotropies in the g and hyperfine tensors, and thus give rise to "averaged" spectra. For this to happen, however, the rate of rotation in solution must be of the order of magnitude of, or greater than, the separation

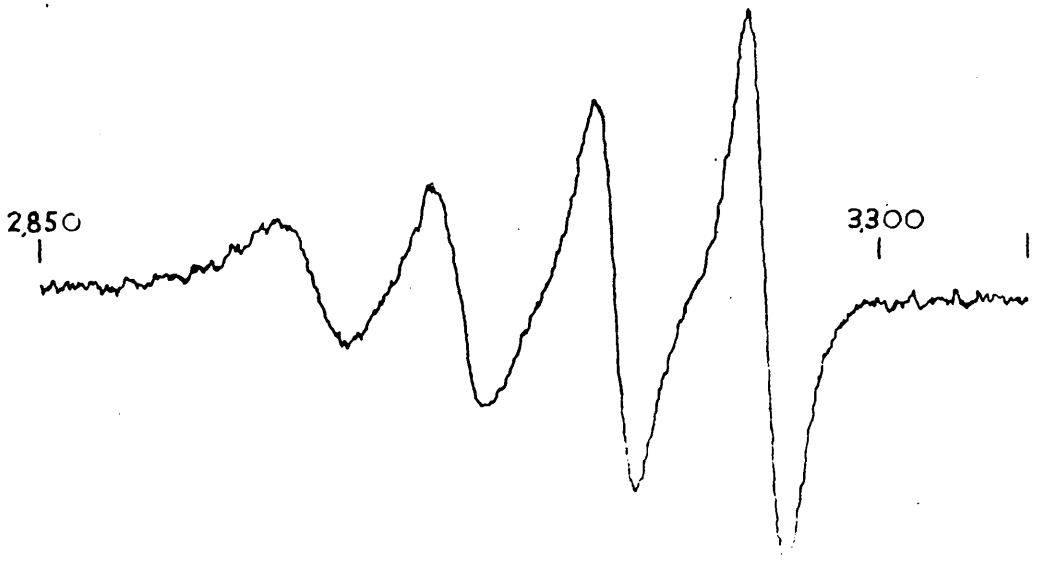

Fig. 11 E.P.R. SPECTRUM OF A 10^{-3}M SOLUTION OF CUPRIC TROPOLONATE IN CHLOROFORM. THE SPECTRUM WAS RECORDED AT 298°K. FIELD MARKERS ARE IN GAUSS UNITS.

(in Hz.) between the different extreme kinds of anisotropic spectra such as are obtained from crystallites in a polycrystalline sample. A simple calculation shows that this averaging will take place in copper tropolonate solution only if the rate of rotation is greater than about 10^9 c/s. Since an averaged spectrum was not obtained, it follows that the rate of rotation must be less than 10^9 c/s. Furthermore, since the line widths are different, it follows that the paramagnetic relaxation time, T_2, depends on the nuclear orientation which is a function of I_z. Hyperfine interactions must therefore contribute to the relaxation of the electron spin.

Magnetic dipolar interactions, exchange interactions, intramolecular vibrations, and tumbling of the complex in solution, all cause time variant magnetic fields to be seen by the unpaired electron. Although these motions are random, nevertheless, the Fourier component at the resonant frequency can result in electron spin-flips which shorten the lifetime of the unpaired electron in a particular energy level and thus broaden the resonance. In the dilute solutions, used, direct magnetic dipolar interactions average out to zero, the exchange interactions can be ignored since the spectrum does not alter on

further dilution, and the vibrations are thought to be negligible. McConnell[20] has considered the effects of the tumbling motions in detail and has shown that these are of primary importance in relaxing electron spins. The rotation of the complex in solution causes the energy of the electron to change with time. The electron effectively experiences a fluctuating magnetic field, and out of this randomly fluctuating magnetic field it extracts the Fourier component at its resonant frequency; thus the lifetime of the electron in any given state decreases and so the e.p.r. line is broadened. In general, the relaxation due to tumbling of the "microcrystal" will increase with increasing $\Delta g = g_{11} - g_{\underline{1}}$, i.e. as Δg increases the linewidth increases.

The Hamiltonian for the complex may be written in terms of a coordinate system based on the complex,

$$\mathcal{H} = \beta_e[g_{11}H_rS_r + g_{\underline{1}}(H_pP_p + H_qS_q)] + AI_rS_r + B(I_pS_p + I_qS_q) + \cdots \quad 4.44$$

where p, q, r, are a set of orthogonal unit vectors fixed in the complex, r being the unit vector parallel to the symmetry axis. The presence of other terms in the Hamiltonian which are not important for the present discussion has been indicated by the + ··· in this

expression. Transformation of this expression to a system of axes, x, y, z, fixed in the laboratory, is now effected. The applied field lies along the z axis. The resulting equation for $\mathcal{H}$ may be considered as compounded from two parts, $\mathcal{H}_o$ and $\mathcal{H}_t$, the former being time-invarient, the latter time-dependent. It may be shown that[20]

$$\mathcal{H}_o = g\beta_e H_o S_z + a\underline{S}.\underline{I} \qquad 4.45$$

where $g = (1/3)(g_{11} + 2g_{\underline{1}})$, and $a = (1/3)(A + 2B)$;

and

$$\begin{aligned}\mathcal{H}_t = {} & [(\Delta g)\beta_e H_o + bI_z][\cos^2\theta(t) - 1/3]S_z \\ & + \tfrac{1}{2}[(\Delta g)\beta_e H_o + bI_z][\sin\theta(t)\cos\theta(t)][S_+\exp(-i\varphi(t)) \\ & + S_-\exp(i\varphi(t))] \\ & - \tfrac{1}{4}b[\cos^2\theta(t) - 1/3][S_+I_- + S_-I_+] \\ & + \tfrac{3}{4}b[\sin^2\theta(t)][I_+S_+\exp(-2i\varphi(t)) + I_-S_-\exp(2i\varphi(t))] \\ & + \tfrac{1}{2}b[\sin\theta(t)\cos\theta(t)][I_+\exp(-i\varphi(t)) + I_-\exp(i\varphi(t))]S_z\end{aligned} \qquad 4.46$$

where $b = A - B$, and θ and φ are the polar and azimuthal angles of the microcrystalline symmetry axis (r) relative to the laboratory x, y, z axes.

The time average value for $\mathcal{H}_t$ is zero, and the centre of gravity of each of the hyperfine multiplet resonances is obtained from the eigenvalues of $\mathcal{H}_o$. The line-broadening arises from the effects of $\mathcal{H}_t$. There is a great similarity between the terms in the expression for $\mathcal{H}_t$ and those in the expression for the dipolar contribution to nuclear relaxation.[21] Spin-lattice relaxation, with characteristic time T_1, arises from the second, third and fourth terms in 4.46 containing the electron spin raising and lowering operators, defined by

$$S_{\pm} = S_x \pm iS_y \qquad 4.47$$

Nuclear relaxation arises from the third, fourth and fifth terms. There is a contribution to the broadening of the electron resonance from the first and last terms in equation 4.46, but the characteristic time for this process is T_2'. Using the Bloembergen-Purcell-Pound notation, T_2 is the total line width parameter,

$$T_2 = \tfrac{1}{2}g(\nu)_{max} \qquad 4.48$$

where $g(\nu)$ is the normalised line shape on a frequency scale. The order-of-magnitude relationship

$$\frac{1}{T_2} \sim \frac{1}{T_2'} + \frac{1}{2T_1} \qquad 4.49$$

is used.

An approximate solution of this perturbation problem has been given by McConnell. If it is assumed that $|\Delta g\beta_e H_o| >> |b|$, the last three terms in 4.46 may be neglected. This implies neglect of nuclear spin-lattice relaxation, so that the time-dependence of matrix elements of I_z in the first two terms is also neglected. The following equations have been derived

$$\frac{1}{T_1} \geq (\frac{8\pi^2}{15})(\Delta g\beta_e H_o + bI_z)^2 h^{-2}\tau_c(1 + 4\pi^2\nu_o^2\tau_c^2)^{-1} \qquad 4.50$$

$$\left(\frac{1}{T_2'}\right)^2 \geq (\frac{32\pi}{45})(\Delta g\beta_e H_o + bI_z)^2 h^{-2}\tan^{-1}(2\tau_c/T_2') \qquad 4.51$$

The inequality arises from the possible presence in equation 4.46 of other relaxation terms. ν_o is the frequency at which resonance occurs; τ_c is the correlation time for the angular functions $[(\cos^2\theta - 1/3)$ and $(\sin\theta\cos\theta)]$ of the microcrystal orientation. In accordance with Bloembergen, Purcell and Pound's use of Debye theory, τ_c is assumed to be the same for both angular functions, and to be given by

$$\tau_c = 4\pi\eta a^3(3kT)^{-1} \qquad 4.52$$

where η is the liquid viscosity and a is the effective radius of the microcrystal in solution.

McConnell has considered only rotational effects, while McGarvey[22] has considered other effects and has shown that, provided the microcrystal maintains its ordered structure for a time that is much greater than its period of tumbling as it moves in solution, then the linewidth may be attributed to two mechanisms.

The first of these is that due to the tumbling of the microcrystal in solution, i.e. the mechanism discussed by McConnell. The second arises from interaction between the ground state and a low lying excited state which can reduce the lifetime of an electron spin in the former.

It should be noticed that these two mechanisms affect line widths in different ways. In the first case, the line width is a function of the symmetry of the electrostatic field surrounding the unpaired electron, and as the symmetry of this electrostatic field decreases, the more anisotropic does the e.p.r. spectrum become. The second mechanism affects spectral line widths in a different way, e.g. in $[Cu(H_2O)_6]^{2+}$ the electrostatic field at the copper(II) ion has almost cubic symmetry, and there is therefore a low lying excited state which limits the lifetime of the positive hole in its ground state. Even in the crystalline state, minute crystal vibrational interactions are strong enough therefore to broaden out the

hyperfine spectrum at room temperature.[23] As the copper(II) complex becomes more distorted, this mixing is reduced until broadening due to it can be neglected in the case of square planar copper(II) complexes, even in solution.

McGarvey concludes that McConnell's arguments are valid in the case of copper(II) complexes, but that in the case of other transition metal ion complexes, particularly when near orbital degeneracies are found, other broadening contributions should be considered.

The Russian authors A. Al'Tshuler and K.A. Valiev[24] have criticised the McConnell-McGarvey theory of line widths in the e.p.r. spectra of transition metal ion complexes on the grounds that it is based on experiments carried out at a single frequency only, and at a single temperature, and they state that B.M. Kozyrev[25] has carried out many sided experimental investigations of paramagnetic resonance in liquid solutions of salts at different temperatures and over a wide frequency range. Kozyrev believes that, in most cases, the experimental dependence of the longitudinal relaxation time on temperature and direction of the applied magnetic field is completely at variance with McConnell's theory. Al'Tshuler and Valiev believe

that T_1 is defined by the vibrations within the complex rather than by rotations of the complex.

The findings of these Russian authors, however, are not substantiated by the very detailed discussion of the e.p.r. linewidths of free radicals and transition metal ions given by D. Kivelson and co-workers.[26-30] He has developed in great detail the theory of line widths of free radicals in diamagnetically "diluted" crystals and in dilute liquid solutions, considering only those cases in which the orbital angular momentum has been almost entirely quenched. His theory is restricted to high (room) temperature, strong applied fields, small anisotropy, and no relaxation through chemical reactions, and he does not consider the effects of intermolecular electron-electron and electron-nuclear dipolar interactions. Nuclear quadrupole moments, zero field splittings, anisotropic Zeeman terms, and intramolecular electron-nuclear dipolar interactions, as well as motional and exchange effects are considered in the strong field case.

The theory is developed in a manner that is particularly adaptable to the study of liquids but it has also been used to study crystals, since the resulting equations, although only applicable for small anisotropies, are

particularly simple. Kivelson has shown that his theory can be used to explain Hausser's results[31] - i.e. the existence of an optimum viscosity for the observation of hyperfine structure.

Rogers and Pake[32] have studied the e.p.r. spectrum of vanadyl ion in solution. They found that the linewidths of the individual hyperfine components depend on the nuclear spin orientation, defined by m_I, and their results obtained at 9250 MHz. and at 24,300 MHz. appear to support McConnell's description of the origin of the anisotropy in the e.p.r spectrum.

On theoretical grounds Kivelson[27] has derived a polynomial relationship between the line width of a hyperfine peak in an e.p.r. spectrum and the nuclear spin quantum number, m_I. If the line width of the hyperfine line corresponding to the nuclear orientation, m_I, is defined as $(\Delta H)_{m_I}$, then

$$(\Delta H)_{m_I} = (\alpha' + \alpha'') + \beta m_I + \gamma m_I^2 + \epsilon m_I^4 \qquad 4.53$$

where all parameters may be temperature dependent. γ arises from modulation of the anisotropic hyperfine tensor; α' arises from modulation of both the anisotropic hyperfine tensor and the anisotropic g-factor; β arises from a cross-correlation between these two; ϵ arises from

quadrupolar relaxation; and α'' arises from other mechanisms, e.g. near degeneracies, chemical exchange, etc. Kivelson showed that for vanadyl acetylacetonate ϵ was too small to be determined from his experiments, but that his data indicated the presence of a small but significant cubic term. His experimental data may be fitted to a polynomial of the form,

$$(\Delta H)_{m_I} = \alpha + \beta m_I + \gamma m_I^2 + \delta m_I^3 \qquad 4.54$$

where $(\Delta H)_{m_I}$ is the peak-to-peak derivative line width of the hyperfine line corresponding to m_I. α is again split into two terms α' and α'', as before. Kivelson has found that the residual line width, α'', is independent of field and of nuclear quantum number, m_I; it is linear in $T\,\eta^{-1}$. He attributes α'' to modulation of rotational angular momentum and the interaction of this momentum with the spin by means of spin-orbit coupling. Kivelson shows that δ arises from modulation of the g and hyperfine tensors by molecular reorientation, as do the terms in α', β and γ.

Kivelson[30] has found that at 237°K. the line widths of the hyperfine components in the e.p.r. spectrum of copper acetylacetonate in chloroform are very unequal, indicating large anisotropic dipolar and g tensor effects. At 331°K the line widths are much less unequal and the two high-field lines are broader than the corresponding lines

in the 237°K spectrum. This is taken as evidence for the onset of significant contributions from spin-rotational coupling.

The general conclusions reached by Kivelson and his co-workers are now summarised. The line widths of hyperfine components in the e.p.r. spectra of copper and vanadyl acetylacetonate in solution may be accounted for in terms of anisotropic nuclear-electronic magnetic dipolar and g tensor interactions, together with spin-rotational interactions. The line widths in dilute solutions appear to fit these three mechanisms, the first two at lower temperatures, the last at higher temperatures. Both the g tensor and the spin-orbit interactions are proportional to the spin-orbit coupling constant; for this reason, the spin-rotational relaxation is more marked for Cu^{2+} than VO^{2+}, being about ten times greater for a given value of $T\,\eta^{-1}$. This simplified theoretical treatment, including approximate expressions for spin-rotational constants, may be used to interpret the experimental data for VO^{++} and for Cu^{++} acetylacetonates, to within 10 to 20%, in terms of one adjustable parameter r for each solution.

That spin-rotational relaxation gives rise to the residual line widths, is supported by the appropriate linear $T\,\eta^{-1}$ dependence, magnetic field independence,

appropriate dependence on spin-orbit coupling constant, and correct order of magnitude results. A pseudo-vibrational Raman process of relaxation is discussed and rejected. It is thought that other vibrational processes may contribute small field-dependent terms to α''.[28] In the case of copper there may be a small quadrupolar contribution to the line width.

12. The mechanism of relaxation in solutions of β-ketoenolates of copper(II)

Table 5 contains the experimental line widths, measured between points of maximum and minimum slope, of the four absorption peaks in the e.p.r. spectra obtained from 10^{-3} M. solutions of cupric tropolonate in chloroform, in toluene, and in chloroform:toluene (60:40) solution, respectively, at 295°K. The line widths of corresponding solutions of compounds (III) and (VII) are similar to those of the tropolonate. For corresponding solutions of (IV) and (VIII) the low field lines are broader. Line widths for (VIII) in chloroform:toluene solution (60:40) are also listed in Table 5.

The line width is related to the overall relaxation time, T_2, by the equation

$$\text{line width} \sim (\sqrt{3}\,\pi\,T_2)^{-1} \qquad 4.55$$

The spin-lattice relaxation time (T_1) and the transverse relaxation time (T_2') are related to the overall relaxation time by the equation

$$\frac{1}{T_2} = \frac{1}{T_2'} + \frac{1}{2T_1} \qquad 4.56$$

and McConnell has derived expressions for T_1 and T_2' in terms of spin Hamiltonian parameters and a correlation time, which have been discussed earlier in this thesis. Using the line widths in Table 5 and the spin Hamiltonian parameters in Table 1, in equations 4.50, 4.51, 4.52, 4.55 and 4.56, shows that, at 295°K, and at a frequency of 9270×10^6 Hz., longitudinal and transverse relaxation processes are equally efficient in relaxing the electron spins. The correlation time is found to be $\tau_c = (4{\cdot}0 \pm 0{\cdot}5) \times 10^{-11}$ sec., and the effective radius of the rotating molecule

$$a = (4{\cdot}0 \pm 0{\cdot}2) \times 10^{-8} \text{ cm}$$

The motion which controls the line widths in these e.p.r. spectra of cupric tropolonate is therefore rotation about the long axis of the molecule.

A change in the radius of the cylinder swept out by this rotation about the long axis results in changes in the correlation time and in the line widths; increasing this radius will result in an increase in τ_c

and in the line widths, whereas increasing the length of the molecule along the rotation axis will have very little effect on the value of τ_c and on the line widths. This agrees with the experimental findings.

Table 5

Line widths (MHz.), measured between points of maximum and minimum slope, at 295°K, of 10^{-3} M solutions of (I) and (VIII) in various solvents

Compound	Solvent	I_z			
		-3/2	$-\frac{1}{2}$	$\frac{1}{2}$	3/2
(I)	chloroform	98	76	62	59
	toluene	112	92	78	73
	chloroform:toluene (60:40)	102	77	64	62
(VIII)	chloroform:toluene (60:40)	122	88	62	49

At the temperatures used in this study, spin-rotational effects may be neglected.

The chloroform exchange reaction, (cupric chelate) $2CHCl_3 \rightleftharpoons$ cupric chelate + $2CHCl_3$ would also broaden

the e.p.r. line widths. In particular, this exchange should broaden the line widths in the spectra of compounds (I) through (VI) and spectra obtained from these compounds in chloroform solution should be broader than the corresponding spectral lines in toluene solution. The data in Table 5 is, however, not consistent with this prediction.

If the microcrystalline unit in toluene solution consists of a sandwich of the copper chelate lying between toluene molecules, then this difficulty is overcome because the increase in line width associated with this increase in the effective radius swept out by rotation about the long axis of this unit, would compensate for the expected reduction in line width compared with the line widths in chloroform solution.

It is interesting to note that these e.p.r. methods may be used to discriminate between different isomers of some of the triacylmethane complexes, or of other polyketonato complexes, of copper (II), e.g. chelates of benzoyl-di-tertiary-butylacylmethane with copper (II) could give rise to either, or to both, of the compounds (XIII) or (XIV).

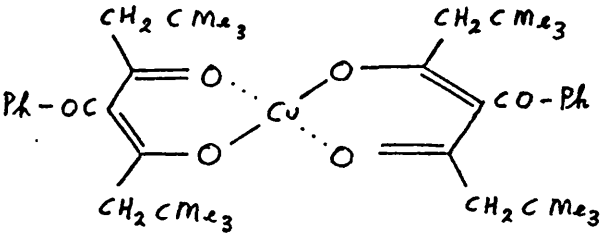

XIII

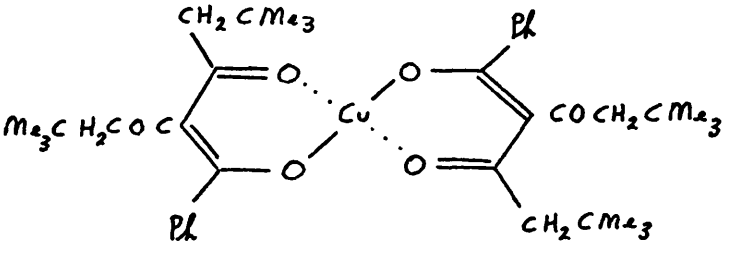

XIV

Electron paramagnetic resonance spectra of 10^{-3} M solutions of this compound in chloroform:toluene glasses at 77°K are doubled. Spin Hamiltonian parameters extracted from these spectra are,

< g >	< A >	g_{11}	$g_{\perp}$	A(^{63}Cu)	B(^{63}Cu)	A(^{65}Cu)	B(^{65}Cu)
2·122	77·5	2·289	2·039	172·0	30·2	176·6	28·0
		2·245	2·061	194·6	18·9	-	-

where the units are those employed in Table 1, and the

line widths of the four absorption peaks in its e.p.r. spectrum at 295°K are,

		I_z	
-3/2	$-\frac{1}{2}$	$\frac{1}{2}$	3/2
145	103	78	55

MHz. respectively. Comparison of these results with the data in Tables 2 and 5 indicates that the structure of this cupric chelate is (XIII). This substantiates the structure assigned to it from infra-red evidence.[33]

13. Summary of Part IV

X-band e.p.r. spectra in chloroform:toluene (60:40) glasses at 77°K show that chloroform forms weak complexes with some planar compounds of copper(II). Spin Hamiltonian parameters for some"isolated" cupric chelates and for some corresponding chloroform-chelate complexes are reported, and these parameters are equated to the atomic orbital coefficients in some of the molecular orbitals involved in bonding in both types of compound. The relative ordering of the energies of the B_{2g} and A_{1g} levels in planar copper(II) compounds may change if the ligand is changed. Effects of axial perturbations which arise from two axial dipoles acting on planar cupric complexes are considered, and first-order perturbation theory is used to obtain relationships which connect the spin Hamiltonian parameters for the "isolated" complexes with those for the perturbed complexes: experimental observations are in accord with the theoretical treatment. Relaxation arising from rotation about the long axis of these cupric complexes controls the line widths in their e.p.r. spectra recorded at 295°K: the effect of chloroform complexing on paramagnetic relaxation phenomena in these complexes is noted. E.p.r. methods may be used

to discriminate between different isomers of poly-ketone complexes of copper(II).

References to Part IV

1. H.A. Bethe, Ann. Physik., 1929, 3, 133.
2. K. Knox, J. Chem. Phys., 1959, 30, 991.
3. J.H. van Vleck, J. Chem. Phys., 1935, 3, 803 and 807.
4. E. Fermi, Z. Phys., 1930, 60, 320.
5. A. Abragam, M.H.L. Pryce, Proc. Roy. Soc., 1951, A, 205, 135.
6. A. Abragam, M.H.L. Pryce, J. Horowitz, Proc. Roy. Soc., 1955, A, 230, 169.
7. B. Bleaney, Phil. Mag., 1951, 42, 441.
8. J.M. Barbour, D.A. Morton-Blake, A.L. Porte, J. Chem. Soc. (A), 1968, 878.
9. R.H. Sands, Phys. Rev., 1955, 99, 1222.
10. R. Neiman, D. Kivelson, J. Chem. Phys., 1961, 35, 156.
11. H.R. Gersmann, J.D. Swalen, J. Chem. Phys., 1962, 36, 3221.
12. H.R. Falle, G.R. Luckhurst, Mol. Phys., 1966, 10, 597.
13. A.H. Maki, B.R. McGarvey, J. Chem. Phys., 1958, 29, 31.
14. D. Kivelson, R. Neiman, J. Chem. Phys., 1961, 35, 149.
15. B.N. Figgis, J. Lewis, "Progress in Inorganic Chemistry," ed. F.A. Cotton, Interscience, London, 1964, Vol. 2, p. 99.

16. A. Abragam, M.H.L. Pryce, Proc. Roy. Soc., 1951, A, 206, 164.

17. T.S. Davis, J.P. Fackler, Inorg. Chem., 1966, 5, 242.

18. W.M. Macintyre, J.M. Robertson, R.F. Zahrobsky, Proc. Roy. Soc. (London), 1965, A, 289, 161.

19. G. Schoffa, O. Ristau, B.E. Wahler, Z. Physik. Chem. (Leipzig), 1960, 215, 203.

20. H.M. McConnell, J. Chem. Phys., 1956, 25, 709.

21. N. Bloembergen, E.M. Purcell, R.V. Pound, Phys. Rev., 1948, 73, 679.

22. B.R. McGarvey, J. Phys. Chem., 1957, 61, 1232.

23. D.M.S. Bagguley, J.H.E. Griffiths, Proc. Phys. Soc. (London), 1952, A, 65, 594.

24. A. Al'Tshuler, K.A. Valiev, Soviet Physics J.E.T.P., 1959, 35, 661.

25. B.M. Kozyrev, Doctoral Dissertation, Phys. Inst. Acad. Sci., Moscow, 1957.

26. D. Kivelson, J. Chem. Phys., 1960, 33, 1094.

27. R. Wilson, D. Kivelson, J. Chem. Phys., 1966, 44, 154.

28. P.W. Atkins, D. Kivelson, J. Chem. Phys. 1966, 44, 169.

19. R. Wilson, D. Kivelson, J. Chem. Phys., 1966, 44, 4440.

30. R. Wilson, D. Kivelson, J. Chem. Phys., 1966, 44, 4445.

31. K.H. Hausser, Naturwissenschaften, 1958, 45, 158.

32. R.N. Rogers, G.E. Pake, J. Chem. Phys., 1960, 33, 1107.

33. D.C. Nonhebel, J. Chem. Soc. (C), 1968. 676.

Appendix A

Analysis of electron paramagnetic resonance spectra of magnetically dilute glasses or of polycrystalline specimens

One of the characteristic features of glasses or of finely powdered samples is the lack of any long range crystalline order. It is possible to regard a glass or powder as being composed of a large number of small crystallites randomly oriented with respect to any axis system such as might be defined by an applied magnetic field. Thus the e.p.r. spectrum of such a system containing a paramagnetic species is composed of a large number of individual spectra, one from each crystallite. Due to anisotropies in the g and hyperfine tensors, the resultant spectrum is spread over a range of magnetic field.

Kneubühl[1] has given a quantitative treatment of such spectra. He assumes that the probability of any e.p.r. transition occurring is independent of the orientation of the crystallite in the magnetic field. Although this approximation is satisfactory for copper chelates and nitroxide radicals, it is not valid in general.[2] With this assumption the probability that an electron absorbs microwave radiation at any given magnetic field H is directly proportioned to the probability of

finding this species in a suitable orientation with respect to the magnetic field such that it undergoes a transition when this value of H is reached. The problem then reduces to an estimation of the probability that a crystallite lies in each orientation.

g factors

Consider first a spin doublet ground state radical or ion ($S = \frac{1}{2}$), with no nuclear interactions ($I = 0$), and distinguish three distinct kinds of environment for this species, these environments differing in the nature of the electrostatic field experienced by the unpaired electron.

Case A. A cubic crystal field

This case includes, for example, structures which consist of a regular tetrahedron or of a regular octahedron. The magnetic properties of the radical or ion must have the same symmetry as that of the local electrostatic field in the crystallite; hence, in this case, the magnetic properties must have cubic symmetry, i.e. the g tensor is isotropic.

Let the z axis be parallel to the applied field. The basis eigenfunctions are $|\ \frac{1}{2}\ >$ and $|\ -\frac{1}{2}\ >$. The spin Hamiltonian is

$$\mathcal{H} = g_e \beta_e S_z H$$

and the basis eigenfunctions are the spin eigenfunctions. The energies of interaction with the magnetic field are:

$E_1 = (\frac{1}{2})g_e\beta_e H$, corresponding to $\psi_1 = |\frac{1}{2}\rangle$

$E_2 = -(\frac{1}{2})g_e\beta_e H$, corresponding to $\psi_2 = |-\frac{1}{2}\rangle$

For resonance, $h\nu = \Delta E = g_e\beta_e H$.

Case B. An axially symmetric crystal field

When the symmetry of the magnetic ion site is tetragonal or trigonal, then the g factor is no longer isotropic, but it must have axial symmetry

i.e. $g_{xx} = g_{yy} \neq g_{zz}$

It is usual to take the trigonal or tetragonal axis direction as the z-axis direction, so that $g_{zz} = g_{11}$ and $g_{xx} = g_{yy} = g_{\underline{1}}$. Let the magnetic field lie at an angle θ to the symmetry axis in the zx plane. This confinement of H to this plane simplifies the treatment without loss of generality, since the location of the x and y axes is arbitrary.

The energy of interaction $E = -\mu.\underline{H}$ and the Hamiltonian is

$$\begin{aligned} \mathcal{H} &= -\mu_x H_x\theta - \mu_z H_z \\ &= g_{\underline{1}}\beta_e S_x H_x + g_{11}\beta_e S_z H_z \\ &= g_{\underline{1}}\beta_e S_x H\sin\theta + g_{11}\beta_e S_z H\cos\theta \end{aligned}$$

$$= \beta_e H(g_{11}\cos\theta . S_z + g_{\perp}\sin\theta . S_x) \qquad A1$$

The spin eigenfunctions are defined as $\psi = c_1\varphi_1 + c_2\varphi_2 = c_1|\tfrac{1}{2}\rangle + c_2|-\tfrac{1}{2}\rangle$. On solving the secular equations, via the secular determinant, the eigenvalues are shown to be

$$E = \pm \tfrac{1}{2}\beta_e H[g_{11}^2\cos^2\theta + g_{\perp}^2\sin^2\theta]^{\frac{1}{2}}$$

and for resonance $h\nu = \beta_e H(g_{11}^2\cos^2\theta + g_{\perp}^2\sin^2\theta)^{\frac{1}{2}}$

$$= g_{effective}\,\beta_e H$$

where $g_{effective} = (g_{11}^2\ell^2 + g_{\perp}^2 m^2)^{\frac{1}{2}}$

and ℓ and m are direction cosines of the field vector with respect to the z and x axes, respectively.

Case C. A rhombic crystal field

If the site symmetry is lower than axial, then the g tensor has three unequal principal values, and the x, y and z axes are uniquely specified. It is easily shown that the application of the magnetic field in a general direction which has direction cosines, ℓ, m, and n with respect to the x, y and z axes respectively, corresponds to the following Hamiltonian,

$$\mathcal{H} = \beta_e H(g_{xx}\ell S_x + g_{yy}mS_y + g_{zz}nS_z)$$

It is straightforward to show that the effective g

factor is given by

$$g_{eff}^2 = g_{xx}^2 \ell^2 + g_{yy}^2 m^2 + g_{zz}^2 n^2$$

It is now necessary to consider orientation probabilities.

<u>To find the probability that a randomly-oriented vector lies in the solid angle interval dθ</u>

If we consider an axially symmetric system, then the semi-vertical angle of the cone generated by the rotation of the axis of symmetry about an axis defined along the applied magnetic field direction, can lie between $-\pi/2 \leqslant \theta \leqslant \pi/2$. The probability that θ lies in the solid angle 2π, i.e. anywhere in the sphere, is equal to unity. The probability that a vector lies anywhere within a circle is proportioned to Ω, the solid angle subtended by the circle. Let this probability be p, then $p \alpha \Omega$. When $\Omega = 2\pi$, $p = 1$, therefore $p = \Omega/2\pi$. Now the solid angle subtented by the spherical cone is equal to

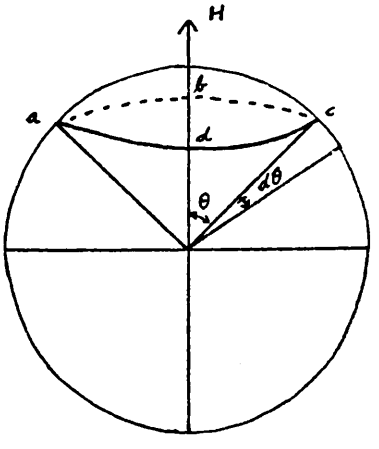

Figure A1

(area of spherical cap a b c d) r^{-2}

$$= 2\pi r h r^{-2}$$

$$= 2\pi r(r - r\cos\theta)r^{-2}$$

$$= 2\pi(1 - \cos\theta)$$

Thus $\Omega = 2\pi(1 - \cos\theta)$ A2

so that the probability that the axis of symmetry lies in this cone of semi-vertical angle θ, is

$$p = \Omega/2\pi = 1 - \cos\theta$$

Therefore, the probability that the axis of symmetry lies in the interval $d\theta$ is equal to $d(\cos\theta)$, since if θ changes by $d\theta$, p changes by

$$dp = \frac{\partial p}{\partial \theta} d\theta$$

$$= \sin\theta d\theta$$

$$= d(\cos\theta) \quad \text{A3}$$

Line shape function

Consider now the e.p.r. spectra of polycrystalline samples of radicals or ions with $S = \frac{1}{2}$ and with no nuclear interactions present. Two kinds of system will be discussed.

1. An axially symmetric system

The probability that the axis of symmetry lies in the angular range θ to $\theta + d\theta$ with respect to the applied field H is $d(\cos\theta)$. Let the normalised line shape

function which describes the intensity of the absorption signal as a function of H be g(H). Then, for resonance, it has already been shown that

$$h\nu = \beta_e H\{g_{11}^2\cos^2\theta + g_{\perp}^2\sin^2\theta\}^{\frac{1}{2}}$$

i.e.

$$\cos\theta = (g_{11}^2 - g_{\perp}^2)^{-\frac{1}{2}}\{(h\nu)^2(\beta_e H)^{-2} - g_{\perp}^2\}^{\frac{1}{2}} \quad \text{A4}$$

A crystallite whose axis of symmetry lies at an angle between θ and $\theta + d\theta$ contributes to that part of the e.p.r. spectrum falling within the field range H to H + dH. Thus, if g(H) and the probability function are both normalised,

$$d(\cos\theta) = g(H)dH$$

$$\therefore\ g(H) = \frac{d}{dH}(\cos\theta)$$

$$= -(g_{11}^2 - g_{\perp}^2)^{-\frac{1}{2}}\{(h\nu)^2(\beta_e H)^{-2} - g_{\perp}^2\}^{-\frac{1}{2}}$$

$$(h\nu)^2\beta_e{}^{-2}H^{-3} \quad \text{A5}$$

When $\theta = 0°$, $h\nu = g_{11}\beta_e H_{11}$, i.e. $g_{11} = h\nu(\beta_e H_{11})^{-1}$

and

when $\theta = 90°$, $h\nu = g_{\perp}\beta_e H_{\perp}$, i.e. $g_{\perp} = h\nu(\beta_e H_{\perp})^{-1}$

so that

$$g(H) = H_{\perp}^2 H_{11}(H_{\perp}^2 - H_{11}^2)^{-\frac{1}{2}}H^{-2}(H_{\perp}^2 - H^2)^{-\frac{1}{2}}$$

For any given system, $g(H) \alpha H^{-2}(H_{\underline{1}}^2 - H^2)^{-\frac{1}{2}}$

$\alpha H^{-2}(c - H^2)^{-\frac{1}{2}}$

The line shape function g(H) and its derivative are plotted below, in Figure A2

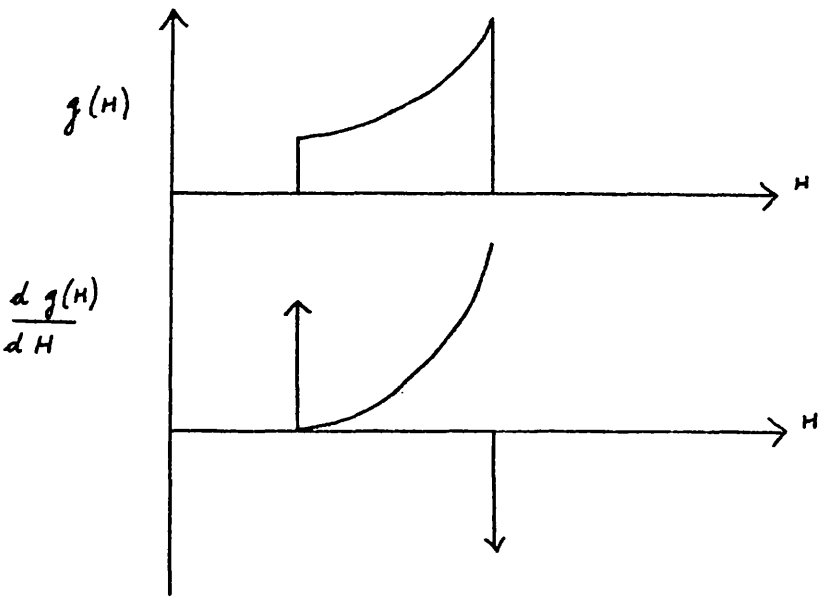

Figure A2

Line shape function g(H) and its derivative, for axially symmetric system.

So far it has been assumed that

(i) the transition probability is independent of the orientation of the given crystallite in the field, and

(ii) the adsorption line shape for each crystallite is

a δ-function. In fact it has been shown[3] that the transition probability is proportional to

$$g_{\perp}^{2}\{g_{11}^{2}g^{-2} + 1\}$$

i.e. the transition probability does change when the orientation of the crystallite is altered. For Cu^{2+} species in a tetragonal field, $g_{11} \sim 2{\cdot}4$ and $g_{\perp} \sim 2{\cdot}1$, so that the ratio of the probability that a given transition will occur when the applied field lies along the symmetry axis to the probability when the field is perpendicular to this axis is 2·0/2·13. For organic radicals, the g tensor components are very much nearer to 2, and it is a good approximation to assume that the probability of a transition taking place is independent of orientation in these cases.

Secondly, the adsorption line shapes are not δ-functions, but may be Lorentzian or Gaussian in nature. For polycrystalline magnetically dilute samples it is a good approximation to consider the line shape of each crystallite as Gaussian, i.e.

$$Y(H - H_o) = (2\pi)^{-\frac{1}{2}}\beta_e^{-1}\exp[-(H - H_o)^2/2\beta_e^{2}] \qquad A6$$

The effect of this is to broaden the lines in the absorption spectrum so that a resonance centred at H contributes to the absorption at H', an amount given by

$$g(H)dHY(H' - H)$$

The total intensity of absorption at H' is the sum of all such contributions,

$$\text{i.e.} \quad S(H') = \sum_{H = H_{11}}^{H = H_1} g(H)dH\Upsilon(H' - H)$$

$$= \int_{H = H_{11}}^{H = H_1} g(H)\Upsilon(H' - H)dH$$

so that

$$S(H') = (2\pi)^{-\frac{1}{2}}\beta_e^{-1} \int_{H_{11}}^{H_1} g(H)\exp[-(H' - H)(2\beta_e^2)^{-1}]dH \qquad A7$$

and

$$\frac{dS(H')}{dH'} = (2\pi)^{-\frac{1}{2}}\beta_e^{-3} \int_{H_{11}}^{H_1} (H - H')g(H)\exp[-(H' - H)(2\beta_e^2)^{-1}]dH \qquad A8$$

These functions are shown in Figure A3, and compared with the original δ-function spectrum shown in Figure A2.

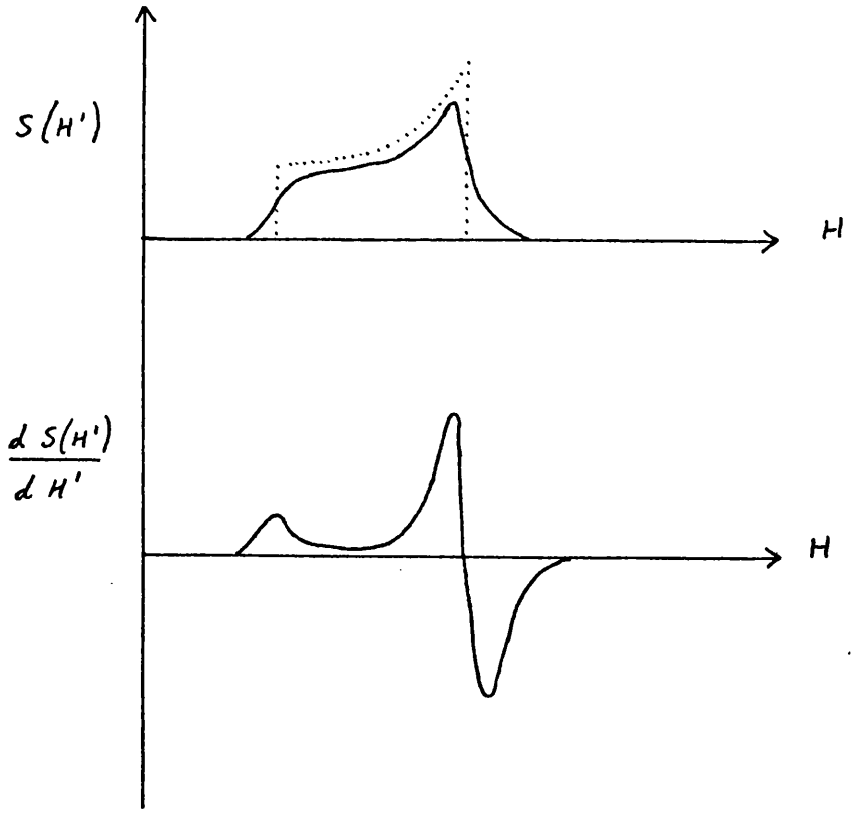

Figure A3.

The line shape function and its derivative, for an axially symmetric system, with broadening.

Effects of hyperfine interaction

Consider now an axially symmetric system with a magnetic nucleus, of quantum number (say) $I = \frac{1}{2}$, interacting with the electron spin ($S = \frac{1}{2}$).

For any one crystallite the resonance spectrum is

a 1:1 doublet separated by T_i gauss, where T_i can have any value between T_{11} and $T_{\underline{1}}$ depending on the orientation of the crystallite in the magnetic field. The polycrystalline spectrum will be as shown below:

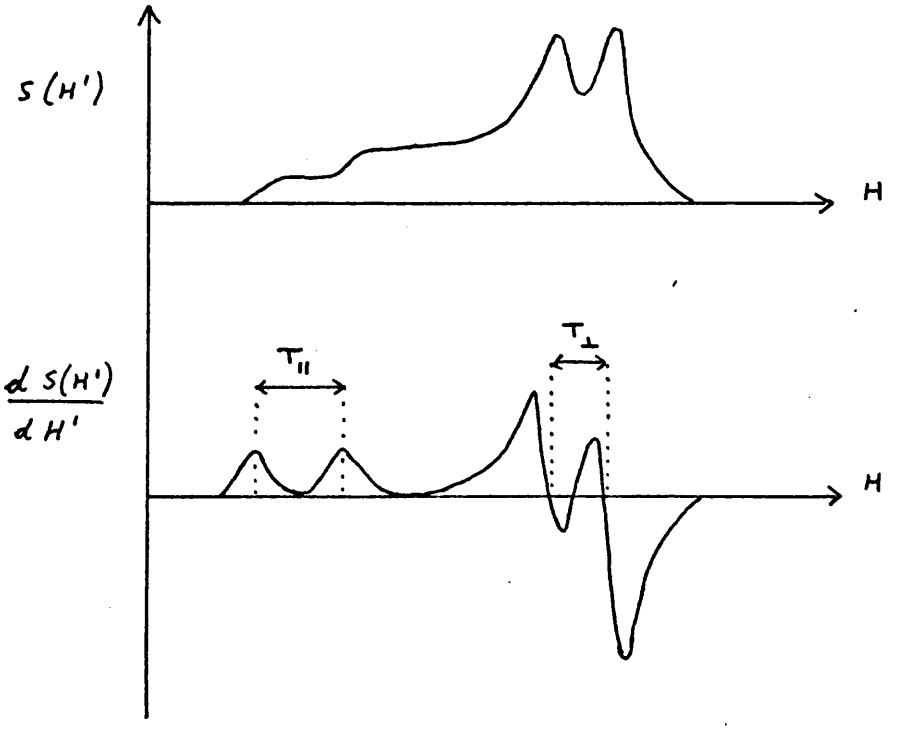

Figure A4.

Line shape function and its derivative for axially symmetric system interacting with a magnetic nucleus with I = $\frac{1}{2}$, and with broadening included.

It is best to construct the spectrum as though there were two kinds of radical present, and then add their

spectra together.

In some such systems, it has been found that certain combinations of the parameters H_{11} and $H_{\underline{1}}$ can result in the appearance of singularities in the function $S(H')$. This causes extra peaks, "polycrystalline peaks", to appear in the derivative spectrum.[4]

2. A system with symmetry lower than axial

Now in e.p.r. spectroscopy, the direction of the magnetic field vector may be defined with respect to the principal axes of the internal electrostatic field experienced by the unpaired electron. It has already been shown that

$$g = \left\{ g_{11}^2 \cos^2\theta_1 + g_{22}\cos^2\theta_2 + g_{33}^2\cos^2\theta_3 \right\}^{\frac{1}{2}} \qquad A9$$

where θ_1, θ_2 and θ_3 are the angles that H makes with these principal directions. Only two of these three angles are independent, since

$$\cos^2\theta_1 + \cos^2\theta_2 + \cos^2\theta_3 = 1$$

If, instead of using the principal axis framework, the direction of H is specified with respect to three axes, x, y, z, fixed in the laboratory, and if this laboratory-fixed set of axes is related to the first set by the Eulerian[5] angles α, β and γ, then by using the substit-

utions,

$$z = \cos\beta$$

and $$\sin^2\gamma = \cos^2\theta_1(1 - \cos^2\theta_3)^{-1}$$

it is easily shown that the relation between the effective g factor for the radical or ion and the principal components of the g tensor may be written,

$$g = \left\{(g_{33}^2 - g_{22}^2)z^2 + (g_{11}^2 - g_{22}^2)(1 - z^2)\sin^2\gamma + g_{22}^2\right\}^{\frac{1}{2}} \qquad \text{A10}$$

The incremental probability that a given crystallite in a powder assumes an orientation (z_1, γ_1) such that

$$z \leqslant z_1 \leqslant z + dz$$

and that $$\gamma \leqslant \gamma_1 \leqslant \gamma + d\gamma$$

may be written

$$p(z_1, \gamma_1) = p(z_1)p(z_1|\gamma_1)$$

where $p(z_1|\gamma_1)$ is the probability that for a given value z_1, γ_1 lies in the range between γ and $\gamma + d\gamma$. If the orientations are random, then $p(z_1)$ and $p(z_1|\gamma_1)$ are proportional to dz and to $d\gamma$ respectively, i.e.

$$dp = cdzd\gamma$$

Thus,

$$\int_{\text{over all space}} dp = c \int_{\text{over all space}} dzd\gamma$$

Therefore, $1 = c\int_{-1}^{1} dz \int_{0}^{2\pi} d\gamma$

so that $c = (4\pi)^{-1}$

and $dp = (4\pi)^{-1} dz d\gamma$

i.e. $|dp| = (4\pi)^{-1} \sin\beta d\beta d\gamma$ A11

since $z = \cos\beta$

Now, let us consider a polycrystalline sample of paramagnetic species with $S = \frac{1}{2}$ and with no nuclear interaction ($I = 0$). A crystallite whose principal axes lie with respect to a fixed frame of reference in such a way that two of the Eulerian angles lie within the ranges β to $\beta + d\beta$ and γ to $\gamma + d\gamma$ respectively, will contribute to the resonance spectrum within the field range H to H + dH where

$$H = h\nu(g\beta_e)^{-1}$$

and g is defined by equation A10. For absorption to occur within the field range H to H + dH, a crystallite must be oriented in such a manner that the electron's g factor lies within the range g to g + dg where

$$H = h\nu(g\beta_e)^{-1}$$

and $dH = -h\nu(g^2\beta_e)^{-1} dg$

i.e. $dg = -g^2\beta_e(h\nu)^{-1} dH$ A12

A representation of the z - g plane is shown in Figure A5; g is a function of z and γ, and there is a range of com-

binations of z and γ values, given by equation A10, which will result in a given value of g, i.e. a number of crystallites with a range of combinations of

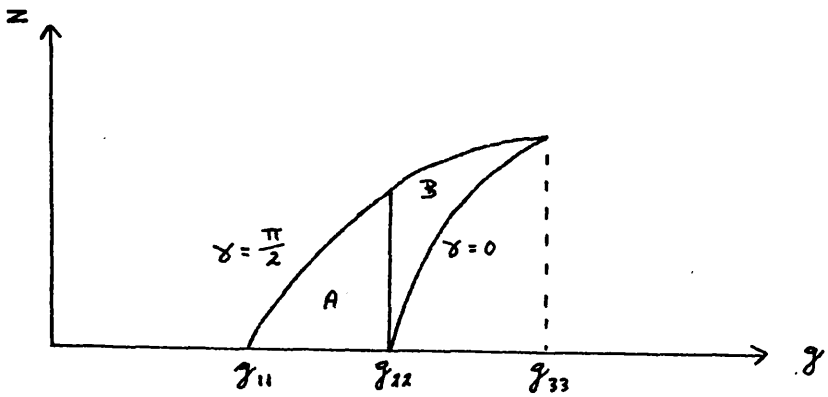

Figure A5

Representation of the z - g plane.

z and γ values contribute to the intensity in the absorption spectrum which lies between H and H + dH. Within the area A of Figure A5, for example, for a given g value, z may have values which lie within the range

$$0 \leqslant z \leqslant z_{\gamma} = \frac{\pi}{2}$$

and within the area labelled B, for any given g value,

$$z_{\gamma} = 0 \leqslant z \leqslant z_{\gamma} = \frac{\pi}{2}$$

Now, if the absorption line shape function is normalised, g(H)dH equals the total probability that a crystallite lies in an orientation such that it gives

absorption at a particular g value,

i.e. $g(H)dH = 8(4\pi)^{-1} \sum dz d\gamma$.

This summation is taken over all z and γ values which result in a g value in the appropriate range,

$$g(H) \leqslant g \leqslant g(H + dH)$$

The factor 8 arises from the fact that in Figure A5, z is allowed to range within $0 \leqslant z \leqslant 1$, and γ within $0 \leqslant \gamma \leqslant \pi/2$, so that only one octant of a sphere has been considered. Now

$$g(H)dH = 2(\pi)^{-1} \sum dz \frac{\partial \gamma}{\partial g} dg$$

$$= -2(\pi)^{-1} \sum dz \left(\frac{\partial \gamma}{\partial g}\right) g^2 \beta_e (h\nu)^{-1} dH$$

so that

$$g(H) = -2(\pi)^{-1} \sum dz \left(\frac{\partial \gamma}{\partial g}\right) g^2 \beta_e (h\nu)^{-1}$$

where the summation is over all z-values in one octant which give rise to the appropriate g value. This expression may be written

$$g(H) = -2g^2 \beta_e (\pi h\nu)^{-1} \int_{z_1}^{z_2} \left(\frac{\partial \gamma}{\partial g}\right) dz \qquad \text{A13}$$

where $z_1 = 0$ and $z_2 =$ z value at $\gamma = \pi/2$, or

z_1 = z value at $\gamma = 0$ and z_2 = z value at $\gamma = \pi/2$, depending on whether the particular g value is not greater than, or else greater than g_{22} in Figure A5.

Before proceeding, it is necessary to evaluate $\frac{\partial\gamma}{\partial g}$. Now, from equation A10

$$\gamma = \sin^{-1}\left(\frac{g^2 - a}{b}\right)^{\frac{1}{2}} \qquad \text{A14}$$

where $a = g_{22}^2 + (g_{33}^2 - g_{22}^2)z^2$

and $b = (g_{11}^2 - g_{22}^2)(1 - z^2)$

Now $\frac{d}{dx}(\sin^{-1}x) = \frac{1}{\sqrt{1 - x^2}}$ and so

$$\frac{\partial\gamma}{\partial g} = \frac{g}{(g_{11}^2 - g^2)^{\frac{1}{2}}(g^2 - g_{22}^2)^{\frac{1}{2}}} \left\{1 - z^2\left(\frac{g_{11}^2 - g_{33}^2}{g_{11}^2 - g^2}\right)\right\}^{-\frac{1}{2}}$$

$$\left\{1 - z^2\left(\frac{g_{33}^2 - g_{22}^2}{g^2 - g_{22}^2}\right)\right\}^{-\frac{1}{2}}$$

Within the range $H_{22} \leqslant H \leqslant H_{11}$, we have

$$g(H) = \frac{-2g^2\beta_e}{\pi h\nu} \int_{z=0}^{z(\text{at } \gamma = \pi/2)} \frac{g\,dz}{(g_{11}^2-g^2)^{\frac{1}{2}}(g^2-g_{22}^2)^{\frac{1}{2}}\{1-z^2k\}^{\frac{1}{2}}\{1-z^2k'\}^{\frac{1}{2}}}$$

$$= \frac{-2g^3\beta_e}{\pi h\nu} \frac{1}{(g_{11}^2-g^2)^{\frac{1}{2}}(g^2-g_{22}^2)^{\frac{1}{2}}} \int_{z=0}^{z(\text{at } \gamma = \pi/2)} \frac{dz}{(1-kz^2)^{\frac{1}{2}}(1-k'z^2)^{\frac{1}{2}}}$$

A15

where $k = (g_{11}^2 - g_{33}^2)(g_{11}^2 - g^2)^{-1}$

and $k' = (g_{33}^2 - g_{22}^2)(g^2 - g_{22}^2)^{-1}$

When $\gamma = \pi/2$, $g^2 = (g_{33}^2 - g_{22}^2)z^2 + (g_{11}^2 - g_{22}^2)(1 - z^2) + g_{22}^2$

$$= (g_{33}^2 - g_{11}^2)z^2 + g_{11}^2$$

so that

$$z = \left(\frac{g^2 - g_{11}^2}{g_{33}^2 - g_{11}^2}\right)^{\frac{1}{2}} = k^{-\frac{1}{2}}$$

Let $u = k^{\frac{1}{2}}z$, so that $dz = k^{-\frac{1}{2}}du$; and when $\gamma = \pi/2$, $z = k^{-\frac{1}{2}}$, and $u = 1$.

Therefore,

$$g(H) = \frac{-2g^3\beta_e}{\pi h\nu} \frac{1}{(g_{11}^2-g^2)^{\frac{1}{2}}(g^2-g_{22}^2)^{\frac{1}{2}}}$$

$$\frac{(g_{11}^2-g^2)^{\frac{1}{2}}}{(g_{11}^2-g_{33}^2)^{\frac{1}{2}}} \int_0^1 \frac{du}{(1-u^2)^{\frac{1}{2}}(1-\ell^2u^2)^{\frac{1}{2}}}$$

where $\ell^2 = \frac{k'}{k} = \left(\frac{g_{33}^2 - g_{22}^2}{g^2 - g_{22}^2}\right)\left(\frac{g_{11}^2 - g^2}{g_{11}^2 - g_{33}^2}\right)$

Thus,

$$g(H) = \frac{-2g^3\beta_e}{\pi h\nu} (g_{11}^2 - g_{33}^2)^{-\frac{1}{2}}(g^2 - g_{22}^2)^{-\frac{1}{2}}K(\ell^2) \qquad \text{A16}$$

where $K(\ell^2)$ is the "elliptic integral of the first kind". From tables of functions, this elliptic integral may be written as

$$K(\ell^2) = \int_0^{\pi/2} \frac{dx}{(1 - \ell^2\sin^2x)^{\frac{1}{2}}}$$

$$= \pi/2\left\{1 + (\tfrac{1}{2})^2\ell^2 + (\tfrac{1.3}{2.4})^2\ell^4 + (\tfrac{1.3.5}{2.4.6})^2\ell^6 + \cdots\right\}$$

for $|\ell^2| < 1$.

It is more convenient to use magnetic field values, and so these expressions become, for $H_{22} \lesssim H \lesssim H_{11}$,

$$g(H) = \frac{2}{\pi} \frac{H_{11}H_{22}H_{33}}{(H_{11}^2 - H_{33}^2)^{\frac{1}{2}}(H^2 - H_{22}^2)^{\frac{1}{2}}H^2} K(\ell^2) \qquad A17$$

where $\ell^2 = \frac{(H_{11}^2 - H^2)(H_{22}^2 - H_{33}^2)}{(H_{33}^2 - H_{11}^2)(H^2 - H_{22}^2)}$.

A similar expression may be derived for the range $H_{33} \lesssim H \lesssim H_{22}$,

$$g(H) = \frac{2}{\pi} \frac{H_{11}H_{22}H_{33}}{H^2(H_{11}^2 - H^2)^{\frac{1}{2}}(H_{33}^2 - H_{22}^2)^{\frac{1}{2}}} K(m^2) \qquad A18$$

where $m^2 = \frac{(H_{11}^2 - H_{22}^2)(H^2 - H_{33}^2)}{(H_{33}^2 - H^2)(H_{11}^2 - H_{22}^2)}$

If, as before, a broadening function, $Y(H' - H)$, is included, then the total absorption intensity at H' is given by

$$S(H') = \int_{\text{all } H} g(H)Y(H' - H)dH$$

Effects of hyperfine interactions

This treatment may be extended to systems where the unpaired electron interacts with magnetic nuclei, by considering each hyperfine component separately, i.e. as a separate polycrystalline spectrum, and then adding all

such spectra together.

This treatment which is due to Kneubühl[1] was used as the basis for a computer program to simulate polycrystalline magnetically dilute e.p.r. spectra; and the parameters relating to such spectra obtained from nitroxide radicals, which are reported in this thesis, were extracted by means of this program.

References to Appendix A

1. F.K. Kneubühl, J. Chem. Phys., 1960, 33, 1074.

2. J.R. Pilbrow, Mol. Phys., 1969, 16, 307.

3. B. Bleaney, Proc. Phys. Soc. (London), 1960, 75, 621.

4. R. Neiman, D. Kivelson, J. Chem. Phys., 1961, 35, 156.

5. H. Margenau, G.M. Murphy, "The Mathematics of Physics and Chemistry," Van Nostrand, New York, 1964, p. 286.

Appendix B

Experimental data obtained from electron paramagnetic resonance spectra of di-tertiary-butylnitroxide in Dianin's compound.

Table I

Second moments of the electron paramagnetic resonance absorption spectrum obtained from polycrystalline samples of Dianin's compound containing di-tertiary-butylnitroxide, recorded within the temperature range $77°K \leqslant T \leqslant 430°K$.

Temperature °K		Second moment gauss^2	Temperature °K		Second moment gauss^2
77	▼	641·0	236	o	397·5
112	▼	651·9	241	▼	397·7
117·5	▼	637·7	254·5	▼	384·0
134	o	564·1	270	o	391·5
136	▼	560·4	278·3	▼	383·7
141	▼	565·2	280	o	384·3
143	o	578·2	283·5	▼	384·0
157	▼	541·0	293	o	372·2
158·5	o	560·6	293	▼	367·1
167·5	▼	500·2	303	o	367·7

Table I (cont'd)

Temperature °K		Second moment gauss^2	Temperature °K		Second moment gauss^2
167·5	o	462·6	314	o	346·8
181·3	o	449·8	327·5	o	359·7
187·5	▾	448·4	351	o	341·0
192·5	o	414·7	369	o	345·1
203·3	o	429·8	403	o	334·0
209	▾	417·2	404	o	330·9 *
214	▾	402·7	415	o	293·7 *
219	o	410·3	433	o	no spectrum
228·5	▾	383·2			

* At this temperature sublimation of the crystal lattice is beginning.

The error on the value of the temperature is ± 2 degrees; and that on the second moment is ± 15 gauss^2; for the linear regions, the error is reduced to ± 10 gauss^2.
The points marked ▾ were obtained as the sample temperature was reduced; those marked o were obtained as the sample temperature was increased.

Experimental data obtained from electron paramagnetic resonance spectra of single crystals of di-tertiary-butylnitroxide in Dianin's compound at 260°K, at 293°K, and at 353°K are presented in the following figures.

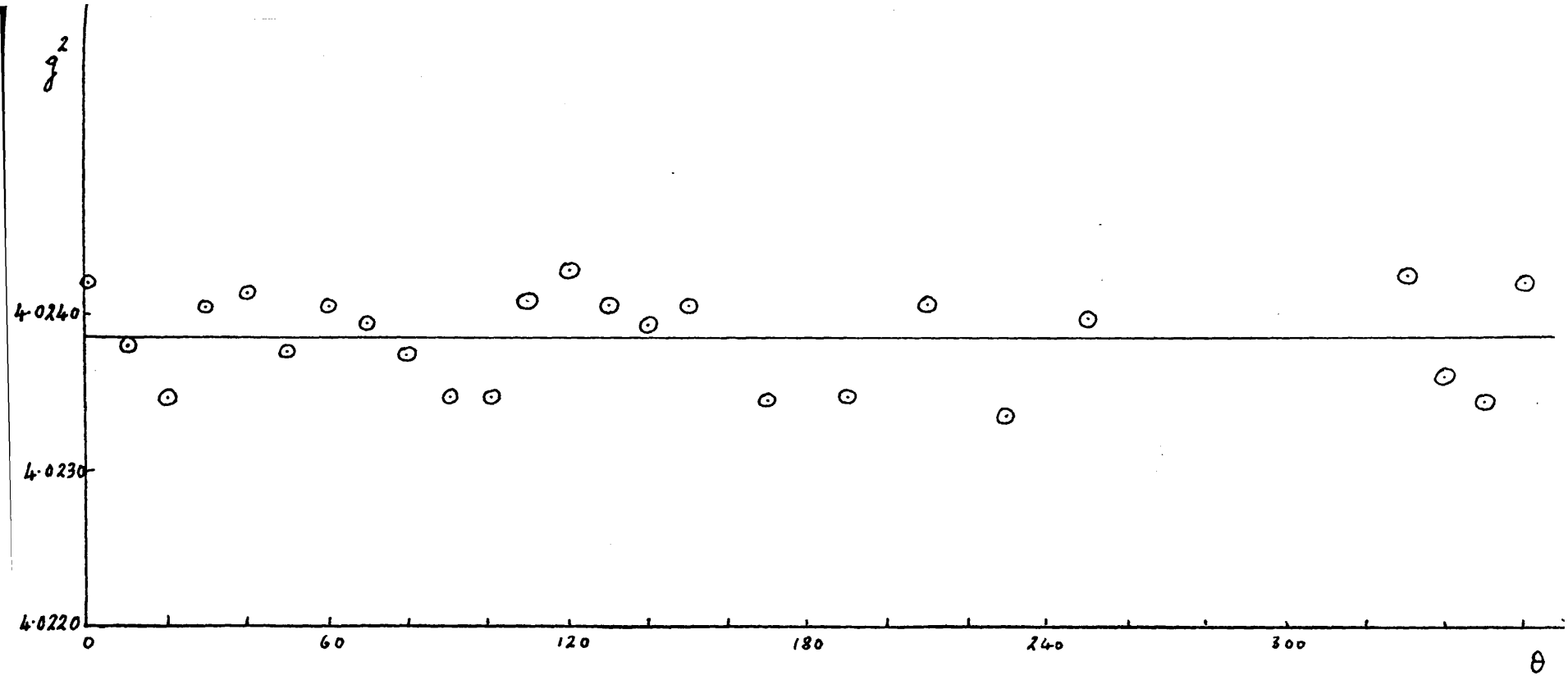

Figure 1

g^2 values obtained for the radical at 260°K with the crystal mounted on axis p.

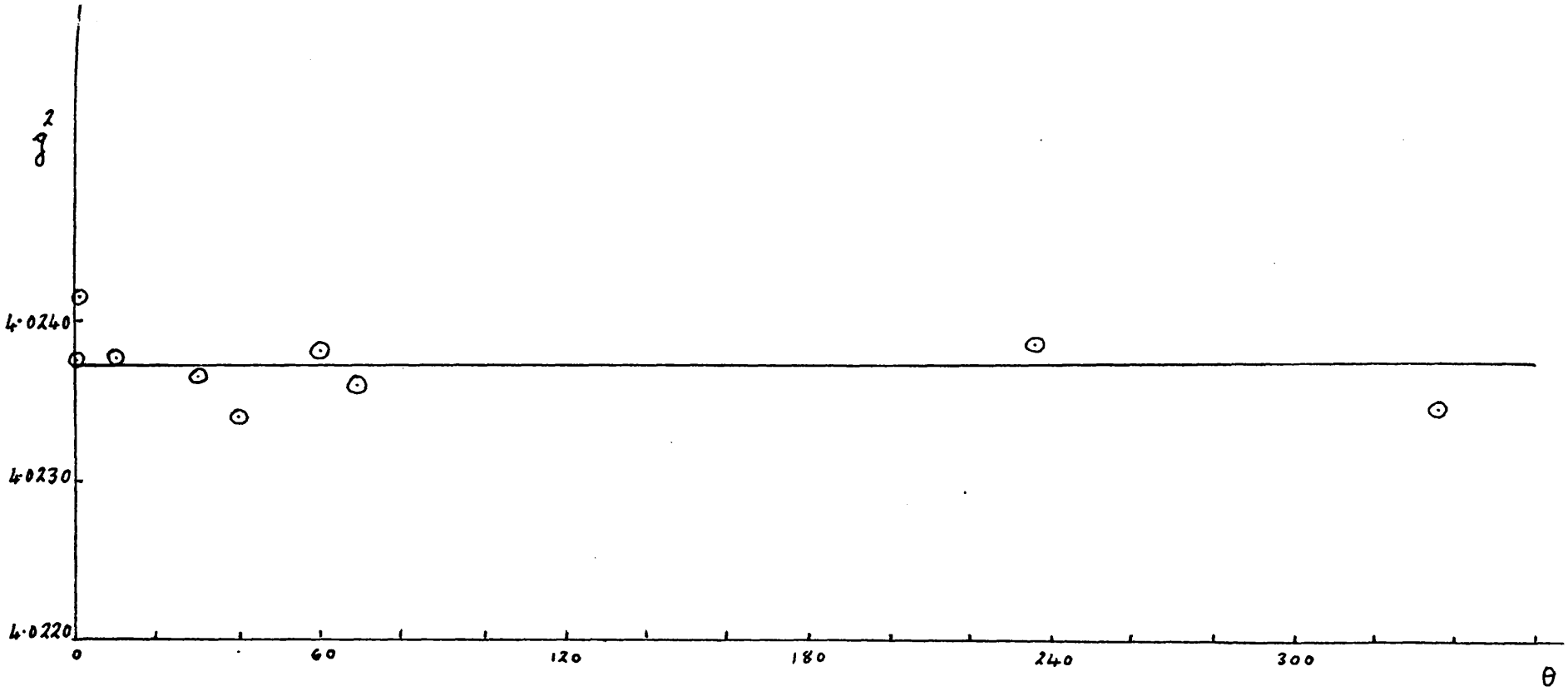

Figure 2

g^2 values obtained for the anisotropic radical at 293°K with the crystal mounted on axis p.

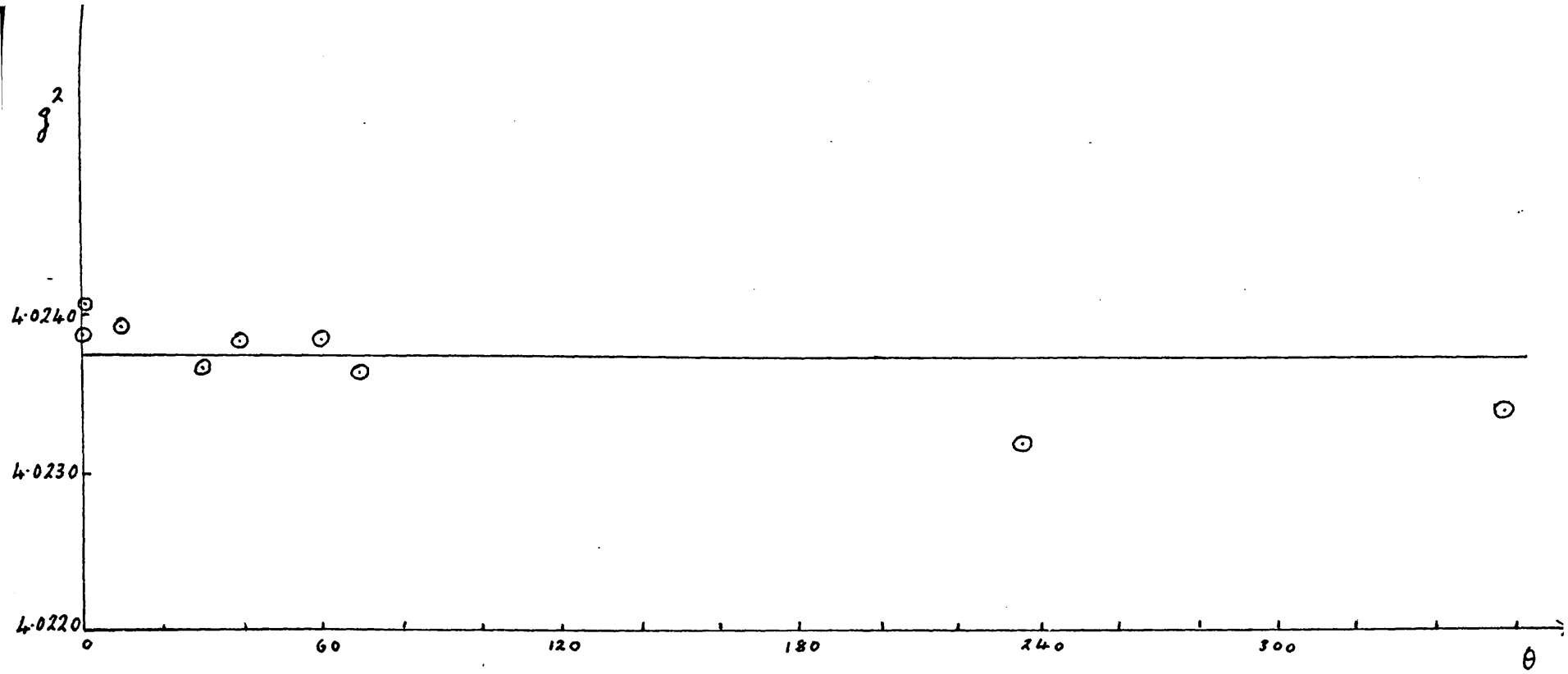

Figure 3

g^2 values obtained for the isotropic radical at 293°K with the crystal mounted on axis p.

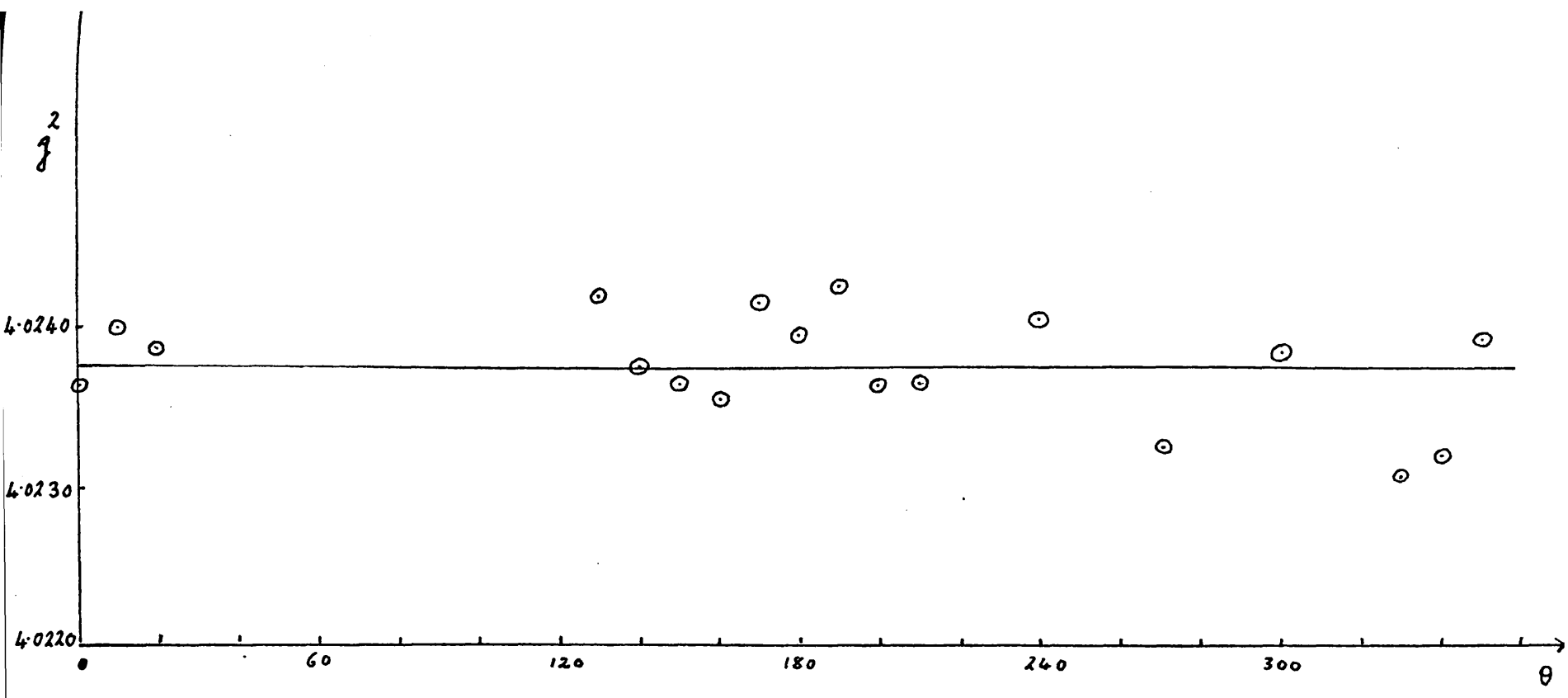

Figure 4

g^2 values obtained for the radical at 353°K with the crystal mounted on axis p.

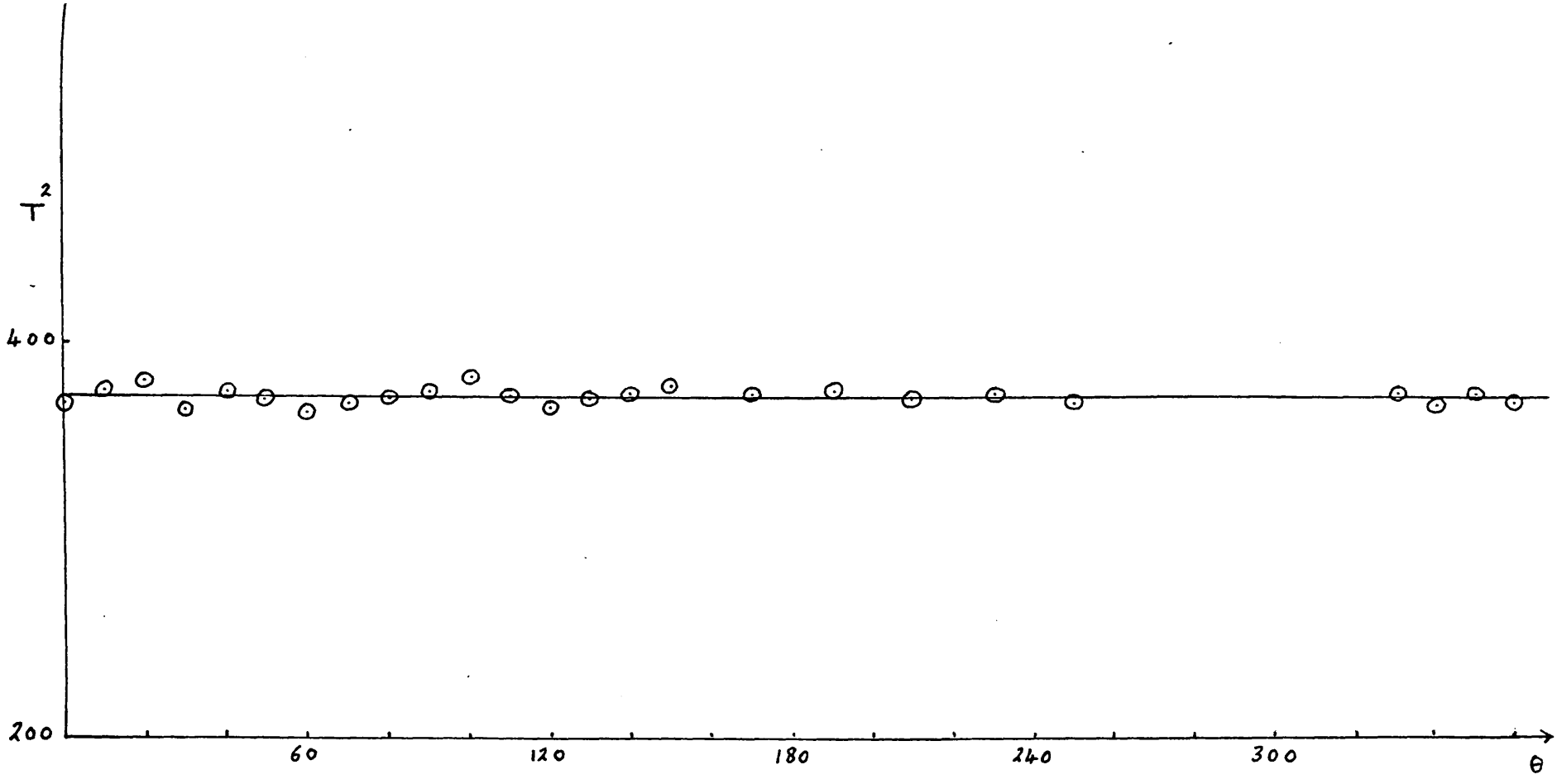

Figure 5

T^2 values obtained for the radical at 260°K with the crystal mounted on axis p.

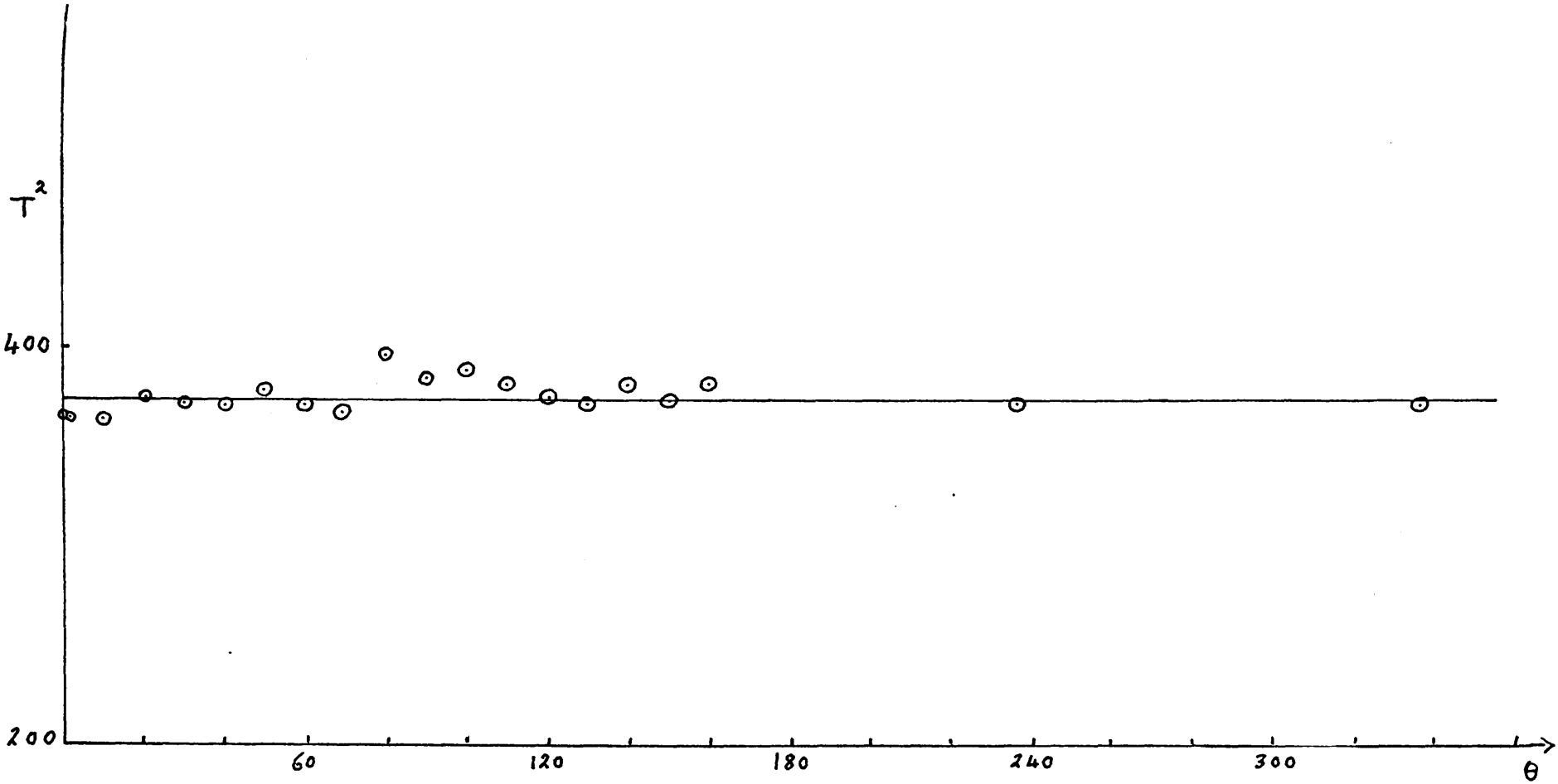

Figure 6

T^2 values obtained for the anisotropic radical at 293°K with the crystal mounted on axis p.

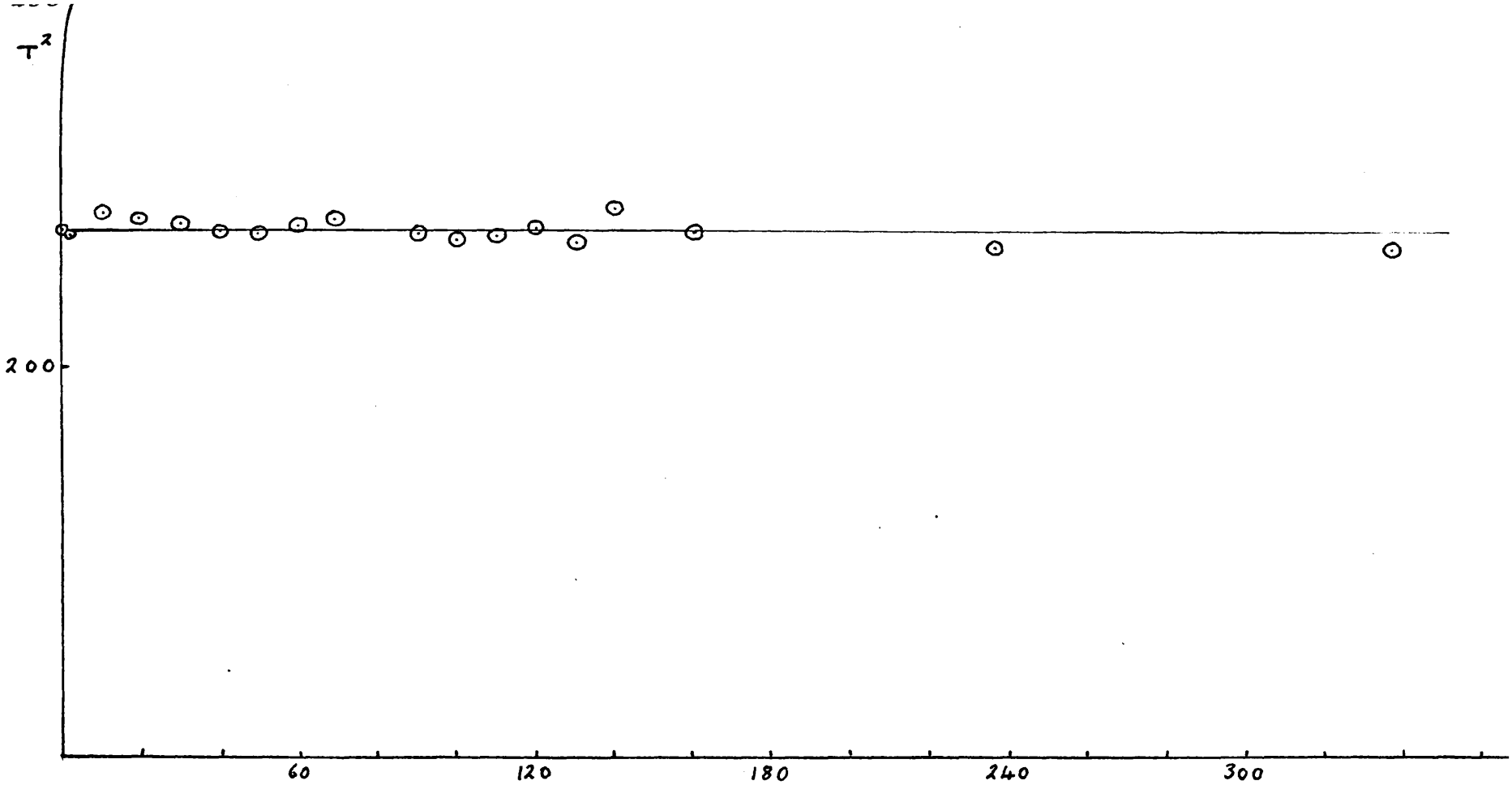

Figure 7

T^2 values obtained for the isotropic radical at 293°K with the crystal mounted on axis p.

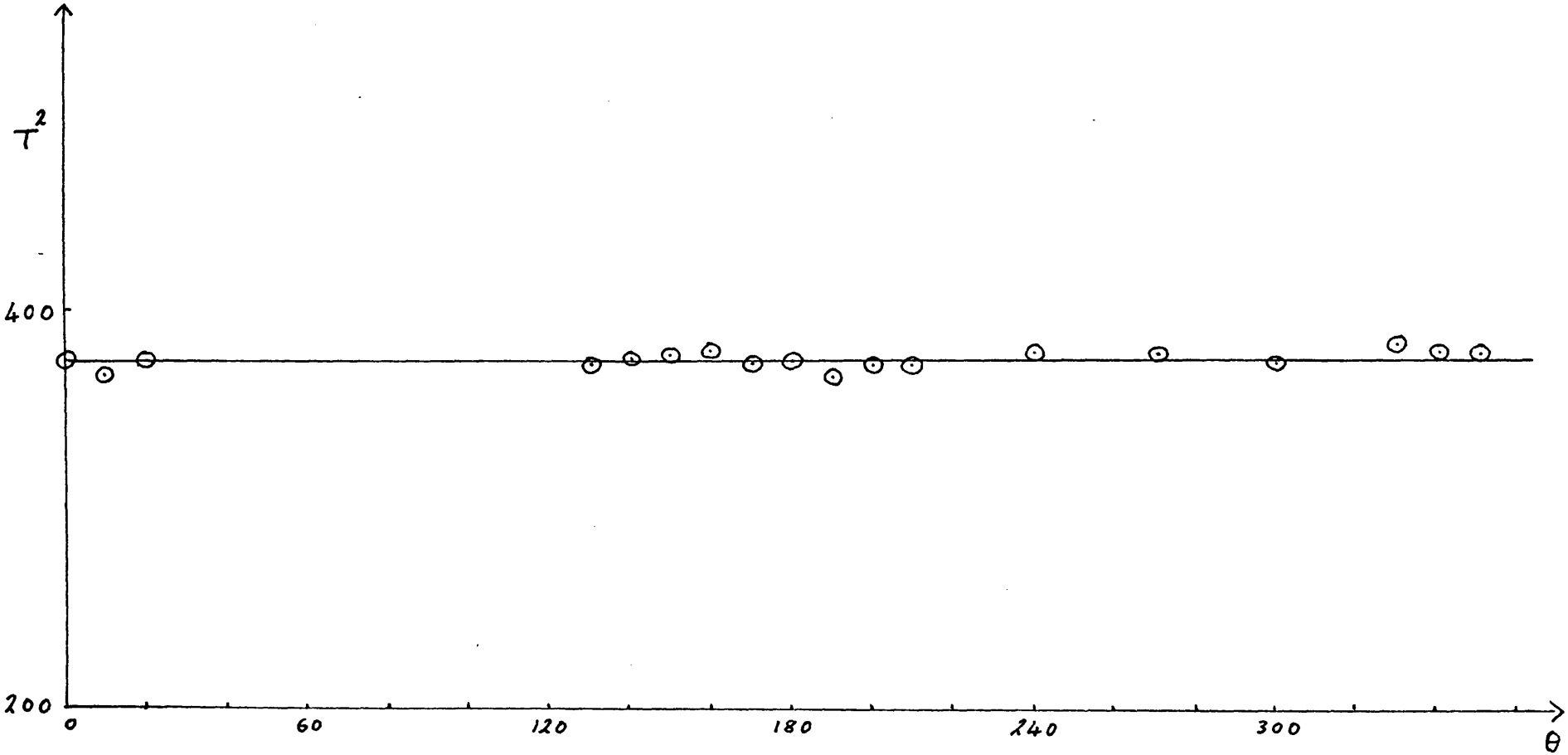

Figure 8

T^2 values obtained for the radical at 353°K with the crystal mounted on axis p.

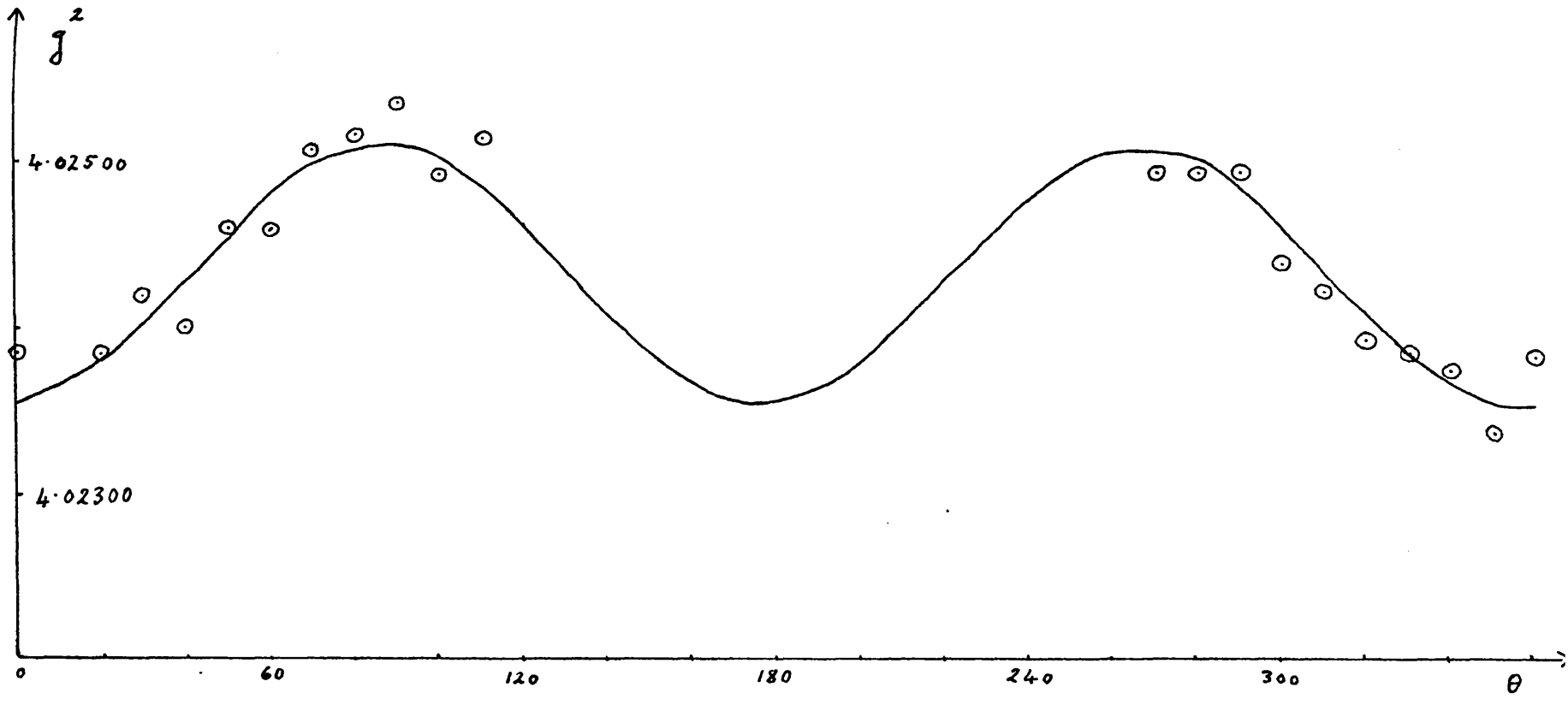

Figure 9

g^2 values obtained for the radical at 260°K with the crystal mounted on axis q.

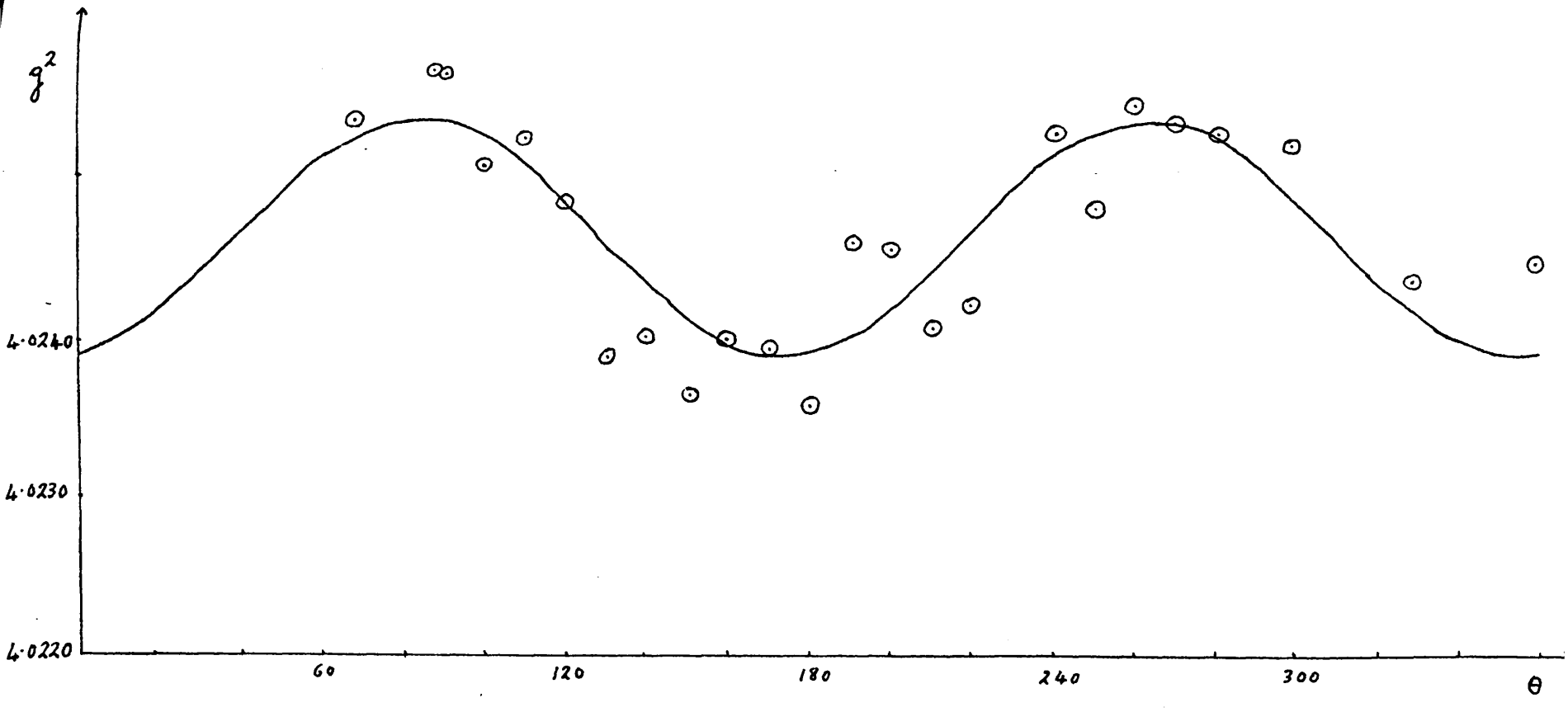

Figure 10

g^2 values obtained for the anisotropic radical at 293°K with the crystal mounted on axis q.

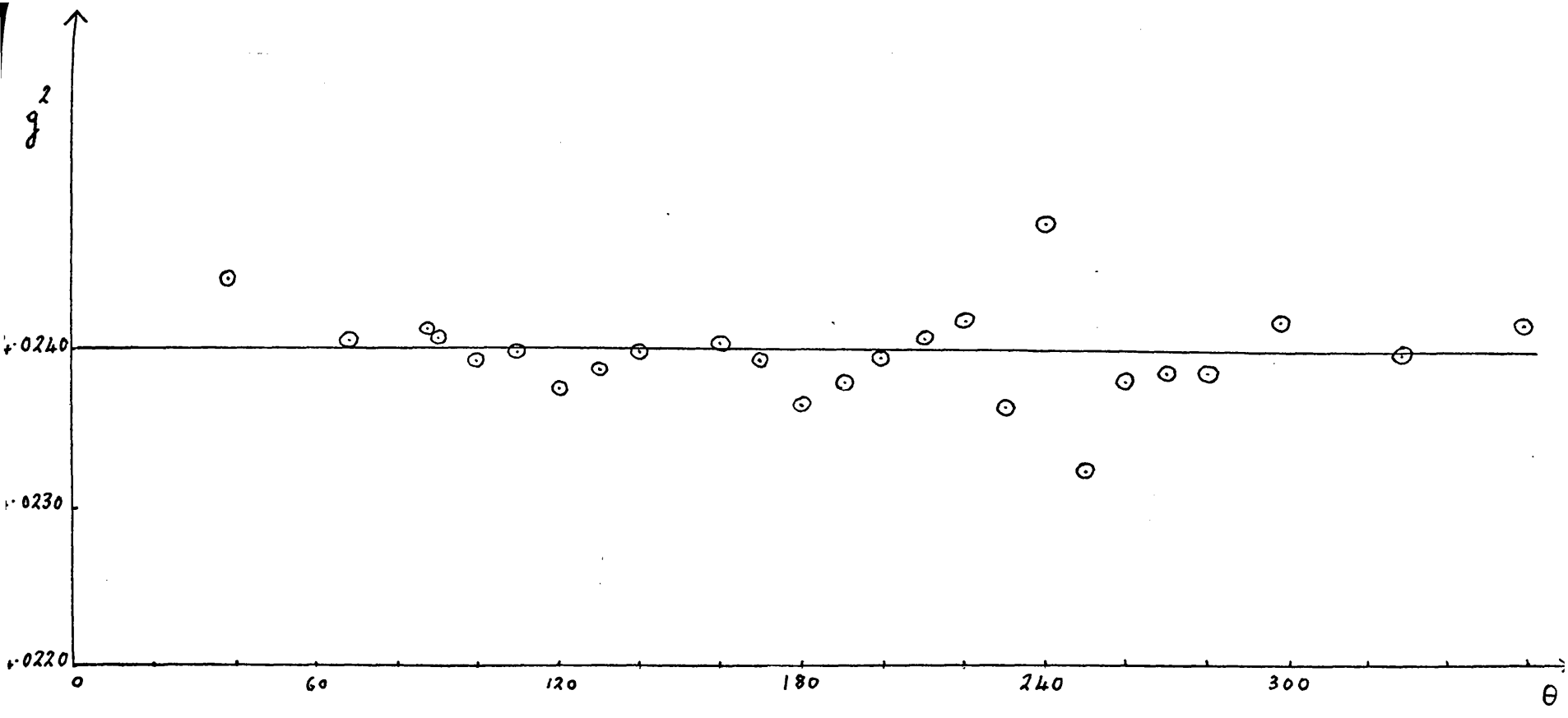

Figure 11

g^2 values obtained for the isotropic radical at 293°K with the crystal mounted on axis q.

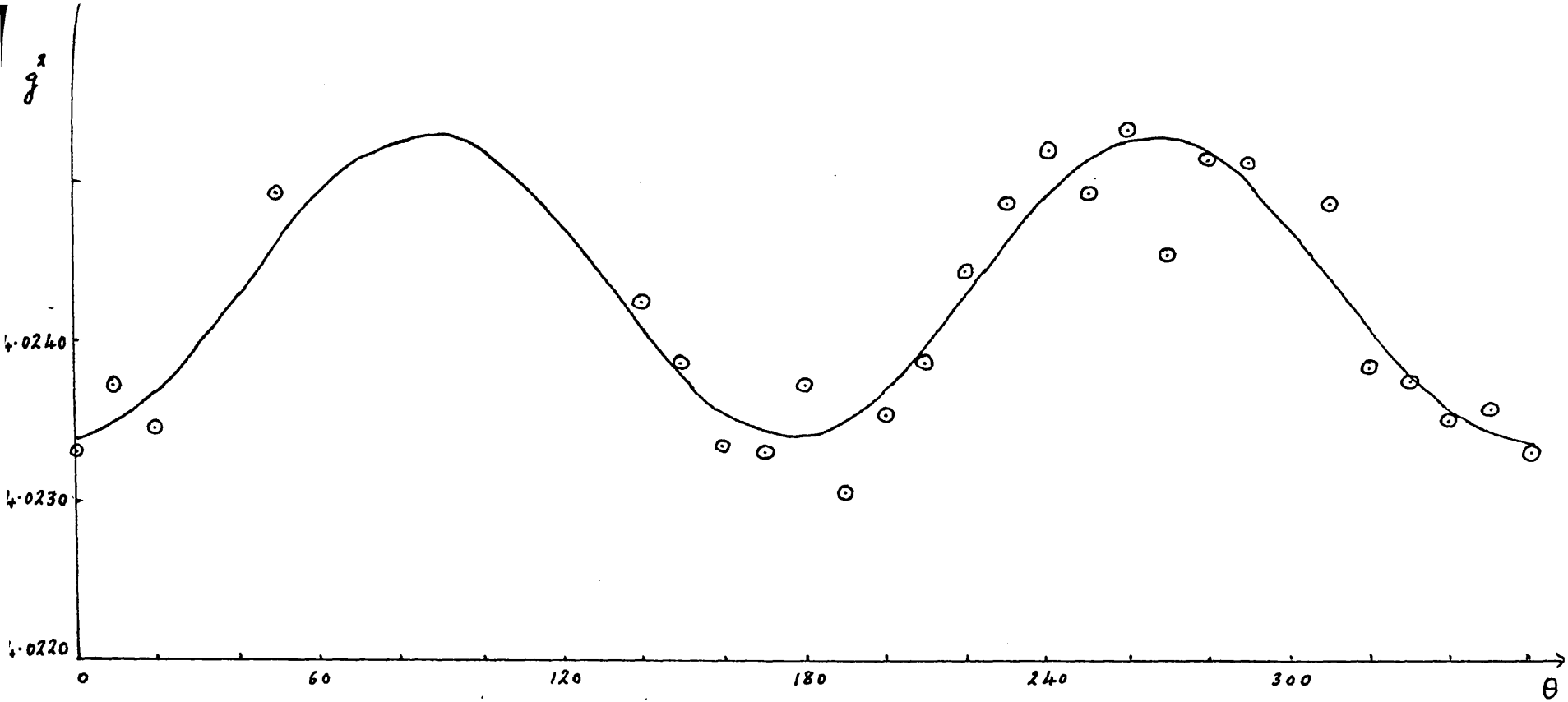

Figure 12

g^2 values obtained for the radical at 353°K with the crystal mounted on axis q.

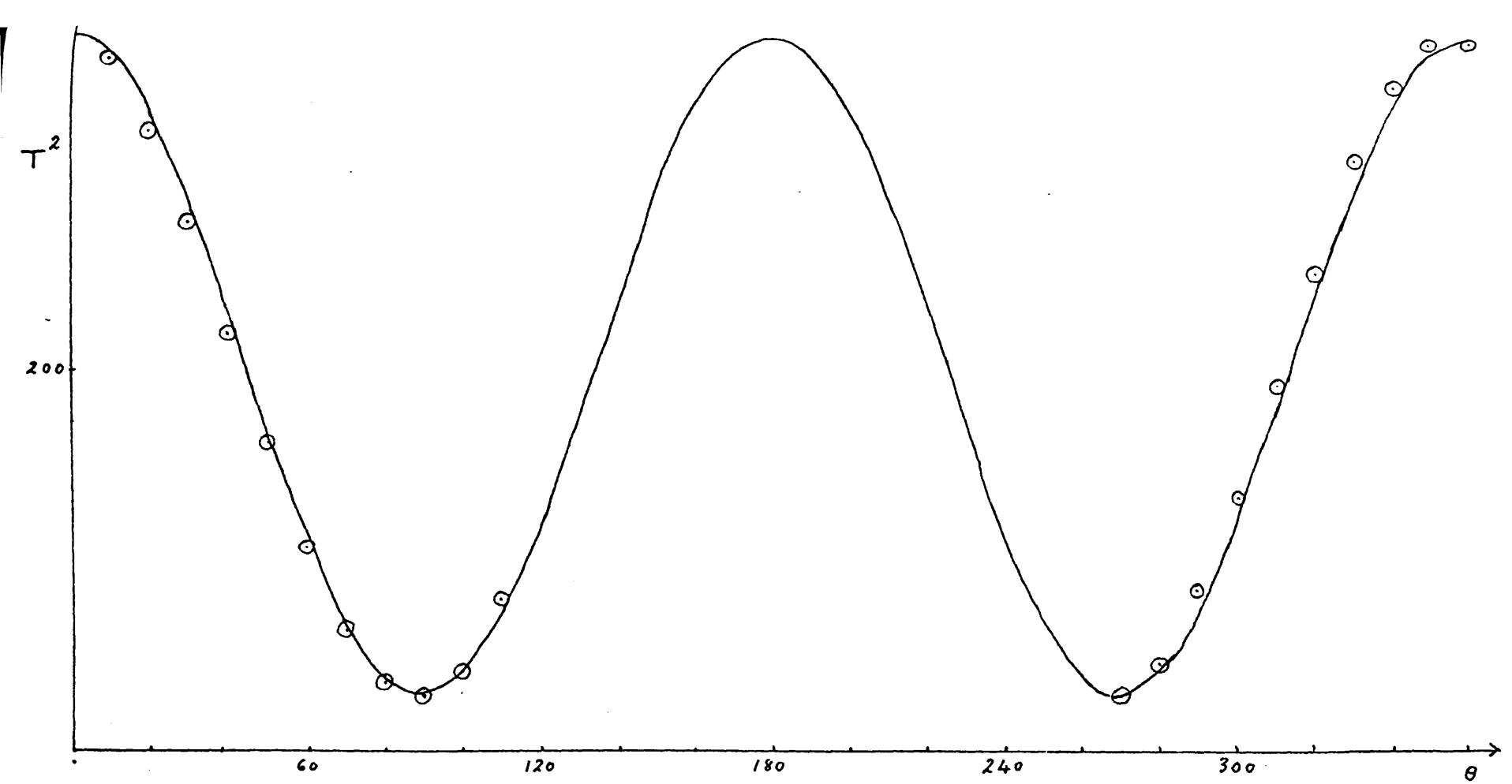

Figure 13

T^2 values obtained for the radical at 260°K with the crystal mounted on axis q.

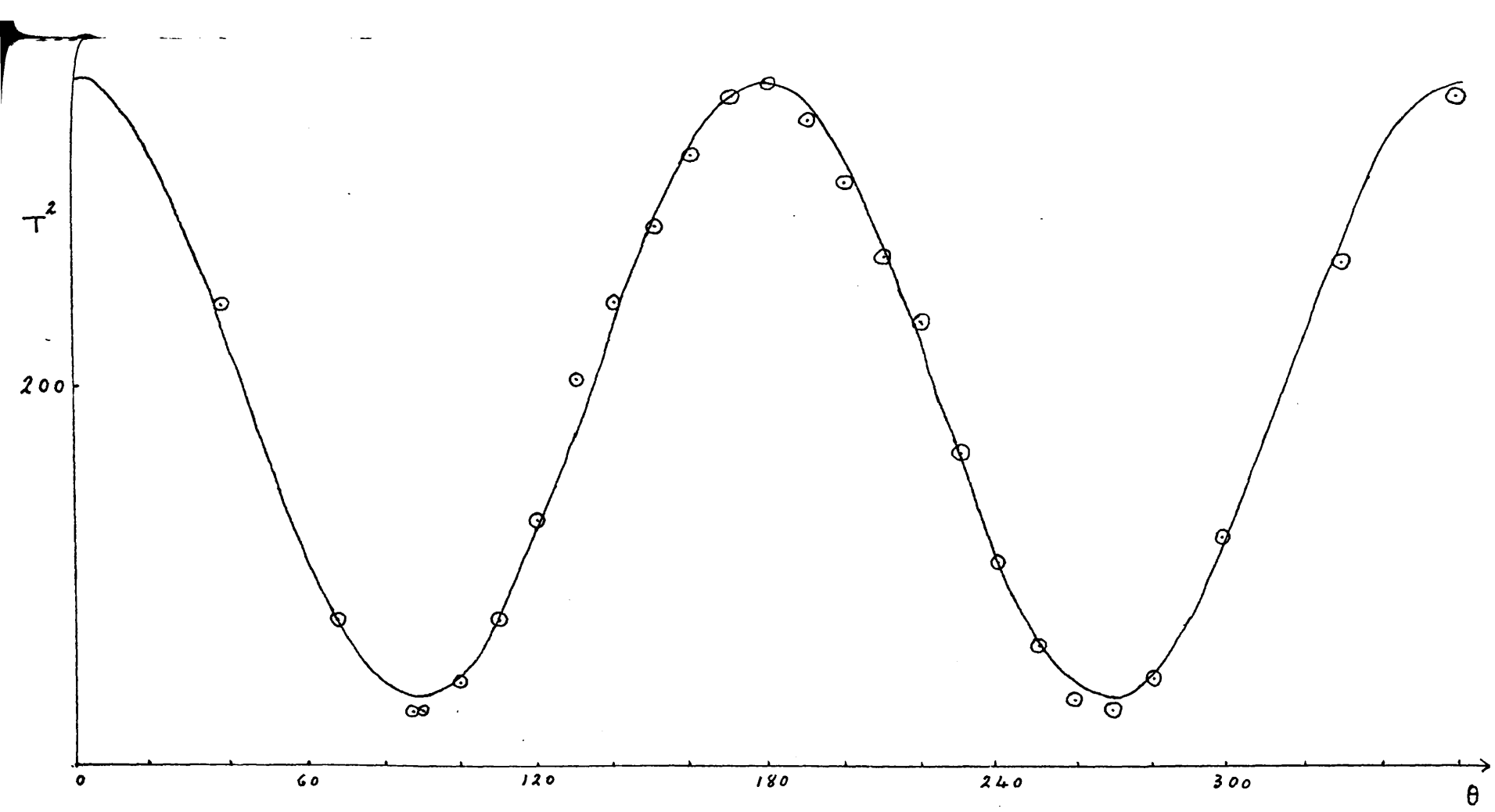

Figure 14

T^2 values obtained for the anisotropic radical at 293°K with the crystal mounted on axis q.

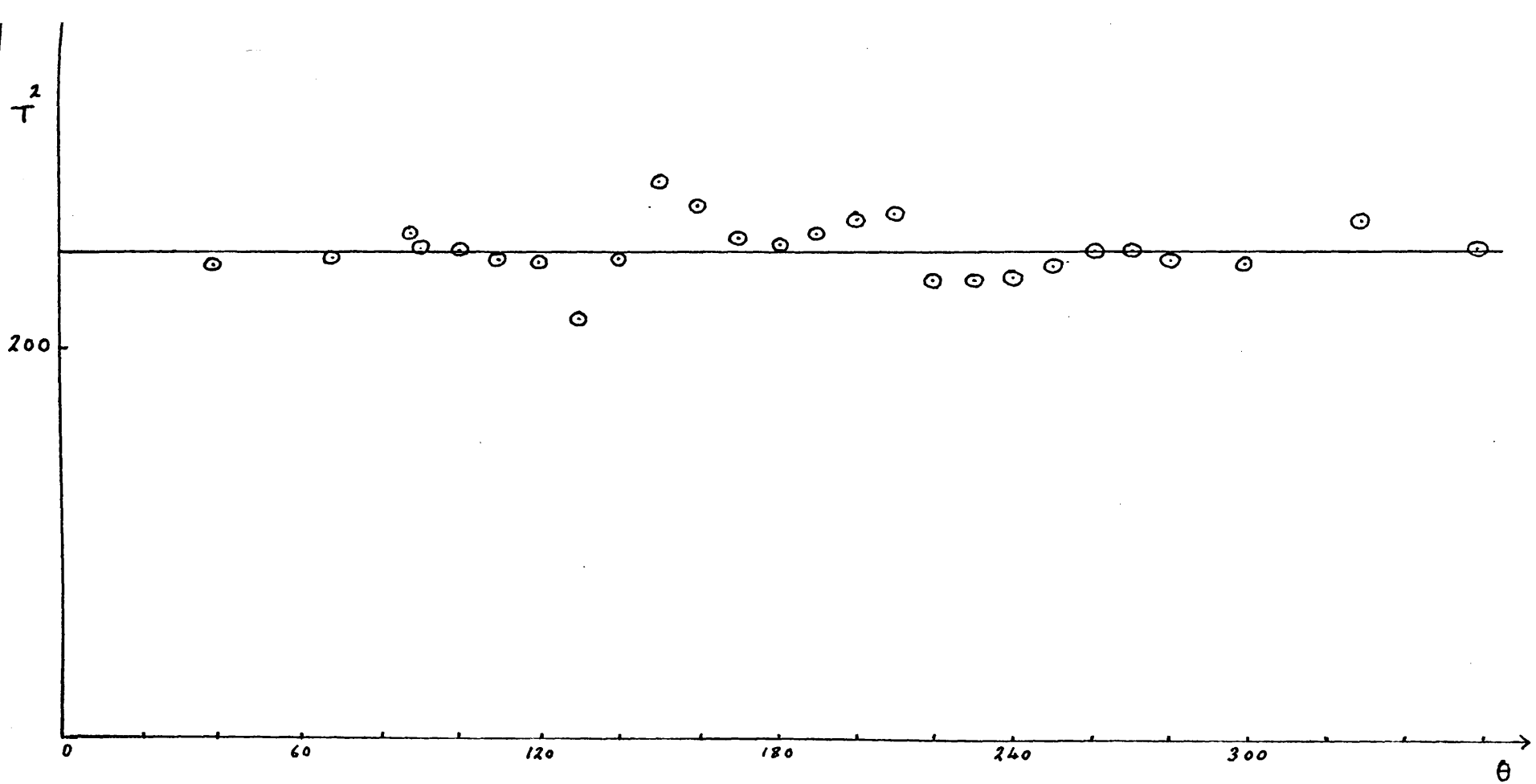

Figure 15

T^2 values obtained for the isotropic radical at 293°K with the crystal mounted on axis q.

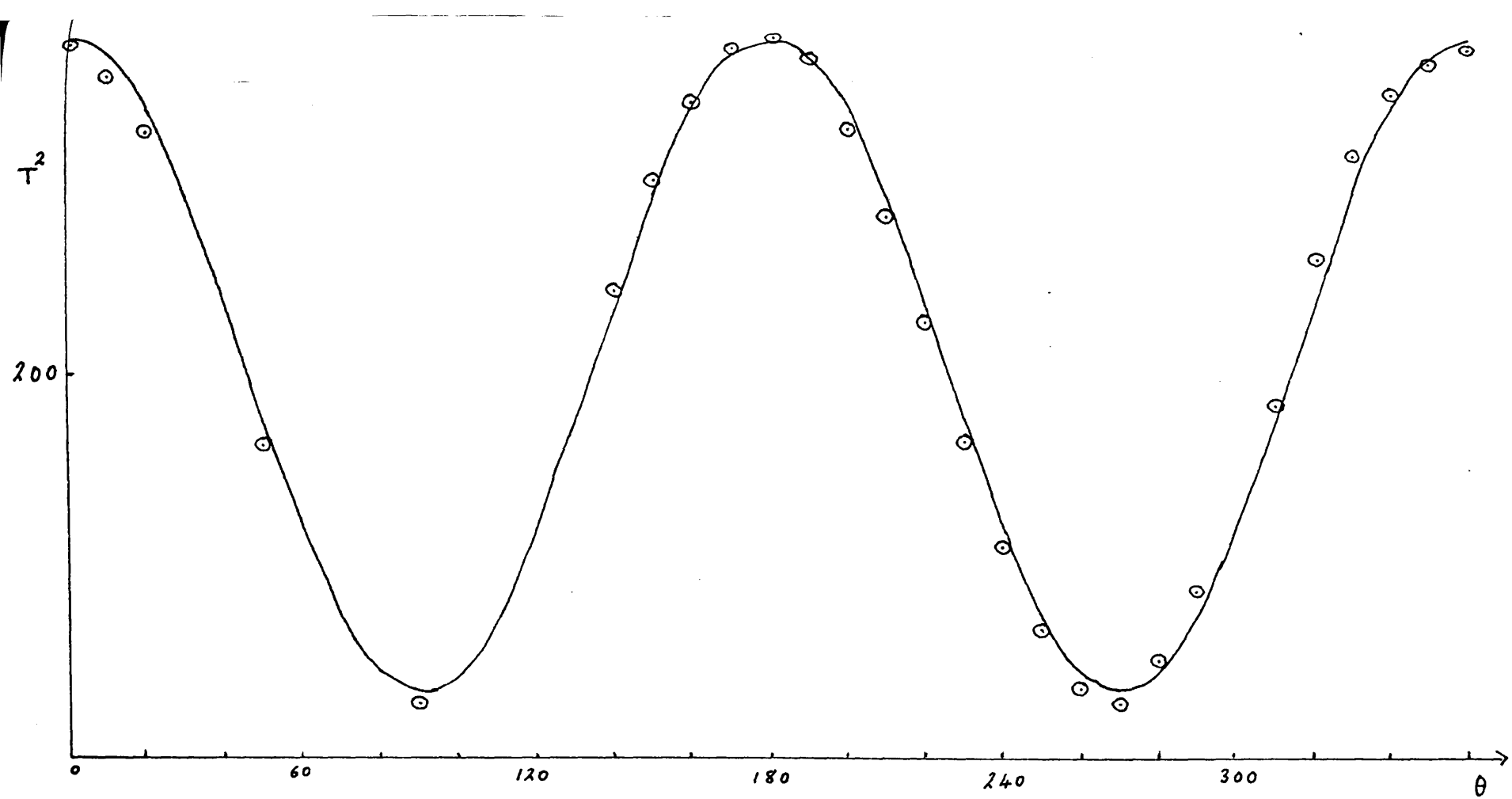

Figure 16

T^2 values obtained for the radical at 353°K with the crystal mounted on axis q.

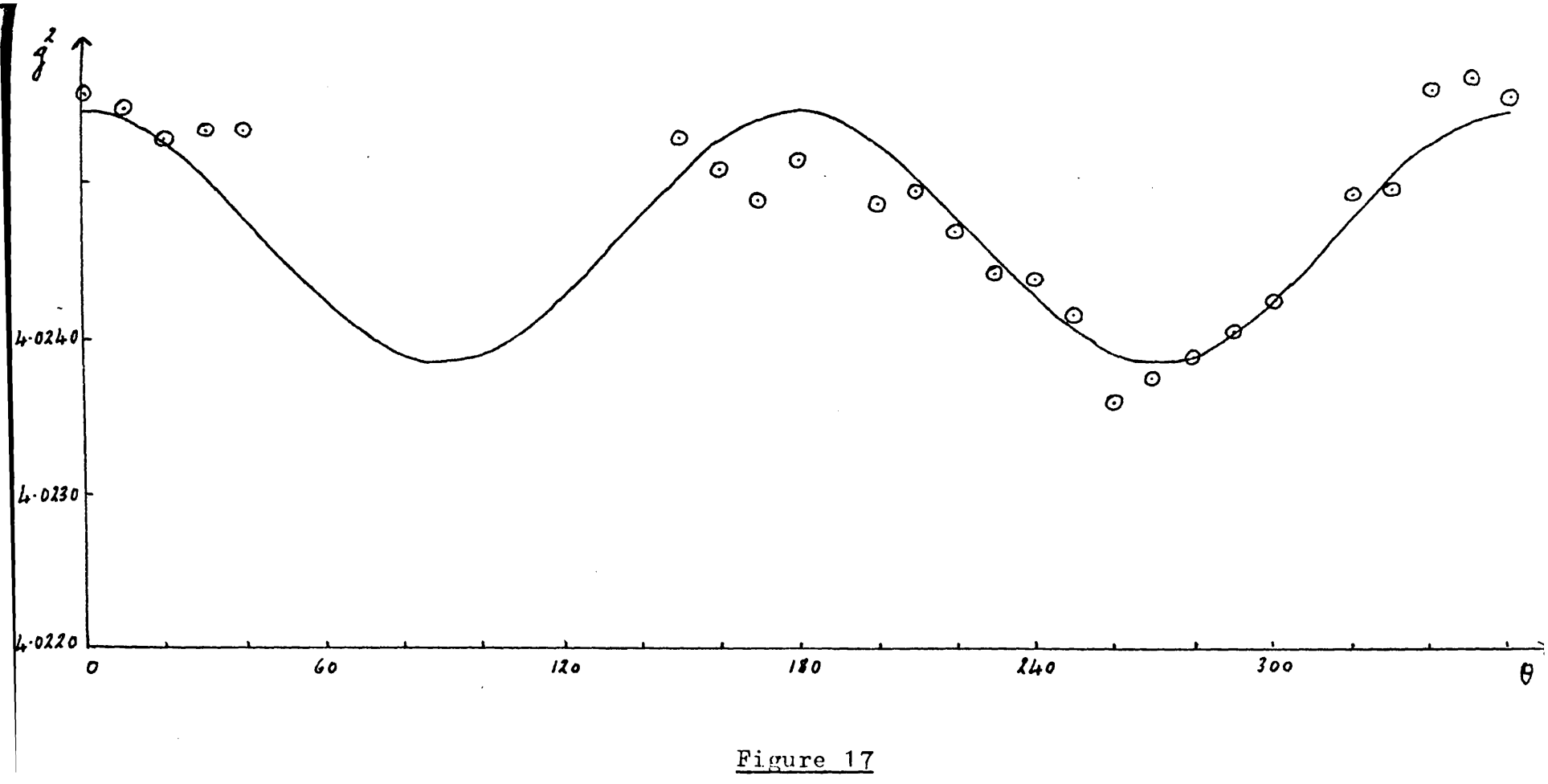

Figure 17

g^2 values obtained for the radical at 260°K with the crystal mounted on axis r.

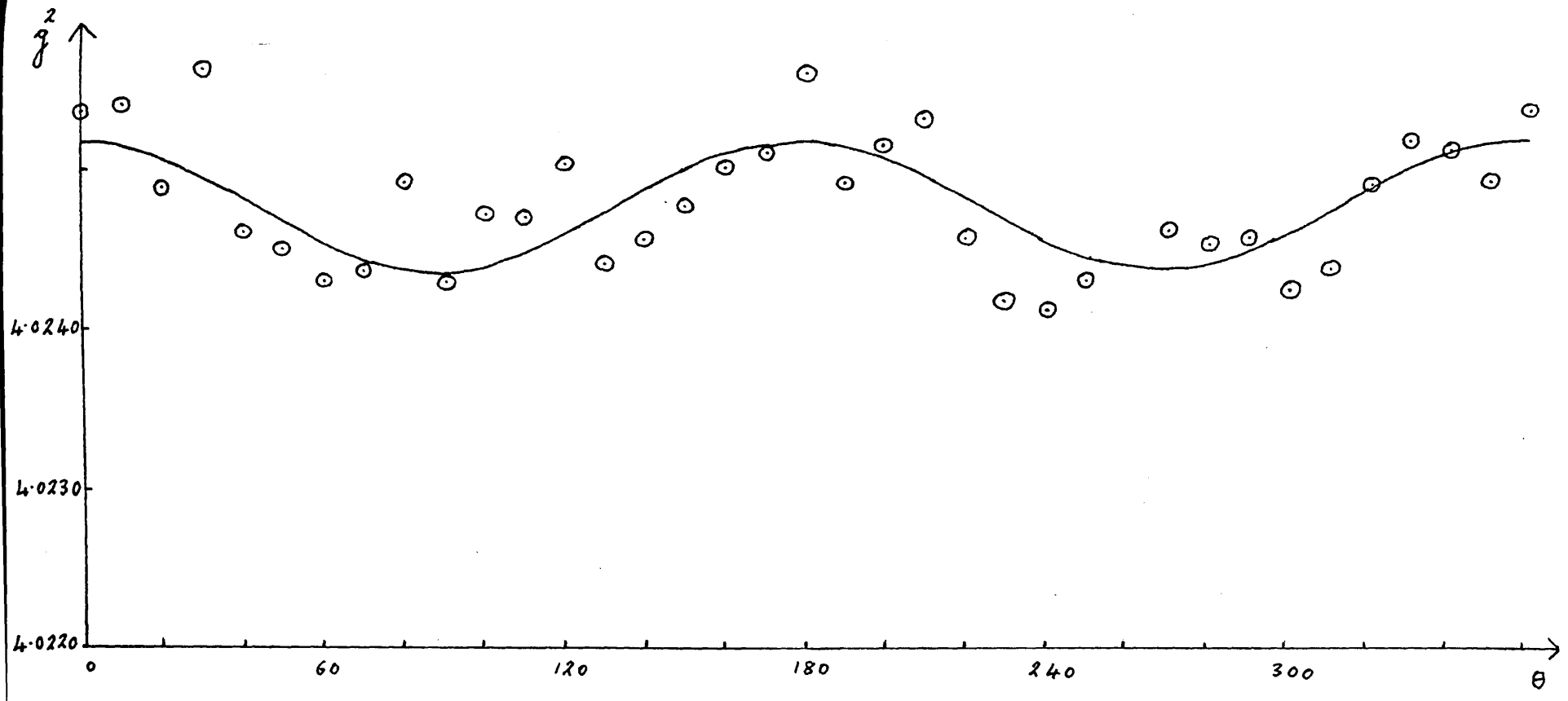

Figure 18

g^2 values obtained for the anisotropic radical at 293°K with the crystal mounted on axis r.

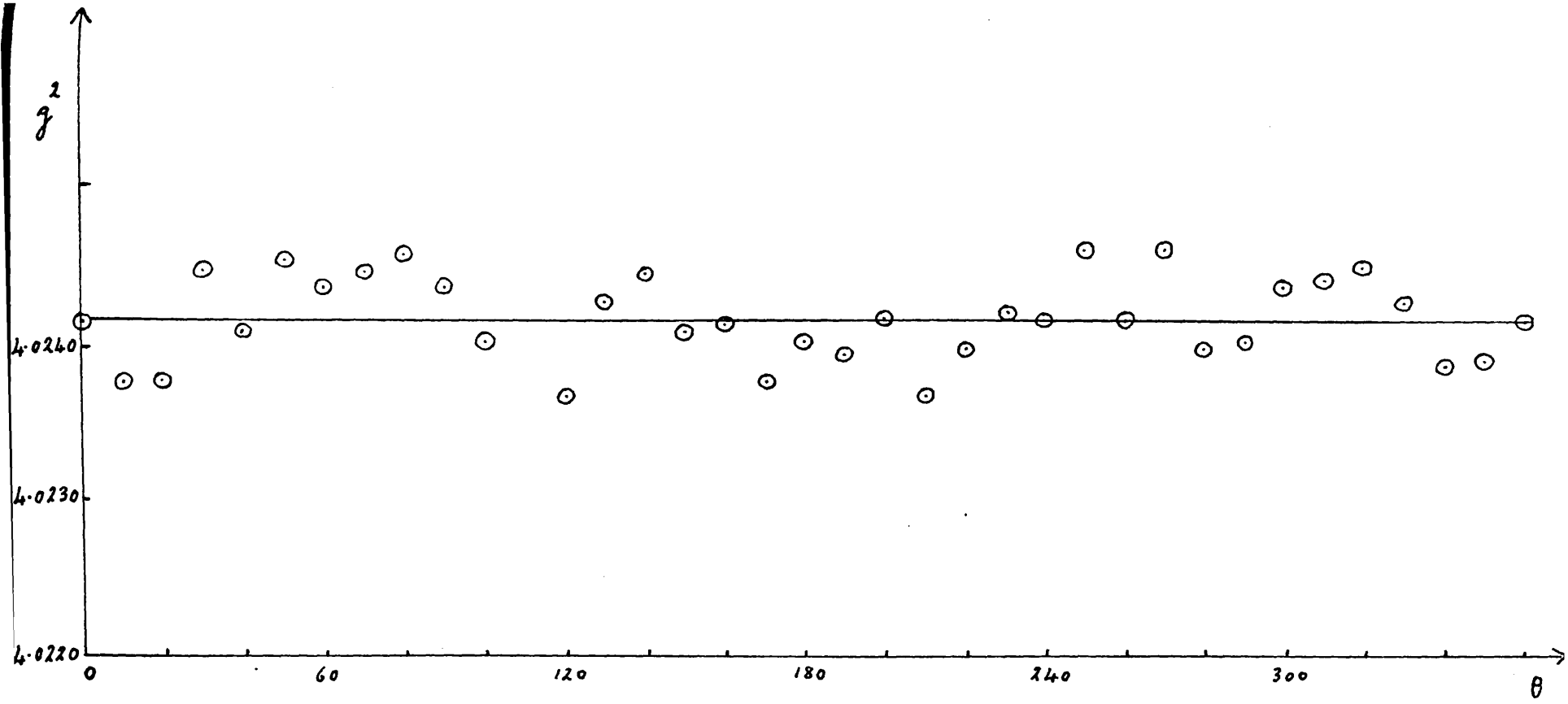

Figure 19

g^2 values obtained for the isotropic radical at 293°K with the crystal mounted on axis r.

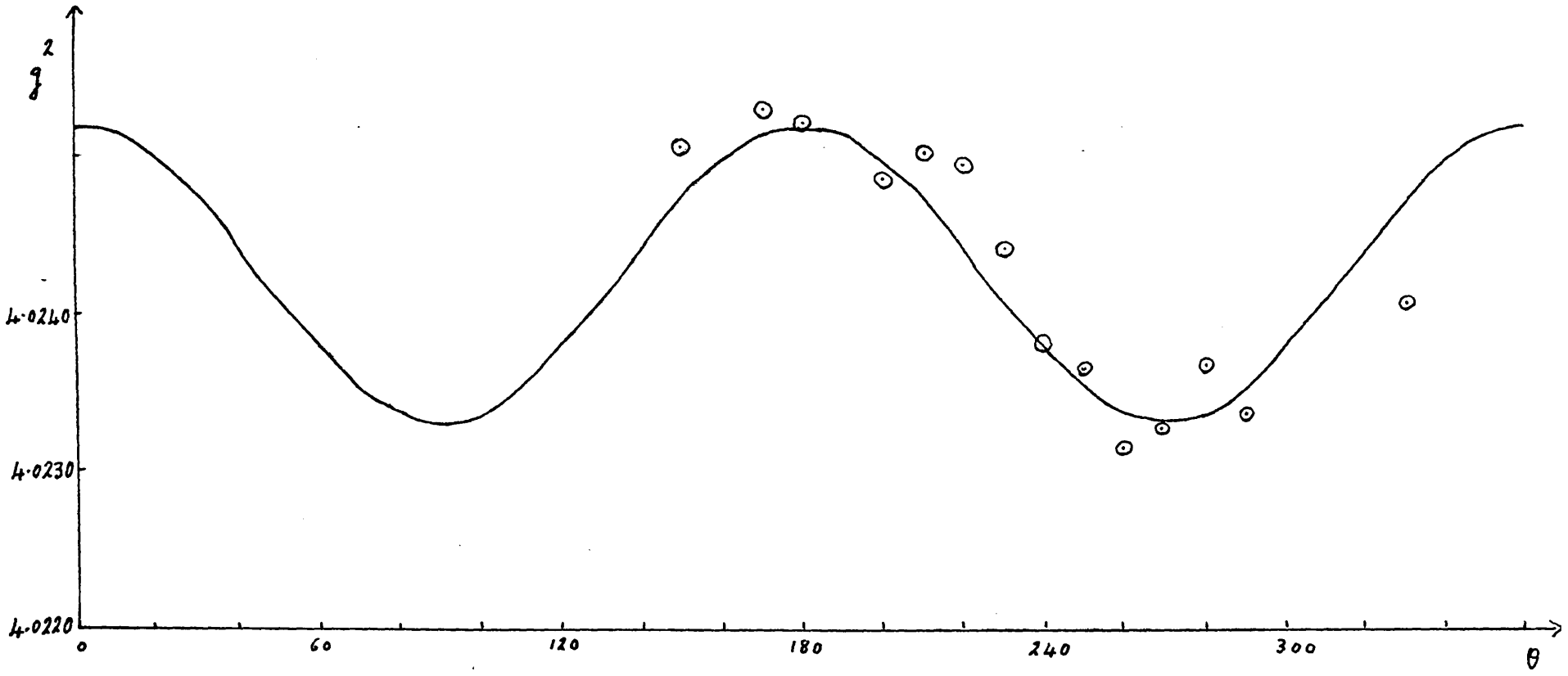

Figure 20

g^2 values obtained for the radical at 353°K with the crystal mounted on axis r.

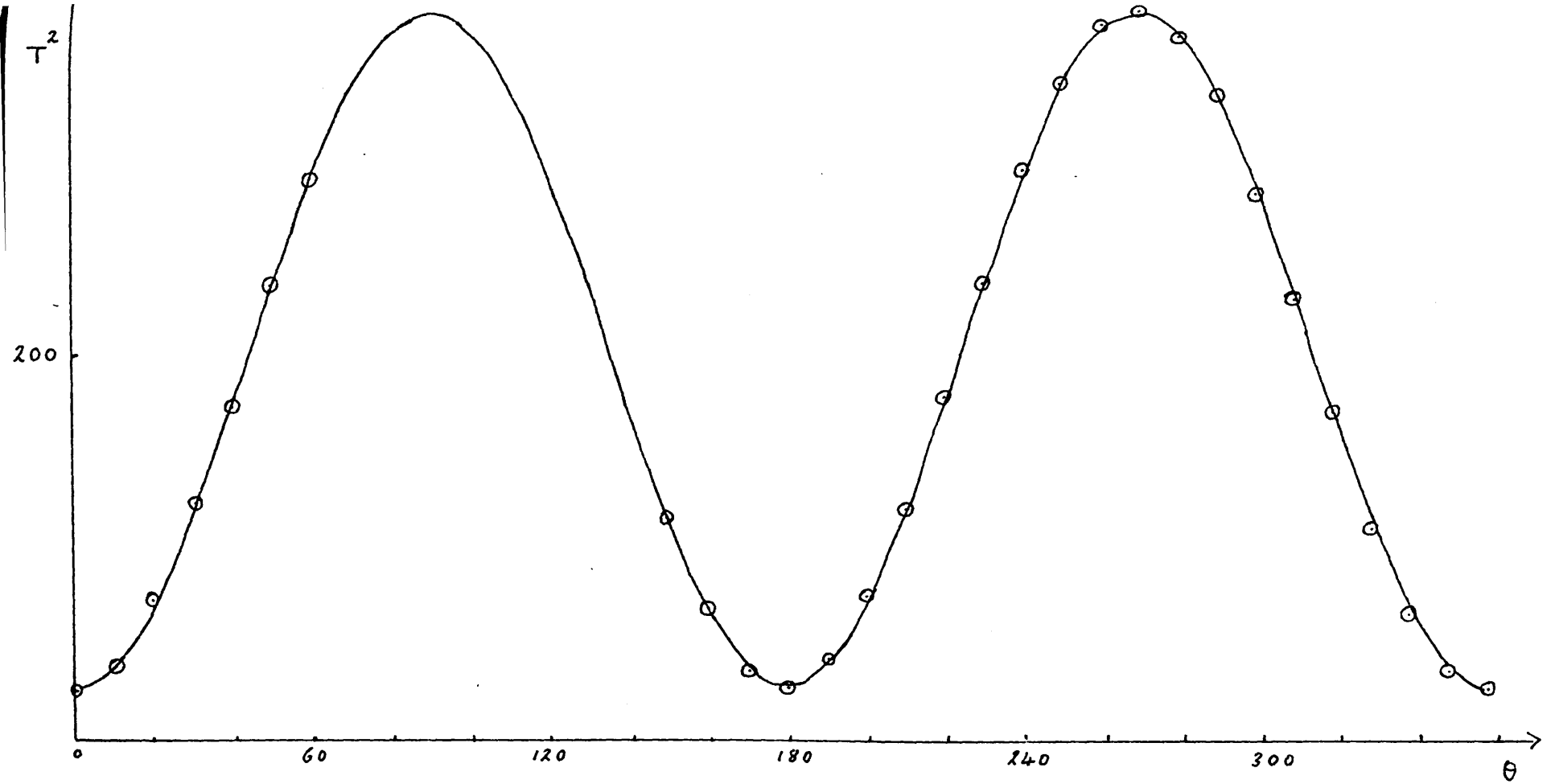

Figure 21

T^2 values obtained for the radical at 260°K with the crystal mounted on axis r.

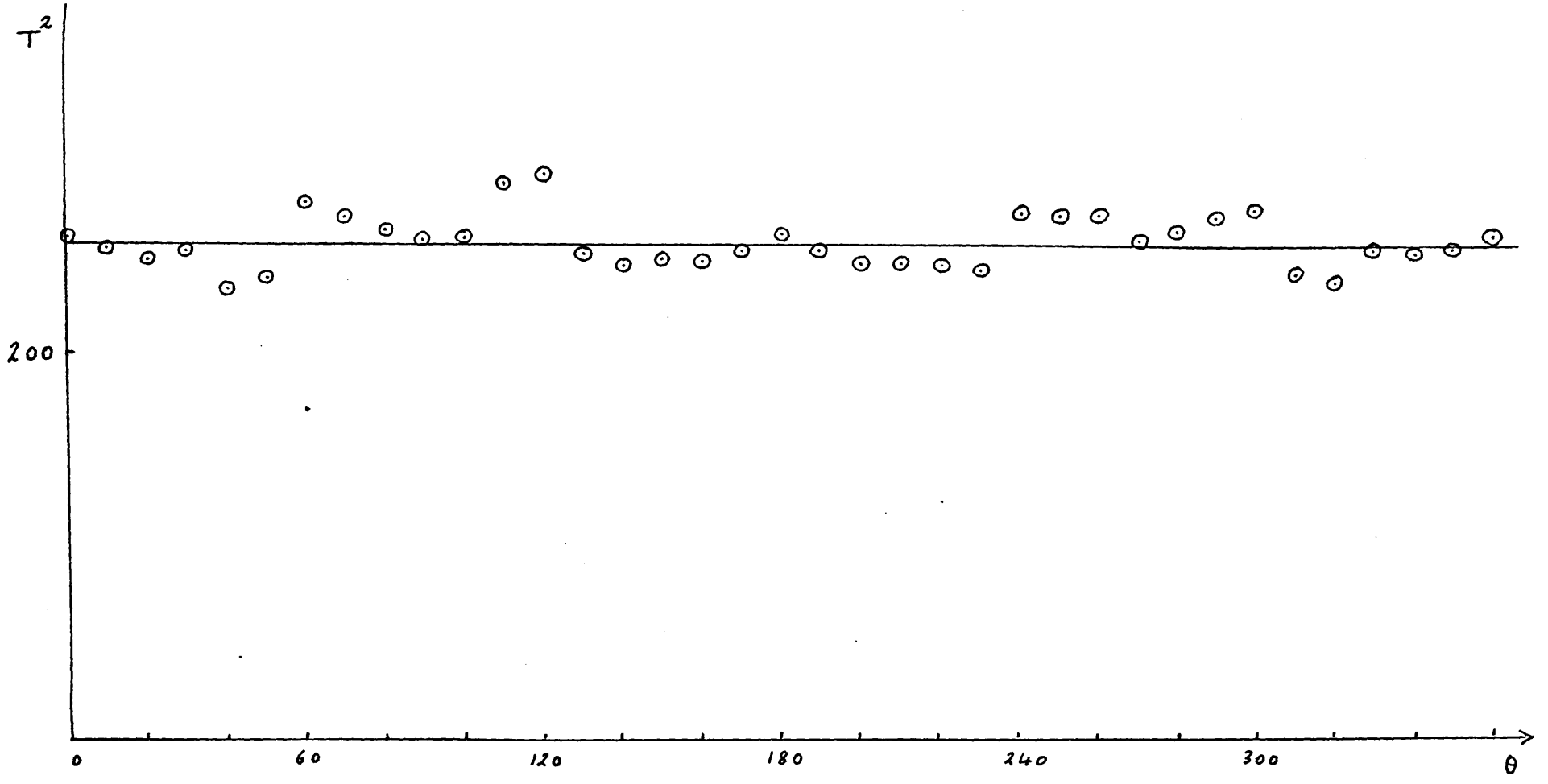

Figure 22

T^2 values obtained for the isotropic radical at 293°K with the crystal mounted on axis r.

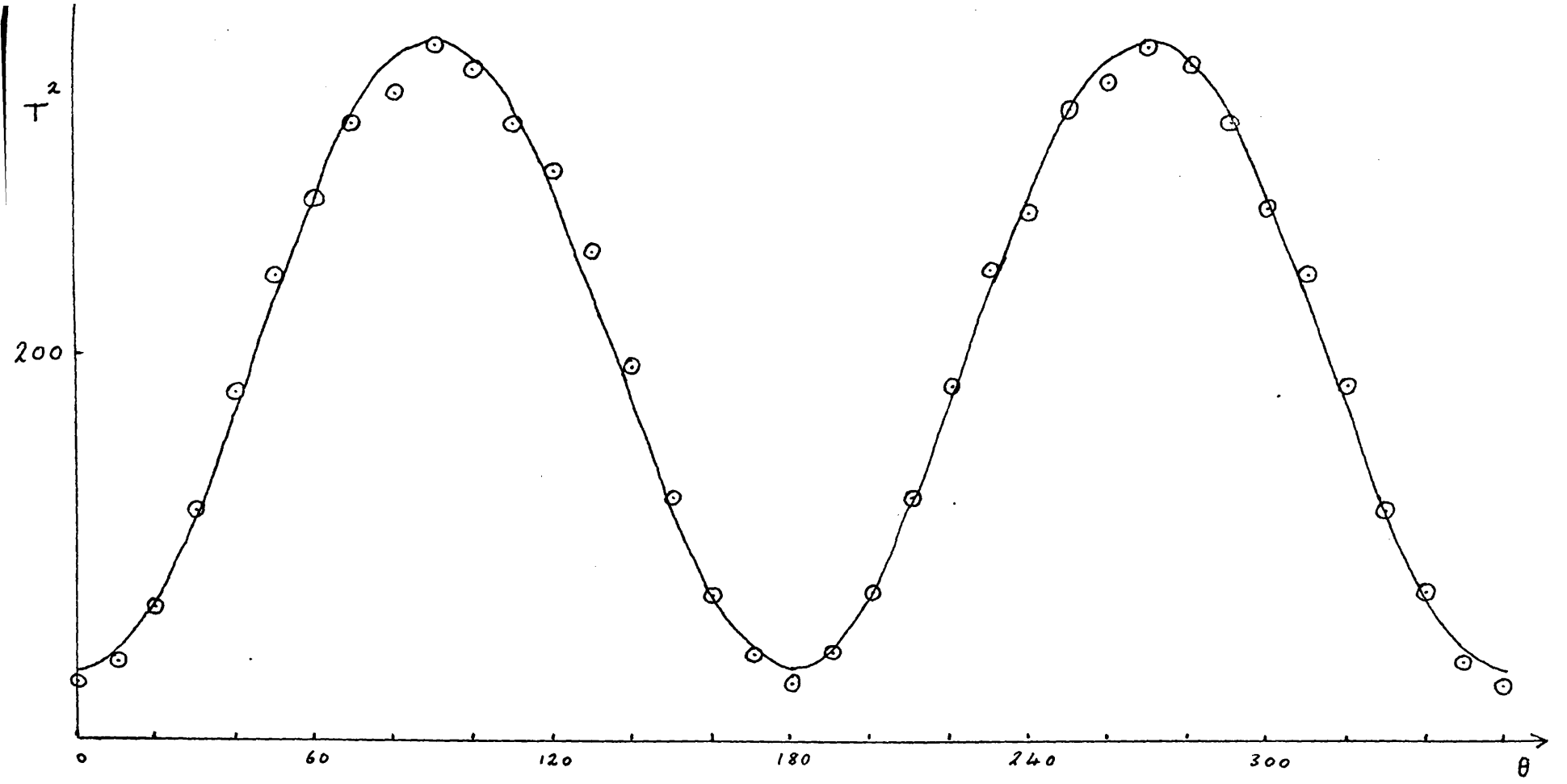

Figure 23

T^2 values obtained for the anisotropic radical at 293°K with the crystal mounted on axis r.

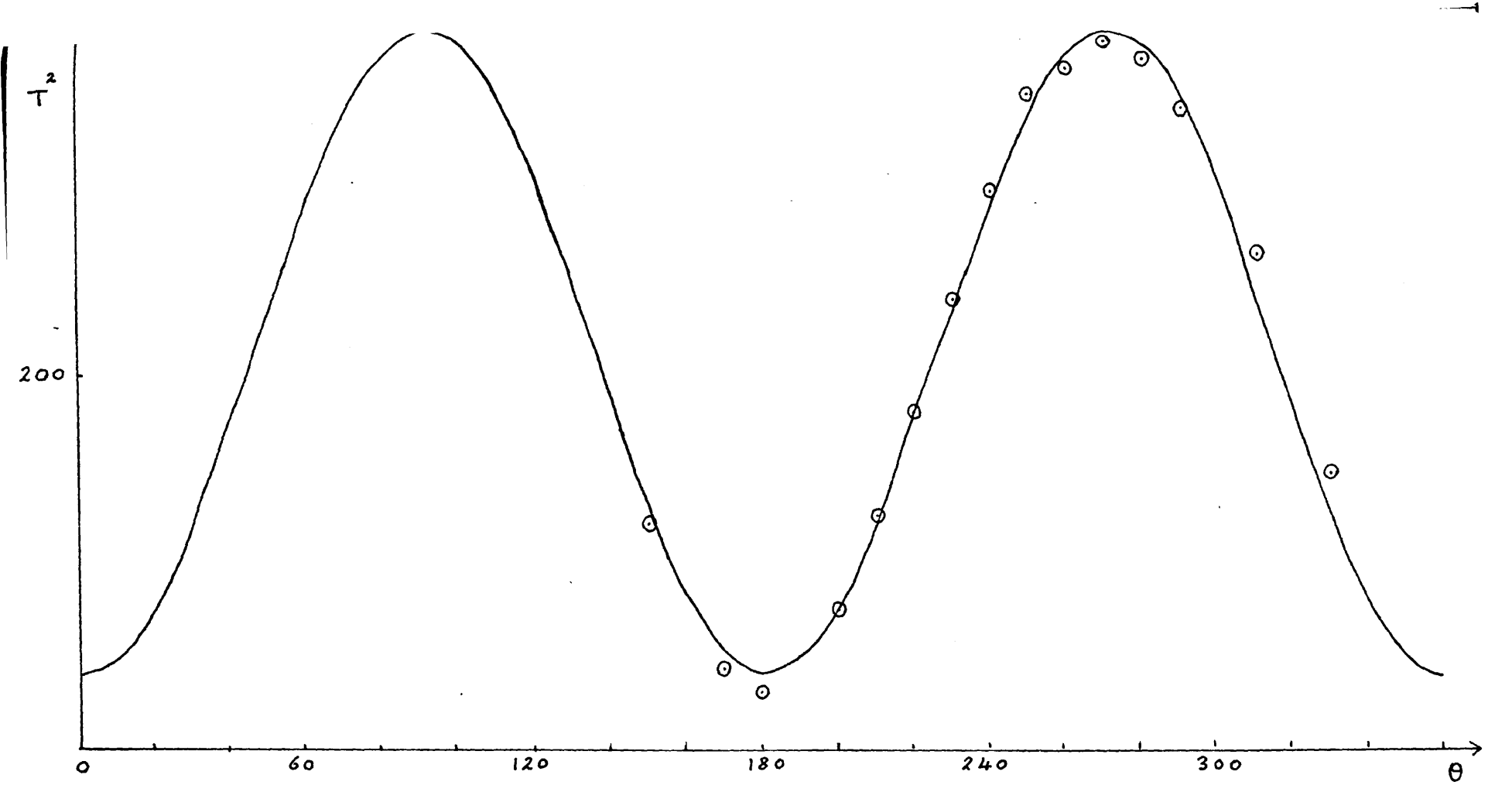

Figure 24

T^2 values obtained for the radical at 353°K with the crystal mounted on axis r.